UNIVERSITEIT GENT

FACULTY OF SCIENCES
Department of Organic and Macromolecular Chemistry
Polymer Chemistry Research Group

Versatile Synthesis of Functional Hyperbranched Polymers by Combination of CRP and Thiol-X Chemistry

Sofie WALLYN

Promotor: Prof. Dr. Filip Du Prez
Co-promotor: Prof. Dr. Richard Hoogenboom
Ghent, 2015

Thesis submitted to obtain the degree of Doctor of Science: Chemistry

Research funded by the Agency for Innovation by Science and Technology

Onderzoek gefinancierd door het Agentschap voor Innovation door Wetenschap en Technologie

Woord Vooraf

Het is algemeen bekend dat wetenschappelijk onderzoek niet altijd van een leien dakje loopt. Dit gaat met vallen en opstaan. Tijdens mijn doctoraat heb ik dit regelmatig moeten ondervinden. Gelukkig stond ik er niet alleen voor. Via deze weg wil ik graag de mensen bedanken die mij de afgelopen vijf jaar door dik en dun steunden.

Eerst en vooral wil ik Prof. Filip Du Prez bedanken om mij de kans te geven om mijn doctoraat uit te voeren binnen zijn onderzoeksgroep. Zijn kennis en onvoorwaardelijke inzet hebben gezorgd voor een motiverende, aangename werksfeer binnen de groep. Ook zijn geduld en begrip wanneer de resultaten al eens tegenvielen zijn zeker het vermelden waard. Zijn deur stond letterlijk en figuurlijk altijd open. Bovendien gaf hij mij de mogelijkheid om kennis op te doen en te presenteren op zowel nationale als internationale congressen. Ook mijn copromotor, Prof. Richard Hoogenboom mag ik zeker niet vergeten te bedanken. Hij had steeds een frisse blik op de zaken en stond steeds open om zijn immense kennis te delen.

I would like to thank the members of the reading committee: Prof. Bruno De Geest, Prof. David Fournier and Dr. Remzi Becer, for reviewing my thesis and for the constructive suggestions and remarks, which improved the quality of the final work.

Alle leden van de PCR-groep wil ik bedanken voor de aangename werksfeer die ervoor zorgden dat 4 jaar doctoreren voorbij vloog. Ik ben dankbaar om te hebben mogen samenwerken met enkele fantastische mensen. Bernhard De Meyer wil ik graag bedanken voor zijn uitstekende technische ondersteuning en steeds klaar te staan wanneer het allemaal wel eens misliep. Je bent de rots in de branding voor de PCR-groep. Stef Vandewalle, wie ik heb mogen begeleiden tijdens zijn masterthesis, heeft een grote bedrage aan het laatste hoofdstuk van deze thesis. Bedankt Stef, het was fantastisch om met je samen te werken, ik kon mij geen betere thesisstudent bedenken. Fabienne Goethals, maatje, een dikke merci voor alles. Je stond/staat altijd klaar voor me en was een grote steun tijdens het schrijven van deze scriptie.

I would also like to thank some people for their interesting collaborations. Prof. Bruno De Geest, Zhiyue Zhang, thank you for your wonderful contribution in Chapter III. Also a special word of thanks to Dr. Lenny Voorhaar, for the nice and intense collaboration on the high throughput experiments. Dr. Becer, thank you for your good advice in the work of the lectin-polymer interactions. It was a honor to working with a professional like you.

Tot slot, wil ik mijn vrienden en familie bedanken voor de onvoorwaardelijke steun en fantastische momenten die we samen beleefden. In het bijzonder wil ik enkele mensen vermelden: Freya en Ellen, middagpauzes zijn nooit meer hetzelfde zonder jullie. De drie musketiers zijn niet meer. Babs, Arne, Dorien, Dries, Lander en Elke: dat er nog vele chemische feestjes mogen volgen! Lien, bedankt voor je luisterend oor tijdens mindere tijden en je vette lach tijdens goede tijden. Maatjes, bedankt allemaal en tot snel. Klaas, schatje, je bent mijn rots in de branding. Bedankt voor je geduld, steun en liefde. *Wat zou ik toch doen zonder jou?* Ook aan mijn ouders, mama en Willy: bedankt voor alles, zonder jullie was dit allemaal niet mogelijk.

Table of Contents

Chapter I

General introduction, aim and outline

I.1 General introduction, aim and outline

The use of polymer materials in our permanently changing, high demanding, technology-driven society is more than ever growing. New developments and application technologies in this field are continuously under investigation by making the synthesis of the macromolecular materials cheaper, faster, greener, more efficient and versatile. Many of these strategies are found in combinations of organic synthesis and controlled radical polymerization reactions. Synthetic polymer-bioconjugates where peptides, proteins and enzymes are modified with well-defined polymeric materials are examples where such combinations are applied.

To achieve straightforward synthesis strategies for the design of well-defined complex macromolecular architectures, a set of efficient reactions is requisite. The introduction of click chemistry in polymer science has been of crucial importance in the synthesis of complex polymer materials, which was before only possible through applying more complicated procedures and intensive work-up.[1-4] The definition of a click reaction entails numerous conditions including the ease in conducting the reaction, its broad applicability in modular approaches and its ability to proceed without the lack of significant side products.[5]

In 2001 Kolb, Finn and Sharpless defined a set of criteria for a reaction to be considered as a click reaction: *"The reaction must be modular, wide in scope, give very high yields, generate only inoffensive byproducts that can be removed by non-chromatographic methods, and be stereospecific (but not necessarily enantioselective). The required process characteristics include simple reaction conditions (ideally, the process should be insensitive to oxygen and water), readily available starting*

materials and reagents, the use of no solvent or a solvent that is benign (such as water) or easily removed, and simple product isolation. Purification—if required—must be by non-chromatographic methods, such as crystallization or distillation, and the product must be stable under physiological conditions. [...] Click processes proceed rapidly to completion and also tend to be highly selective for a single product: we think of these reactions as being 'spring- loaded' for a single trajectory".[6] Our research group, in combinations with some others, have made a critical evaluation of those conditions, in macromolecular science.[5] In this context, a new set of requirements has been proposed for click reactions in macromolecular synthesis, taking into account the different needs and perspectives for polymers (Figure I-1). Besides the original criteria of being modular, chemoselective, wide in scope and proceeding by a single reaction trajectory (in blue), some polymer-specific, stricter requirements are adapted and added to the definition (in green and green-blue).

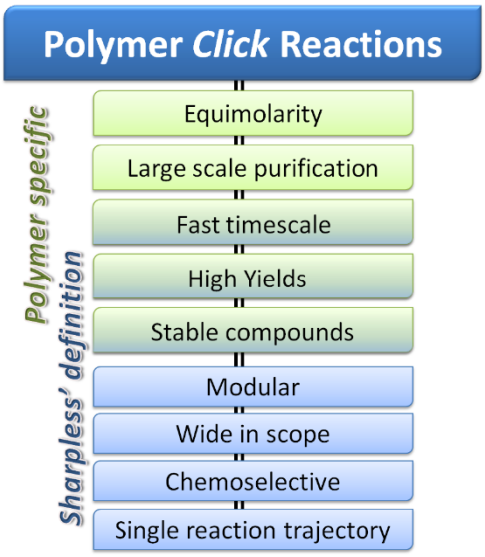

Figure I-1: Requirements for click reactions involving one or more polymeric reagents (blue: originally defined by Sharpless; green and blue–green: adapted requirements related to synthetic polymer chemistry).[5]

A major part of new investigations in polymer science are dealing with the introduction of new functionalities in order to obtain new complex well-defined macromolecular structures. Click chemistry plays an important role in these synthesis approaches. Next to the popular Cu(I)-catalyzed azide-alkyne cycloaddition click reaction[7-10], historically the first introduced one, more and more attention goes to thiol-based click chemistries.[2, 11-16]

Another highly investigated topic in polymer science is the synthesis of hyperbranched polymers with well-defined end-group functionalities *via* a straightforward procedure. The unique properties of these three-dimensional structures make them attractive for many new applications ranging from drug delivery systems[17, 18] to rheology modifiers[19]. The concept of hyperbranched structures was already described by Flory in the early 1950s.[20] In the meantime, many new synthetic strategies have been developed for the preparation of these unique structures, which have led to the development of a broad range of dendritic structures that are applicable in different fields. Recently, different studies handling the synthesis of hyperbranched structures using click chemistry are reported making the synthesis of multi-functional hyperbranched structures more straightforward.[21-27]

In this PhD project, well-defined AB_2 macromonomers are synthesized *via* controlled radical polymerization (CRP) techniques, and then further reacted upon thiol-X chemistry, resulting in functional hyperbranched polymers. Next to the frequently used reversible addition-fragmentation chain transfer (RAFT), the recently developed Cu(0)-mediated radical polymerization is applied as CRP technique for the preparation of protected AB_2 macromonomers. Both a CTA group and thiolactone moiety are known precursors for thiols and used to avoid the common problems occurring when working with thiols such as their instability towards oxidation reactions. Aminolysis of the protecting groups with small amines or NH_2–oligomers, releases a thiol resulting in the AB_2 macromonomers, which then can further react to hyperbranched polymers upon thiol-X chemistry. Moreover, these synthesis strategies are used to synthesize thermo-responsive hyperbranched glycopolymers, which are tested on their interaction abilities with their specific lectins.

I.2 Outline

The first part of **Chapter II** highlights the new synthetic developments in thiol-based chemistries for polymer synthesis together with some new insight in controlled radical polymerization techniques. Next to the traditional CRP techniques such as ATRP and RAFT, the new developments in Cu(0)-mediated controlled polymerization techniques are described. This latter technique is fast, can proceed at ambient temperatures and gives structures with a high end-group fidelity even at high conversions. These properties make the Cu(0)-mediated polymerization a

suitable technique for the preparation of hyperbranched polymers. Moreover, in combination with efficient click chemistries, a broad range of hyperbranched polymers can be synthesized. In a second part of **Chapter II**, hyperbranched polymers are defined together with their unique properties. New developments in the synthesis strategies of these structures are described together with their potential in several application fields. In a last part, the need and use of glycopolymers and their applicability in certain fields are reported.

Chapter III describes the straightforward synthesis of heterotelechelic, hydrophilic polymers with a primary amine and thiol group at the α– and ω-chain end *via* reversible addition-fragmentation chain transfer (RAFT) polymerization. These structures were subsequently used for the design of dual-responsive polymer/gold nanohybrids. End-group conversions were monitored by ^{1}H NMR spectroscopy, MALDI-TOF MS analysis and UV-Vis spectroscopy, confirming that quantitative modifications were obtained during each stage. The amino groups of these heterotelechelic polymer chains were modified with citraconic anhydride, after which the obtained polymers were grafted with the thiol group onto citrate stabilized gold nanoparticles resulting in the creation of dual temperature- and pH-responsive gold particles. Furthermore, incorporation of two different dye components at the PNIPAM structure yielded thermo-responsive polymeric dyes whose sensing capacities are tested by using a biphasic aqueous/organic system below and above the cloud point temperature of the polymeric structure.

In the next chapter, **Chapter IV**, the findings on the use of thiol-yne chemistry of AB_2 oligomers for the preparation of hyperbranched polymers is reported. Two different approaches are followed. In the first approach, a suitable CTA, containing an alkyne functionality at the ω-chain end, is synthesized and evaluated on its polymerization capacities of different monomer types. Subsequent aminolysis yielded the AB_2 thiol-alkyne oligomers with narrow dispersity. Applying photo(UV)-initiated thiol-yne chemistry in the presence of a photo-catalyst hyperbranched polymers were obtained. In the other approach, a monomer containing both an alkyne and thiolactone moiety was synthesized. Opening of the thiolactone ring upon aminolysis with an RAFT-derived oligomer containing a primary amine at the α-chain end yielded the AB_2 thiol-alkyne oligomers. Using this strategy, a new functionality is introduced into the structure originating from the amine molecule. Again, photo(UV)-initiated thiol-yne chemistry was applied for the preparation of hyperbranched structures.

As alternative CRP technique to RAFT, which is used in the previous chapters, Cu(0)-mediated polymerization was considered as a technique to synthesize the AB_2 oligomers. Therefore, in **Chapter V,** the optimization of the Cu(0)-mediated polymerization of *n*-butyl acrylate and 2-methoxyethyl acrylate is reported using an automated parallel synthesizer. Using this robot, up to 16 kinetic reactions could be performed in parallel, resulting in a fast screening of different reaction conditions. Several parameters were optimized to determine the optimal reaction conditions with regard to control over the polymerization and reaction rate. These optimal reaction conditions were then used for the one-pot two-step synthesis of diblock copolymers by sequential monomer addition.

Finally, in **Chapter VI**, the synthesis of hyperbranched glycopolymers in which thermo-responsive poly(*N*-isopropylacrylamide) (PNIPAM), connected by redox-responsive disulfide bonds, forms the skeleton and for which mannose units are present at each branching point are described. Degradation of the hyperbranched structure via chemical reduction of the disulfide bond was demonstrated. Moreover, the thermo-responsive behaviour of the glycopolymer was studied. Finally, the lectin-polymer interaction was investigated to understand the influence of both the polymer concentration and different chain conformations below and above cloud point, respectively. Furthermore, it is attempted to prepare thermo-responsive hyperbranched glycopolymers with adjustable amount of sugar units per branching unit.

I.3 References

[1] C. R. Becer, R. Hoogenboom, U. S. Schubert, *Angew. Chem.-Int. Edit.* **2009**, *48*, 4900.
[2] B. S. Sumerlin, A. P. Vogt, *Macromolecules* **2010**, *43*, 1.
[3] J.-F. Lutz, H. Schlaad, *Polymer* **2008**, *49*, 817.
[4] R. K. Iha, K. L. Wooley, A. M. Nystrom, D. J. Burke, M. J. Kade, C. J. Hawker, *Chem. Rev.* **2009**, *109*, 5620.
[5] C. Barner-Kowollik, F. E. Du Prez, P. Espeel, C. J. Hawker, T. Junkers, H. Schlaad, W. Van Camp, *Angew. Chem.-Int. Edit.* **2011**, *50*, 60.
[6] H. C. Kolb, M. G. Finn, K. B. Sharpless, *Angew. Chem.-Int. Edit.* **2001**, *40*, 2004.
[7] J. A. Johnson, M. G. Finn, J. T. Koberstein, N. J. Turro, *Macromol. Rapid Commun.* **2008**, *29*, 1052.
[8] M. Meldal, C. W. Tornoe, *Chem. Rev.* **2008**, *108*, 2952.
[9] P. L. Golas, K. Matyjaszewski, *Chemical Society Reviews* **2010**, *39*, 1338.
[10] H. Nandivada, X. Jiang, J. Lahann, *Advanced Materials* **2007**, *19*, 2197.
[11] A. B. Lowe, *Polymer Chemistry* **2014**, *5*, 4820.
[12] G. Franc, A. K. Kakkar, *Chem. Soc. Rev.* **2010**, *39*, 1536.
[13] R. Hoogenboom, *Angew. Chem.-Int. Edit.* **2010**, *49*, 3415.
[14] C. E. Hoyle, A. B. Lowe, C. N. Bowman, *Chem. Soc. Rev.* **2010**, *39*, 1355.
[15] M. J. Kade, D. J. Burke, C. J. Hawker, *J. Polym. Sci. Pol. Chem.* **2010**, *48*, 743.
[16] A. B. Lowe, C. E. Hoyle, C. N. Bowman, *J. Mater. Chem.* **2010**, *20*, 4745.

[17] S. Chen, X.-Z. Zhang, S.-X. Cheng, R.-X. Zhuo, Z.-W. Gu, *Biomacromolecules* **2008**, *9*, 2578.
[18] M. Irfan, M. Seiler, *Industrial & Engineering Chemistry Research* **2010**, *49*, 1169.
[19] C. Kavitha, K. P. Dasan, *Chimica Oggi-Chemistry Today* **2013**, *31*, 46.
[20] P. J. Flory, *J. Am. Chem. Soc.* **1952**, *74*, 2718.
[21] G. Franc, A. K. Kakkar, *Eur. Polym. J.* **2009**, *15*, 5630.
[22] D. Konkolewicz, A. Gray-Weale, S. Perrier, *J. Am. Chem. Soc.* **2009**, *131*, 18075.
[23] D. Konkolewicz, M. J. Monteiro, S. Perrier, *Macromolecules* **2011**, *44*, 7067.
[24] Z. a. Li, G. Yu, P. Hu, C. Ye, Y. Liu, J. Qin, Z. Li, *Macromolecules* **2009**, *42*, 1589.
[25] A. Qin, J. W. Y. Lam, C. K. W. Jim, L. Zhang, J. Yan, M. Haussler, J. Liu, Y. Dong, D. Liang, E. Chen, G. Jia, B. Z. Tang, *Macromolecules* **2008**, *41*, 3808.
[26] M. Semsarilar, V. Ladmiral, S. Perrier, *Macromolecules* **2010**, *43*, 1438.
[27] J. Xu, L. Tao, C. Boyer, A. B. Lowe, T. P. Davis, *Macromolecules* **2010**, *43*, 20.

Chapter II

Theoretical description

II.1 Controlled radical polymerization

The discovery of living polymerization reactions by Szwarc in 1956 has been essential for the synthesis of well-defined polymers with precisely designed architectures. The term living polymerization was denoted as a chain growth polymerization for which termination or transfer reactions are absent.[1] In this way, the polymer chain keeps growing until all monomer is consumed. Moreover, all chains are initiated immediately and grow simultaneously. This makes living polymerization suitable for the synthesis of a large range of polymers with some interesting properties, such as a low dispersity and a high end-group fidelity.

The first living polymerizations were based on anionic and cationic polymerization methods. Termination and transfer reaction could be excluded because of the fact that similar charges do not react with each other whereby the active centres are retained. However, this method has also some drawbacks such as the need for stringent reaction conditions, the incompatibility with some functional groups and the number of monomers amenable with this method is rather low.[2] Generally, it can be stated that ionic polymerization reactions are often not very attractive for the synthesis of polymers on industrial scale, although their use is in some cases inevitable (e.g. polybutadiene, SBS rubbers,…).

On the other hand, radical polymerization techniques are frequently used for the commercial synthesis of high molecular polymers as they can be carried out under relatively mild reaction conditions and show tolerance to several functional groups, solvents and impurities.[3] Because of this, the majority of the commercially materials are made by free radical polymerization (FRP)

techniques. Despite this, the main disadvantage of FRP is the lack of control over some key elements of the molecular structure (molecular weight, dispersity and end-group functionality), which is a prerequisite for obtaining materials with well-defined material properties.

The development of controlled radical polymerization (CRP) techniques made it possible to overcome the above limitations and to synthesize well-defined polymers with a good control over the molecular weight, dispersity, composition and architecture.[4-6] These properties enable exceptional opportunities in many fields, where materials with precise control of the molecular structure are needed. All of these polymerization techniques rely on a dynamic equilibrium between the active propagating radicals and various dormant species, as shown in Scheme II-1.a. Hence, the concentration of propagating radicals is lowered dramatically (10^{-7} - 10^{-8} M) compared to FRP. Termination reactions can therefore be virtually neglected. This effect is further amplified by the fact that termination reactions are from the second rate order, while propagation is a first order rate process (eqs II.1 and II.2). Moreover, the fast equilibrium between the active and dormant species guarantees that all polymer chains propagate at the same rate resulting in homogeneous products. Apart from the aforementioned mechanism where the presence of a dormant species prevents termination and transfer, another mechanism for controlled radical polymerization is based on degenerative exchange processes as shown in Scheme II-1.b.

$$R_P = k_p[P_n \cdot][M] \quad \text{(II.1)}$$

$$R_t = 2k_t[P_n \cdot]^2 \quad \text{(II.2)}$$

R_p = propagation rate

R_t = termination rate

k_p = propagation rate coefficient

k_t = termination rate coefficient

$[P_n \cdot]$ = radical concentration

$[M]$ = monomer concentration

In the past 20 years, a number of controlled radical polymerization methods have been developed based on these dynamic equilibria where nitroxide mediated polymerization (NMP; also called stable free radical polymerization (SFRP)), reversible addition-fragmentation chain transfer polymerization (RAFT) and copper-mediated polymerizations (such as atom transfer radical polymerization (ATRP)) can be regarded as the three most important examples. Both RAFT and a specific type of copper-mediated polymerization are frequently used in this thesis and will thus be discussed into more detail in the next sections. For NMP the reader is referred to literature.[7-9]

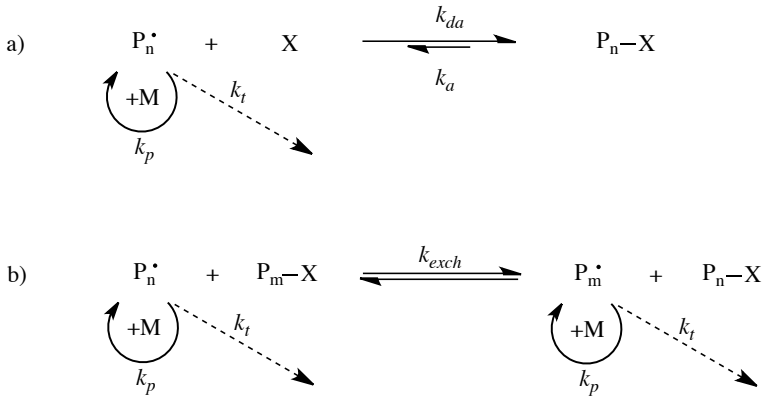

Scheme II-1: Controlled radical polymerization mechanism: a) Deactivation/activation process; b) Degenerative exchange process.

II.1.1 Reversible addition-fragmentation chain transfer polymerization (RAFT)

The RAFT polymerization technique was reported for the first time in 1998 by Rizzardo *et al.*[10-14] and the group of Charmot[15]. Until today, this versatile process has been extensively used for the synthesis of well-defined homo-, gradient, multi-block, star and hyperbranched polymers as well as more complex architectures such as polymer brushes.[16] The wide range of functional monomers polymerizable via RAFT (acrylics, methacrylics, styrenics, dienes, and other vinyl monomers) and the possibility to introduce different end-group functionalities at the α-terminus (e.g. -OH, -COOH (not compatible with ATRP), -NR_2, -$CONR_2$, -SO_3H,…) via the chain transfer agent (CTA) enables the synthesis of well-defined complex macromolecules (narrow dispersities, linear evolution of number average molar mass (M_n) with conversion and good agreement with theoretical M_n). Moreover, the high thiocarbonylthio end-group fidelity enables not only further chain growth or block extension by subsequent monomer addition, but it also allows further post-polymerization reactions at the ω-terminus. Aminolysis easily converts the CTA into a thiol moiety, opening various possibilities for thiol modification reactions (see section II.2.2).[17-19]

The key factor of this CRP method relies on a degenerative exchange process where a thiocarbonylthio compound is used as a chain transfer agent (CTA) to create a free living radical polymerization system as shown in Scheme II-2. The effectiveness of the CTA, which has general structure of (ZC=S)SR, depends on the monomer being polymerized and the properties of both the Z- and R-group. The Z-group is chosen in such a way that the thiocarbonylthio double bond has sufficient reactivity with the monomers and that the stability for the intermediate radicals is high

enough to avoid side reactions. On the other hand, the R-group, which is a free radical leaving group, should be rapidly converted into a propagating radical, and should effectively reinitiate the polymerization. The use of a wide variety of RAFT agents has already been reported including dithioesters, dithiocarbamates, trithiocarbonates and xanthates. For more detail for the selection of CTAs for various polymerizations, the reader is referred to literature.[10, 16]

The mechanism of the RAFT process involves a series of reversible addition-fragmentation steps (Scheme II-2). In the early stages of the polymerization, addition of a propagating radical $P_n^{\cdot}$ to the thiocarbonylthio compound gives an adduct radical that fragments to a polymeric thiocarbonylthio compound and a new radical $R^{\cdot}$. Reaction of this radical with monomers forms a new propagating radical $P_m^{\cdot}$. A fast equilibrium between the active propagating radicals ($P_n^{\cdot}$ and $P_m^{\cdot}$) and the dormant polymeric thiocarbonylthio compound ensures that all polymer chains have the same opportunity to grow, which provides polymers with a narrow molecular weight distribution.

Initiation

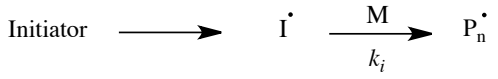

Reversible chain transfer

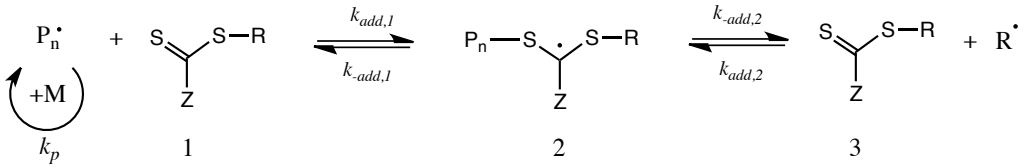

Reinitiation

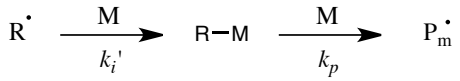

Chain equilibration

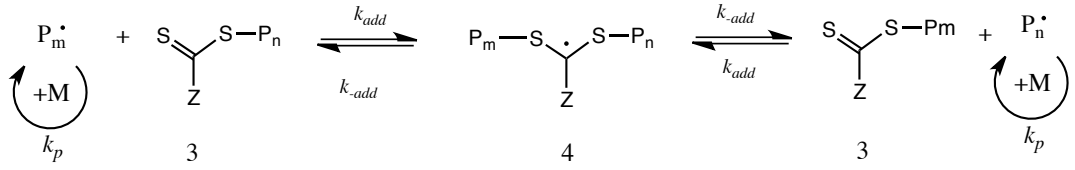

Termination

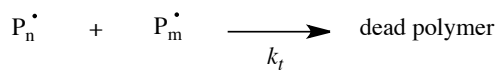

Scheme II-2: Mechanism of RAFT polymerization.

The RAFT process is not only tolerant for unprotected functionalities (in monomer, solvent or initiating system), but it is also compatible with a wide range of reaction conditions (e.g. organic or aqueous solvents, bulk, suspension, emulsion) which make this technique applicable for both academic and industrial purposes. As an example relevant for this thesis, Perrier *et al.* used this technique to synthesize well-defined oligomers with an alkyne functionality at the ω-chain end which, after aminolysis of the CTA group, reacted with the free thiol, yielding hyperbranched polymers.[20-22]

II.1.2 Atom transfer radical polymerization (ATRP)

ATRP, which is one of the most commonly used CRP technique was developed in 1995 and further optimized including the groups of Sawamoto[23-26] and Matyjaszewski[27-32] are the most important ones. The commercial availability of the ATRP reagents allowed a widespread academic and first industrial use of this technique.

The mechanism of ATRP polymerizations differs fundamentally from that of RAFT polymerizations. It involves a homolytic cleavage of an alkyl halide R-X (or macromolecular P_n-X) by a transition metal complex Mt^n/L with a ligand (L) in its lower oxidation state. This reaction reversibly generates an alkyl radical $R^{\cdot}$ (or an active polymer chain $P_n^{\cdot}$) (k_{act}), while the metal complex is transformed into its higher oxidation state (X-Mt^{n+1}/L). Subsequently, this activated radical $R^{\cdot}$ can propagate with a vinyl monomer (k_p), reversibly transformed into a dormant species (Pn-X) by addition of a halide atom (k_{deact}) or terminate by coupling and/or disproportionation (k_t). These termination reactions are negligible due to the fact that the equilibrium is shifted toward the dormant species to keep the radical concentration low ($k_{act} << k_{deact}$). This CRP technique is already successfully used for the polymerization of monomer types such as styrenes, (meth)acrylates, (meth)acrylamides and acrylonitriles generating polymers with predetermined molecular weights, narrow dispersities and good control of the functionalities. However, ATRP of nitrogen containing monomers and certain dienes is very challenging as monomer or polymer complexation with the catalyst can lower its activity.

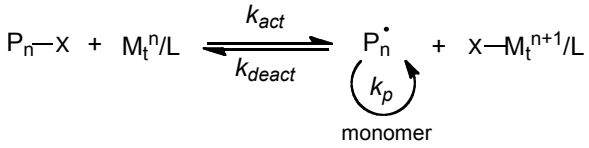

Scheme II-3: Equilibrium between active and dormant polymer species in ATRP.

Via ATRP, a wide range of polymer architectures e.g. block copolymers, star copolymers, random copolymers, gradient polymers can be synthesized. Moreover, another advantage of this method is the fact that the terminal halogen group in the polymer, originating from the initiator, can be easily displaced to other end-group functionalities using various electrophilic, nucleophilic and radical reactions (Scheme II-4).

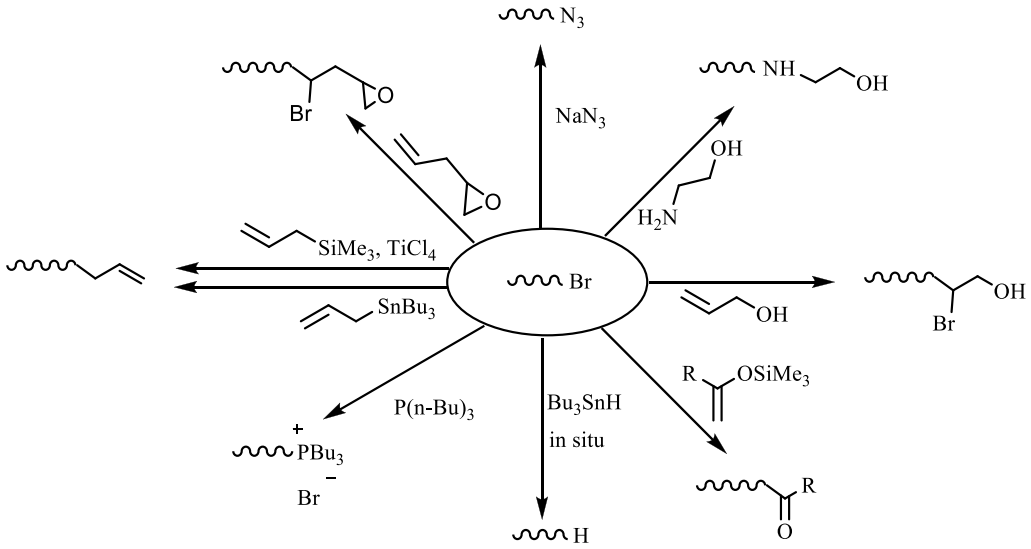

Scheme II-4: Examples of the displacement of the terminal halogen in ATRP polymers using electrophilic, nucleophilic and radical reactions. [29]

However, the major disadvantage of conventional ATRP is the need of a transition metal catalyst, mostly copper, in relatively high concentrations. Various post-polymerization purification processes have been developed to avoid end-products that are contaminated with transition metal impurities. Because such procedures are, in general, prohibitively expensive and time-consuming, a lot of research has been done to diminish the concentration of catalyst in the reaction to such levels that purification is no longer necessary.

A breakthrough towards reducing the amount of catalyst necessary to achieve controlled polymerization, was the development of three new concepts by Matyjaszewski *et al.* (Scheme II-5). One concept, called *activators regenerated by electron transfer* (ARGET) ATRP, uses an excess of reducing agent (e.g. ascorbic acid, derivatives of hydrazine, sugars,…) which reacts with the Cu(II) to generate Cu(I) ATRP catalyst. As such good control over the polymerization has been established using 10-50 ppm of Cu catalyst. In the *initiators for continuous activator regenerating* (ICAR) ATRP system, the role of the reducing agent in ARGET is replaced by radical initiators which constantly reduce and regenerate Cu(I) species that accumulates as a persistent radical. In this way, the mechanism behind ICAR ATRP closely resembles the RAFT mechanism. Moreover, it was shown that externally applying an electrochemical potential over the polymerization mixture can reversibly activate the copper catalyst for ATRP by a one-electron reduction of an initially added air-stable cupric species (Cu(II)/Ligand), giving rise to the e-ATRP concept.

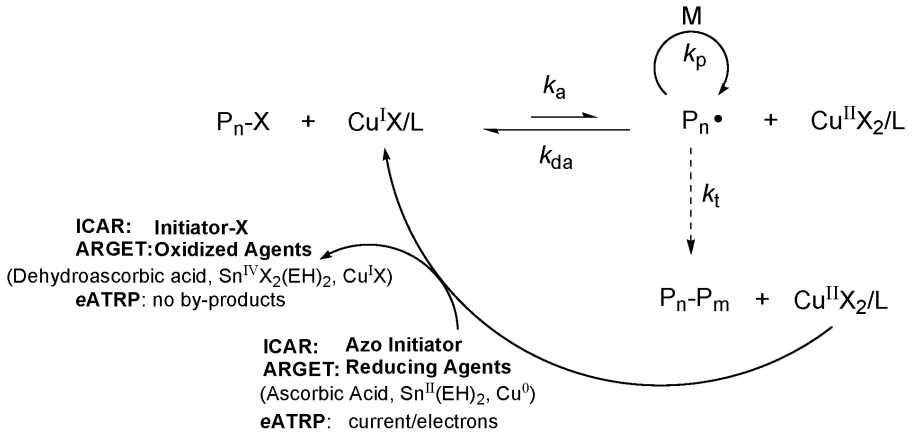

Scheme II-5: The three different main concepts to reduce the Cu(I) concentration: ICAR ATRP, ARGET ATRP and e-ATRP. [33]

II.1.2.1 *Cu(0)-mediated living radical polymerization (Cu(0)-LRP)*

At almost the same time when ARGET and ICAR ATRP were being developed, Percec *et al.* defined another controlled radical polymerization system to reduce the copper concentration. This technique, called single electron transfer-living radical polymerization (SET-LRP) uses ligands and an initiator commonly used in conventional ATRP in combination with elemental copper as active species. The proposed mechanism for the Cu(0)-mediated polymerization method is shown in Scheme II-6. In the Cu(0)-mediated polymerization technique, the polymer chains are activated through a Cu(0) mediated outer-sphere electron transfer (OSET) process to generate the active

radical chains. These chains can now undergo propagation, termination or deactivation via halogen exchange with a Cu(II) species. Just like in conventional ATRP, the Cu(II)X_2/ligand complex acts as a deactivator to cap radicals to establish an equilibrium between active and dormant polymer chains. Both these activation and deactivation steps generate Cu(I) species, which undergo spontaneous disproportionation into Cu(0) and Cu(II) when an appropriate combination of is used. A survey of different ligand/solvent combinations revealed that strong coordinating ligands (Me_6TREN, TREN, PMDETA) favour the disproportionation in certain polar or coordinating solvents (DMSO, alcohols, binary mixtures of water and other organic solvents), which is required to complete the Cu(0)-mediated polymerization cycle. Because of their extremely high catalytic activity with Cu(0), only a small amount is needed (about in the same range as in ARGET and ICAR; ppm level).

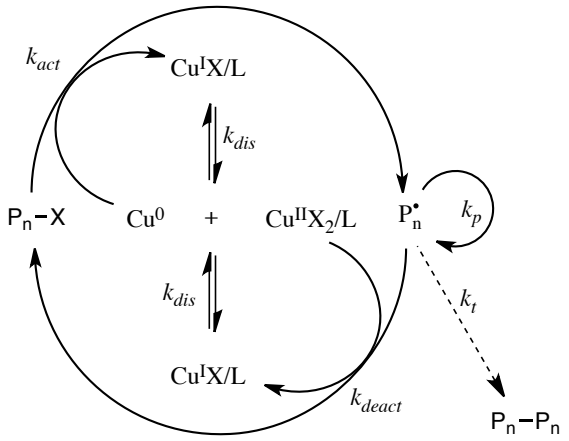

Scheme II-6: Proposed mechanism of reversible-deactivation radical polymerization by Percec et al. (SET-LRP).[34]

However, recently a debate is going on in literature regarding the mechanism of reversible-deactivation radical polymerization in the presence of Cu(I). Besides the mechanism proposed by Percec (*vide supra*), the group of Matyjaszewski introduced the *supplemental activator and reducing agent atom transfer radical polymerization* (SARA ATRP) concept. In SARA ATRP, Cu(I) is the major activator of alkyl halides, Cu(0) is a supplemental activator and reducing agent of excess Cu(II) through comproportionation, and disproportionation is negligible. It is important to note that both mechanisms are used to describe the same polymerization process, and thus the names SET-LRP and SARA ATRP should not be used if the assumptions underlying the mechanism are not backed up by experimental data. Nevertheless, Matyjaszewski reported that a body of experimental and theoretical data indicates that Cu(I) species are typically more than 100 times more active than Cu(0)

species and that the kinetics of the process dictate that Cu(I) species activate alkyl halides at least 10^5 times faster than they disproportionate, agreeing with the SARA ATRP mechanism.[35] As the debate is still ongoing and no general mechanism is accepted yet, the term Cu(0)-mediated living radical polymerization (Cu(0)-LRP) is used in this thesis.

The advantages of the Cu(0)-mediated polymerization over conventional ATRP and other forms of low copper concentration ATRP are remarkable. First of all, the use of elemental copper enables simple removal of the catalyst from the polymer, as it is heterogeneous to the reaction mixture. Further, the polymerization rates are higher than in comparable ATRP systems (≤ 2 hours), and polymerizations are often performed at room temperature or even below. Moreover, the control and retention of the end-groups (even at 99% conversion) makes this technique successful for the synthesis of poly(acrylate)s, poly(methacrylate)s and poly(acrylamide)s, including functional macromolecules with complex architectures.[36-38] This high end-group fidelity, which leads to polymers with a high degree of livingness, enables the synthesis of polymers with high molecular weights as well as the facile generation of multi-block polymers by simple monomer addition.

II.2 Click chemistry

Current advances in material science, organic chemistry and pharmaceutics areas, increasingly demand structural materials with a well-defined chemical composition through rational design. Moreover, also the industrial applicability of reaction strategies is becoming more and more important. The introduction of the concept of click chemistry by Sharpless *et al.* in 2001, made it possible to fulfil the different requirements needed for such a design and rapidly triggered great interest in the field of polymers.[39, 40]

According to the definition of Sharpless[39], click chemistry must meet a set of stringent criteria: "*The reaction must be modular, wide in scope, give very high yields, generate only inoffensive by-products that can be removed by nonchromatographic methods, and be stereospecific (but not necessarily enantioselective). The required process characteristics include simple reaction conditions (ideally, the process should be insensitive to oxygen and water), readily available starting materials and reagents, the use of no solvent or a solvent that is benign (such as water) or easily removed, and simple product isolation. Purification—if required—must be by nonchromatographic methods, such as crystallization or distillation, and the product must be stable under physiological conditions."* All these characteristics can be attributed by the fact that click reactions have a high thermodynamic driving force, usually bigger than 20 kcal.mol^{-1}.

The term click chemistry is not limited to one specific type of reaction but includes a wide range of reactions with different mechanisms, which fulfill all above criteria. In general, click reactions can be divided in four categories[39, 41, 42]:

- Cycloadditions of unsaturated species, particularly the 1,3-dipolar cycloaddition reaction but also the hetero-Diels-Alder cycloaddition reaction;
- Nucleophilic substitution reactions; such as the ring-opening of strained hetero-cyclic electrophiles;
- Carbonyl chemistry of the 'non-aldol'-type, such as the formation of hydrazones;
- Additions to carbon-carbon multiple bonds, such as for certain types of thiol-ene chemistry.

In the beginning, the term click chemistry was almost exclusive denoted to the 1,3-dipolar cycloaddition reaction between terminal alkynes and azides. The possible use of this reaction, also known as the Huisgen 1,3-dipolar azide-alkyne cycloaddition, is very high as the azide and alkyne can be incorporated in an easy way into a wide range of substituents, while azides lack reactivity with other functional groups. Nevertheless, this uncatalyzed reaction proceeds relatively slow as azides are generally poor 1,3-dipolar acceptors, requiring elevated temperatures or pressures. The harsh conditions required for the non-catalyzed 1,3-dipolar addition leads to a loss of regioselectivity and leads to the formation of a mixture of 1,4- and 1,5-substituted triazoles. These major drawbacks were overcome in 2002 when the research groups of Sharpless[43] and Meldal[42] discovered, nearly simultaneously, that the use of copper(I) as catalyst in the 1,3-dipolar cycloaddition reaction makes the reaction not only faster but also regioselective. In this manner, only the 1,4-substituted 1,2,4-triazole product is formed and the reaction is accelerated by a factor of 10^7 (relative to the thermal process), making it sufficiently fast at room temperature (Scheme II-7). The mechanism of this efficient reaction is depicted in Figure II-1, whereby the copper-acetylide complexes are responsible for the catalytic effect.[43] As such, Cu(I) catalyst makes the acetylene moiety more active towards the 1,3 dipolar azide.

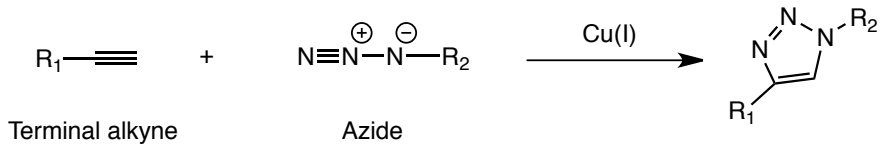

Scheme II-7: Cu(I)-catalyzed 1,3-dipolar cycloaddition of azides and terminal alkynes.

Nowadays, this copper(I) catalyzed azide-alkyne cycloaddition reaction (CuAAC) is undoubtedly the most popular type of click reaction and finds applications in many different fields of research, ranging from pharmaceutical science to nanotechnology. However, despite the advantages, the need of the metal catalyst and safety issues related to the use of azides, make the reaction unsuitable for bio-related or industrial applications. These considerations have inspired researchers to explore other, metal-free reactions exhibiting characteristics fitting the click chemistry philosophy. The most prominent examples are the strain-promoted azide-alkyne cycloaddition reaction (SPAAC), the Diels-Alder reactions and some reactions involving thiols.

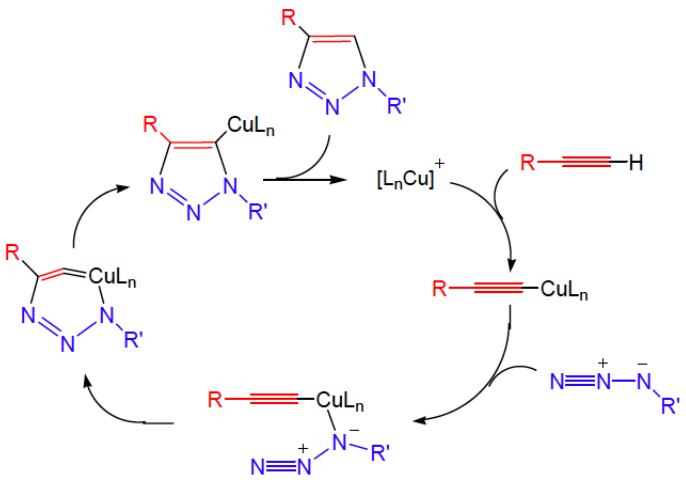

Figure II-1: Proposed mechanism of the Cu(I)-catalyzed cycloaddition of azides and terminal alkynes. [43]

Thiol-based click reactions have become very attractive the last years in polymer science, due to the versatility and the high reactivity of the thiol functionality. Many types of thiol-X chemistry are developed: e.g. thio-bromo[44, 45], thio-isocyanate[46, 47], thiol-epoxy[48], thiol-ene[49, 50] and thiol-yne[51] chemistry. In this thesis, several of those thiol-X reactions are used and will be shortly discussed below. For a more detailed overview of click reactions, the reader is referred to literature.[52, 53]

II.2.1 Azide-alkyne based click reactions

The introduction of the click chemistry concept in polymer science had a huge impact on the design and synthesis strategies for macromolecular architectures. Click chemistry not only facilitates the synthesis of new polymer materials, it also increases the range of structures that can be prepared while simplified purification techniques can be used.[40, 54] In 2004, both Hawker and Fréchet introduced this concept in the polymer world by preparing dendrimers and dendronized linear polymers via CuAAC reactions.[55, 56] Since then, the amount of publications dealing with the combination polymers/click chemistry has increased tremendously.

A very common strategy, is the post-modification of ATRP derived polymers by converting the halogen end-group into an azide moiety, which can then subsequently be clicked with several functional alkynes.[57] Such approaches can lead to telechelic polymers, block copolymers, dendrimers or other complex macromolecular architectures.[58, 59] Next to that, functional initiators

and monomers (i.e. azide or alkyne functional compounds) can be used in ATRP for the synthesis of clickable polymers.[59-62] Haddleton *et al.* reported the copper(I) catalyzed one-pot simultaneous CuAAC/LRP process where the relative rate of the CuAAC and LRP can be tuned by appropriate changing certain parameters (concentration of copper species, solvent, temperature).[62] Next to ATRP, also RAFT and other commonly used polymerization techniques were successfully applied in conjugation with the CuAAC click chemistry for the preparation of functional polymers or other complex macromolecules. As such, Perrier *et al.* described the synthesis of highly branched and hyperbranched glycopolymers by combining RAFT with CuAAC as highly efficient post-modification reaction (Figure II-2).[63]

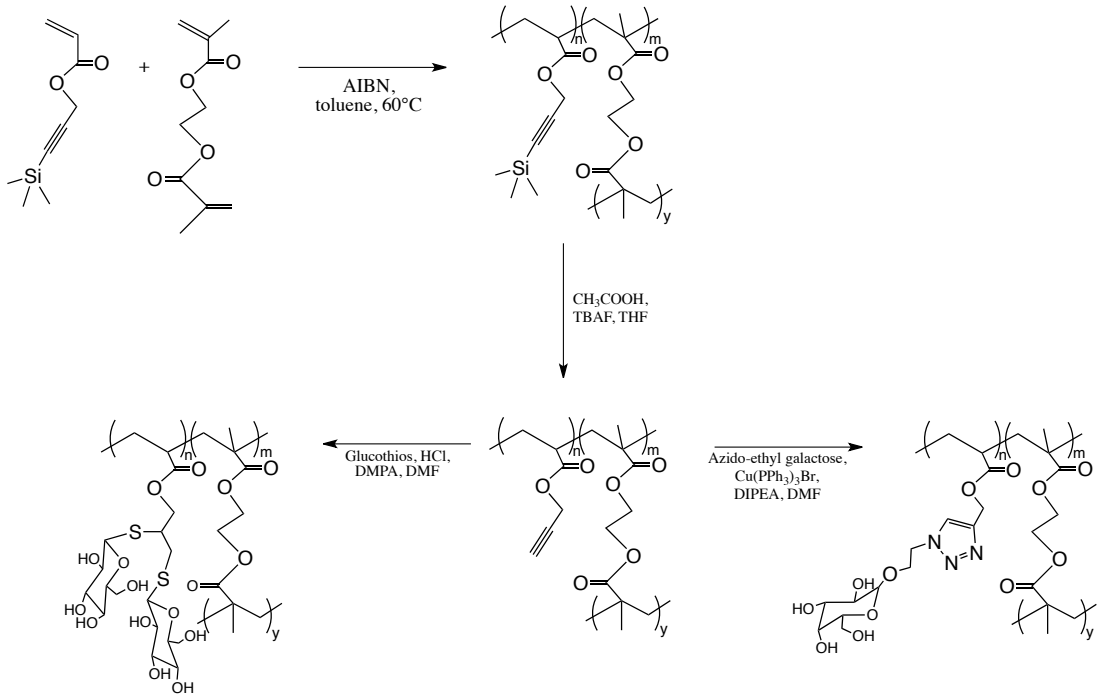

Figure II-2: Synthetic strategy for the preparation of highly branched glycopolymers using CuAAC or thiol-yne chemistry as highly efficient post-modification reaction.[63]

II.2.2 Thiol based click reactions

It has already been demonstrated that thiol-click reactions are essential in the development of new functional materials, due to the versatility and high reactivity of the thiol functionality. The combination of d-orbitals and the inherent electron density associated with sulfur, makes that thiols are classified as soft nucleophiles compared to their hard alcohol and amine counterparts. Thiols typically exhibit high reactivity with substrates prone to reactions with strong nucleophiles. Both thiolate anions and thiyl radicals are highly activated species, giving high yields under relatively mild

conditions. Thiol structures can be classified in four basic types, which are all different with respect to participation in radical and Michael addition reactions: simple alkyne thiols, thiolpropionate thiols, thiolacetate thiols and aromatic thiols (Figure II-3). In addition to the basic thiol structures, also the corresponding thiolates and thiyl radical structures are depicted. The direction of increasing pK_a of the conjugate acids, hydrogen abstractability (by radical), nucleophilicity (thiolates) and electrophilicity (thiyl radical) is indicated by arrows.

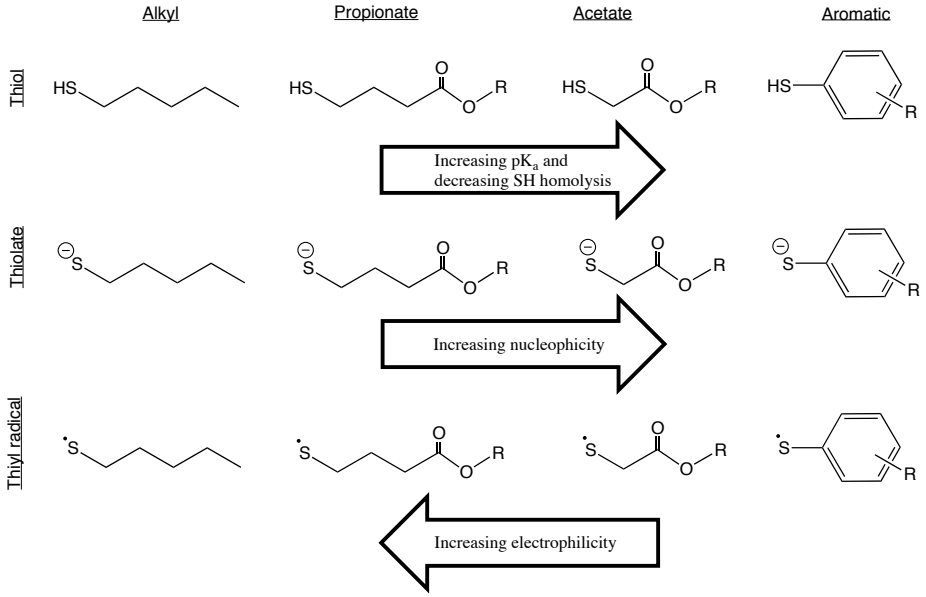

Figure II-3: Structure of various thiol, thiolate and thiyl radical types. [64]

Depending specifically on the catalyst type and methodology employed, the thiol-functionality is capable of readily participating in a large range of click reactions with a variety of functional groups: electron rich enes (radical), electron poor enes (Michael addition), alkynes (thiol-yne), isocyanates (carbonyl addition), epoxies (S_N2 ring-opening), and halogens (S_N2 nucleophilic substitution) All these reactions constitute a toolbox of thiol-based reactions which all fulfil (most of) the requirements for a click reaction (*vide supra*) (Scheme II-8).[64]

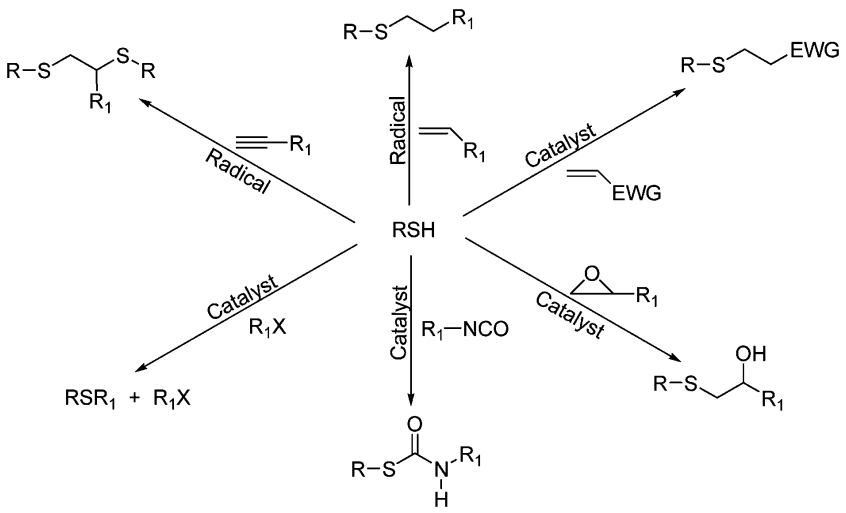

Scheme II-8: Toolbox of thiol-X click reactions. EWG = electron withdrawing group, X = Br or I, R_1= aliphatic or aromatic group and catalyst = base. [64]

A kinetic study of 13 different thiol-X click reactions using FT-IR has been performed by our group.[52] It was observed that the thiol-maleimide reaction is the fastest without need of a catalyst. For a detailed overview we refer the reader to the paper, which can serve as a useful guide for selecting the most appropriate ligation reaction.

Nevertheless, despite the enormous popularity of thiol-X reactions in polymer science, it should be denoted that some reactions are susceptible to multiple simultaneous side reactions, which violates the definition of click chemistry. The term click chemistry can only be given to reactions which are not only fast, but also are chemoselective and orthogonal to a broad range of reagent, solvents and other functional groups. Therefore, researchers have extended the original definition of click chemistry by Sharpless *et al.* with some additional requirements specifically for polymer chemistry, such as the criterium of equimolarity.[40] This implies that not all thiol-X reactions can be considered as click reactions, which is exemplified by the polymer-polymer thiol-ene conjugation limitations reported by Junkers *et al*.[65]

The thiol-X chemistry set comprises two different basic types of reactions, namely those proceeding via radical chain processes and those proceeding via nucleophilic reactions, which both will be discussed into more detail below.

II.2.2.1 *Nucleophilic thiol-X chemistry*

This group of reactions is governed by the nucleophilicity of the thiol component and proceeds with different rates depending on the substrate. When an appropriate catalyst is selected, this reactions show propensity to achieve fast rates and high conversions. As such, a strong base is needed for the initiation of thiol-epoxy, thiol-isocyanate, thiol-halogen and thiol-Michael addition reaction.

II.2.2.1.1 Thiol-epoxy click reaction

The proposed thiol-epoxy reaction mechanism is a simple nucleophilic ring-opening reaction by the thiolate anion, followed by protonation of the alcoholate anion via the protonated tertiary ammonium ion, which is initially formed by the reaction of the tertiary amine base (catalyst) and the thiol when generating the initial thiolate anion.[66] Combinations of different types of polymerization techniques with this thiol-X click reaction were already used to construct a variety of functionalized polymer architectures.[48, 67-71] It is expected that this thiol-X click type of reactions will continue to develop in the field of drug synthesis, in the synthesis of biologically active components, and in the synthesis of numerous organic synthons useful in a variety of synthetic procedures. For a more detailed overview about the mechanics, kinetics and applications of this type of click chemistry, the reader is referred to literature.[72]

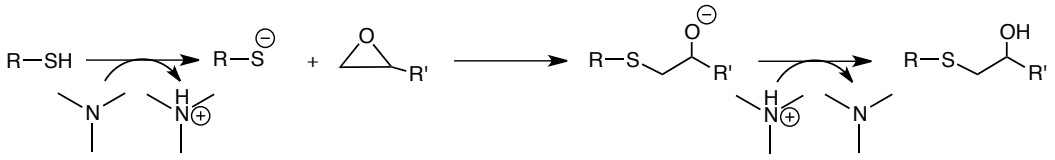

Figure II-4: Reaction mechanism proposed in literature for catalyzed epoxy-thiol ring-opening coupling reaction.

II.2.2.1.2 Thiol-isocyanate reaction

Polyurethanes are known as one of the commodity classes of polymeric structures with an extremely high versatility and they find applications in a wide range of industrial areas such as coatings, adhesives, elastomers and foams. In addition, polythiourethanes, the sulphur analogue of polyurethanes, have gained a lot of attention the last years, due to the ability to form thiourethane linkages by an efficient, high-yield click reaction with no side-products in the presence of a mild catalyst at low concentrations (Figure II-5).[73-75] Successful industrial and commercial applications of

polyurethane-based materials with interesting optical properties demonstrate the potential utility of this click reaction.[76] Moreover, thiol-isocyanate reactions have also been used to functionalize RAFT-based polymers by a straightforward sequence of aminolysis, followed by coupling of the obtained thiol with the isocyanate, allowing the introduction of a wide variety of functional groups.[46, 53]

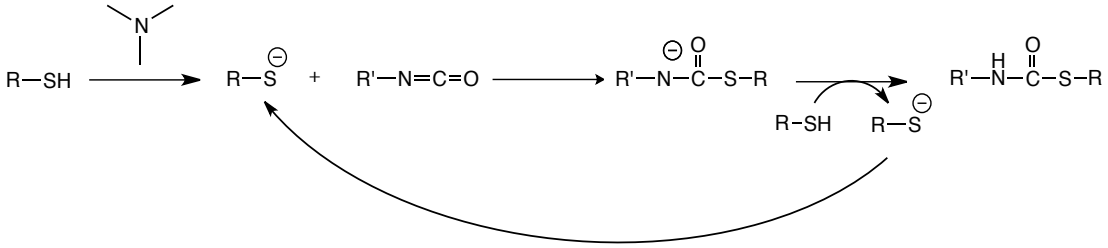

Figure II-5: Mechanism for thiol-isocyanate reaction.

II.2.2.1.3 Thiol-Michael addition click reaction

Thiol-Michael addition reactions have become an important tool in material science due to their highly modular click nature with the ability to produce highly stereospecific and regiospecific products. Generally, Michael additions involve the reaction of an enolate-type nucleophile in the presence of a catalyst to an α, β-unsaturated carbonyl, yielding thioether addition products. The catalyst can either be a base (an amine) or a nucleophile, which implies that two different pathways can be applied (Scheme II-9).[77, 78]

The base-catalyzed pathway involves the abstraction of the thiol proton by a common base (Et_3N), forming a thiolate anion together with the conjugated acid. This strong nucleophilic thiolate anion attacks subsequently the electrophilic β-carbon of the C=C bond, yielding the intermediate carbon-centred anion. Being a strong base, this anion abstracts a hydrogen from the conjugated acid, generating the thioether as the thiol-ene product while the base catalyst is regenerated in the process. The overall reaction rate and yield are influenced by several parameters such as the base catalyst strength, the pH and polarity of the solvent, the thiol pK_a and the chemical structure of ene and thiol components.

The second pathway, the nucleophile-mediated thiol-Michael addition, involves the conjugate addition of a nucleophile (amine or phosphine) to the activated C=C bond. Therefore, the reaction kinetics are dependent on the nucleophilicity of the catalyst: the higher the nucleophilicity, the more active thiolate anion intermediates can be generated. Phosphine-based nucleophiles are commonly used, as they are known to be quite reactive, even at lower catalyst loading.[79]

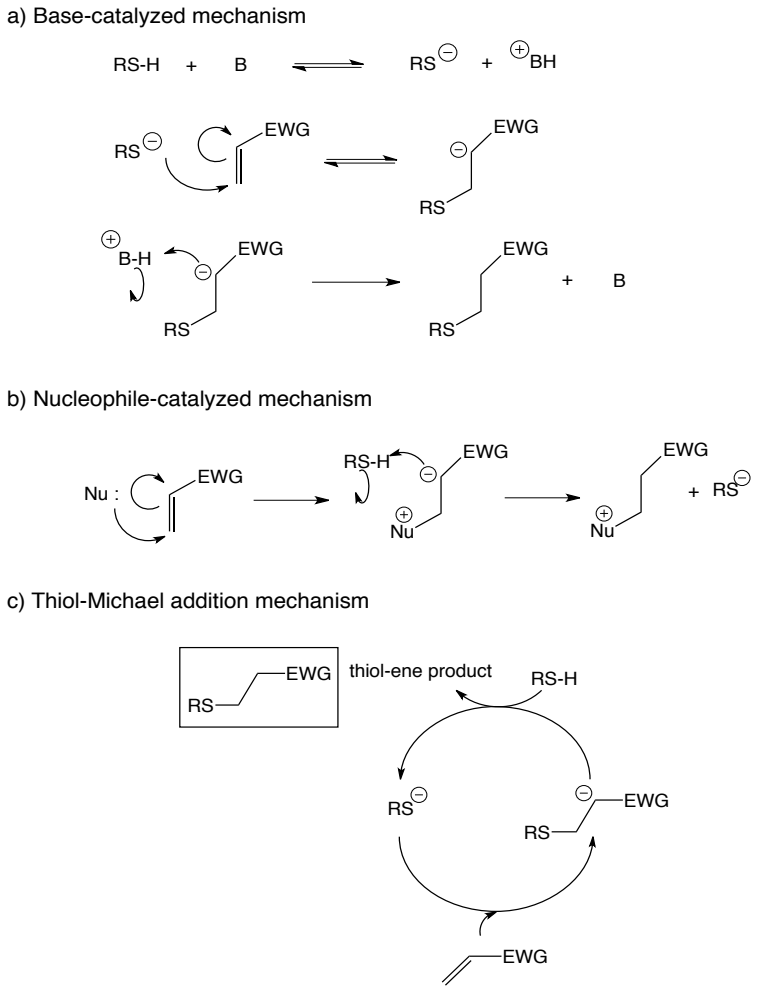

Scheme II-9: The base- and nucleophile-catalyzed thiol-Michael addition reaction mechanisms.

Thiol-Michael addition reaction are extensively used to provide an efficient route for the synthesis of linear and crosslinked polymers, dendrimers, hyperbranched polymers, and hydrogels from commercially available or easily synthesizable monomers. Lately, this type of click reaction has gained attention as post-polymerization reaction of the α-chain end of many RAFT-derived polymers, also aided by readily available electron poor ene components (Figure II-6).[77, 80-82] In addition, thiol-

Michael addition reactions are also commonly employed in the field of bio-conjugation as is exemplified by Hubbell *et al.*.[83]

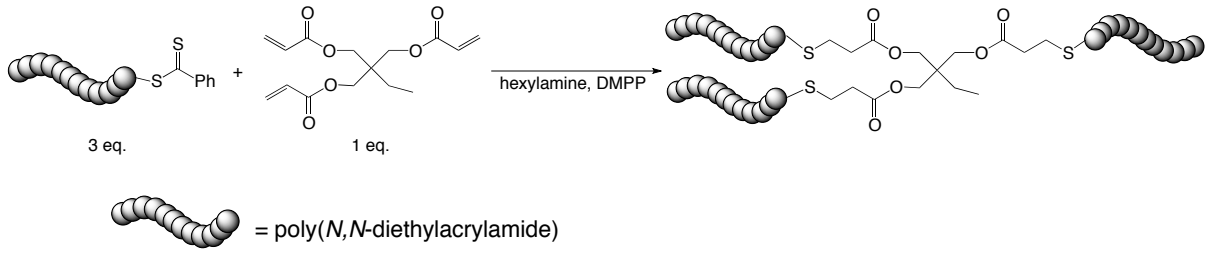

Figure II-6: Synthetic outline for the preparation of 3-arm star polymers under nucleophile-catalyzed conditions by sequentially reacting a RAFT prepared poly(N,N-diethylacrylamide) polymer via a thiol-vinyl Michael click reaction.[82]

Recently, an interesting publication was reported by Dove *et al.* on the base-catalyzed addition of alkyl thiols to electron-deficient alkynes with high levels of regioselectivity that can be directed based on the choice of catalyst and solvent.[84] Furthermore, it was shown that the single addition ene product from the thiol-yne Michael addition can be isolated with good yields (Figure II-7). Therefore, depending on the reaction conditions as well as the structures of the substrates, the electron-deficient yne can be selected to be either monofunctional (i.e. reacting with only one thiol) or difunctional.

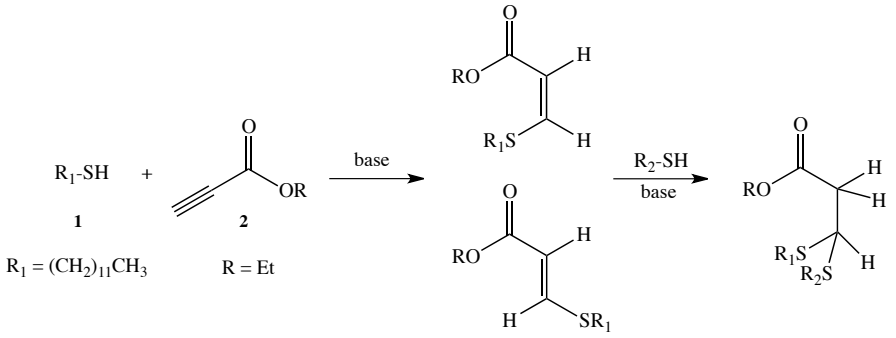

Figure II-7: Base-catalyzed thiol-yne Michael addition of dodecane-1-thiol (2) to ethyl propiolate (1).

II.2.2.1.4 Thiol-halogen click reaction

Thiol compounds have the ability to rapidly and efficiently participate in substitution reactions with reactive substrates bearing readily available leaving groups (*e.g.* halogens) resulting in the thiol-

halogen nucleophilic substitution click reaction. This click reaction is catalyzed by relatively mild organic bases such as trialkyl amine, which can be easily removed after reaction as halogenated salts. Recently, the fast displacement of reactive bromine groups with a wide variety of thiols was demonstrated by Percec *et al.*, which proves that the S_N2 nucleophilic substitution reaction can be considered as a click reaction (Figure II-8).[44] They showed that this type of click reaction could be effectively used for the divergent synthesis of dendrimers of the fourth generation.

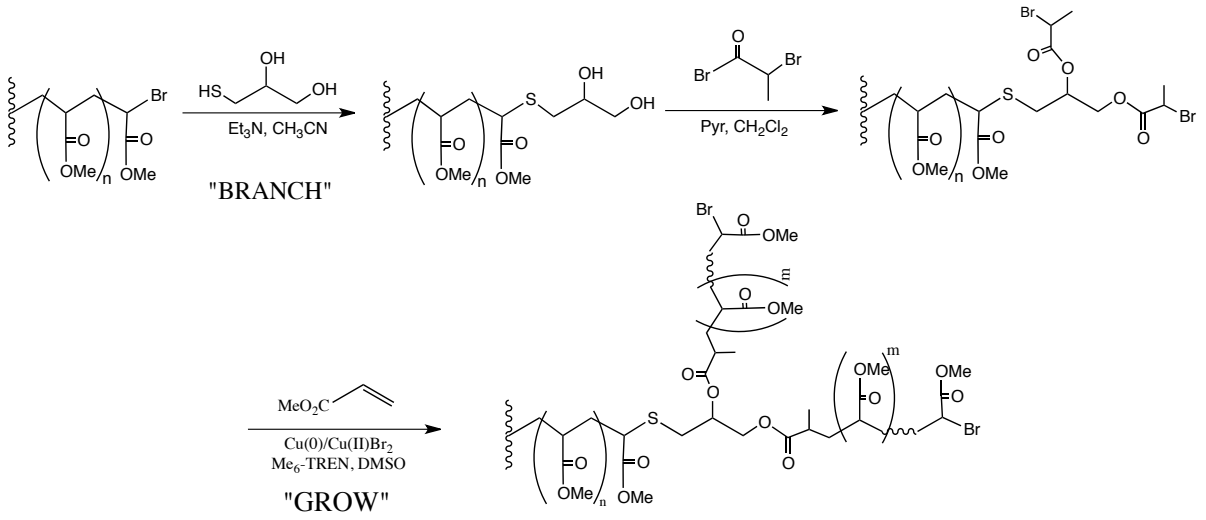

Figure II-8: Synthesis of bromo-terminated macromolecular dendrimers via thio-bromo click and acylation reactions.

Moreover, Haddleton *et al.* employed this thiol-bromo click reaction in combination with Cu(0)-LRP for the synthesis of functional multiblock glycopolymers with defined sequence.[85] However, it should be mentioned that research of Du Prez *et al.* pointed out that compared to other commonly used thiol-X chemistries, thiol-bromo reactions are relatively slow and the formation of HBr is not favourable.

Next to that, Becer *et al.* prepared glycopolymers consisting of styrene and pentafluorostyrene by a combination of NMP and the nucleophilic substitution of the *p*-fluorine atoms with thiol-glucose units. It was observed that this reaction proceeds with high yields and kinetics were relatively fast (less than 1 hour).[86]

II.2.2.2 *Thiol-radical chemistries*

The radical-mediated thiol-ene reaction was identified for the first time in 2007 by Schlaad and coworkers as a "click" reaction.[87] It was revealed that the radical addition of mercaptans to an ene functionality can be performed under sufficient (no metal catalyst needed) and mild conditions (under UV-light at room temperature) and goes to 100% conversion within a day. In fact, there are two different types of radical-mediated thiol-X processes, namely thiol-ene and thiol-yne reactions. Both of these radical-mediated processes are used in this thesis and will be described below into more detail.

II.2.2.2.1 Radical thiol-ene chemistry

Thiol-ene reactions are not a discovery of the last century but were already employed in polymer/material science for the synthesis of networks and film as been exemplified by the work of Hoyle and coworkers[82, 88-93] and Bowman *et al.*[94-96]. However, thiol-ene reactions have gained a lot of attention the last decade in other research fields due to its (often wrong) recognition as click reactions. Hoyle *et al.* pointed out in several reviews the broad scope of this click reaction to afford novel polymeric materials with specific properties as well as their historical and on-going industrial perspectives.[49, 64, 90, 97]

Mostly, radical thiol-ene reactions are photochemically induced, whereby it proceeds *via* a typical chain process with initiation, propagating, transfer and termination steps (Scheme II-10). During the initiation, a thiyl radical is generated by the irradiation of a thiol in the presence of a photoinitiator. In the next step, the propagation, this radical readily reacts with both electron rich and poor C=C bonds, generating an intermediate carbon-centred radical. This radical adduct subsequently abstracts a proton from another thiol molecule, resulting in the thiol-ene product (with mainly anti-Markovnikov orientation) and a new thiyl radical. Possible termination reactions involve typical radical–radical coupling processes. From this mechanistic viewpoint, it can be concluded that radical thiol-ene (photo)-polymerization reactions are actually radical step-growth polymerizations, which means it combines the characteristics of step-growth polymerizations with the benefits of a rapid, photo-initiated radical-mediated process.

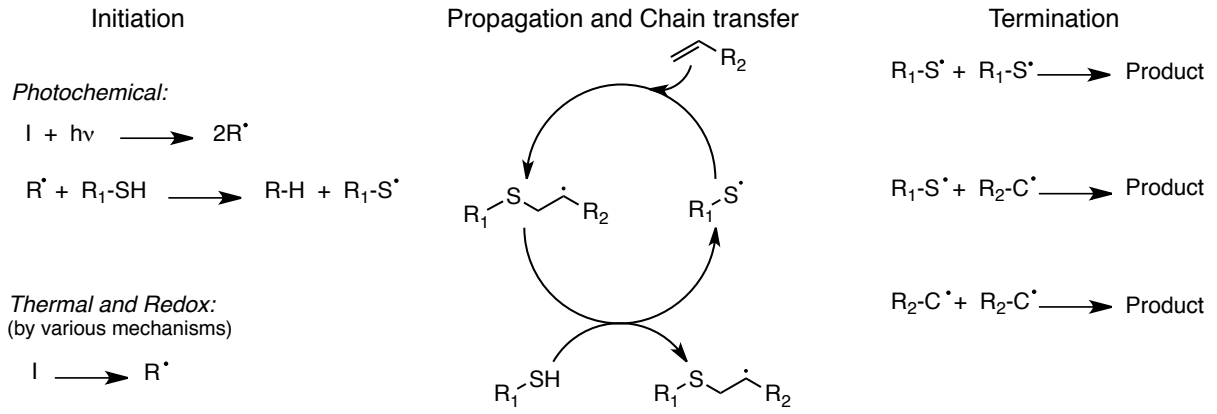

Scheme II-10: The radical-mediated thiol–ene reaction mechanism.

The reactivity of the radical thiol-ene reaction strongly depends on the chemical structure of the used ene and thiol molecules. Kinetic studies revealed that the propagation to chain transfer ratio (k_p/k_{ct}) influences the reaction rates dramatically.[94] This ratio significantly depends on the nature of the ene functional groups. It was observed that the ene reactivity falls with decreasing electron density of the double bond.[90] Despite all the advantages of this reaction, it has been observed that it is not always efficient for polymer-polymer conjugations, which favours the nucleophilic thiol-ene reactions for such applications.[65] However, many applications using radical thiol-ene chemistry are reported. As such, Du Prez *et al.* developed a synthetic platform for the preparation of various norbornenyl (Nb) containing CTAs, which after RAFT polymerization were modified with different thiols via radical thiol-ene chemistry (Figure II-9), yielding α-semi-telechelic polymers with high end-group fidelity.[98]

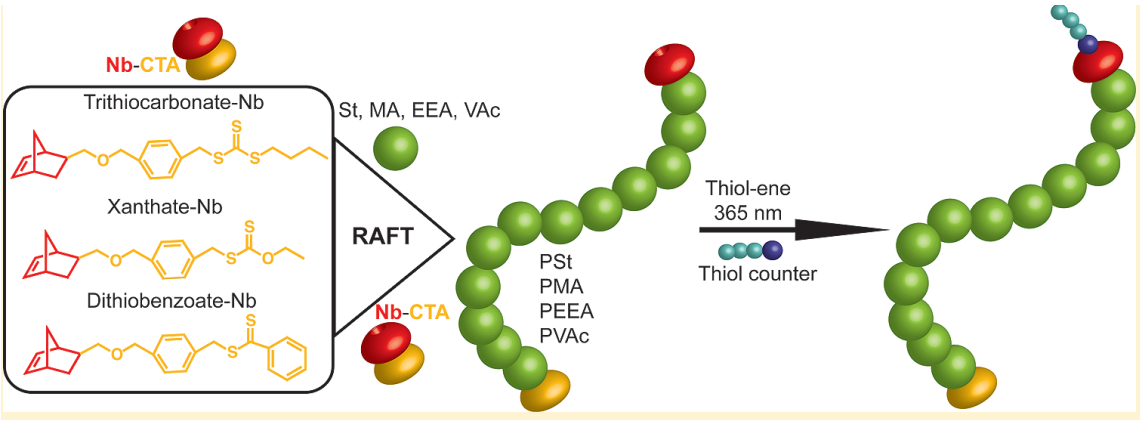

Figure II-9: Synthesis of α-semi-telechelic polymers via combination of RAFT and radical thiol-ene chemistry. *[98]*

II.2.2.2.2 Thiol-yne chemistry

Complementary to the radical thiol-ene reaction, thiol-yne radical reactions involve the coupling of two thiols to one yne bond using either a chemical radical source, UV irradiation or sunlight at ambient temperature.[51, 99] Mechanistically, the addition of the two equivalents proceeds in a similar way to the radical thiol-ene reaction (*vide supra,* Scheme II-10), yielding the 1,2-bisaddition dithioether product (Scheme II-11). The beauty of this coupling reaction is the fact that it combines the readily available building blocks of the CuAAC reaction (alkynes) with the thiol compounds of the thiol-ene chemistry to create multifunctional materials. Fairbanks and coworkers evaluated the relative rate of addition of the two thiol equivalents by applying stoichiometrically unbalanced systems, from which it can be determined that the thiol addition to the intermediate vinylthioether is approximately three times faster than thiol addition to the alkyne. As such, significant concentrations of vinylthioether should never be present in balanced formulations.[99, 100] It should be noted that double hydrothiolation also results in the generation of a chiral center that, while less important in synthetic polymer chemistry and macromolecular modification, is an important consideration in the preparation of small molecules and especially those of biological significance.

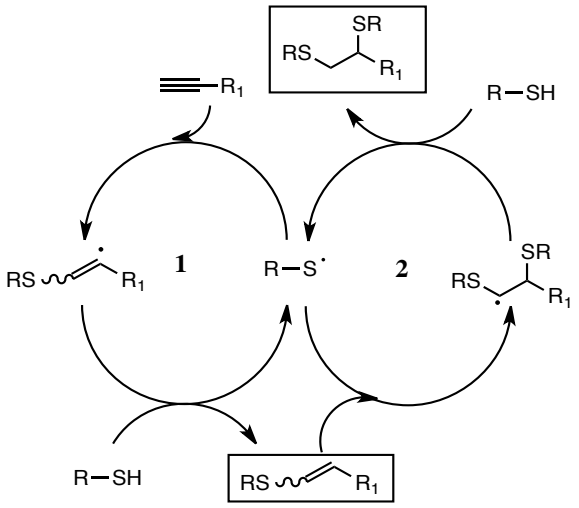

Scheme II-11: Generally accepted mechanism for the double hydrothiolation reaction, under radical conditions, of terminal alkynes.

Perrier *et al.* employed the branching character of the thiol-yne reaction for the synthesis of hyperbranched polymers (Figure II-10).[20-22] Suitable AB_2 oligomers, where A stands for a thiol functionality and B_2 for a single alkyne moiety, were prepared via RAFT and subsequently reacted with each other under UV light to yield highly functional hyperbranched polymers. It is remarkable

that the degree of branching (DB) of the hyperbranched polymers is nearly one, which implies that the alkyne functionalities either reacted twice with a thiol or remained unreacted. From this observation it can be concluded that the first addition of the thiol to the yne functionality is the rate-limiting step in this radical click reaction, while the second addition proceeds much faster. Moreover, the same group presented the preparation of branched glycopolymers whereby the sugar units are clicked on the alkyne-containing hyperbranched structure by thiol-yne chemistry.[63]

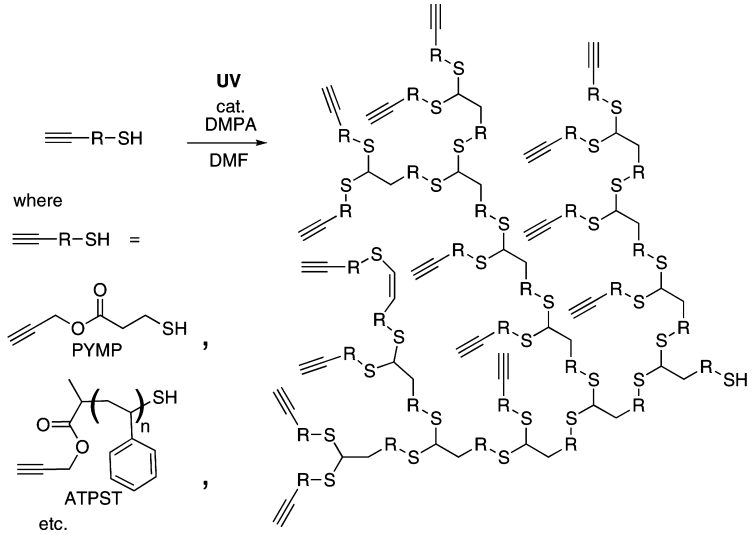

Figure II-10: Polymerization of a molecule bearing an alkyne and a thiol to give a hyperbranched polymer.

II.2.2.3 *Thiolactone as latent thiol*

As described above, the use of the robust and efficient click reactions became indispensable for scientists in different research fields. Moreover, more and more attention goes out to the metal-free conjugation and modification reactions involving thiols, or shortly thiol-X click chemistries. However, these types of click reactions show problems related with the thiol functionality such as an unpleasant smell, a poor shelf life due to oxidation reactions and low synthetic availability. A lot of research is already done to use latent thiol groups to avoid these issues.[101, 102] Undoubted, the most known protecting group for thiol functionalities is the thiocarbonylthio group of CTAs. After the RAFT polymerization, this group can be modified into a thiol upon aminolysis at room temperature in the presence of a primary amine. A recent review by O'Reilly *et al.* addresses the end-group removal and the subsequent modification of RAFT polymers.[103]

Another way to protect thiols is the conversion into disulfides. Numerous examples of the use of disulfide-containing monomers[104, 105] and initiators[106] have already been reported. Another commonly used protecting groups is methyldithiosulfonate, which is an activated disulfide.[107, 108] Theato *et al.* described the ω-end-group functionalization of RAFT polymers with sodium methanethiosulfonate resulting in ω-alkyne functionalized polymers through the formation of a disulfide linkage.[108] Also ATRP polymers have already been modified with methanethiosulfonate groups as they easily can undergo nucleophilic substitution with the halogen end-group. Davis and coworkers made use of this reactivity to create polymers with latent thiol groups.[107] (Figure II-11) Other frequently used methods to protect thiol groups are as their corresponding thioesters[109-111] and thioureas[112] or by the use of photolabile latent thiols[113, 114].

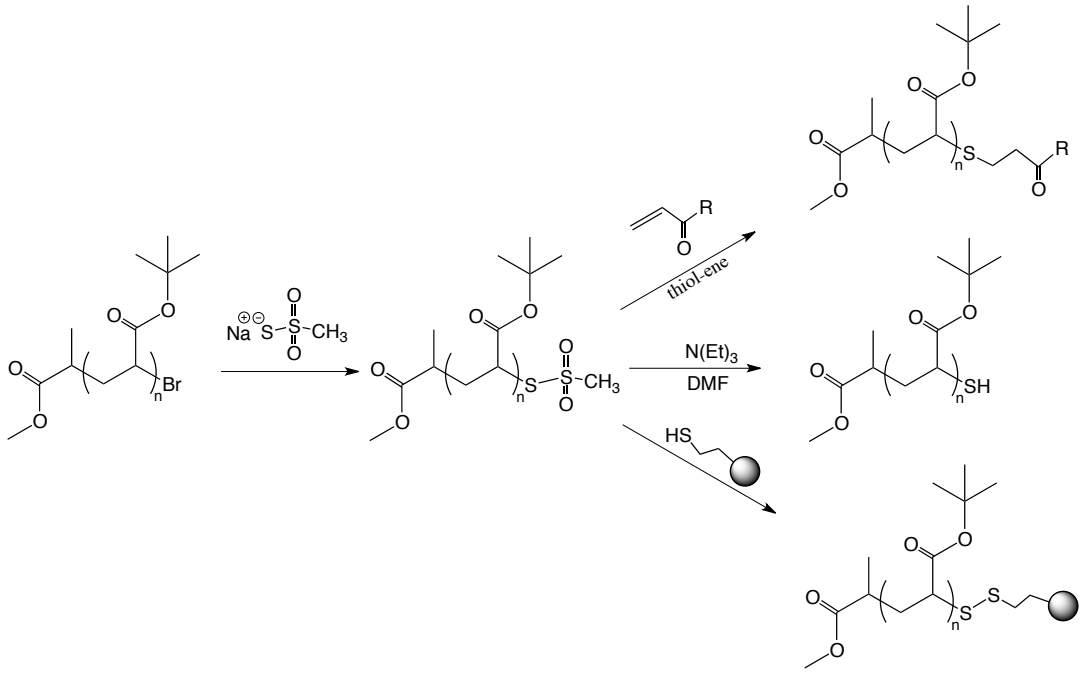

Figure II-11: Chemical modification of a halide end-group using sodium methanethiosulfonate and its post-modification.

Recently, our group developed a new concept in polymer science, which makes use of a thiolactone moiety (a cyclic thioester) as latent thiol functionality. Thiols are generated by nucleophilic ring-opening (aminolysis) of the thiolactone moiety and subsequently reacted with a thiol 'scavenger' in an efficient one-pot multistep process (Scheme II-12). The beauty of this concept is that as the thiol is released, a new functionality, originating from the amine, is introduced in the structure.

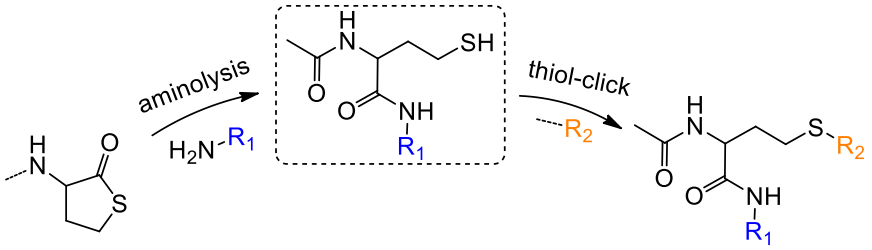

Scheme II-12: A thiolactone as latent thiol functionality: the thiol is released by nucleophilic ring-opening followed by a thiol-X reaction.

This simple, efficient and modular synthetic process is shown to be a relevant extension of the popular thiol-X chemistries and is extensively used by our group and other groups world wide in several different strategies. For example, monomers containing both a thiolactone unit and a double bond are synthesized, which can be seen as A'B type monomers as the thiolactone can be considered as a precursor for a thiol functionality. Ring-opening upon aminolysis and subsequent UV-curing generates novel polymeric architectures (linear polymers or networks, depending on the amine used) (Figure II-12).[115] Moreover, linear copolymers with pendant thiolactone groups were prepared via RAFT and NMP.[116] The ring-opening upon aminolysis and subsequent thiol-click modification demonstrated the successful extension of this concept. For more papers dealing with this new concept, the reader is referred to literature.[117-122]

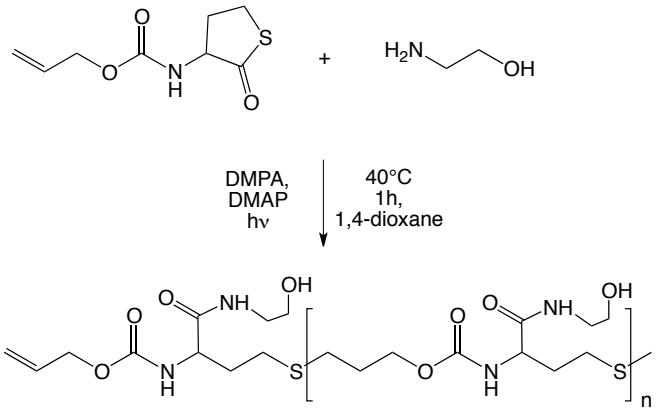

Figure II-12: Stepwise photopolymerization of the Alloc-Thiolactone monomer in a one-pot process yielding a linear polymer with a polythioether/polyurethane backbone and pendant hydroxyl groups.

II.3 Hyperbranched polymers

II.3.1 Introduction

Macromolecules with several architectures are already successfully prepared going from linear polymers to very complex macromolecular structures such as dendritic brush-like polymers. The last decade, a lot of attention went out to the synthesis and applications of dendritic macromolecules, due to their unique properties. Dendritic polymers can be described as highly 3D branched macromolecular structures with a functional surface. The most known classes of dendritic polymers are dendronized polymers, dendrigrafts, dendrimers and hyperbranched polymers (Figure II-13).[123] Tomalia and coworkers started this topic in 1980 with the synthesis of the first dendrimers.[124]

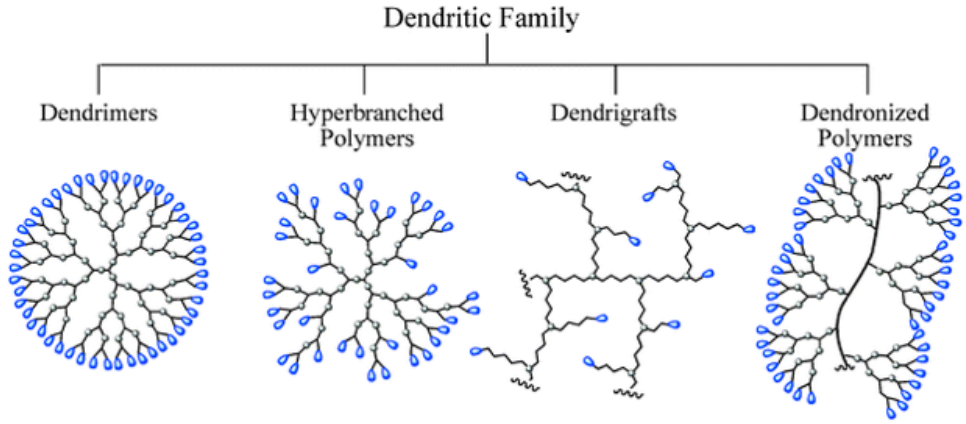

Figure II-13: The four most important classes of dendritic macromolecular structures: dendrimers, hyperbranched polymers, dendrigrafts and dendronized polymers.[123]

Hyperbranched polymers (HBP) are a special type of dendritic polymers and have as common feature their high branching density.[125, 126] They are often prepared via a one-pot synthesis without protecting steps, which limits the control over the molar mass and structure resulting in heterogeneous products with a certain distribution in molecular weight and branching degree. These properties distinguish HBP from dendrimers, which are monodisperse structures with perfectly branched architectures. The last decade, a lot of attention went out to the synthesis and the use of both HBP and dendrimers as they possess some interesting properties such as high number of functional end-groups and a relatively low viscosity as compared to their linear counterparts. However, the challenging synthesis steps (i.e. the iterative protection and deprotection steps) needed for the preparation of dendrimers make HBP much more attractive for large-scale applications (e.g. coating or resins) due to their easy and reasonable synthesis routes.[127]

II.3.2 Synthesis methodologies

The first reports of hyperbranched polymers originate from the 19th century dealing with the synthesis of resins made out of tartaric acid (A_2B_2 monomer) and glycerol (B_3 monomer), followed by the reports on the reaction of phthalic anhydride (latent A_2 monomer) or phthalic acid (A_2 monomer) with glycerol.[128] Nowadays, several synthetic routes can be applied for the preparation of hyperbranched polymers. Two main categories can be distinguished; namely the single-monomer methodology (SMM) and the double-monomer methodology (DMM) (Scheme II-13). Using the first methodology, hyperbranched structures are prepared by the polymerization of AB_n, AB* or latent AB_n monomers while in the second strategy two monomer types are combined.[126]

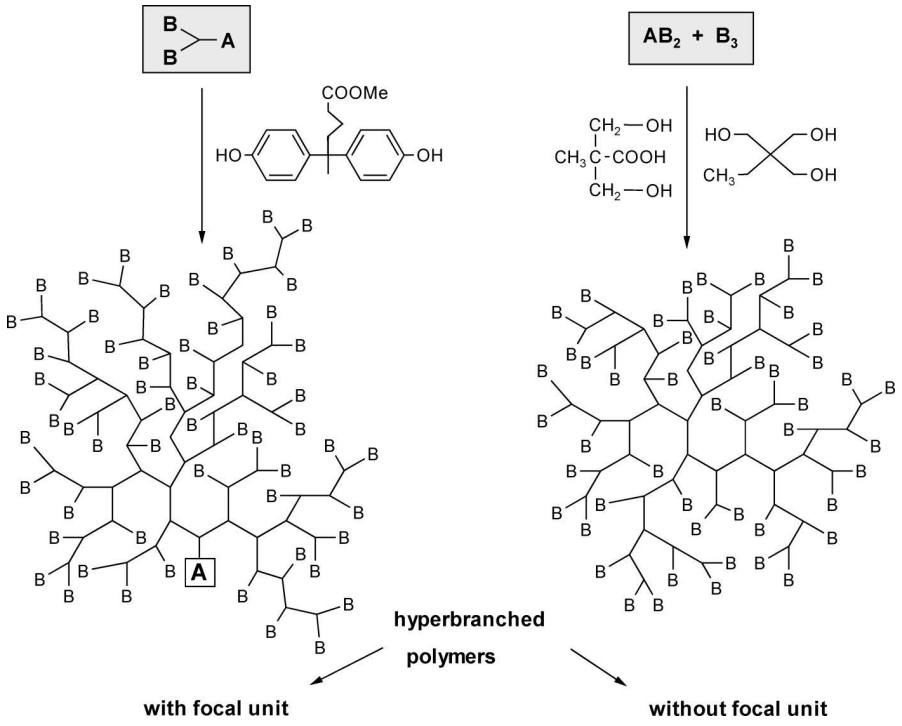

Scheme II-13: Schematic representation of the synthesis of hyperbranched polymers through the AB_x and $AB_x + B_y$ approach ($x \geq 2$; here, 2; $y \geq 3$; here, 3).

II.3.2.1 *Single monomer methodology (SMM)*

Four specific reaction types can be distinguished in the SMM approach according to their reaction mechanism: (1) step-growth polycondensation of AB_x monomers (the classical Flory approach); (2) step-growth self-condensing vinyl polymerization (SCVP) of AB* monomers; (3) ring-opening multibranching polymerization (ROMBP) of latent AB_x monomers and (4) proton-transfer polymerization (PTP) to form polysiloxanes or polyesters with epoxy or hydroxyl end-groups.

The most commonly used technique is the polycondensation of an AB_n monomer ($n \geq 2$), whereby A selectively reacts with B without side reactions and all the B functionalities having the same reactivity. The reaction involves the typical characteristics of a step-growth polymerization of multifunctional monomers. After polymerization, the HBP is built up out of dendritic (D) (fully reacted B functions), terminal (T) (no reacted B functions) and linear (L) (partially reacted B functions) units and one focal point (an A functionality) (Figure II-14). The use of AB_2 monomers is the most frequently applied variant of this approach and was already applied for the synthesis of many different hyperbranched macromolecular structures (e.g. hyperbranched polyphenylenes, polyethers, polyesters, polyamides, polycarbonates). Especially the synthesis of highly branched polyesters was favoured due to the readily availability of the monomers. Recently, Perrier *et al.* prepared AB_2 oligomers via RAFT and subsequent aminolysis, which were subsequently reacted under UV-irradiation yielding hyperbranched polymers (Figure II-10).[21, 22] Next to that, occasionally, AB_3, AB_4 and even AB_6 monomers were reported for the preparation of hyperbranched macromolecules. Examples are given in the work of Hayes[129], Yan, Gao and Frey[126, 127, 130], Fréchet[124, 131], Voit[125] and many more.

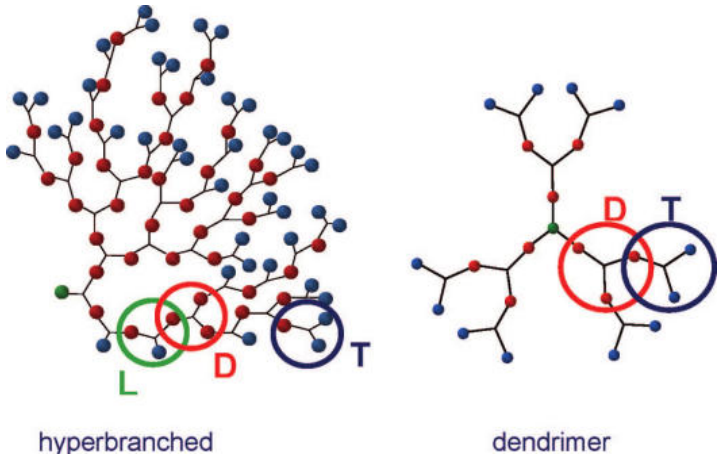

Figure II-14: Schematic representation of the dendritic polymeric unit of a hyperbranched structure compared to dendrimers.[125]

Another approach for the synthesis of hyperbranched polymers (the self-condensing vinyl polymerization (SCVP)), first reported by Fréchet and coworkers in 1995[132], uses a vinyl monomer which contains an initiator group ('inimer' = initiator + monomer)[133]. Chain growth is achieved by the double bond of the monomer, while addition of the initiator to the double bond ensures the step-growth polymerization resulting in hyperbranched macromolecular structures. This one-pot synthesis approach allows branching in each unit, which allows a degree of branching up to 50%. This

SMM methodology to prepare hyperbranched polymers was reported for the first time by Walter and co-workers in 1993.[134] The extension of this methodology to other chain-growth polymerization techniques, such as controlled radical polymerization reactions did not take a long time.[135-138]

Ring-opening multibranching polymerization (ROMBP), another SMM method, relies on the same principle of inimers. In this case, the monomer function is a heterocyclic group and a cationic or anionic mechanism is applied. Hyperbranched polyamines[139], polyethers[140, 141] and polyesters[142] have been prepared *via* this technique.

II.3.2.2 *Double monomer methodology (DMM)*

The DMM can be classified into two main subclasses based on the selected monomer pairs and different reaction pathways.[126] The first most classical approach includes the polymerization of A_2 and B_3 monomers and has been applied to synthesize three main polymer structures including polyamides, polycarbonates and polyureas.[129] Combination of 'A_2+B_3'methodology with the basic SMM synthetic principles results in another DMM, called the couple-monomer methodology (CMM) (Figure II-15). This approach is based on the *in situ* formation of AB_n intermediates from specific monomers due to the non-equal reactivity of the different functional groups.[130, 143] Different types of hyperbranched polymers, such as poly(sulfone amine)s, poly(ester amine)s and polyureas are synthesized via this technique.

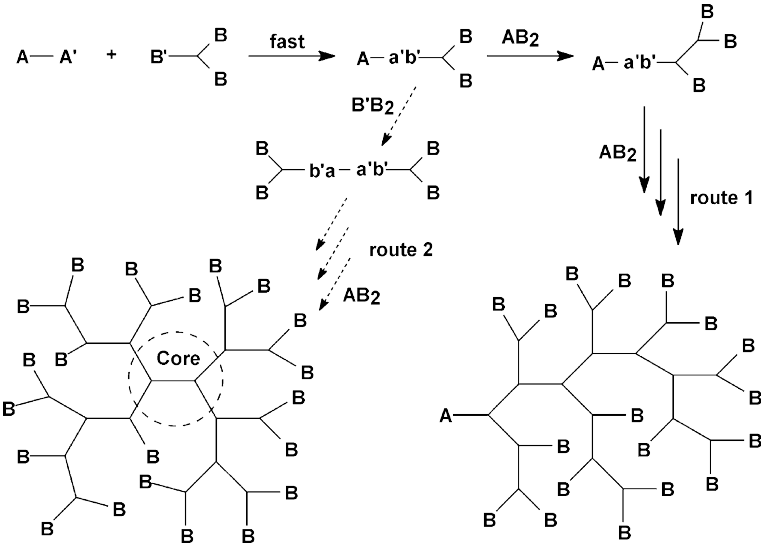

Figure II-15: 'A_2+B_3' approach to hyperbranched polymers as a typical example for the basic principle description of couple-monomer methodology.

II.3.3 Structural characterization

The high attention hyperbranched polymers have received the last 20 years is the result of their new and specific characteristics, which strongly influence the properties and consequently the application possibilities of these macromolecular structures. Next to the synthesis of these structures, research is done to characterize, understand and theoretically describe the properties of the HBP in order to have a better understanding of their structure-property relationships. It was shown that they possess different solution and bulk properties compared to their linear analogous.[144, 145]

II.3.3.1 *Degree of branching*

The degree of branching (DB) is one of the most important parameters of hyperbranched structures since it determines several physical properties of the polymers such as the viscosity, chain entanglement and glass transition temperature (T_g).[146] The DB is namely directly correlated with the density of the structure and with the number and location of the end-groups. Moreover, it is the most commonly used parameter describing the average architecture of highly branched structures. As is depicted in Figure II-14, the perfectly branched dendrimers only possess dendritic (D) and terminal (T) units, while the randomly branched HBP structures also incorporate linear units. A definition for the DB of hyperbranched polymers synthesized by polycondensation of AB_2 monomers was proposed by Fréchet *et al.*. [147]

$$DB_{Fréchet} = \frac{T+D}{T+D+L}$$

This definition has been frequently used for the determination of the DB via nuclear magnetic resonance (NMR) measurements. It is clear that the branching degree for dendrimers is equal to one as there are no linear units present. Even for fully linear polymers a DB > 0 is observed due to the presence of, in most cases, one or two end-groups. Most reports dealing with HBPs prepared from AB_2 monomers have DBs close to 0.5. Another definition, which is also valid for low molar mass regions, is given by Frey and coworkers[148] and the group of Müller[146].

$$DB_{Frey} = \frac{2D}{2D+L}$$

Determination of the DB is mostly done by making use of the powerful tool NMR. Fréchet *et al.* reported the synthesis of a hyperbranched polyester achieved by the self-condensing polymerization of an AB_2 monomer (3,5-bis(trimethylsiloxy)benzoyl chloride).[147] By characterization of a series of model compounds via ^{1}H NMR and ^{13}C NMR, they were able to assign the characteristic peaks of the dendritic, linear and terminal units of the hyperbranched polyester and thus to determine the branching degree. For hyperbranched polymers containing a heteroatom, ^{15}N, ^{19}F, ^{29}Si and ^{31}P NMR spectroscopies can also be used to determine the DB.[149-151] Recently also 2D NMR has been used to calculate the DB values of some complicated hyperbranched polymers as it resolves overlapping peaks into several individual peaks.[152, 153] Next to that, Hawker and Wooley proposed another approach to measure the DB of degradable systems via NMR spectroscopy.[154, 155] After modification of the functional groups, the polymer is degraded into the dendritic, linear and terminal subunits from which the DB can be calculated.

Moreover, the DB could be altered or even tuned to some extent.[156] Five different methods could be applied to increase the DB:

- The enhancement of the reactivity of the functional groups associated with linear units [157];
- The slow addition of multifunctional core molecules during the polymerization process[158];
- The use of dendrons without linear units for polycondensation polymerization[159];
- Several post-modification reactions[160];
- The use of an appropriate catalyst [161].

These methods make it possible to synthesize HBP with a degree of branching higher than 0.5, sometimes even close to 1. On the other hand, by copolymerization of AB_2 and AB monomers with different feed ratios, by changing the conditions or by host-guest inclusion, the DB can be tuned to certain values. As stated above, the DB stands in close relationship with several polymer properties, which consequently can be controlled to a certain extent through adjusting the DB. For

example, Yan *et al.* discovered that the T_g decreased practically linearly and the degree of crystallization exponentially with an increase of DB of poly(3-ethyl-3-(hydroxymethyl)oxetane).[162, 163]

II.3.3.2 *Molar mass and molar mass distributions*

Next to the DB, molecular weight and dispersity of hyperbranched polymers are important parameters. Because of the statistically driven polymerization process, hyperbranched polymers based on AB_n monomers show very broad molar mass distributions. It is observed that for HBP, the higher the degree of polymerization the broader the molar mass distribution. This broadness is strongly influenced by the reactivity of the functional groups, using slow monomer addition methods, or adding a multifunctional core molecule. The determination of the molar mass and molar mass distribution of hyperbranched polymers is not straightforward because of their increased overall molecular density compared with their linear analogues. Using size exclusion chromatography (SEC) with linear standards can thus lead to strong deviations from the actual values. When coupled to static light-scattering detector (MALLS, multi-angle laser light-scattering) SEC gives the absolute molar mass values, also for complex macromolecular architectures.[125, 126]

II.3.4 Physical properties

The key factor that made hyperbranched polymers highly successful, both in industry and academia, relies on their interesting set of chemical and physical properties such as a low bulk and solution viscosity which strongly depends on weight average molecular weight and DB. The correlation between the intrinsic viscosity [η] and the viscosity-average molecular weight M_v is given by the Mark-Houwink equation (eq II.3). This relationship, which is depicted in Figure II-16, offers an indirect approach for the evaluation of the structure of complex macromolecular architectures. The intrinsic viscosity of a HBP is lower than that of its linear analogues, but higher than that of dendrimers. Moreover, the Mark-Houwink exponent α of hyperbranched polymers is much lower due to the compactness and fewer chain entanglements.

$$[\eta] = KM_v^{\alpha} \qquad (II.3)$$

The values of the Mark-Houwink constants, K and α, depend on the specific polymer-solvent system. In general, the α of a randomly coiled linear polymer is in the range 0.5 to 1, while for hyperbranched polymers it is typically smaller than 0.5.[164, 165] This means that branching reduces the viscosity of the solution.

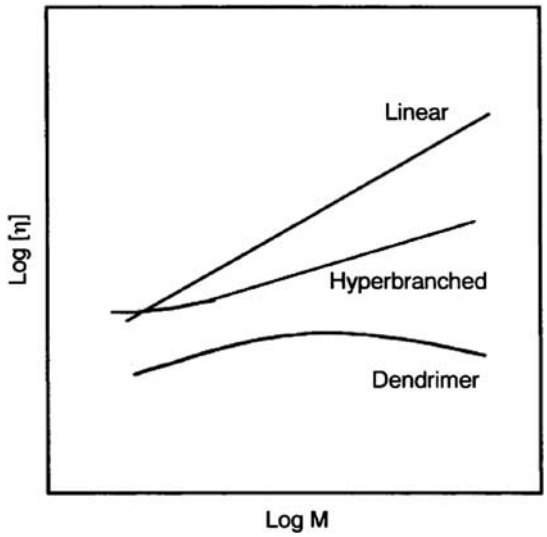

Figure II-16: Schematic plots for the relationship between the intrinsic viscosity and molecular weight for various polymer topologies.

Next to the viscosity, also the thermal properties of polymers are strongly influenced by branching. It is known that crystallization and melting behaviour are closely related to their chain architecture. It was shown that the degree of crystallization reduces with increased degree of branching.[163] The extent of this effect is mainly determined by the branching topology and length of the polymer chain between the branching units. On the other hand, glass transition temperature (T_g) in general depends on the free volume and the chain mobility of the polymer. As HBP differ from linear polymers in architecture, amount of end-groups, compactness and crystallization ability, the T_g is altered as well. As a consequence of the decrease in molecular mobility with the degree of branching and branching density, an increase of the T_g is observed.[162] Nevertheless, the effect of the end-groups on the T_g of hyperbranched polymers should also be taken into account. Hawker and coworkers prepared a series of hyperbranched poly(ether ketone)s with different functional end-groups and concluded that the thermal properties heavily depended on the nature of these end-groups.[151]

II.3.5 Applications

Within different sectors, there is a huge demand for polymeric materials with a high degree of functionalization and specific properties, depending on the end-groups. Typical examples of such materials are dendrimers, which due to their highly compact structure and high surface functionality since their invention in 1978, were investigated for applications in medicine, medicinal chemistry, catalysis, coatings and many others. However, despite the more than 15,000 publications and patents published on dendrimers, and 37 years of development since their invention in 1978, there is currently only one dendrimer-borne commercial application, namely a pharmaceutical anti-HIV-agent VivaGel®.[166]

On the other hand, an extensive patent and market study revealed that today hyperbranched polymers have been widely used in different applications because of their analogue properties obtained through a simple one-pot synthesis. Companies such as Perstorp[167] (coatings), Evonik[168] (additives and carriers), DSM[169] (coatings and resins) and BASF[170] (coatings and crosslinkers) have already marketed different varieties.[171] Their easy synthesis and the fact that certain features, such as their solubility of HBP can be controlled quite effectively, make them applicable in different areas.

The excellent flow and processing properties of HBPs have made them very attractive as base for various coatings, such as powder coatings, high solid coatings, flame retardant coatings and barrier coatings for flexible packaging[172], depending on their solubility, viscosity and abundant functional groups. The first HBPs studied in this field were aliphatic polyesters based on bis-hydroxymethyl propionic acid (BHMPA) which are commercialized by Perstorp under the name Boltorn™ (Figure II-17).[173] Next to that, DSM commercialized in 1999 poly(esteramides)s for coating and resin applications under the trade name Hybrane™ (Figure II-17).[174] Further modification of these structures with a wide range of reactive groups such as acrylates, methacrylates, and epoxy functionalities, allows their use in thermosets, resins or additives.

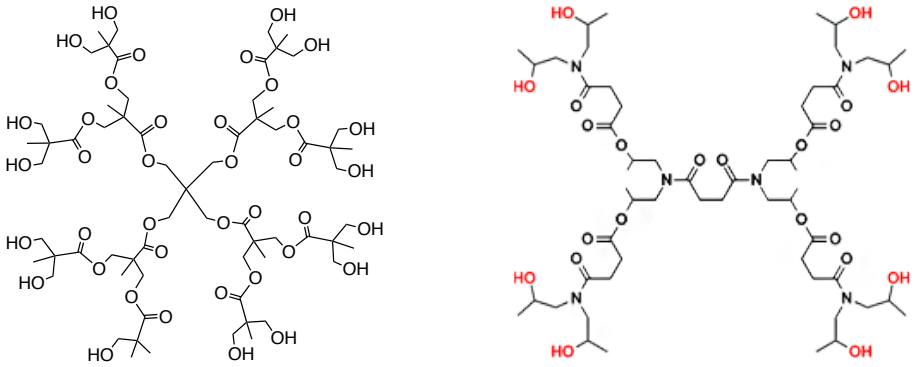

Figure II-17:Structures of Boltorn (left) and Hybrane (right); two commercially available hyperbranched structures.

The use of hyperbranched structures as gene delivery carriers of drug delivery systems, either by covalent or non-covalent drug loading, has been studied extensively.[126, 175] As carrier, both the interior as the peripheral functional groups of the hyperbranched polymers can be applied to fix bio-objects or guest molecules. For example, it was found that hyperbranched poly(ethyleneimine) (PEI) has certain advantages over its linear analogues. The densely branched structure ensures stronger complexation while the higher dispersity may increase the transfection efficiency.[176, 177]

Because of their tuneable solubility and exceptional processability, conjugated hyperbranched polymers such as polythiophene and poly(phenylenevinylene) (PPV) are extremely well-suited as novel optical, electronic and magnetic materials.[178] Li *et al.* described the "A_2+B_3" synthesis of partially conjugated hyperbranched PPV starting from the oligomer distrylbenzene, which possesses a high fluorescence quantum yield. Properties, such as a high thermal stability, a high T_g and high fluorescent quantum yield were observed and found to be better than the fully conjugated hyperbranched PPV.[179] The group of Ludwigs investigated the opto-electronic properties of hyperbranched polythiophenes p3T and p4T synthesized via a straightforward one-pot procedure by the oxidative coupling of branched trithiophene and tetrathiophene monomers with $FeCl_3$ (Figure II-18).[180] It was found that these materials are applicable in organic solar cell devices as the HOMO and LUMO levels are shifted towards lower energy levels compared to the linear P3HT.

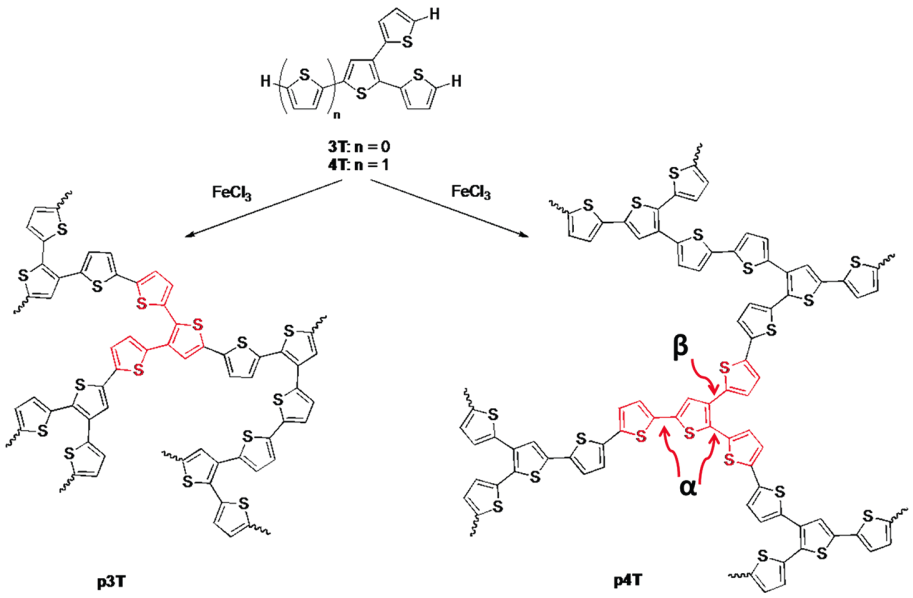

Figure II-18: Synthesis of p3T and p4T via oxidative coupling with $FeCl_3$; Visualization of α- and β-conjugation in hyperbranched polythiophenes.

Hyperbranched polymers containing ethylene glycol (EG) units have been synthesized and employed as novel polymeric electrolytes or ion-conducting elastomers. Hawker and coworkers prepared hyperbranched poly(ether ester)s containing linear EG units with varying lengths by polymerization of AB_2 monomers. It was seen that complexes of these HBP with lithium perchlorate salt behave as polymeric electrolytes and the ionic conductivity increases with both temperature and concentration of Li^+.[181]

The use of HBP as nanomaterials for host-guest encapsulation and the formation of organic-inorganic materials is another important application of the dendritic structures. Amphiphilic hyperbranched polyglycerols consisting of a hydrophilic core and a hydrophobic shell were prepared via the partial esterification of branched prepolymers with fatty acids.[182] Different water-soluble dyes were subsequently irreversibly encapsulated in the core via phase transfer process, confirmed via UV-Vis measurements.

Based on their unique properties HBPs can also be used as toughеners for thermosets, curing, crosslinking or adhesive agents, compatibilizers, dispersants and rheology modifiers. For a more detailed overview of all applications, the reader is referred to a review on HBPs.[125, 126]

II.4 Glycopolymers

The last decade, there has been an increasing interest in the development of glycopolymers, synthetic sugar-containing macromolecules, because of their unique recognition properties, such as the binding interaction with lectins. These specific interactions make glycopolymers applicable in fields like drug and gene delivery. Controlled radical polymerization techniques such as RAFT, ATRP and NMP are mainly used to synthesize those polymers as they provide control over the reaction and can be combined with most click chemistries.[183]

II.4.1 Introduction

Natural saccharides (carbohydrates) are already a hot research topic in many fields for different decades. It has been shown that sugars play an important role in many biological processes which led to the development of new fields, like chemical glycobiology. The development of the automatic synthesis of polysaccharides made it possible to prepare synthetic polysaccharides which resulted in the development of carbohydrate-vaccines, drug delivery systems but also to applications in tissue engineering.[184] It was found that glycopolymers exhibit specific interactions with lectins and proteins. This interaction proved to be much stronger compared to the equivalent specific interaction between a single carbohydrate unit and a lectin. This effect of enhanced interaction by the presence of multiple carbohydrate units is called the 'glycocluster effect'. This multivalent interaction feature has inspired many polymer scientists to develop various functional glycopolymers and to investigate their interaction properties with lectins. The strategies in the glycopolymer synthesis are generally carried out as either direct polymerization of glycomonomers or by post-glycosylation of preformed polymers.[185, 186]

II.4.2 Synthesis methodologies

Combination of living polymerization and click chemistry is undoubtedly the most commonly followed approach for the synthesis of functional glycopolymers. Different types of architectures, from linear to dendritic glycopolymers with different functional groups, molecular weight and density are already reported and discussed in several reviews by *inter alia* Stenzel, Haddleton and

Cameron.[183, 185-188] The most common synthesis strategies of glycopolymers developed the last decade are discussed in the paragraphs below.

II.4.2.1 *Glycopolymers from the direct polymerization of glycomonomers*

The synthesis of glycopolymers via the direct polymerization of carbohydrate-containing monomers can be carried out by many different polymerization techniques, including free radical polymerization (FRP), ring-opening polymerization (ROP), ring-opening metathesis polymerization (ROMP) and controlled radical polymerization (CRP). In this thesis only the latter polymerization strategy will be discussed while for the other strategies, the reader is referred to the interesting review of the group of Stenzel and Haddleton *et al.*.[185, 187]

NMP was the pioneer of the CRP techniques for the preparation of glycopolymers, but has only been applied a few times, due to the required high temperatures. The group of Stenzel reported in 2009 the copolymerization of methacrylate based monomer, 2-(2',3',4',6'-tetra-O-acetyl-β-D-galactosyloxy)ethyl methacrylate (AcGalEM) and styrene (10%) which was done at lowered temperature of 85°C. Subsequent chain extension with styrene resulted in block copolymers that were able to self-assembly into glyco-micelles or honeycomb structured films which were both tested on their bioactivity with the PNA lectin (Figure II-19).[189]

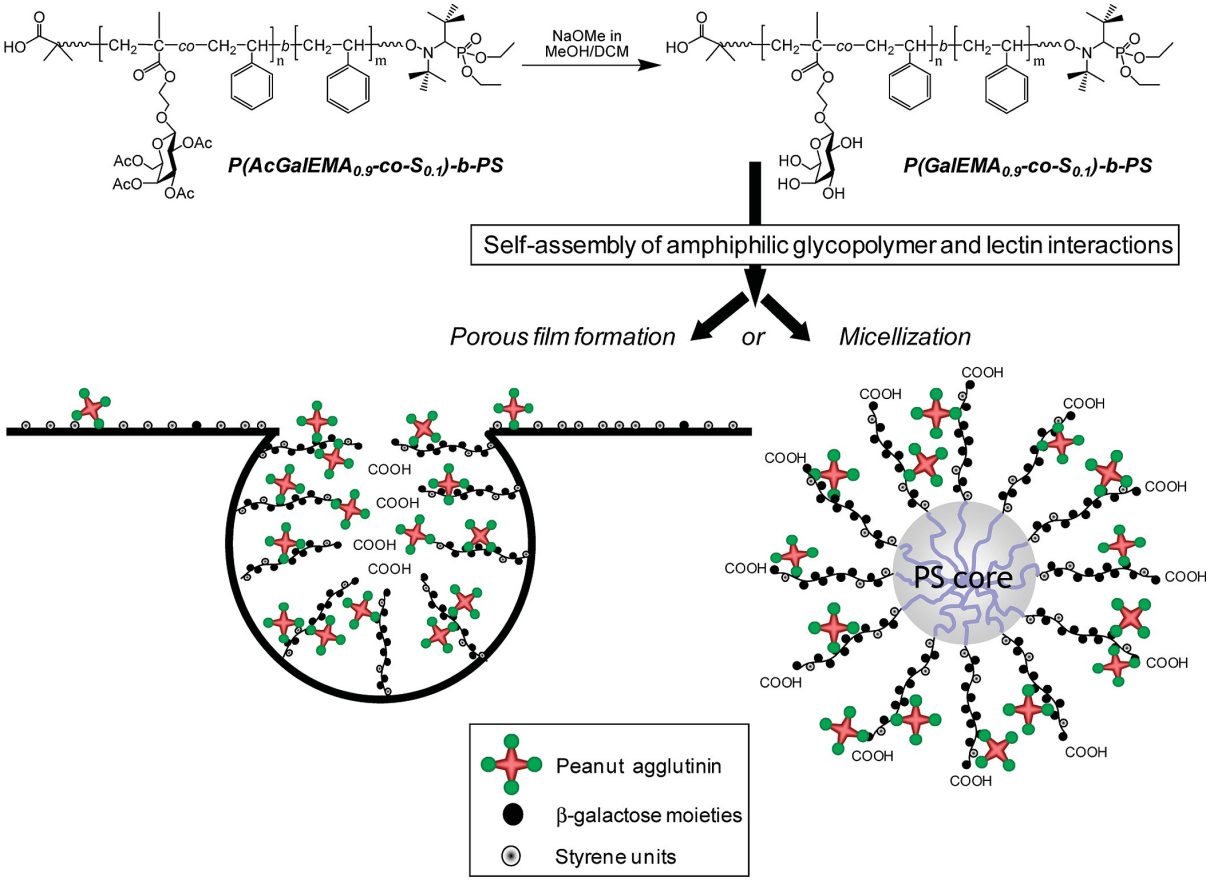

Figure II-19: Schematic approach to micelles with glycopolymer shell based on β-galactose moieties and honeycomb structured porous films with glycopolymer enriched inside the pore; as materials in solution and in solid state that can selectively recognize peanut agglutinin, PNA. [189]

The direct polymerization of glycomonomers via ATRP was first reported in 1998 by the group of Fukuda who polymerized protected glycofuranose monomers in veratrole at 80°C in the presence of the CuBr/bipyridine catalyst.[190] Generally, ATRP polymerizations of unprotected glycomonomers are performed in polar solvents such as DMSO and DMF for solubility reasons of the sugar monomers. Extensive research was done by Haddleton *et al.* and the group of Becer on the synthesis of glycopolymers *via* the combination of ATRP and click chemistry (Figure II-20).[186] A variety of carbohydrate monomers was prepared by CuAAC and subsequently polymerized, yielding well-defined glycopolymers with narrow dispersity.

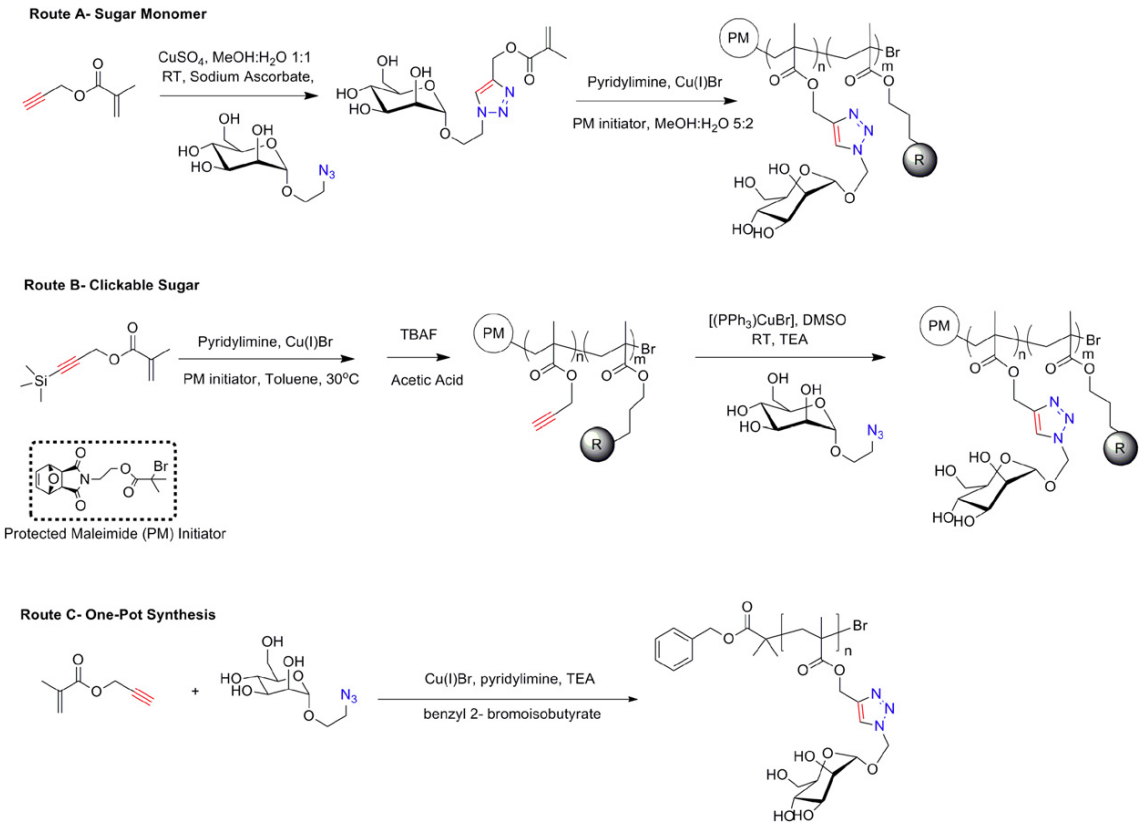

Figure II-20: Various synthetic routes to glycopolymers using ATRP and CuAAC employed by Haddleton et al.. [186]

Recently, the synthesis of well-defined glycopolymers *via* Cu(0)-LRP has become a hot topic as it provides good control and a high end-group fidelity. Moreover, the same group reported the synthesis of multi-block glycopolymers with a high degree of monomer sequence control in various compositions from glycomonomers containing mannose, glucose, and fucose moieties by using Cu(0)-LRP.[71] These narrow dispersity glycopolymers were then tested for binding and inhibition of DC-SIGN, a protein important for HIV infection, which shows a higher binding affinity for the polymers with higher mannose content.

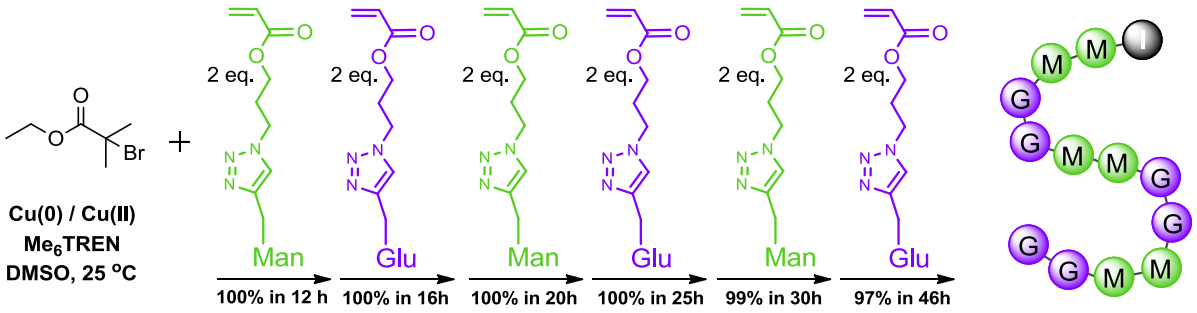

Figure II-21: Synthesis of multi-block glycopolymers with a high degree of monomer sequence control in various compositions from glycomonomers containing mannose, glucose, and fucose moieties by using Cu(0)-LRP. [71]

RAFT polymerization has become the most popular technique for the synthesis of glycopolymers due to its robustness and tolerance to the presence of various functional groups. In addition, relatively low temperatures are required for polymerization. Moreover, the fact that no toxic catalyst is needed and that the polymerization can be performed in water, makes this method highly applicable in bio-related fields. Different strategies have been developed for the polymerization of both protected as unprotected carbohydrate monomers. As example, McCormick *et al.* reported the polymerization of 2-methacryloxyethyl glycoside *via* RAFT in aqueous media at 70°C yielding well-defined carbohydrate macromolecules.[191]

II.4.2.1.1 Post-modification of preformed polymers with sugar moieties

Although polymerization of sugar-containing monomers has been proven successful, modification of preformed polymers using saccharide-containing reagents offers an excellent alternative synthetic route. This approach is suitable to produce libraries of glycopolymers with the same macromolecular architecture by attaching different sugar moieties to preformed polymer scaffolds. Moreover, the top-down preformed scaffold method shows some additional advantages as compared with the bottom-up glycomonomer polymerization: 1) the synthesis of glycomonomers requires multiple steps and 2) the monomer may self-polymerize during purification or storage.

A frequently used method for polymer modification is the use of amino-sugar moieties via amide linkages between the polymer and the sugar unit, which can proceed without the need of

protecting groups as a result of the good nucleophilicity of amines. Various polymer backbones were already applied in this approach. The most relevant ones are depicted in Figure II-22.

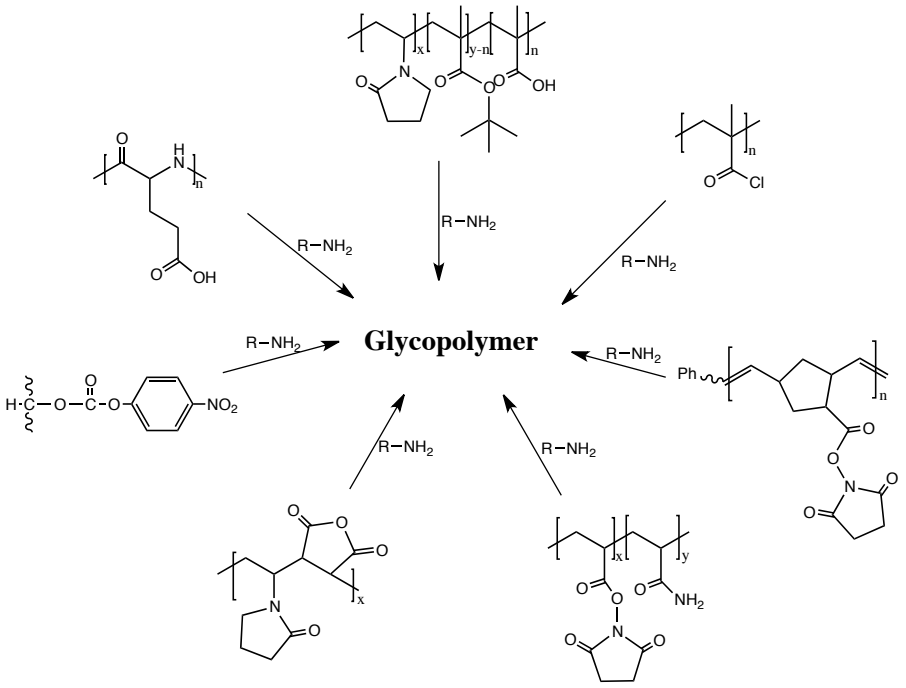

Figure II-22: Synthesis of glycopolymers via amide linkages.

Another approach to the formation of hyperbranched glycopolymers includes the use of click reactions. CuAAC reactions have been widely used in the post-modification reaction of preformed polymers with pendant (protected) alkyne functionalities. After removal of the protecting group, click reaction with azido functional sugar unit can be performed.[186] The disadvantage of this approach is the demanding removal of the toxic Cu(I) species, which makes their biological applicability more difficult. As described in section II.2.2, thiol-X has become very popular, also in the synthesis of glycopolymers. As such, thiol-ene coupling has been used by Chen *et al.* for the post-modification of RAFT derived block copolymers containing pendant alkene groups with glucothiose.[192] Successful glycosylation of both linear polymers as dendrimers can be performed *via* radical-mediated thiol-alkyne click reaction where a thiol-containing sugar is clicked with the alkyne groups of the polymer backbone.[193] Thiol-halogen reactions, such as nucleophilic substitution reactions of thiocarbohydrate sodium salt with halogen-containing polymers, have been used for direct synthesis of glycopolymers. Despite the fact that these reactions are relatively slow, no catalyst is needed and hazardous side product are avoided.[194]

Stenzel *et al.* reported the synthesis of thermo-responsive copolymers with pendant thiolactone functionalities that are reacted with various amines to liberate the corresponding thiol which is consequently reacted *in situ* with bromo-containing mannosepyranose moieties.[117] The resulting double-modified graft copolymers show the characteristic self-assembly behavior due to their amphiphilic nature, affording glycopolymer-based nanoparticles.

II.4.3 Biomedical applications

An important property of glycopolymers is their specific interaction with a wide range of complex carbohydrate binding proteins. These proteins are better known as lectins and play an essential role in the initiation of biochemical processes as a result of specific carbohydrate-lectin interaction with oligosaccharides at the cell membrane. The binding between glycopolymers and lectins could give a better insight in biological interaction in plants and the human body. This binding property between glycopolymer and lectins is also used for therapeutic applications. In the paragraphs below, an overview is given of the most recent applications of glycopolymers. For a more detailed overview of the application of glycopolymers, several reviews are available.[185, 188, 195-197]

II.4.3.1.1 Therapeutics

Haddleton *et al.* reported the potential of mannose-containing glycopolymers to interact with human dendritic cell associated lectin (DC-SIGN) and the ability of these glycopolymers to disrupt/inhibit the interaction between DC-SIGN and the HIV envelope glycoprotein gp120, which could be seen as a new approach for therapeutics.[198, 199]

The group of Cameron described the synthesis of a series of *N*-acetyl-D-glucosamine based glycopolymers by RAFT and the subsequent conjugation of these glycopolymers to gold nanoparticles, yielding a type of multicopy multivalent nanoscale glycoconjugates.[200] Moreover, they showed that these generate a significant immune response *in vivo*, with promising indications that the generated antibodies are capable of recognizing natural Tn-antigen glycans and mammalian-mucin glycoproteins (Figure II-23).

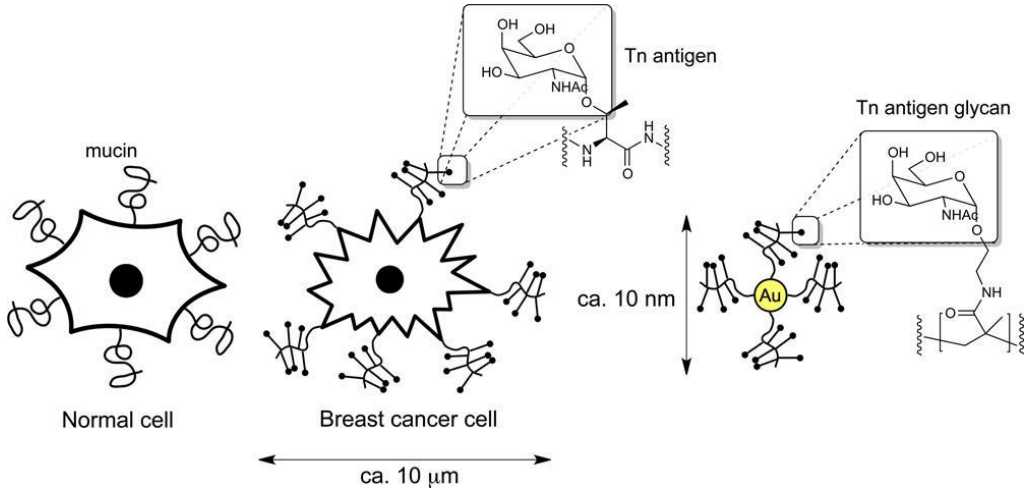

Figure II-23: Multicopy multivalent glycopolymer-stabilized gold nanoparticles as potential synthetic cancer vaccines. [200]

Carbohydrate based anticancer agents have been explored with the aim of increasing the effectiveness and to decrease the side effects of traditional anticancer Pt-based drugs.[201] In the study of Narain *et al.*, glycopolymer based dithiocarbamate-conjugates are prepared by RAFT and subsequently modified with gold(I) phosphine. These compounds are tested or their in vitro toxicity in both normal and cancer cell lines, which showed that the gold conjugates have a higher accumulation in cancer cells due to the presence of glycopolymers.[202] Moreover, it was seen that light enhanced the cytotoxic effect of the polymer, which makes this technique applicable in cancer imaging and photodynamic therapy.

II.4.3.1.2 Delivery systems

Glucose-sensitive polyelectrolyte nanocapsules based on phenylboronic acid and carbohydrates were prepared successfully by the layer-by-layer method. The nanocapsules were sensitive to glucose and insulin could be encapsulated into the hollow structure whereby the release of insulin depended on glucose concentration and pH value of the release medium, which give these capsules potential applications in self-regulated drug delivery systems.[203]

II.5 References

[1] M. Szwarc, *Nature* **1956**, *178*, 1168.
[2] K. Matyjaszewski, *Macromol. Symp.* **2001**, *174*, 51.
[3] K. Matyjaszewski, T. P. Davis, "*Handbook of Radical Polymerization*", John Wiley & Sons, New Jersey 2002.
[4] K. Matyjaszewski, "*Controlled Radical Polymerization*", American Chemical Society, Washington, D.C., 1998, p. 484.
[5] K. Matyjaszewski, "*Controlled/Living Radical Polymerization: Progress in ATRP, NMP, and RAFT*", American Chemical Society, Washington, D.C., 2000, p. 496.
[6] K. Matyjaszewski, "*Advances in Controlled/Living Radical Polymerization*", American Chemical Society, Washington, D.C., 2003, p. 704.
[7] J. Nicolas, Y. Guillaneuf, C. Lefay, D. Bertin, D. Gigmes, B. Charleux, *Prog. Polym. Sci.* **2013**, *38*, 63.
[8] M. F. Cunningham, *Comptes Rendus Chimie* **2003**, *6*, 1351.
[9] R. B. Grubbs, *Polym. Rev.* **2011**, *51*, 104.
[10] J. Chiefari, Y. K. Chong, F. Ercole, J. Krstina, J. Jeffery, T. P. T. Le, R. T. A. Mayadunne, G. F. Meijs, C. L. Moad, G. Moad, E. Rizzardo, S. H. Thang, *Macromolecules* **1998**, *31*, 5559.
[11] R. T. A. Mayadunne, E. Rizzardo, J. Chiefari, Y. K. Chong, G. Moad, S. H. Thang, *Macromolecules* **1999**, *32*, 6977.
[12] G. Moad, J. Chiefari, Y. K. Chong, J. Krstina, R. T. A. Mayadunne, A. Postma, E. Rizzardo, S. H. Thang, *Polym. Int.* **2000**, *49*, 993.
[13] E. Rizzardo, J. Chiefari, B. Y. K. Chong, F. Ercole, J. Krstina, J. Jeffery, T. P. T. Le, R. T. A. Mayadunne, G. F. Meijs, C. L. Moad, G. Moad, S. H. Thang, *Macromol. Symp.* **1999**, *143*, 291.
[14] D. G. Hawthorne, G. Moad, E. Rizzardo, S. H. Thang, *Macromolecules* **1999**, *32*, 5457.
[15] D. Charmot, P. Corpart, H. Adam, S. Z. Zard, T. Biadatti, G. Bouhadir, *Macromol. Symp.* **2000**, *150*, 23.
[16] G. Moad, E. Rizzardo, S. H. Thang, *Polymer* **2008**, *49*, 1079.
[17] G. Moad, E. Rizzardo, S. H. Thang, *Aust. J. Chem.* **2005**, *58*, 379.
[18] G. Moad, E. Rizzardo, S. H. Thang, *Aust. J. Chem.* **2006**, *59*, 669.
[19] G. Moad, E. Rizzardo, S. H. Thang, *Aust. J. Chem.* **2009**, *62*, 1402.
[20] R. Barbey, S. Perrier, *Acs Macro Letters* **2013**, *2*, 366.
[21] D. Konkolewicz, A. Gray-Weale, S. Perrier, *J. Am. Chem. Soc.* **2009**, *131*, 18075.
[22] D. Konkolewicz, C. K. Poon, A. Gray-Weale, S. Perrier, *Chem. Commun.* **2011**, *47*, 239.
[23] T. Ando, M. Kato, M. Kamigaito, M. Sawamoto, *Macromolecules* **1996**, *29*, 1070.
[24] Y. Kotani, M. Kato, M. Kamigaito, M. Sawamoto, *Macromolecules* **1996**, *29*, 6979.
[25] M. Kamigaito, T. Ando, M. Sawamoto, *Chem. Rev.* **2001**, *101*, 3689.
[26] M. Kato, M. Kamigaito, M. Sawamoto, T. Higashimura, *Macromolecules* **1995**, *28*, 1721.
[27] J. S. Wang, K. Matyjaszewski, *Macromolecules* **1995**, *28*, 7901.
[28] J. S. Wang, K. Matyjaszewski, *J. Am. Chem. Soc.* **1995**, *117*, 5614.
[29] K. Matyjaszewski, J. H. Xia, *Chem. Rev.* **2001**, *101*, 2921.
[30] V. Coessens, T. Pintauer, K. Matyjaszewski, *Prog. Polym. Sci.* **2001**, *26*, 337.
[31] T. E. Patten, J. H. Xia, T. Abernathy, K. Matyjaszewski, *Science* **1996**, *272*, 866.
[32] T. E. Patten, K. Matyjaszewski, *Adv. Mater.* **1998**, *10*, 901.
[33] N. Bortolamei, A. A. Isse, A. J. D. Magenau, A. Gennaro, K. Matyjaszewski, *Angew. Chem.-Int. Edit.* **2011**, *50*, 11391.
[34] B. M. Rosen, V. Percec, *Chem. Rev.* **2009**, *109*, 5069.
[35] D. Konkolewicz, Y. Wang, P. Krys, M. Zhong, A. A. Isse, A. Gennaro, K. Matyjaszewski, *Polym. Chem.* **2014**, *5*, 4396.
[36] V. Percec, T. Guliashvili, J. S. Ladislaw, A. Wistrand, A. Stjerndahl, M. J. Sienkowska, M. J. Monteiro, S. Sahoo, *J. Am. Chem. Soc.* **2006**, *128*, 14156.
[37] N. H. Nguyen, B. M. Rosen, V. Percec, *J. Polym. Sci. Part A* **2010**, *48*, 1752.
[38] N. H. Nguyen, B. M. Rosen, V. Percec, *J. Polym. Sci. Pol. Chem.* **2011**, *49*, 1235.
[39] H. C. Kolb, M. G. Finn, K. B. Sharpless, *Angew. Chem.-Int. Edit.* **2001**, *40*, 2004.
[40] C. Barner-Kowollik, F. E. Du Prez, P. Espeel, C. J. Hawker, T. Junkers, H. Schlaad, W. Van Camp, *Angew. Chem.-Int. Edit.* **2011**, *50*, 60.
[41] H. C. Kolb, K. B. Sharpless, *Drug Discovery Today* **2003**, *8*, 1128.
[42] C. W. Tornoe, C. Christensen, M. Meldal, *J. Org. Chem.* **2002**, *67*, 3057.

[43] V. V. Rostovtsev, L. G. Green, V. V. Fokin, K. B. Sharpless, *Angew. Chem.-Int. Edit.* **2002**, *41*, 2596.
[44] B. M. Rosen, G. Lligadas, C. Hahn, V. Percec, *J. Polym. Sci. Pol. Chem.* **2009**, *47*, 3931.
[45] J. Xu, L. Tao, C. Boyer, A. B. Lowe, T. P. Davis, *Macromolecules* **2010**, *43*, 20.
[46] H. Li, B. Yu, H. Matsushima, C. E. Hoyle, A. B. Lowe, *Macromolecules* **2009**, *42*, 6537.
[47] X. K. D. Hillewaere, R. F. A. Teixeira, L.-T. T. Nguyen, J. A. Ramos, H. Rahier, F. E. Du Prez, *Adv. Funct. Mater.* **2014**, n/a.
[48] S. De, A. Khan, *Chem. Commun.* **2012**, *48*, 3130.
[49] C. E. Hoyle, C. N. Bowman, *Angew. Chem.-Int. Edit.* **2010**, *49*, 1540.
[50] M. J. Kade, D. J. Burke, C. J. Hawker, *J. Polym. Sci. Pol. Chem.* **2010**, *48*, 743.
[51] R. Hoogenboom, *Angew. Chem.-Int. Edit.* **2010**, *49*, 3415.
[52] L.-T. T. Nguyen, M. T. Gokmen, F. E. Du Prez, *Polym. Chem.* **2013**, *4*, 5527.
[53] M. Le Neindre, R. Nicolay, *Polym. Int.* **2014**, *63*, 887.
[54] C. Barner-Kowollik, A. J. Inglis, *Macromol. Chem. Phys.* **2009**, *210*, 987.
[55] B. Helms, J. L. Mynar, C. J. Hawker, J. M. J. Frechet, *J. Am. Chem. Soc.* **2004**, *126*, 15020.
[56] P. Wu, A. K. Feldman, A. K. Nugent, C. J. Hawker, A. Scheel, B. Voit, J. Pyun, J. M. J. Frechet, K. B. Sharpless, V. V. Fokin, *Angew. Chem.-Int. Edit.* **2004**, *43*, 3928.
[57] J. F. Lutz, H. G. Borner, K. Weichenhan, *Macromolecules* **2007**, *40*, 7060.
[58] J. A. Johnson, M. G. Finn, J. T. Koberstein, N. J. Turro, *Macromol. Rapid Commun.* **2008**, *29*, 1052.
[59] M. Meldal, *Macromol. Rapid Commun.* **2008**, *29*, 1016.
[60] U. Mansfeld, C. Pietsch, R. Hoogenboom, C. R. Becer, U. S. Schubert, *Polym. Chem.* **2010**, *1*, 1560.
[61] B. S. Sumerlin, N. V. Tsarevsky, G. Louche, R. Y. Lee, K. Matyjaszewski, *Macromolecules* **2005**, *38*, 7540.
[62] J. Geng, J. Lindqvist, G. Mantovani, D. M. Haddleton, *Angew. Chem.-Int. Edit.* **2008**, *47*, 4180.
[63] M. Semsarilar, V. Ladmiral, S. b. Perrier, *Macromolecules* **2010**, *43*, 1438.
[64] C. E. Hoyle, A. B. Lowe, C. N. Bowman, *Chem. Soc. Rev.* **2010**, *39*, 1355.
[65] S. P. S. Koo, M. M. Stamenovic, R. A. Prasath, A. J. Inglis, F. E. Du Prez, C. Barner-Kowollik, W. Van Camp, T. Junkers, *J. Polym. Sci. Pol. Chem.* **2010**, *48*, 1699.
[66] J. A. Carioscia, J. W. Stansbury, C. N. Bowman, *Polymer* **2007**, *48*, 1526.
[67] I. Gadwal, A. Khan, *Polym. Chem.* **2013**, *4*, 2440.
[68] S. Binder, I. Gadwal, A. Bielmann, A. Khan, *J. Polym. Sci. Pol. Chem.* **2014**, *52*, 2040.
[69] N. Cengiz, J. Rao, A. Sanyal, A. Khan, *Chem. Commun.* **2013**, *49*, 11191.
[70] Y. Jian, Y. He, Y. Sun, H. Yang, W. Yang, J. Nie, *J. Mater. Chem. C* **2013**, *1*, 4481.
[71] Q. Zhang, A. Anastasaki, G.-Z. Li, A. J. Haddleton, P. Wilson, D. M. Haddleton, *Polym. Chem.* **2014**, *5*, 3876.
[72] A. Braendle, A. Khan, *Polym. Chem.* **2012**, *3*, 3224.
[73] E. Dyer, J. F. Glenn, E. G. Lendrat, *J. Org. Chem.* **1961**, *26*, 2919.
[74] J. Shin, H. Matsushima, J. W. Chan, C. E. Hoyle, *Macromolecules* **2009**, *42*, 3294.
[75] R. M. Hensarling, S. B. Rahane, A. P. LeBlanc, B. J. Sparks, E. M. White, J. Locklin, D. L. Patton, *Polym. Chem.* **2011**, *2*, 88.
[76] N. Droger, O. Primel, J. L. Halary, *J. Appl. Polym. Sci.* **2008**, *107*, 455.
[77] J. W. Chan, C. E. Hoyle, A. B. Lowe, M. Bowman, *Macromolecules* **2010**, *43*, 6381.
[78] D. P. Nair, M. Podgorski, S. Chatani, T. Gong, W. Xi, C. R. Fenoli, C. N. Bowman, *Chem. Mater.* **2014**, *26*, 724.
[79] D. Tejedor, A. Santos-Exposito, G. Mendez-Abt, C. Ruiz-Perez, F. Garcia-Tellado, *Synlett* **2009**, 1223.
[80] M. Li, P. De, S. R. Gondi, B. S. Sumerlin, *J. Polym. Sci. Pol. Chem.* **2008**, *46*, 5093.
[81] M. Li, P. De, H. Li, B. S. Sumerlin, *Polym. Chem.* **2010**, *1*, 854.
[82] J. W. Chan, B. Yu, C. E. Hoyle, A. B. Lowe, *Chem. Commun.* **2008**, 4959.
[83] M. Heggli, N. Tirelli, A. Zisch, J. A. Hubbell, *Bioconj. Chem.* **2003**, *14*, 967.
[84] V. X. Truong, A. P. Dove, *Angew. Chem.-Int. Edit.* **2013**, *52*, 4132.
[85] Q. Zhang, A. Anastasaki, G. Z. Li, A. J. Haddleton, P. Wilson, D. M. Haddleton, *Polym. Chem.* **2014**, *5*, 3876.
[86] C. R. Becer, K. Babiuch, D. Pilz, S. Hornig, T. Heinze, M. Gottschaldt, U. S. Schubert, *Macromolecules* **2009**, *42*, 2387.
[87] A. Gress, A. Volkel, H. Schlaad, *Macromolecules* **2007**, *40*, 7928.
[88] J. W. Chan, C. E. Hoyle, A. B. Lowe, *J. Am. Chem. Soc.* **2009**, *131*, 5751.
[89] N. B. Cramer, S. K. Reddy, M. Cole, C. Hoyle, C. N. Bowman, *J. Polym. Sci. Pol. Chem.* **2004**, *42*, 5817.
[90] C. E. Hoyle, T. Y. Lee, T. Roper, *J. Polym. Sci. Part A* **2004**, *42*, 5301.
[91] J. A. Pojman, B. Varisli, A. Perryman, C. Edwards, C. Hoyle, *Macromolecules* **2004**, *37*, 691.
[92] H. Wei, A. F. Senyurt, S. Jonsson, C. E. Hoyle, *J. Polym. Sci. Pol. Chem.* **2007**, *45*, 822.

[93] B. Yu, J. W. Chan, C. E. Hoyle, A. B. Lowe, *J. Polym. Sci. Pol. Chem.* **2009**, *47*, 3544.
[94] N. B. Cramer, S. K. Reddy, A. K. O'Brien, C. N. Bowman, *Macromolecules* **2003**, *36*, 7964.
[95] V. S. Khire, A. W. Harant, A. W. Watkins, K. S. Anseth, C. N. Bowman, *Macromolecules* **2006**, *39*, 5081.
[96] A. E. Rydholm, S. K. Reddy, K. S. Anseth, C. N. Bowman, *Polymer* **2007**, *48*, 4589.
[97] C. E. Hoyle, T. Y. Lee, T. Roper, *J. Polym. Sci. Part A* **2004**, *42*, 5301.
[98] M. M. Stamenovic, P. Espeel, W. Van Camp, F. E. Du Prez, *Macromolecules* **2011**, *44*, 5619.
[99] B. D. Fairbanks, T. F. Scott, C. J. Kloxin, K. S. Anseth, C. N. Bowman, *Macromolecules* **2009**, *42*, 211.
[100] B. D. Fairbanks, E. A. Sims, K. S. Anseth, C. N. Bowman, *Macromolecules* **2010**, *43*, 4113.
[101] M. Le Neindre, R. Nicolay, *Polym. Chem.* **2014**.
[102] P. Espeel, F. E. Du Prez, *Macromolecules* **2015**, *48*, 2.
[103] H. Willcock, R. K. O'Reilly, *Polym. Chem.* **2010**, *1*, 149.
[104] Q. Zhang, J. W. Hwang, K. N. Kim, H. W. Jung, S. M. Noh, J. K. Oh, *J. Polym. Sci. Pol. Chem.* **2013**, *51*, 2860.
[105] X. L. Sun, W. D. He, J. Li, L. Y. Li, B. Y. Zhang, T. T. Pan, *J. Polym. Sci. Pol. Chem.* **2009**, *47*, 6863.
[106] J. A. Syrett, M. W. Jones, D. M. Haddleton, *Chem. Commun.* **2010**, *46*, 7181.
[107] C. Boyer, A. H. Soeriyadi, P. J. Roth, M. R. Whittaker, T. P. Davis, *Chem. Commun.* **2010**, *47*, 1318.
[108] P. J. Roth, D. Kessler, R. Zentel, P. Theato, *J. Polym. Sci. Pol. Chem.* **2009**, *47*, 3118.
[109] E. Hrsic, I. Zografou, B. Schulte, A. Pich, H. Keul, M. Moeller, *Polymer* **2013**, *54*, 495.
[110] M. Liras, O. Garcia, I. Quijada-Garrido, R. Paris, *Macromolecules* **2011**, *44*, 1335.
[111] M. Liras, O. Garcia, N. Guarrotxena, M. Palacios-Cuesta, I. Quijada-Garrido, *Polym. Chem.* **2013**, *4*, 5751.
[112] L. Garamszegi, C. Donzel, G. Carrot, T. Q. Nguyen, J. Hilborn, *React. Funct. Polym.* **2003**, *55*, 179.
[113] R. M. Hensarling, E. A. Hoff, A. P. LeBlanc, W. Guo, S. B. Rahane, D. L. Patton, *J. Polym. Sci. Pol. Chem.* **2013**, *51*, 1079.
[114] G. Delaittre, T. Pauloehrl, M. Bastmeyer, C. Barner-Kowollik, *Macromolecules* **2012**, *45*, 1792.
[115] P. Espeel, F. Goethals, F. E. Du Prez, *J. Am. Chem. Soc.* **2011**, *133*, 1678.
[116] P. Espeel, F. Goethals, M. M. Stamenovic, L. Petton, F. E. Du Prez, *Polym. Chem.* **2012**, *3*, 1007.
[117] Y. Chen, P. Espeel, S. Reinicke, F. E. Du Prez, M. H. Stenzel, *Macromol. Rapid Commun.* **2014**, *35*, 1128.
[118] P. Espeel, L. L. G. Carrette, K. Bury, S. Capenberghs, J. C. Martins, F. E. Du Prez, A. Madder, *Angew. Chem.-Int. Edit.* **2013**, *52*, 13261.
[119] P. Espeel, F. Goethals, F. Du Prez, "Thiolactones as Functional Handles for Polymer Synthesis and Modification", in *Thiol-X chemistries in Polymer and Materials Science*, A.L.a.C. Bowman, Ed., RSC publishing, 2013.
[120] F. Goethals, S. Martens, P. Espeel, O. van den Berg, F. E. Du Prez, *Macromolecules* **2014**, *47*, 61.
[121] S. Reinicke, P. Espeel, M. M. Stamenovic, F. E. Du Prez, *Acs Macro Letters* **2013**, *2*, 539.
[122] M. M. Stamenovic, P. Espeel, E. Baba, T. Yamamoto, Y. Tezuka, F. E. Du Prez, *Polym. Chem.* **2013**, *4*, 184.
[123] A. Carlmark, C. J. Hawker, A. Hult, M. Malkoch, *Chem. Soc. Rev.* **2009**, *38*, 352.
[124] D. A. Tomalia, J. M. J. Frechet, *J. Polym. Sci. Pol. Chem.* **2002**, *40*, 2719.
[125] B. I. Voit, A. Lederer, *Chem. Rev.* **2009**, *109*, 5924.
[126] C. Gao, D. Yan, *Prog. Polym. Sci.* **2004**, *29*, 183.
[127] D. Yan, C. Gao, H. Frey, "*Hyperbranched Polymers: Synthesis, properties and applications"*, John Wiley & Sonc, Inc, **2009**.
[128] R. H. Kienle, A. G. Hovey, *J. Am. Chem. Soc.* **1929**, *51*, 509.
[129] C. R. Yates, W. Hayes, *Eur. Polym. J.* **2004**, *40*, 1257.
[130] D. Y. Yan, C. Gao, *Macromolecules* **2000**, *33*, 7693.
[131] D. A. Tomalia, J. M. Frechet, *Prog. Polym. Sci.* **2005**, *30*, 217.
[132] J. M. J. Frechet, M. Henmi, I. Gitsov, S. Aoshima, M. R. Leduc, R. B. Grubbs, *Science* **1995**, *269*, 1080.
[133] A. H. E. Muller, D. Y. Yan, M. Wulkow, *Macromolecules* **1997**, *30*, 7015.
[134] O. Nuyken, F. Gruber, S. D. Pask, A. Riederer, M. Walter, *Macromol. Chem. Phys.* **1993**, *194*, 3415.
[135] C. J. Hawker, J. M. J. Frechet, R. B. Grubbs, J. Dao, *J. Am. Chem. Soc.* **1995**, *117*, 10763.
[136] M. W. Weimer, J. M. J. Frechet, I. Gitsov, *J. Polym. Sci. Pol. Chem.* **1998**, *36*, 955.
[137] K. Matyjaszewski, S. G. Gaynor, A. Kulfan, M. Podwika, *Macromolecules* **1997**, *30*, 5192.
[138] S. Carter, S. Rimmer, A. Sturdy, M. Webb, *Macromol. Biosci.* **2005**, *5*, 373.
[139] M. Suzuki, A. Ii, T. Saegusa, *Macromolecules* **1992**, *25*, 7071.
[140] M. Bednarek, T. Biedron, J. Helinski, K. Kaluzynski, P. Kubisa, S. Penczek, *Macromol. Rapid Commun.* **1999**, *20*, 369.
[141] H. Magnusson, E. Malmstrom, A. Hult, *Macromol. Rapid Commun.* **1999**, *20*, 453.
[142] M. J. Liu, N. Vladimirov, J. M. J. Frechet, *Macromolecules* **1999**, *32*, 6881.
[143] C. Gao, D. Y. Yan, *Macromolecules* **2001**, *34*, 156.

[144] M. G. McKee, S. Unal, G. L. Wilkes, T. E. Long, *Prog. Polym. Sci.* **2005**, *30*, 507.
[145] W. Burchard, *Branched Polymers I* **1999**, *143*, 113.
[146] D. Y. Yan, A. H. E. Muller, K. Matyjaszewski, *Macromolecules* **1997**, *30*, 7024.
[147] C. J. Hawker, R. Lee, J. M. J. Frechet, *J. Am. Chem. Soc.* **1991**, *113*, 4583.
[148] D. Holter, A. Burgath, H. Frey, *Acta Polymerica* **1997**, *48*, 30.
[149] G. Maier, C. Zech, B. Voit, H. Komber, *Macromol. Chem. Phys.* **1998**, *199*, 2655.
[150] L. J. Hobson, A. M. Kenwright, W. J. Feast, *Chem. Commun.* **1997**, 1877.
[151] C. J. Hawker, F. K. Chu, *Macromolecules* **1996**, *29*, 4370.
[152] L. Chen, X. Y. Zhu, D. Y. Yan, Y. Chen, Q. Chen, Y. F. Yao, *Angew. Chem.-Int. Edit.* **2006**, *45*, 87.
[153] Z. F. Jia, H. Chen, X. Y. Zhu, D. Y. Yan, *J. Am. Chem. Soc.* **2006**, *128*, 8144.
[154] P. Kambouris, C. J. Hawker, *J. Chem. Soc.* **1993**, 2717.
[155] D. H. Bolton, K. L. Wooley, *J. Polym. Sci. Pol. Chem.* **2002**, *40*, 823.
[156] D. Holter, H. Frey, *Acta Polymerica* **1997**, *48*, 298.
[157] J. Y. Wang, D. M. Johnson, *Polym. Int.* **2009**, *58*, 1234.
[158] W. Radke, G. Litvinenko, A. H. E. Muller, *Macromolecules* **1998**, *31*, 239.
[159] Y. Ishida, A. C. F. Sun, M. Jikei, M. Kakimoto, *Macromolecules* **2000**, *33*, 2832.
[160] C. Lach, H. Frey, *Macromolecules* **1998**, *31*, 2381.
[161] W. Huang, L. Su, Z. Bo, *J. Am. Chem. Soc.* **2009**, *131*, 10348.
[162] Q. Zhu, J. Wu, C. Tu, Y. Shi, L. He, R. Wang, X. Zhu, D. Yan, *J. Phys. Chem. B* **2009**, *113*, 5777.
[163] Y. Y. Mai, Y. F. Zhou, D. Y. Yan, J. Hou, *J Phys.* **2005**, *7*.
[164] A. H. Widmann, G. R. Davies, *Comput. Theor. Polym. Sci.* **1998**, *8*, 191.
[165] P. F. W. Simon, A. H. E. Muller, T. Pakula, *Macromolecules* **2001**, *34*, 1677.
[166] G. Franc, A. K. Kakkar, *Chem. Soc. Rev.* **2010**, *39*, 1536.
[167] E. Zagar, M. Zigon, *J. Chromatogr.* **2004**, *1034*, 77.
[168] M. Seiler, *Evonik Science Letter; Hanau, Germany* **2008**, 12.
[169] P. Froehling, *J. Polym. Sci. Part A* **2004**, *42*, 3110.
[170] J. F. Stumbe, B. Bruchmann, *Macromol. Rapid Commun.* **2004**, *25*, 921.
[171] M. Irfan, M. Seiler, *Industrial & Engineering Chemistry Research* **2010**, *49*, 1169.
[172] J. Lange, E. Stenroos, M. Johansson, E. Malmstrom, *Polymer* **2001**, *42*, 7403.
[173] A. Hult, M. Johansson, E. Malmstrom, *Branched Polymers Ii* **1999**, *143*, 1.
[174] P. Froehling, *J. Polym. Sci. Part A* **2004**, *42*, 3110.
[175] S. E. Stiriba, H. Frey, R. Haag, *Angew. Chem.-Int. Edit.* **2002**, *41*, 1329.
[176] D. Fischer, T. Bieber, Y. X. Li, H. P. Elsasser, T. Kissel, *Pharm. Res.* **1999**, *16*, 1273.
[177] H. Petersen, P. M. Fechner, A. L. Martin, K. Kunath, S. Stolnik, C. J. Roberts, D. Fischer, M. C. Davies, T. Kissel, *Bioconj. Chem.* **2002**, *13*, 845.
[178] L. M. Dai, B. Winkler, L. M. Dong, L. Tong, A. W. H. Mau, *Adv. Mater.* **2001**, *13*, 915.
[179] H. Q. Wang, N. Song, H. Y. Li, Y. F. Li, X. Y. Li, *Synthetic Metals* **2005**, *151*, 279.
[180] H. S. Mangold, T. V. Richter, S. Link, U. Wurfel, S. Ludwigs, *J. Phys. Chem. B* **2012**, *116*, 154.
[181] C. J. Hawker, F. K. Chu, P. J. Pomery, D. J. T. Hill, *Macromolecules* **1996**, *29*, 3831.
[182] A. Sunder, M. Kramer, R. Hanselmann, R. Mulhaupt, H. Frey, *Angew. Chem.-Int. Edit.* **1999**, *38*, 3552.
[183] V. Vazquez-Dorbatt, J. Lee, E.-W. Lin, H. D. Maynard, *Chembiochem* **2012**, *13*, 2478.
[184] D. S. Kohane, R. Langer, *Pediatr Res* **2008**, *63*, 487.
[185] S. R. S. Ting, G. Chen, M. H. Stenzel, *Polym. Chem.* **2010**, *1*, 1392.
[186] S. Slavin, J. Burns, D. M. Haddleton, C. R. Becer, *Eur. Polym. J.* **2011**, *47*, 435.
[187] V. Ladmiral, E. Melia, D. M. Haddleton, *Eur. Polym. J.* **2004**, *40*, 431.
[188] S. G. Spain, M. I. Gibson, N. R. Cameron, *J. Polym. Sci. Part A* **2007**, *45*, 2059.
[189] S. R. S. Ting, E. H. Min, P. Escale, M. Save, L. Billon, M. H. Stenzel, *Macromolecules* **2009**, *42*, 9422.
[190] K. Ohno, Y. Tsujii, T. Fukuda, *J. Polym. Sci. Pol. Chem.* **1998**, *36*, 2473.
[191] A. B. Lowe, B. S. Sumerlin, C. L. McCormick, *Polymer* **2003**, *44*, 6761.
[192] G. Chen, S. Amajjahe, M. H. Stenzel, *Chem. Commun.* **2009**, 1198.
[193] J. Kumar, A. Bousquet, M. H. Stenzel, *Macromol. Rapid Commun.* **2011**, *32*, 1620.
[194] Y. Chen, G. Chen, M. H. Stenzel, *Macromolecules* **2010**, *43*, 8109.
[195] Y. Miura, *J. Polym. Sci. Pol. Chem.* **2007**, *45*, 5031.
[196] S. G. Spain, N. R. Cameron, *Polym. Chem.* **2011**, *2*, 60.
[197] R. J. Ma, L. Q. Shi, *Polymer Chemistry* **2014**, *5*, 1503.
[198] C. R. Becer, M. I. Gibson, J. Geng, R. Ilyas, R. Wallis, D. A. Mitchell, D. M. Haddleton, *J. Am. Chem. Soc.* **2010**, *132*, 15130.
[199] Q. Zhang, J. Collins, A. Anastasaki, R. Wallis, D. A. Mitchell, C. R. Becer, D. M. Haddleton, *Angew. Chem.-Int. Edit.* **2013**, *52*, 4435.

[200] A. L. Parry, N. A. Clemson, J. Ellis, S. S. R. Bernhard, B. G. Davis, N. R. Cameron, *J. Am. Chem. Soc.* **2013**, *135*, 9362.
[201] V. T. Huynh, G. J. Chen, P. de Souza, M. H. Stenzel, *Biomacromolecules* **2011**, *12*, 1738.
[202] M. Ahmed, S. Mamba, X.-H. Yang, J. Darkwa, P. Kumar, R. Narain, *Bioconj. Chem.* **2013**, *24*, 979.
[203] H. L. Guo, Q. Q. Guo, T. C. Chu, X. G. Zhang, Z. M. Wu, D. M. Yu, *J. Mater. Sci.-Mater. Med.* **2014**, *25*, 121.

Abstract

Heterotelechelic, hydrophilic polymers with a primary amine and thiol group at the α– and ω-chain end respectively were synthesized *via* reversible addition-fragmentation chain transfer (RAFT) polymerization in a straightforward and versatile way and subsequently used for the design of dual-responsive polymer/gold nanohybrids. Therefore, a phthalimido-containing chain transfer agent (CTA) was synthesized and used for the polymerization of the hydrophilic monomers *N*-isopropylacrylamide (NIPAM) and *N,N*-dimethylacrylamide (DMA). After polymerization, the trithiocarbonate functionality at the ω-chain end, originating from the CTA, was converted into a thiol upon aminolysis. In a next step, the phthalimido α-chain end was hydrolyzed into a primary amine, resulting in heterotelechelic, hydrophilic polymers. End-group conversions were monitored by ^{1}H NMR spectroscopy, MALDI-TOF MS analysis and UV-Vis spectroscopy, confirming that quantitative modifications were obtained during each stage. The amino groups of these heterotelechelic polymer chains were modified with citraconic anhydride, after which the obtained polymers were grafted with the thiol group onto citrate stabilized gold nanoparticles resulting in the creation of dual temperature- and pH-responsive gold particles. Furthermore, incorporation of two different dye components at the PNIPAM structure yielded thermo-responsive polymeric dyes whose sensing capacities are tested by using a biphasic aqueous/organic system below and above the cloud point temperature of the polymeric structure.

Part of this chapter was published as:

S. Wallyn, Z. Zhang, F. Driessen, J. Pietrasik, B. G. De Geest, R. Hoogenboom, F. E. Du Prez, Macromol. Rapid Commun. 2014, 35, 405.

Chapter III

Straightforward RAFT-procedure for the synthesis of heterotelechelic poly(acrylamide)s

III.1 Introduction

Much attention goes to the synthesis of well-defined macromolecular structures with appropriate end-group functionalities because of their use in research fields like gene and drug delivery systems, sensors, etc.[1-3] Controlled radical polymerization (CRP) techniques provide control over both the architecture and the molecular weight distribution of the resulting polymers as well as the chain end functionalities.[4, 5] Amongst them, RAFT (reversible addition-fragmentation chain transfer) polymerization offers the ability to control the polymerization of most monomers such as acrylates, methacrylates, styrenics or dienes.[6-12] Moreover, this technique is mostly tolerant to unprotected functionalities and is compatible with a wide range of reaction conditions.[13] Another major advantage of the RAFT process is that the functional group present on the chain transfer agent (CTA) is retained at the end of the polymerization, enabling the incorporation of a wide range of functional end-groups at the α-terminus. On the other hand, the CTA thiocarbonylthio end-group can easily be converted into a thiol functional group at the ω-terminus, opening manifold opportunities for thiol modification reactions.[14, 15] These features make RAFT the ideal technique for the synthesis of heterotelechelic systems, *i.e.* polymer chains with two different end-groups.[16-19] Much attention goes to systems with end-groups, including carboxylic acids and amines, with a high impact for biological research, such as proteins or targeting molecules.[17]

Therefore, polymers with a primary amine end-group gained much interest due to their potential application areas, not only in various biomedical applications but also in fields such as surface science and adhesion materials.[20, 21] The introduction of primary amine groups in polymers synthesized *via* RAFT is not straightforward as the trithiocarbonate functionality is sensitive to aminolysis.[22] Therefore, an important challenge is the development of a versatile and easy RAFT synthesis method for heterotelechelic polymers with a primary amine as one of the end-groups.[23, 24]

On the other hand, thermo-responsive polymers have gained a lot of attention, especially poly(*N*-isopropyl acrylamide) (PNIPAM) because aqueous solutions of PNIPAM exhibit a cloud point temperature (T_{cp}) in the range of 28–32 °C, depending on the aqueous solution composition.[25, 26] When heated in water above the T_{cp} PNIPAM undergoes a reversible phase transition from a swollen hydrated state to a shrunken dehydrated state. This very sharp transition (over ca. 5°C) in water is attributed to the disruption of the hydrogen bonding of water molecules around the amide group of the side chain, which is accompanied with a strong, increase in entropy.[27-29] This feature has been used to control enzymatic activity[30], in affinity precipitation separation[31] and as a protein recycling system[32, 33].

The aim of this first part of the PhD project was to develop and investigate a straightforward method for the synthesis of heterotelechelic polymers. This knowledge has been applied in the next chapters to synthesize well-defined AB_2 oligomers for the preparation of functional hyperbranched polymers. Narrow-disperse PNIPAM and PDMA structures are synthesized *via* RAFT using a phthalimido-containing CTA.[24, 34, 35] The RAFT polymerization of PNIPAM has been already well described as those structures possess a cloud point temperature of 32°C, which makes them useful in many biomedical applications.[36, 37] After aminolysis, the phthalimido group was hydrolysed into a primary amine, yielding polymers with a primary amine at the α-chain end and a free thiol at the ω-chain end. Even though some recent reports describe the synthesis of amino-functionalized polymers using similar phthalimido-CTAs[1, 23], subsequent modification of both the amino and thiol groups has not been explored. In our study, in collaboration with the UGent research groups of Richard Hoogenboom and Bruno De Geest, we focused on the use of heterotelechelic structures to prepare dual-responsive polymer/gold nanohybrids by grafting the thiol-functional terminus of the polymer prepared by RAFT polymerization onto citrate stabilized gold nanoparticles. Such nanohybrids could find potential applications as sensor or in a biomedical context.[38] For this, the primary amine is converted into an amide with a pending carboxylic acid group and subsequently grafted onto the

gold particle *via* ligand exchange between the thiol of the polymer and the metallic gold. It is shown that these nanohybrids are temperature- and pH-responsive as they agglomerate above the cloud point temperature of the polymers or by lowering the pH. Moreover, both chain-ends of the heterotelechelic PNIPAM structures are functionalized with a dye and subsequently tested on their sensing capabilities as thermo-responsive polymeric dye in a biphasic system (Scheme III-1).

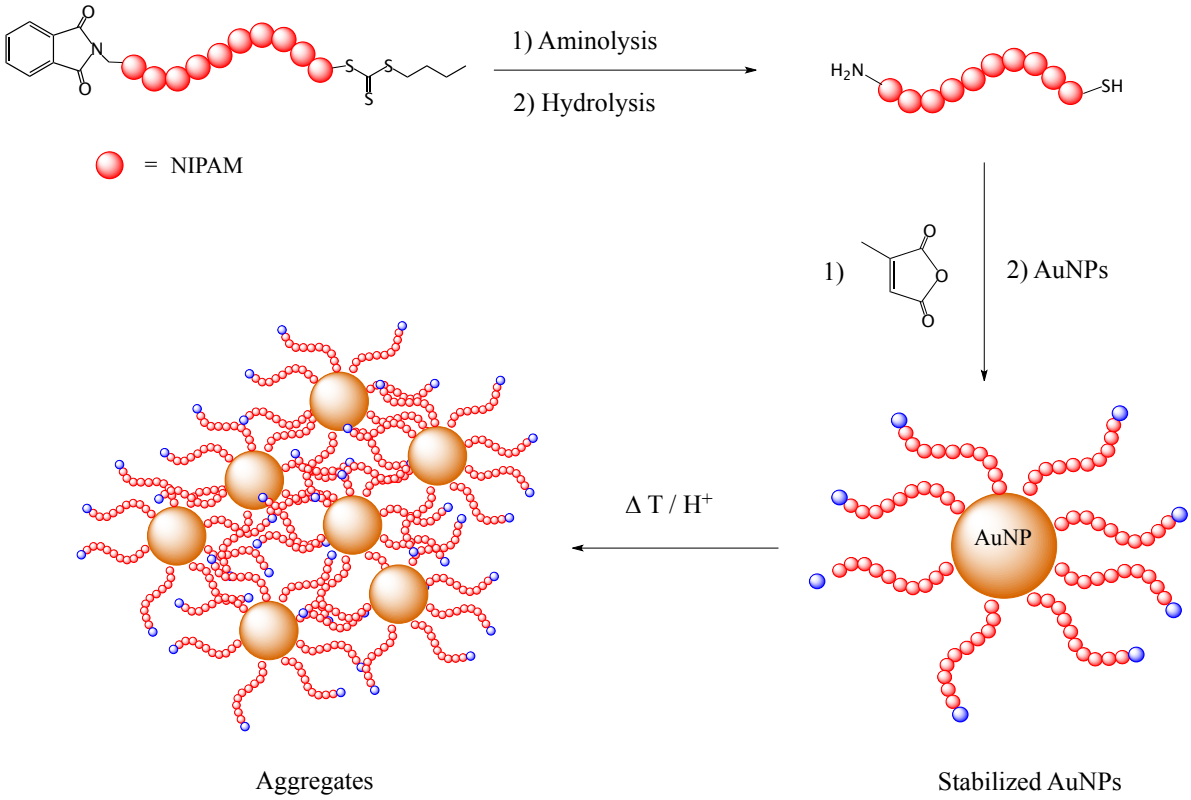

Scheme III-1: Graphical overview of the different steps for the synthesis of dual responsive gold nanohybrids.

III.2 Synthesis of heterotelechelic polymers

A phthalimido-containing CTA was synthesized *via* one-pot synthesis (Figure III-1; ~10 gram scale) and used for the polymerization of hydrophilic monomers, namely NIPAM and DMA, using AIBN as initiator (Scheme III-2 (**1**)). This type of CTA (butyl phthalimidomethyl trithiocarbonate) is known to mediate the RAFT polymerization of different type of monomers (acrylates, methacrylates, styrenics,...) with good control over both the molecular weight distribution and end-group fidelity, but subsequent modification of both amino and thiol groups has not been fully explored.[24, 39]

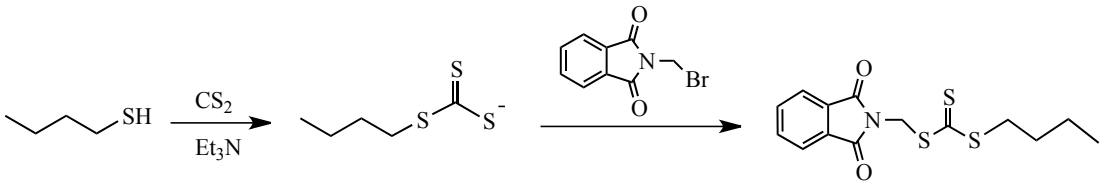

Figure III-1: Synthesis of butyl phthalimidomethyl trithiocarbonate CTA for the preparation of heterotelechelic polymers via RAFT.

The polymerization for the two types of acrylamides was followed using SEC and ^{1}H NMR spectroscopy. The results show that the theoretical molecular weights are in good agreement with the molecular weights obtained (between 2.5 and 6 kDa) and the dispersities are relatively narrow (≤ 1.2) in all cases (Table III-1). To avoid the loss of the end-groups due to radical side reactions at high conversion, conversions of about 70% were targeted, confirmed *via* ^{1}H NMR spectroscopy. MALDI-TOF MS analysis demonstrates the end-group fidelity as the experimental masses are in good agreement with the theoretical ones (Figure III-2). Next to the main (Na+)-distribution, a minor distribution is detected from which the origin could not be attributed.

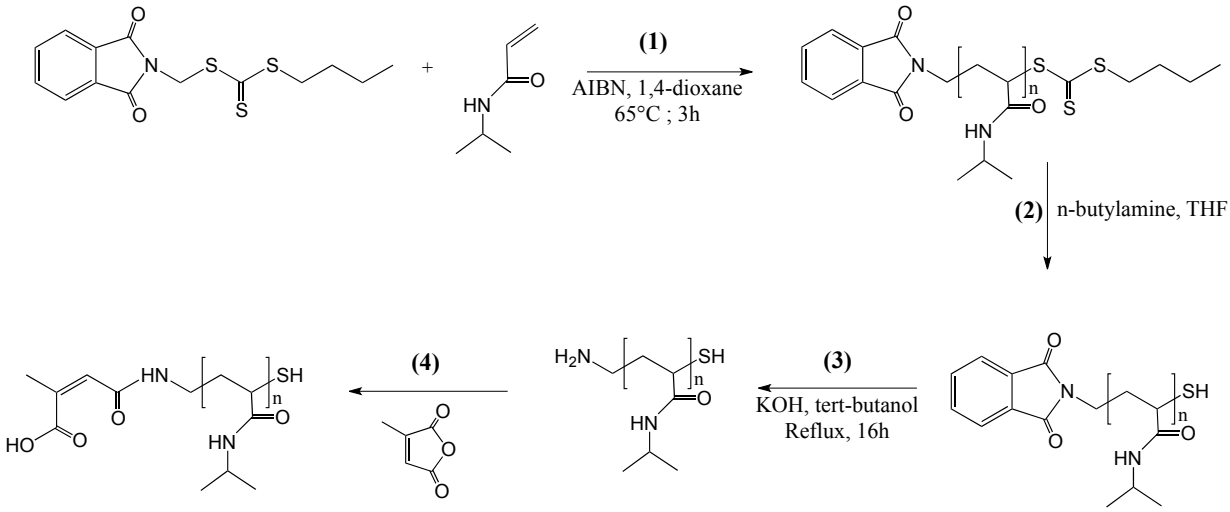

Scheme III-2: General synthesis scheme of heterotelechelic PNIPAM structures ((1)-(3)) and their further modification with citraconic anhydride (4), to enable the synthesis of dual-responsive polymer/gold nanohybrids by grafting them onto gold nanoparticles.

However, *via* end-group modification (Scheme III-2, **(2)** and **(3)**), it was observed that these series also contain both end-groups, indicating a high end-group conservation during the RAFT polymerization of the acrylamides. Most probably, the series can be attributed to a fragmentation reaction during the MALDI-process since in each step a mass difference of 18 Da compared to the main (Na+)-distribution is seen. Moreover, no distributions were detected that can be attributed to recombination (m/z = 3712.38 Da), disproportionation (m/z = 3669.47 Da) reactions or initiation by AIBN (m/z = 3701.51 Da), indicating the controlled character of the polymerization process.

Table III-1: Reaction conditions and results for the synthesis of PNIAM and PDMA via RAFT polymerization. All polymerizations were performed in dry 1,4-dioxane at 65°C.

M	$[M]_0/[CTA]_0/[I]_0$	t [h]	$M_{n,\,SEC}$ [a] [g/mol]	$M_{n,\,NMR}$ [g/mol]	$M_{n,\,th}$ [g/mol]	Đ	Conv. [%]
NIPAM	30/1/0.11	4	3900	2300	2630	1.19	68
NIPAM	50/1/0.11	3	5600	3600	4000	1.15	65
NIPAM	60/1/0.11	3	6200	4000	4390	1.15	60
DMA	40/1/0.11	3	3900	2300	2580	1.18	50
DMA	70/1/0.11	3	5800	4000	5540	1.15	66

[a] *Determined via DMA SEC calibrated with PMMA standards.* $M_{n,\,th} = M_w(CTA) + conv\ x$ [M]/[CTA] x M_w(M).

In order to obtain the heterotelechelic polymer chains, the trithiocarbonate group at the ω-chain end was first converted into a thiol functionality upon aminolysis with an excess of *n*-butylamine in THF (Scheme III-2 (**2**)). The conversion of this reaction was followed *via* UV-Vis spectroscopy, as the trithiocarbonate group has a characteristic absorbance at 310 nm while the thiol does not absorb.[40] After two hours, complete disappearance of the signal at 310 nm was observed, reflecting the complete conversion of the trithiocarbonate into a thiol (Figure III-3). Also MALDI-TOF MS analysis confirmed the successful deprotection of the thiol and revealed that no disulfides were formed during the reaction. Moreover, SEC analysis showed that the molecular weight distribution showed no significant shift, confirming the absence of double molar mass polymers coupled *via* disulfide formation (Figure III-2).

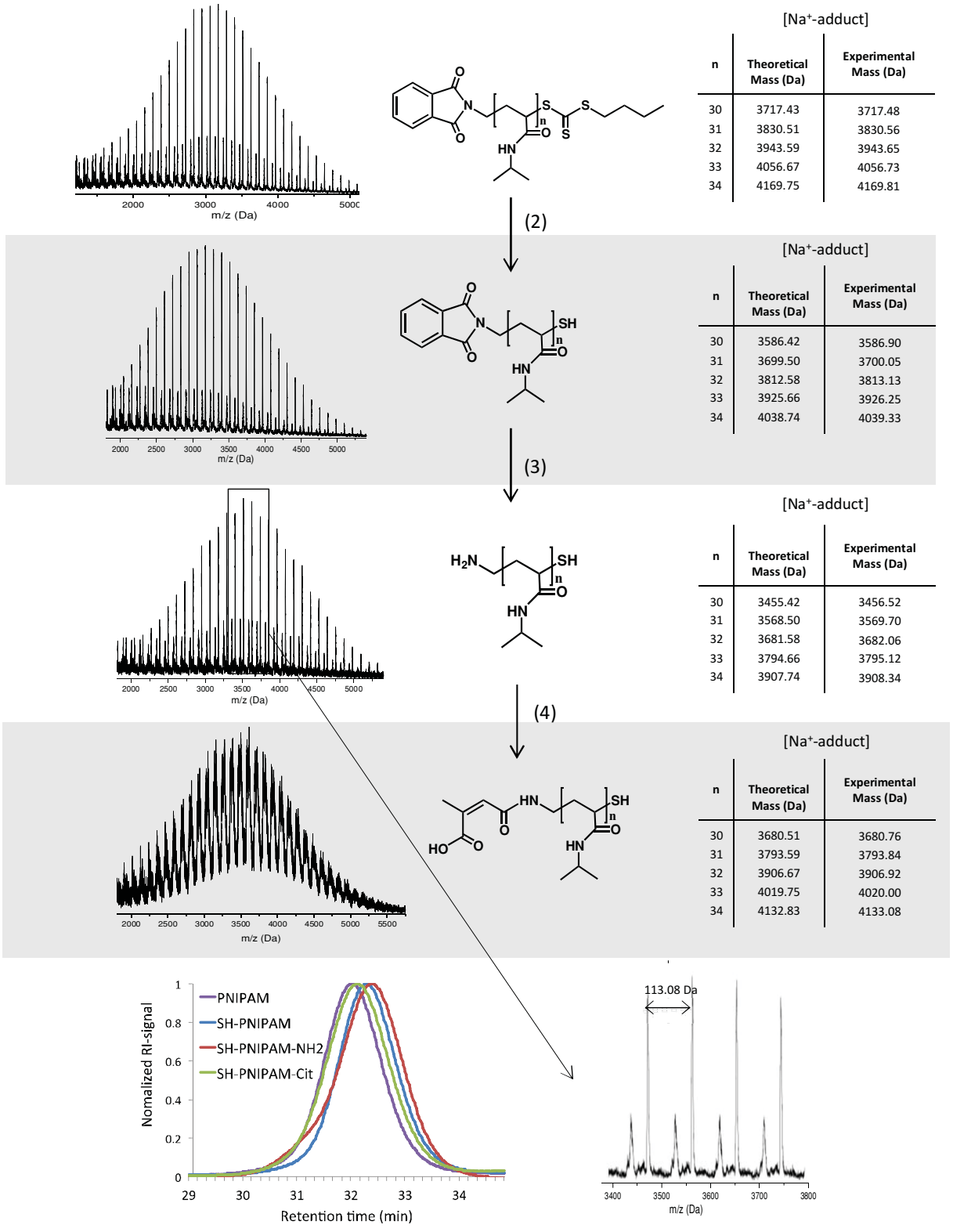

Figure III-2: MALDI-TOF analysis of PNIPAM (top), SH-PNIPAM (upper middle), SH-PNIPAM-NH_2 (lower middle) and SH-PNIPAM-Cit (bottom). The experimental masses are in good agreement with the theoretical masses, confirming the presence of end-groups during each step. SEC analysis shows that the dispersity during each step remains low (no disulfide formation).

The third and last step for the synthesis of heterotelechelic poly(acrylamide)s is the isolation of the primary amine by hydrolysis of the phthalimido functionality at the α-chain end (Scheme III-2, (**3**)). The polymer obtained after aminolysis was reacted overnight with potassium hydroxide in refluxing *tert*-butanol. In this step, known from the Gabriel synthesis, *tert*-butanol not only acts as a solvent but also as a reactant.[35] Again, quantitative conversion was proven *via* ^{1}H NMR spectroscopy and MALDI-TOF MS analysis.

The characteristic ^{1}H NMR chemical shifts of the phthalimido group at δ 7.70 and 7.85 ppm completely disappeared after hydrolysis, proving the conversion into the α-amine (Figure III-4). Due to overlay of the broad signal of the polymer backbone, the primary amine could not be assigned to its chemical shift, typically appearing between δ 2.0 and 4.0 ppm. The presence of the primary amine at the α-chain end was also confirmed *via* MALDI-TOF MS measurements (Figure III-2). A nearly symmetrical distribution is observed with a repeating mass difference of 113.08 Da, corresponding to one NIPAM repeating unit. Besides the main (Na^{+})-distribution, which proves the conversion to the α-amine, a minor distribution is observed, again attributed to fragmentation reactions during the MALDI-ionization process.

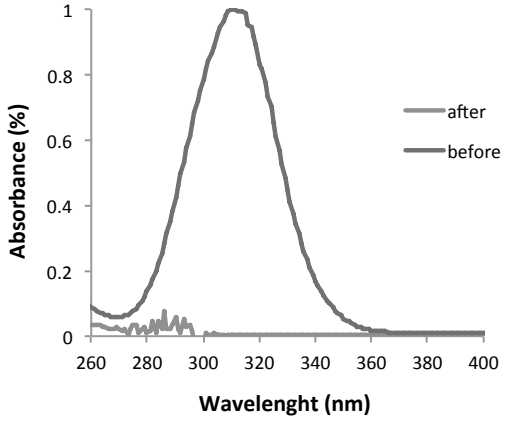

Figure III-3: UV-Vis spectra of PNIPAM before (dark grey) and after (light grey) aminolysis with n-butylamine (Scheme III-2 (1)), indicating full conversion.

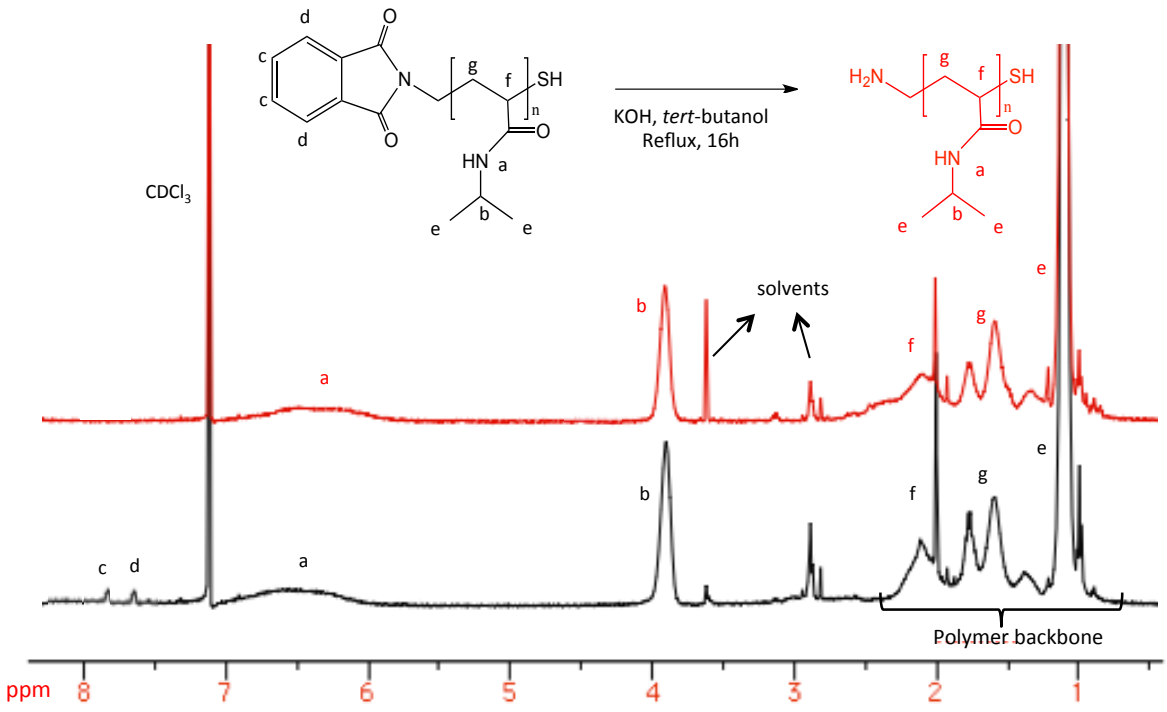

Figure III-4: ^{1}H NMR ($CDCl_3$; 500 MHz) of PNIPAM before (black) and after (red) hydrolysis of the phthalimido-group. The typical signals from the phthalimide functionality at 7.7 and 7.8 ppm disappeared after the reaction, confirming the completion of the reaction.

III.3 Grafting the heterotelechelic polymers onto gold particles

As proof of concept that the heterotelechelic SH-PNIPAM-NH_2 polymers can be used for the design of 'intelligent' higher order structures, we aimed at creating dual-responsive polymer/gold nanohybrids. Although it is known that polymer chains obtained by RAFT could be directly grafted onto gold particles *via* the CTA group[41, 42], we opted to reduce the CTA into a thiol to avoid uncontrolled side reactions of the primary amines onto the CTA.[43, 44] Moreover, the same thiol group could be applied for further post-polymerization modification through thiol-X chemistries (not part of this study).[45, 46] This part of the chapter reports the work that was done in collaboration with Zhiyue Zhang from the group of Prof. Dr. Bruno De Geest (Department of Pharmaceutics, Ghent University).

Citrate stabilized gold nanoparticles can be easily modified with polymers that have a thiol end-group *via* ligand exchange, leading to a quasi covalent bond between sulphur and metallic gold.[47, 48] The stability of a gold nanoparticles solution can be visually assessed from the change of its plasmonic properties, with citrate based gold nanoparticles (goldNP) prepared via direct reduction in the presence of an excess of citrate exhibiting a typical surface plasmon peak at 520 nm (leading to a reddish colour) for particles with a mean diameter of about 13 nm (Figure III-5). Upon destabilization and agglomeration of the particles, the colour of the solution turns blue and finally colourless when the particles fully precipitate from solution.

We found that these citrate stabilized goldNP cannot be decorated with SH-PNIPAM-NH_2 due to electrostatic interaction between the NH_2 groups and the citrate ions on the goldNP surface or by direct adsorption of the NH_2 groups on the metallic gold surface. Both phenomena lead to irreversible aggregation of the goldNP from solution. This prompted us to reason whether we could engineer the polymer coating in such a way that we could convert the NH_2 group to a carboxylic acid group to avoid agglomeration while a physiologically relevant stimulus could be used to reveal the original NH_2 group and destabilize the goldNP solution.

To address this aim, we modified the terminal primary amine group of the SH-PNIPAM-NH_2 with citraconic anhydride (further denoted as SH-PNIPAM-Cit) as shown in Scheme III-2 **(4)**, which converts the primary amine to an amide with a pending carboxylic acid group. MALDI-TOF MS analysis confirms the complete conversion of this modification reaction while SEC analysis provides evidence that no diblocks were formed through disulfide formation between two polymer chain ends (Figure III-2). Interestingly, the amide moiety hydrolyzes under acidic conditions, revealing the original NH_2 group.[49, 50]

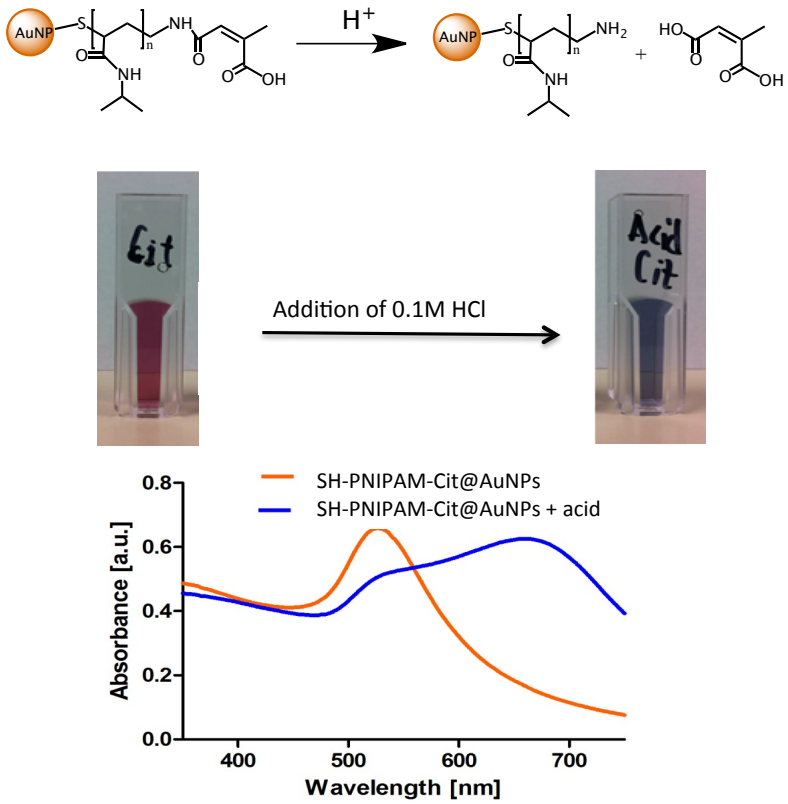

Figure III-5: The SH-PNIPAM-Cit is grafted onto the goldNP via a ligand exchange reaction without compromising their colloidal stability. The citraconic acid moiety could be hydrolysed into the original NH2 polymer end-group under acid conditions inducing a shift in the plasmon peak.

The resulting SH-PNIPAM-Cit could be grafted onto the goldNP without compromising their colloidal stability as was evidenced by the fact that after polymer grafting, the goldNP could be repeatedly centrifuged and redispersed in pure water without a visual shift in colour. On the contrary, bare citrate goldNP irreversibly aggregated when the excess of citrate is removed *via* centrifugation and redispersion. Next we assessed whether these goldNPs could respond to stimuli of

temperature and pH. Temperature-responsive behavior of the polymer coated gold nanoparticles was measured in aqueous medium containing 0.1 M NaCl. Recently Zhang and co-workers reported on the effect of salt on the temperature-responsive properties of PNIPAM coated citrate based gold nanoparticles.[51] In pure water, the particles remain stabilized at any temperature due to electrostatic repulsion of the remaining citrate ions on the goldNP surface. However, in the presence of salt the electrostatic charges are screened and the PNIPAM grafted goldNP do show aggregation above the T_{cp} of the PNIPAM.

Figure III-6 depicts the shift in plasmon peak to higher wavelengths upon heating of the particle solution from an initial value of 526 to 554 nm. This is also visually confirmed by the shift from red to pink of the particle solution. DLS measurements provide evidence that agglomerates are formed as the particle size increases from 43 nm to 400 nm (Figure III-7). Secondly, we assessed whether a pH drop could be used to trigger destabilization of the SH-PNIPAm-Cit decoated goldNP. Therefore we lowered the pH of the solution by adding a small portion of 0.1 M HCl (100 µL; final pH = 1.4), which hydrolysed the amide functionality of the citraconic acid moiety and restored the NH_2 polymer end-group. Immediately the goldNP solution turned bluish.

The corresponding shift in plasmon peak from 526 to 533 nm is depicted in Figure III-5, along with the visual colour shift of the particle solution. Interestingly, the pH induced shift is much larger than the temperature-induced shift, indicating a stronger plasmon coupling, likely due to the formation of larger agglomerates. These observations are confirmed by DLS measurements which show the presence of aggregates with a size of 1056 nm. Control experiments with SH-PNIPAM-COOH, also prepared *via* RAFT, but using a carboxylic acid functional CTA, showed goldNP decorated with this polymer to remain stable at acidic pH.

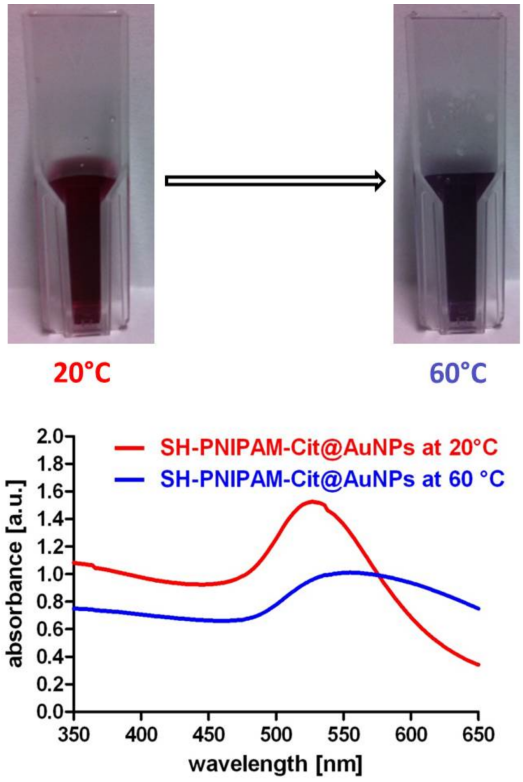

Figure III-6: The shift in plasmon peak from an initial value of 526 to 554 nm upon heating of the particle solution from room temperature to 60°C as a result of the thermo-responsive character of the grafted gold nanoparticles.

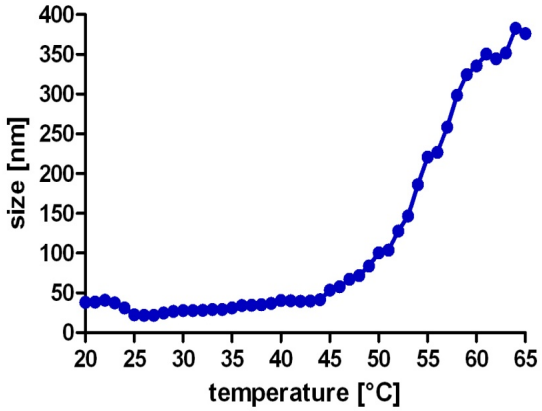

Figure III-7: DLS-spectrum of the particle solution in aqueous medium (0.1M NaCl) measured using a temperature program in which the temperature increases from 20°C to 65°C at a rate of 1 °C/min.

Summarizing, these data show that the presence of the different end groups on the heterotelechelic, thermo-responsive polymer, SH-PNIPAM-NH_2, allow the design of goldNP with dual temperature and pH-responsive properties.

III.4 Functionalization of the heterotelechelic polymer to obtain thermo-responsive sensors

During the last decades, there is an increased interest in smart functional materials due to the desire to control and create systems that adapt or respond to the environment.[52, 53] Such materials are playing an important role in diverse application fields such as biotechnology,[54, 55] drug delivery[56, 57] and particle transport[58]. Moreover, it is known that stimuli-responsive polymer systems facilitate the efficient transduction mechanisms making them suitable for use in sensor applications.[52, 59, 60] As proof of concept of this project, both chain-ends of the heterotelechelic polymer are functionalized with a compatible dye generating thermo-responsive dye sensors (Scheme III-3). Disperse red 1 acrylate (DR1A) is synthesized and reacted with the thiol functionality of the polymer upon thiol-Michael click reaction, while the amine moiety remained unreacted. On the other hand, the α-chain end could be functionalized with rhodamine B isothiocyanate (RITC) *via* a straightforward reaction, leaving the thiol available for other modification reactions.

PNIPAM structures with different molecular weight are synthesized according to Scheme III-2, (**1**). Low dispersities and molecular weights, which are in good agreement with the theoretical masses, are observed using SEC and MALDI-TOF MS analysis. Both aminolysis and hydrolysis are performed as described in section III.2. UV-Vis and MALDI-TOF MS confirmed the complete conversion of all trithiocarbonate groups to thiol functionalities, while combination of NMR (^{1}H and ^{13}C) with MALDI-TOF MS prove the full hydrolysis of the phthalimide chain-ends to primary amines.

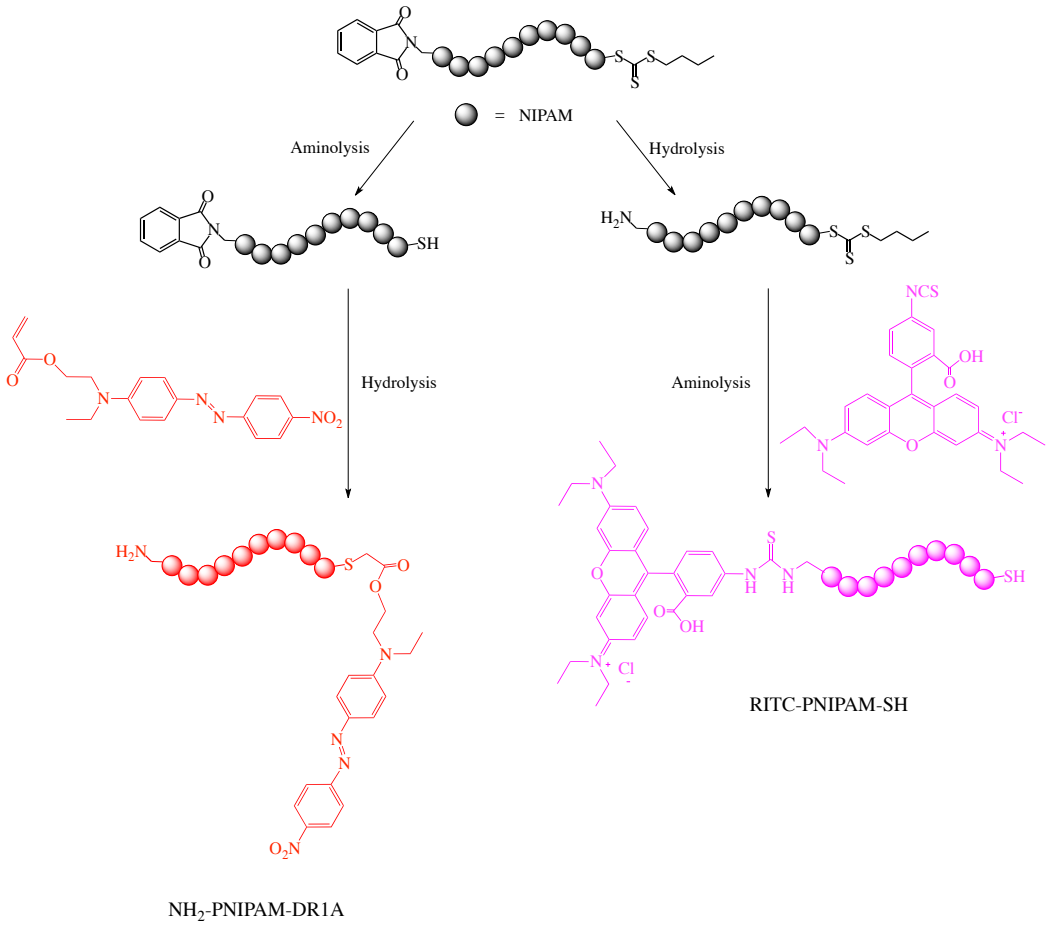

Scheme III-3: Overview of the different steps of the synthesis strategy of two different thermo-responsive dye sensors.

For the synthesis of the NH_2-PNIPAM-DR1A dye sensors, disperse red 1 acrylate is synthesized by the esterification of the hydroxy group of disperse red 1 with acryloyl chloride (Figure III-8). In the next step, this dye functionalized acrylate is clicked with the thiol chain-end of PNIPAM-SH by a thiol-Michael type click reaction. It is expected that the incorporation of the pH-responsive solvatochromic dye (disperse red 1) into the polymer leads to not only thermo- but also to pH-responsiveness, due to dye's sensitivity to changes in solvent polarity (Figure III-9). This phenomenon is the result of the interaction between the solute and the solvent causing a shift in the tautomeric equilibrium accompanied by a change in the energy difference between the ground and excited states.[61]

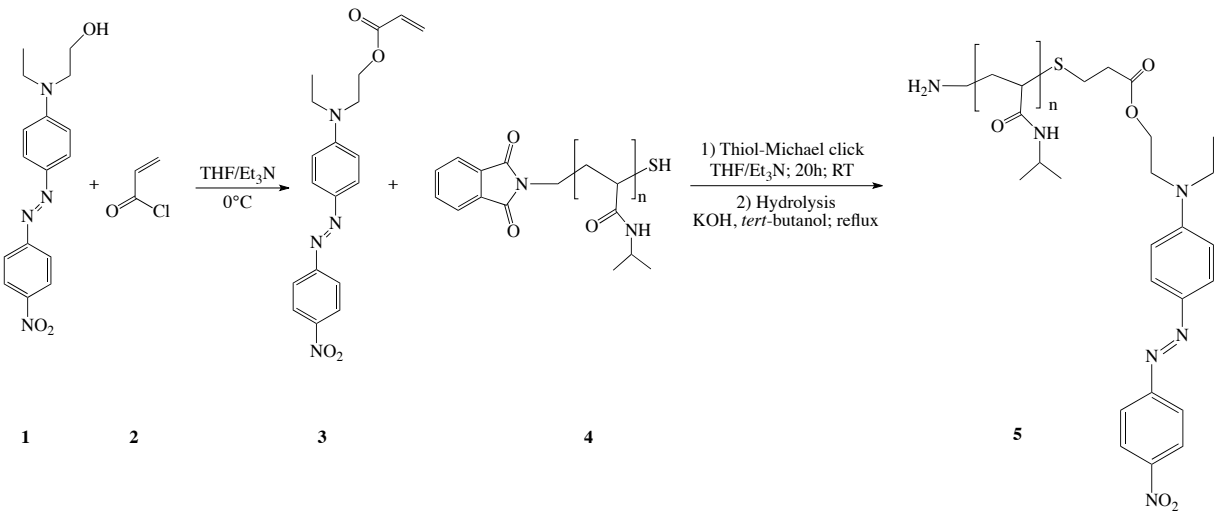

Figure III-8: Synthesis of disperse red 1 acrylate (DR1A; 3) and subsequent thiol-Michael click reaction with PNIPAM-SH (4) to yield a dual pH- and thermo-responsive polymers (5).

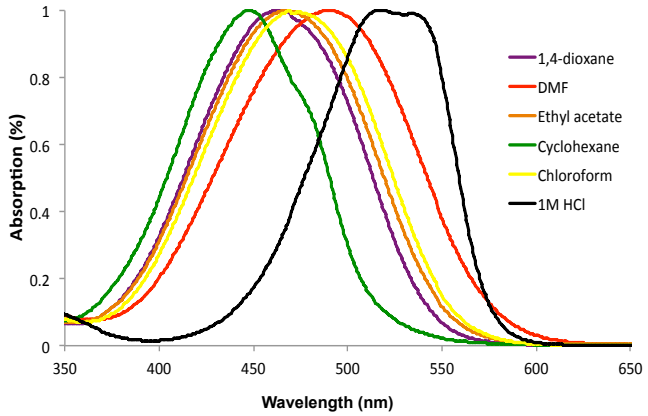

Figure III-9: Solvatochromic behavior of disperse red 1 acrylate in different solvents: upon changing the polarity of the solvent, the maximum absorption wavelength (color) of the dye solution changes.

During the SEC analysis with a diode array detector (DAD) of the different PNIPAM structures, UV-spectra were recorded resulting both in 3D-plots of the UV absorbance (µAU) as a function of the retention time (min) and wavelength (nm) as well as in the corresponding contour diagrams (Figure III-10). The 3D-plot indicates the covalent incorporation of the disperse red 1 acrylate in the PNIPAM structure. The polymer before modification, which is active at a wavelength of 310 nm (due to the presence of the phthalimide chain-end) has the same retention time (19.5 min) as the DR1A modified polymer, which is active at a wavelength of 480 nm. Besides the polymer signal, the 3D plot also reveals the DR1A UV-spectrum at a retention time of 22.5 min indicating that a small fraction of unreacted DR1A is still present in the isolated polymer, which further is not problematic for the testing of the thermo-responsive sensor, due to its low concentration.

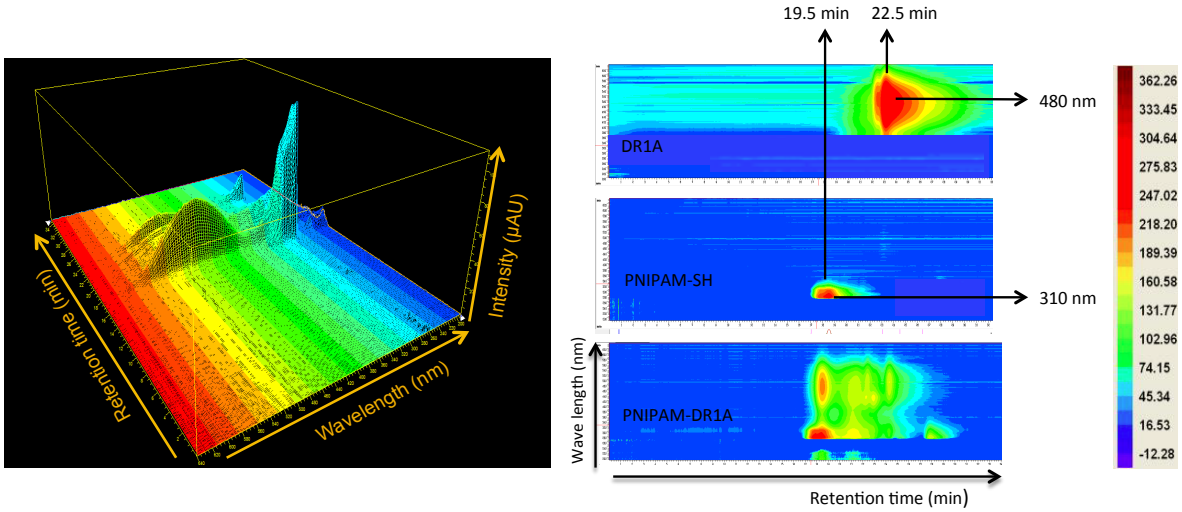

Figure III-10: DAD-SEC trace showing the absorbance intensity (µAU) as a function of the retention time (min) and the wavelength (nm) for NH_2-PNIPAM-DR1A (left); Contour diagrams of disperse red 1 acrylate, PNIPAM-SH and PNIPAM-DR1A (right).

As the molecular weight of the polymers is kept low (≤ 3.6 kDa), it is expected that the cloud point temperature (T_{cp}) of the polymers slightly changes upon changing the chain-end of the polymer. Transmission measurements indeed show indeed that T_{cp} after aminolysis increases 6°C. Incorporation of DR1A does decrease the T_{cp} to 29°C, while hydrolysis of the phthalimide chain-end sets the T_{cp} at 42°C. This is an important observation to consider in the application as thermo-responsive sensor (Figure III-11).

Code	$Mn_{,GPC}$ [g/mol]	$Mn_{,MALDI-TOF}$ [g/mol]	Đ	T_{cp} [°C]
PNIPAM	6200	3350	1.15	32
PNIPAM-SH	6150	3300	1.18	38
PNIPAM-DR1A	6300	3600	1.20	29
NH2-PNIPAM-DR1A	6700	3500	1.22	42

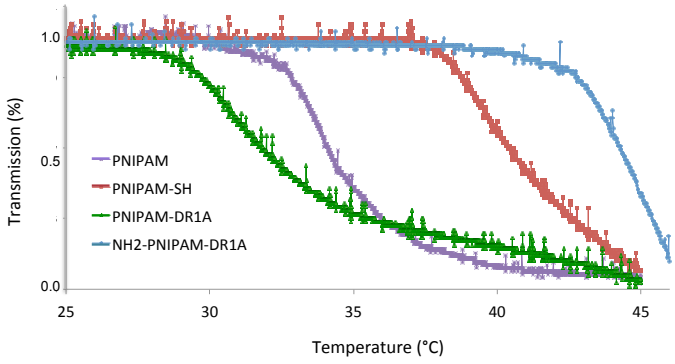

Figure III-11: Cloud point temperature determination via transmisssion measurements of PNIPAM, PNIPAM-SH, PNIPAM-DR1A and NH_2-PNIPAM-DR1A (bottom). Determination of molecular weight and dispersity of the polymer after each modification step (top).

To evaluate the sensing capabilities of this thermo-responsive polymeric dye, a biphasic aqueous/organic system was used. However, finding the selective organic solvent was cumbersome, as the solvent should fulfill several characteristics. Firstly, it must be immiscible with water and secondly it must solubilize PNIPAM-DR1A above the T_{cp}. However, the affinity of the solvent towards the polymeric dye should be limited below T_{cp}, such that after cooling the two-phase system to room temperature, PNIPAM-DR1A returns to the aqueous phase. Finally it must have a relatively high boiling point as the system needs be heated above the T_{cp} value.[37] From earlier studies, it is known that the only solvent that fulfills these conditions is ethyl acetate. Figure III-12 gives a schematic overview of the different steps of the sensing capabilities of the thermo-responsive polymeric dye in a biphasic system.

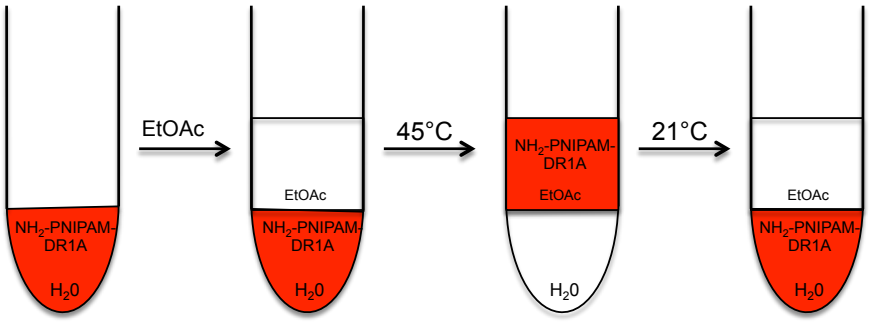

Figure III-12: General principle of the use of the thermo-responsive polymeric dye NH_2-PNIPAM-DR1A in a biphasic system below and above the T_{cp}.

Below the T_{cp} (at room temperature), the polymeric dye prefers to stay in the aqueous phase as it is in completely hydrated state as a result of the strong specific intermolecular interactions (hydrogen bonds) between the polymer chain and the solvent molecules. The lower layer of the two-phase system is hereby coloured red while the upper layer stays colourless. When heating above the T_{cp}, the PNIPAM-DR1A migrates to the EtOAc phase as a result of the thermo-responsive character, resulting in a red organic phase while the aqueous has became colorless. This indicates visually that most of the polymer chains migrated to the organic phase, which is confirmed by SEC analysis. By cooling down again to temperatures under the T_{cp} (21°C, room temperature), the polymeric dye migrates again to the aqueous phase, making it red, while the organic phase turns colorless. This procedure shows the capability of the polymeric dye to be used as a thermo-responsive sensor. The presence of the primary amine at the α-chain end makes it possible to use this thermo-responsive polymeric dye in fields such as surface science, adhesion and various biomedical applications.

For the synthesis of the thermo-responsive RITC-PNIPAM-SH polymers, hydrolysis of the phthalimide functionality and subsequent introduction of the commercially available RITC were performed before aminolysis of the trithiocarbonate (Scheme III-3). The covalent incorporation of this dye colors the polymer pink. SEC/DAD analysis confirms this covalent linking upon thiourea formation as the polymer signal shows an absorption at 550 nm, which corresponds with a RITC labeled polymer (Figure III-13).

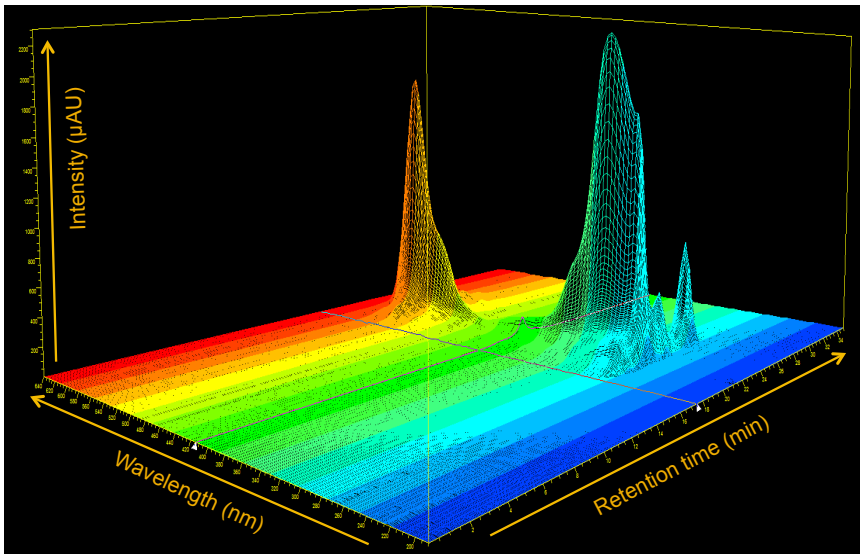

Figure III-13: :DAD-SEC trace showing the absorbance intensity (µAU) as a function of the retention time (min) and the wavelength (nm) for RITC-PNIPAM-SH, confirming the covalent incorporation of the dye in the polymer structure.

Turbidimetry analysis was again applied for the determination of the T_{cp} of the polymer structure. However, it was seen that the transition was not sharp, which is unexpected for PNIPAM structures (Figure III-14). Nevertheless, the sensing capacities of this thermo-responsive polymeric dye were tested, again using a EtOAc/H_2O biphasic system (same procedure as shown in Figure III-12). It was seen that when heated above the T_{cp} the polymeric dye migrates to the organic phase, but when cooling down again, the polymeric dye does not go back to aqueous phase. Most probably, this polymeric dye shows a high affinity for the organic phase, which makes the return to the aqueous phase difficult. Moreover, the unsharp transition of the polymers also contributes to this irreversible transition. An extensive search towards other potential solvents, which would fulfill the requirements for the organic phase, did not yield any solution.

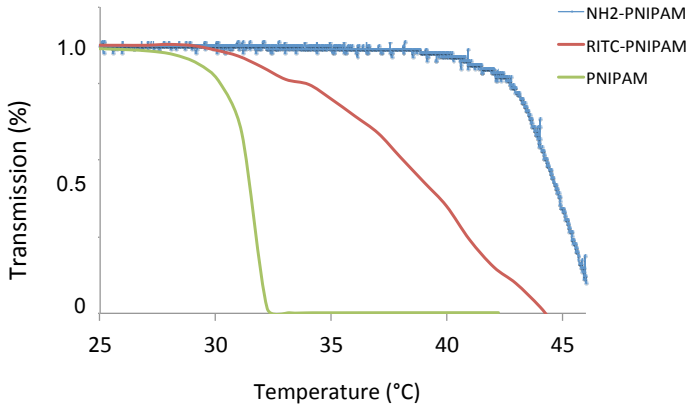

Code	$Mn_{,GPC}$ [g/mol]	Đ	T_{cp} [°C]
PNIPAM	6200	1.15	32
NH_2-PNIPAM	6200	1.20	44
RITC-PNIPAM	6500	1.23	n.d
RITC-PNIPAM-SH	6550	1.27	33-36

**n.d= not determined.*

Figure III-14: Determination of molecular weight and dispersity of the different polymer structures via SEC analysis (PMMA standards) (bottom) and turbidimetry analysis of RITC-PNIPAM-SH for the determination of the cloud point temperature (top).

It can be concluded that NH_2-PNIPAM-DR1A is a good thermo-responsive polymeric sensor in the applied two-phase system, while RITC-PNIPAM-SH does not show a reversible character, which limits its sensing capabilities.

III.5 Conclusion

A straightforward and versatile method for the synthesis of heterotelechelic poly(acrylamide)s containing an α-amine and a ω-thiol was demonstrated. Therefore, PNIPAM and PDMA macromolecules are synthesized *via* RAFT using a phthalimido CTA. After aminolysis, the phtalimido functionality was hydrolysed into a primary amine, yielding α-amino-ω-thiol heterotelechelic polymers. This approach provides polymers with well-defined structures (architecture and molecular weight distribution) and high end-group fidelity at each step, proven by MALDI-TOF MS analysis and ^{1}H NMR spectroscopy. These heterotelechelic polymers were modified and used to create dual-responsive polymer/gold nanohybrids by grafting them onto gold nanoparticles *via* ligand exchange between the thiol end-group of the polymer and the metallic gold.

Furthermore, incorporation of disperse red 1 acrylate at the α-chain end of the PNIPAM structure yielded a thermo-responsive polymeric dye whose sensing capacities are confirmed by using a biphasic aqueous/organic system below and above the cloud point temperature of the polymeric structure.

III.6 Experimental part

III.6.1 Materials

1-Butanethiol (Aldrich, 99%), carbon disulfide (Aldrich, ≥99%), *N*-(bromomethyl)phthalimide (Aldrich, 97%), chloroform (Aldrich, HPLC grade), triethylamine (Aldrich, HPLC grade), tetrahydrofuran (THF) (Aldrich, HPLC grade), dry DMF (Aldrich, 99.8%) *n*-hexane (Aldrich, HPLC grade), toluene (Aldrich, HPLC grade), H_2SO_4 (Aldrich, 99.9%), potassium hydroxide (KOH) (Aldrich, 90%), *tert*-butanol (Aldrich, ≥ 99%), citraconic anhydride (Aldrich, 98%), $HAuCl_4$ (Aldrich, 99.9%), acryloyl chloride (Aldrich, 97%), disperse red 1 (Aldrich, 95%), rhodamine B isothiocyanate (Aldrich, mixed isomers) were used as received. *N*-Isopropyl acrylamide (NIPAM) (Aldrich) was recrystallized twice from a 50/50 toluene/*n*-hexane mixture. Dimethyl acrylamide (DMA) (Aldrich, 99%) was stripped from the inhibitor by passing over basic alumina before use. 2,2'-Azobis(isobutyronitrile) (AIBN) (Aldrich) was recrystallized twice from methanol. 1,4-Dioxane (Aldrich, HPLC grade) was dried by distillation from sodium/benzophenone. Citrate stabilized gold nanoparticles were synthesized according to literature and their size was measured *via* TEM to be 13 nm.[62]

III.6.2 Characterization and equipment

Nuclear magnetic resonance (^{1}H- and ^{13}C-NMR) spectra were recorded at 300 or 500 MHz in $CDCl_3$ (Eurisotop) solution at room temperature on a Bruker Avance 300 or Bruker DRX500 spectrometer, respectively. Chemical shifts are presented in parts per million (δ) relative to $CHCl_3$ (7.26 ppm in ^{1}H- and 77.2 ppm in ^{13}C NMR) as internal standard. Coupling constants (J) in ^{1}H NMR spectra are given in Hz. The resonance multiplicities are described as s (singlet), d (doublet), t (triplet), q (quartet) or m (multiplet).

Size-exclusion chromatography (SEC) was performed on a Agilent 1260-series HPLC system equipped with a 1260 online degasser, a 1260 ISO-pump, a 1260 automatic liquid sampler (ALS), a thermostatted column compartment (TCC) at 50°C equipped with a PSS Gram30 column in series with a PSS Gram1000 column, a 1260 diode array detector (DAD) and a 1260 refractive index detector (RID). The used eluent was DMA containing 50mM of LiCl at a flow rate of 1 mL/min. The

spectra were analyzed using the Agilent Chemstation software with the SEC add on. Molar mass and PDI values were calculated against Varian PS standards.

UV-Vis measurements were performed on an AnalytikJena Specord 200 in quartz cuvettes with a thickness of 10 mm at a wavelength range of 200 to 700 nm. The concentration of each sample was 1 mg/mL.

Matrix assisted laser desorption/ionization time of flight mass spectroscopy (MALDI-TOF MS) was performed on an Applied Biosystems Voyager De STR MALDI-TOF mass spectrometer equipped with 2 m linear and 3 m reflector flight tubes, and a 355 nm Blue Lion Biotech Marathon solid state laser (3.5 ns pulse). All mass spectra were obtained with an accelerating potential of 20 kV in positive ion and in reflectron mode. *Trans*-2-[3-(4-*tert*-butylphenyl)-2-methyl-2-propenylidene]malononitrile, (DCTB) (30 mg/mL in DCM) was used as a matrix, NaTFA (19 mg/mL in acetone) was used as a cationizing agent, and polymer samples were dissolved in THF (4 mg/mL). Analyte solutions were prepared by mixing 10 µL of the matrix, 10 µL of the polymer and 1 µL of the salt solution. Subsequently, 0.5 µL of this mixture was spotted on the sample plate, and the spots were dried in air at room temperature. A poly(ethylene oxide) standard (Mn = 2000 g/mol) was used for calibration. All data were processed using the Data Explorer 4.0.0.0 (Applied Biosystems) software package.

Dynamic light scattering (DLS) was performed on a Zetasizer Nano-ZS Malvern apparatus (Malvern Instruments Ltd) using disposable cuvettes. The excitation light source was a He−Ne laser at 633 nm, and the intensity of the scattered light was measured at 173°. This method measures the rate of the intensity fluctuation and the size of the particles is determined through the Stokes−Einstein equation. Grafted gold particle solutions with a concentration of 0.18 mg/mL were measured in both aqueous (0.1 M NaCl) and acidic media. For the sample in aqueous media, a temperature program was set up in which the temperature increases from 20°C to 65°C at a rate of 1 °C/min. The sample in acidic media was measured at 20°C. Before starting the measurements, samples were incubated for at least 300s to reach equilibrium. All samples were filtered through Millipore membranes with pore sizes of 0.2 µm prior to measurement.

III.6.3 Synthesis of the CTA: Butyl phthalimidomethyl trithiocarbonate

The compound was synthesized using the general procedure described elsewhere.[24] 1-Butanethiol (6.0 g, 0.066 mol), carbon disulfide (10.12 g, 0.132 mol) and chloroform (40 mL) were placed in a three-neck flask. To this mixture, triethylamine (13.8 g, 0.136 mol) was added dropwise and the solution was stirred for 3 hours. *N*-(bromomethyl)phthalimide was added slowly and the solution was stirred for another 16 hours. Next, the mixture was diluted with additional chloroform (50 mL) and washed with water, H_2SO_4, water and brine. Subsequently, the organic phase was dried over $MgSO_4$ and the solvent was evaporated under reduced pressure to give a yellow solid (yield: 91%). ^{1}H NMR ($CDCl_3$, 500.0 MHz); δ (ppm): 0.95 (t, 3H, C**H$_3$**-), 1.35 (m, 2H, CH_3C**H$_2$**CH_2CH_2-), 1.65 (m, 2H, CH_3CH_2C**H$_2$**CH_2-), 3.30 (t, 2H, -CH_2C**H$_2$**S-), 5.60 (s, 2H, N-C**H$_2$**-S), 7.70 (m, 2H, Ar**H**), 7.85 (m, 2H, Ar**H**). ^{13}C NMR ($CDCl_3$, 500 MHz); δ (ppm): 13.5 (**C**H_3-), 22.0 (CH_3**C**$H_2CH_2CH_2$-), 29.8 (CH_3CH_2**C**H_2CH_2-), 36.9 (-CH_2**C**H_2S), 41.9 (N**C**H_2S), 123.7 (2 × *o*-Ph, **C**H), 131.8 (2 × Ph, **C**), 134.4 (2 × *p*-Ph, **C**H), 166.6 (**C**O), 220.8 (**C**S_3). M.W.= 325.0 g/mol; ESI-MS (m/z): 326.0 g/mol [M+H$^+$].

III.6.4 RAFT Polymerization of NIPAM or DMA

In a typical experiment, NIPAM (5.2 g, 0.046 mol) or DMA (4,56 g, 0.046 mol), CTA (0.5 g, 0.00154 mol), AIBN (0,0278 g, 0,169 mmol) as the thermal initiator ($[CTA]_0$:$[AIBN]_0$ = 1:0.11) and dry 1,4-dioxane were placed in a 20 mL Schlenk flask, which was degassed by three freeze-pump-thaw cycles, backfilled with nitrogen, sealed and heated under stirring to 65°C. After 3 hours, the reaction was quenched by placing the flask in an ice/water bath under air. The polymer was isolated by a two-fold precipitation in cold diethyl ether and dried under vacuum, yielding a slightly yellow fine powder.

III.6.5 Aminolysis of the trithiocarbonate group (SH-PNIPAM)

The polymer was reacted with an excess (30 equivalents) *n*-butylamine in THF for two hours. The color of the solution changed from light yellow to colorless. A few drops of *n*-tributylphosphine were added to the mixture to minimize disulfide formation. The polymer was subsequently isolated by two-fold precipitation in cold diethyl ether and obtained as a white solid after drying.

III.6.6 Hydrolysis of the phthalimide α-chain end (SH-PNIPAM-NH_2)

After aminolysis, the polymer and 10 equivalents of potassium hydroxide were added to refluxing *tert*-butyl alcohol. After 16 hours of refluxing, the solvent was evaporated and 10 mL of water was added. The obtained aqueous phase was acidified to pH 2, extracted with dichloromethane (3 x 20 mL) and then lyophilized to obtain a white solid.

III.6.7 Synthesis of Citraconic Amide Substituted SH-PNIPAM-NH_2 (SH-PNIPAM-Cit)

SH-PNIPAM-NH_2 (44 mg, 0.011 mmol) was dissolved in 3 mL of 1M NaOH solution and stirred overnight. Citraconic anhydride (472 µL, 5.25 mmol) was added dropwise to the SH-PNIPAM-NH_2 solution, and the reaction mixture was stirred overnight at room temperature. Meanwhile, 1M NaOH was added to maintain the pH of reaction solution above 8 during the reaction. After that, the resulting mixture was dialyzed against water (adjusted to pH > 8 using 1M NaOH) for 4 days and lyophilized to yield the final product as a white powdery solid.

III.6.8 SH-PNIPAM-Cit coating of gold nanoparticles

4.4 mg of SH-PNIPAM-Cit was dissolved in 100 µL of 1 wt% sodium citrate (pH > 8), then added to 4 mL of a citrate stabilized gold nanoparticles solution and stirred overnight at room temperature. The resulting conjugates were purified three times by centrifugation at 4°C with 10 000 rpm for 30 min, followed by redispersion in water (adjusted to pH > 7 using NaOH).

III.6.9 Synthesis of disperse red 1 acrylate (DR1A)

To a solution of 1.0 g (3.2 mmol) disperse red 1 (DR1) in 50 mL of anhydrous THF, 1.46 mL of triethylamine (10.5 mmol) were added followed by a dropwise addition of acryloyl chloride (0.77 mL, 9.5 mmol). The resulting mixture was stirred at 0°C and allowed to heat up to room temperature during 24 hours. Subsequently, the solvent was evaporated under reduced pressure and the solid residue was solved in diethyl ether (50 mL) and washed with water (3 x 50 mL). After evaporation of the diethyl ether, the crude product DR1-acrylate (DR1A) was purified by silica gel chromatography eluting with dichloromethane. ^{1}H NMR ($CDCl_3$, 500.0 MHz); δ (ppm): 1.25 (s, 3H, C**H$_3$**CH_2N-), 3.53 (q, 2H, CH_3C**H$_2$**N-), 3.69 (t, 2H, -NC**H**$_2$$CH_2$O-), 4.32 (t, 2H, -$NCH_2$**$CH_2$**O-), 5.70 (d, 1H, -COCH**CH**$_2$), 6.15 (q,

1H, -CO**CH**CH_2), 6.30 (d, 1H, -COCH**C**$\mathbf{H}_2$), 6.80 (d, 2H, -Ph**H**), 7.91 (dd, 4H, -Ph**H**), 8.35 (d, 2H, Ph**H**-NO_2). M.W.= 369.34 g/mol; ESI-MS (m/z): 371.0 g/mol [$M+H^+$].

III.6.10 Synthesis of PNIPAM-DR1A

PNIPAM-SH (1 g; 0.3 mmol) was dissolved in a mixture of anhydrous THF (100 mL) and Et_3N (0.2 mL; 1.5 mmol) and stirred for 30 min under inert atmosphere. DR1A (0.6 g; 1.5 mmol) was added and the red mixture was stirred overnight at room temperature. The polymer was isolated by two-fold precipitation in cold diethyl ether and dried under vacuum yielding a red powder.

III.6.11 Synthesis of RITC-PNIPAM

A solution of 500 mg of NH_2-PNIPAM (0.17 mmol) in 60 mL borate buffer (0.1 M – pH 8.5 – 9.5) and a solution of 0.18 mg of rhodamine B isothiocyanate (0.33 mmol) in 60 mL borate buffer were mixed and stirred overnight at room temperature under inert atmosphere. The resulting mixture was dialyzed against water for 5 days and lyophilized to yield the final product as a pink powdery solid.

III.7 References

[1] O. Shimoni, A. Postma, Y. Yan, A. M. Scott, J. K. Heath, E. C. Nice, A. N. Zelikin, F. Caruso, *Acs Nano* **2012**, *6*, 1463.
[2] L. Weipeng, Q. Junjie, F. Wengian, Z. Guoliang, Z. Fengbao, F. Xiaobin, *J. Mater. Chem.* **2012**, *22*, 11290.
[3] N. Akeroyd, B. Klumperman, *Eur. Polym. J.* **2011**, *47*, 1207.
[4] K. Matyjaszewski, J. H. Xia, *Chem. Rev.* **2001**, *101*, 2921.
[5] C. J. Hawker, A. W. Bosman, E. Harth, *Chem. Rev.* **2001**, *101*, 3661.
[6] J. Chiefari, Y. K. Chong, F. Ercole, J. Krstina, J. Jeffery, T. P. T. Le, R. T. A. Mayadunne, G. F. Meijs, C. L. Moad, G. Moad, E. Rizzardo, S. H. Thang, *Macromolecules* **1998**, *31*, 5559.
[7] G. Moad, E. Rizzardo, S. H. Thang, *Aust. J. Chem.* **2005**, *58*, 379.
[8] G. Moad, E. Rizzardo, S. H. Thang, *Aust. J. Chem.* **2009**, *62*, 1402.
[9] A. Favier, M.-T. Charreyre, *Macromol. Rapid Commun.* **2006**, *27*, 653.
[10] A. Gregory, M. H. Stenzel, *Prog. Polym. Sci.* **2012**, *37*, 38.
[11] K. Nilles, P. Theato, *Polym. Chem.* **2011**, *2*, 376.
[12] C. Barner-Kowollik, S. Perrier, *J. Polym. Sci. Pol. Chem.* **2008**, *46*, 5715.
[13] D. Roy, J. N. Cambre, B. S. Sumerlin, *Chem. Commun.* **2008**, 2477.
[14] G. Moad, E. Rizzardo, S. H. Thang, *Polym. Int.* **2011**, *60*, 9.
[15] M. A. Harvison, A. B. Lowe, *Macromol. Rapid Commun.* **2011**, *32*, 779.
[16] X. Xiong, Z. Tang, L. Cai, *Prog. Chem.* **2012**, *24*, 1751.
[17] H. Xin, C. Boyer, T. P. Davis, V. Bulmus, *Polym. Chem.* **2011**, *2*, 1505.
[18] R. Guo, X. Wang, C. Guo, A. Dong, J. Zhang, *Macromol. Chem. Phys.* **2012**, *213*, 1851.
[19] W. Birnbaum, D. Kuckling, *Polym. Chem.* **2012**, *3*, 2039.
[20] Pankaj, M. Verma, S. Goyal, P. K. Patnala, *Mater. Sci. Forum* **2012**, *712*, 147.
[21] F. Croisier, C. Jerome, *Eur. Polym. J.* **2013**, *49*, 780.
[22] J. Xu, J. He, D. Fan, X. Wang, Y. Yang, *Macromolecules* **2006**, *39*, 8616.
[23] J. Jacobs, N. Gathergood, A. Heise, *Macromol. Rapid Commun.* **2013**, *34*, 1325.
[24] A. Postma, T. P. Davis, R. A. Evans, G. Li, G. Moad, M. S. O'Shea, *Macromolecules* **2006**, *39*, 5293.
[25] W. Loos, F. Du Prez, *Macromol. Symp.* **2004**, *210*, 483.
[26] N. A. Plate, T. L. Lebedeva, L. I. Valuev, *Polym. J.* **1999**, *31*, 21.
[27] X. Yin, A. S. Hoffman, P. S. Stayton, *Biomacromolecules* **2006**, *7*, 1381.
[28] J. G. McGrath, R. D. Bock, J. M. Cathcart, L. A. Lyon, *Chem. Mater.* **2007**, *19*, 1584.
[29] B. Brugger, W. Richtering, *Adv. Mater.* **2007**, *19*, 2973.
[30] T. Shiroya, N. Tamura, M. Yasui, K. Fujimoto, H. Kawaguchi, *Colloids Surf. B* **1995**, *4*, 267.
[31] J. P. Chen, A. S. Hoffman, *Biomaterials* **1990**, *11*, 631.
[32] Y. G. Takei, T. Aoki, K. Sanui, N. Ogata, T. Okano, Y. Sakurai, *Bioconjugate Chem.* **1993**, *4*, 341.
[33] Y. G. Takei, T. Aoki, K. Sanui, N. Ogata, T. Okano, Y. Sakurai, *Bioconjugate Chem.* **1993**, *4*, 42.
[34] A. Postma, T. P. Davis, G. Li, G. Moad, M. S. O'Shea, *Macromolecules* **2006**, *39*, 5307.
[35] S. Monge, O. Giani, E. Ruiz, M. Cavalier, J.-J. Robin, *Macromol. Rapid Commun.* **2007**, *28*, 2272.
[36] X. Wang, S. Li, Y. Su, F. Huo, W. Zhang, *J. Polym. Sci. Pol. Chem.* **2013**, *51*, 2188.
[37] S. Wallyn, M. Lammens, R. K. O'Reilly, F. Du Prez, *J. Polym. Sci. Pol. Chem.* **2011**, *49*, 2878.
[38] E. C. Dreaden, A. M. Alkilany, X. Huang, C. J. Murphy, M. A. El-Sayed, *Chem. Soc. Rev.* **2012**, *41*, 2740.
[39] J. Skey, R. K. O'Reilly, *Chem. Commun.* **2008**, 4183.
[40] K. Skrabania, A. Miasnikova, A. M. Bivigou-Koumba, D. Zehm, A. Laschewsky, *Polym. Chem.* **2011**, *2*, 2074.
[41] M. Liang, I. C. Lin, M. R. Whittaker, R. F. Minchin, M. J. Monteiro, I. Toth, *Acs Nano* **2010**, *4*, 403.
[42] I. C. Lin, M. Liang, T.-Y. Liu, M. J. Monteiro, I. Toth, *Nanomedicine-Nanotechnology Biology and Medicine* **2012**, *8*, 8.
[43] A. S. Duwez, P. Guillet, C. Colard, J. F. Gohy, C. A. Fustin, *Macromolecules* **2006**, *39*, 2729.
[44] A. Glaria, M. Beija, R. Bordes, M. Destarac, J.-D. Marty, *Chem. Mater.* **2013**, *25*, 1868.
[45] P. Theato, H.-A. Klok, "*Functional Polymers by Post-Polymerization Modification: Concepts, Guidelines and Applications*", 2012.
[46] K. A. Guenay, P. Theato, H.-A. Klok, *J. Polym. Sci. Pol. Chem.* **2013**, *51*, 1.
[47] S. Rucareanu, M. Maccarini, J. L. Shepherd, R. B. Lennox, *J. Mater. Chem.* **2008**, *18*, 5830.
[48] J. C. Love, L. A. Estroff, J. K. Kriebel, R. G. Nuzzo, G. M. Whitesides, *Chem. Rev.* **2005**, *105*, 1103.
[49] Y. Lee, S. Fukushima, Y. Bae, S. Hiki, T. Ishii, K. Kataoka, *J. Am. Chem. Soc.* **2007**, *129*, 5362.

[50] X. Liu, J. Zhang, D. M. Lynn, *Soft Matter* **2008**, *4*, 1688.
[51] Z. Y. Zhang, S. Maji, A. B. D. Antunes, R. De Rycke, Q. L. Zhang, R. Hoogenboom, B. G. De Geest, *Chemistry of Materials* **2013**, *25*, 4297.
[52] C. Pietsch, R. Hoogenboom, U. S. Schubert, *Angew. Chem.-Int. Edit.* **2009**, *48*, 5653.
[53] M. A. C. Stuart, W. T. S. Huck, J. Genzer, M. Muller, C. Ober, M. Stamm, G. B. Sukhorukov, I. Szleifer, V. V. Tsukruk, M. Urban, F. Winnik, S. Zauscher, I. Luzinov, S. Minko, *Nat. Mater.* **2010**, *9*, 101.
[54] S. Aoshima, S. Kanaoka, in *Nanocomposites, Stimuli-Responsive Polymers*, 2008, p. 169.
[55] E. S. Gil, S. M. Hudson, *Prog. Polym. Sci.* **2004**, *29*, 1173.
[56] C. Alexander, K. M. Shakesheff, *Adv. Mater.* **2006**, *18*, 3321.
[57] D. Schmaljohann, *Adv. Drug Deliv. Rev.* **2006**, *58*, 1655.
[58] E. W. Edwards, M. Chanana, D. Wang, H. Moehwald, *Angew. Chem.-Int. Edit.* **2008**, *47*, 320.
[59] C. Koopmans, H. Ritter, *J. Am. Chem. Soc.* **2007**, *129*, 3502.
[60] I. Roth, A. A. Jbarah, R. Holze, M. Friedrich, S. Spange, *Macromol. Rapid Commun.* **2006**, *27*, 193.
[61] L. De Boni, C. Toro, A. E. Masunov, F. E. Hernandez, *J. Phys. Chem. A* **2008**, *112*, 3886.
[62] J. Turkevich, P. C. Stevenson, J. Hillier, *Disc. Faraday Soc.* **1951**, *11*, 55.

Abstract

In this chapter, the findings on the use of thiol-yne chemistry for the preparation of hyperbranched polymers, starting from AB_2 oligomers, is reported. For this, two different approaches are followed. In the first approach, a suitable CTA, containing an alkyne functionality at the ω-chain end, is synthesized and evaluated on its polymerization capacities of different monomer types (styrene (S), *N*-isopropyl acrylamide (NIPAM), ethoxyethyl acrylate (EEA)). It was seen that for all type of monomers, a linear correlation between molar mass and conversion was present, while the polymers possess a narrow dispersity (≤ 1.25). Moreover, a high end-group fidelity was observed, even when no protecting group for the alkyne functionality was used during polymerization, when conversion was kept below 70%. Aminolysis of the typical trithiocarbonate group into a thiol functionality, yields the AB_2 oligomers (where A stands for a thiol and B_2 for a single alkyne functionality) with narrow dispersity. Photo (UV)-initiated thiol-yne chemistry was applied, yielding hyperbranched polymers. According to NMR, the degree of branching was relatively high, which implies only a little amount of internal double bonds remained in the hyperbranched structure, suggesting that the first step in the thiol-yne chemistry is the rate-determining step. In the second approach a monomer containing both an alkyne and thiolactone was synthesized. The thiolactone ring, which can be seen as a precursor for a thiol moiety, was opened upon aminolysis with an RAFT-derived oligomer containing a primary amine at the α-chain end. As such, AB_2 thiol-alkyne oligomers are formed and a new functionality is introduced into the structure. Again, photo(UV)-initiated thiol-yne chemistry was applied for the preparation of hyperbranched structures.

Chapter IV

Synthesis of hyperbranched polymers derived from RAFT-derived AB_2 oligomers

IV.1 Introduction

In Chapter II, the different synthesis methodologies of hyperbranched polymers and the unique properties of these structures are discussed extensively. It is clear that those polymers are expected to play an important role in different disciplines in both science and technology in the 21st century.[1] Despite the fact that these structures are already been used a lot the last decade, both in academic and industrial context, for more specific applications there is need for new synthesis strategies, which enable the introduction of new functionalities and thus enhanced properties. Moreover, the synthesis of the AB_n monomers is frequently not straightforward and requires multiple steps, which hamper the upscalability.

The introduction of controlled radical polymerization brought some major advantages for the preparation of hyperbranched polymers as it ensures high end-group fidelity and enables to fully capitalize the unique properties of the hyperbranched structures. To achieve this, it is generally beneficial to control the number of branch points and the length of the branches such that the overall macromolecular properties can be tuned.[2] Fréchet *et al.* proposed the principles of self-condensing vinyl polymerization wherein an AB* inimer containing both a polymerizable double bond (A) and an initiating moiety (B*) participate in the homopolymerization or copolymerization with other monomers resulting in highly branched structures.[3]

Up to now, plenty of reports demonstrate its synthetic capacities to facilitate the good control over branched polymer architectures in combination with controlled radical polymerization (CRP). For example, Fréchet *et al.* synthesized the first hyperbranched polymers (polystyrenes) *via* nitroxide-mediated radical polymerization (NMP)[4], while Matyjaszewski and other researchers prepared hyperbranched polystyrenes[5, 6] and hyperbranched polyacrylates[7] *via* atom transfer radical polymerization (ATRP).

Reversible addition-fragmentation chain transfer (RAFT) polymerization has also proven to be a versatile CRP technique for the preparation of well-defined highly branched macromolecular topologies under a variety of reaction conditions.[8, 9] RAFT has recently employed for the preparation of highly branched (co)polymers by employing AB* chains transfer agents, divinyl (co)monomers and pendant xanthate copolymers. Wang and coworkers reported the RAFT polymerization mediated by a CTA containing a polymerizable styrenic group and a benzyl dithiobenzoate moiety.[10] On the other hand, the group of Rimmer reported the synthesis of highly branched temperature-responsive polymers with a polymerizable CTA that contains an imidazole thiocarbonylthio RAFT moiety.[11] Moreover, Perrier *et al.* reported the use of click chemistry for the preparation of styrenic hyperbranched polymers.[12-14] As click chemistry comprises a set of efficient reactions, it is a powerful tool for the synthesis of hyperbranched polymers out of AB_x (macro)monomers. The research of Perrier on the use of thiol-yne chemistry for the synthesis of hyperbranched polymers appeared simultaneously with this part of the PhD project and therefore shows some similarities with the first followed approach. However, the use of thermo-responsive oligomers as AB_2 macromonomers, and especially the use of a thiolactone group as precursor for thiols clearly differs and make our strategies more accessible for the introduction of various functionalities. The strategies will be discussed in more detail in the next paragraphs.

One of the first aims of this PhD project is to evaluate the synthesis of hyperbranched structures derived from AB_2 oligomers *via* the efficient, robust and orthogonal thiol-yne chemistry, which fulfils most criteria of the click philosophy.[15, 16] At the start of this PhD project, several research groups world-wide, including ours, started to investigate intensively the use of thiol-ene and thiol-yne chemistry as a metal-free alternative for the copper-catalyzed Huisgen reaction.

The AB_2 oligomers itself, where A stands for a thiol moiety while the B_2 represents a single alkyne functionality with the possibility for a double reaction, are prepared *via* RAFT polymerization using a specific CTA. In the first approach, oligomers with narrow dispersity (≤ 1.25) are synthesized *via* RAFT using a CTA containing a protected alkyne at the α-chain end. After aminolysis of the trithiocarbonate and deprotection of the alkyne, AB_2 oligomers are obtained, which further can react upon thiol-yne chemistry under UV-irradiation, yielding hyperbranched polymers. In the second approach, a monomer containing both an alkyne and thiolactone moiety was synthesized. Aminolysis of the thiolactone ring was done by an oligomer containing a primary amine at the α-chain end, yielding the AB_2 thiol-alkyne oligomers. Photo (UV)-irradiation generated the hyperbranched structures upon thiol-yne click reaction.

IV.2 Approach 1: Synthesis of the hyperbranched polymers upon thiol-yne reaction of RAFT derived AB_2 oligomers

As stated in the introduction section, two different strategies are followed for the synthesis of functional hyperbranched polymers. In the first approach, a suitable CTA containing a protected alkyne moiety at the α-chain end was synthesized and used for the polymerization of different types of monomers. After deprotection of the alkyne functionality and aminolysis of the trithiocarbonate group, thiol-yne chemistry upon photo UV-irradiation yields the hyperbranched polymers with a high degree of branching (Scheme IV-1).

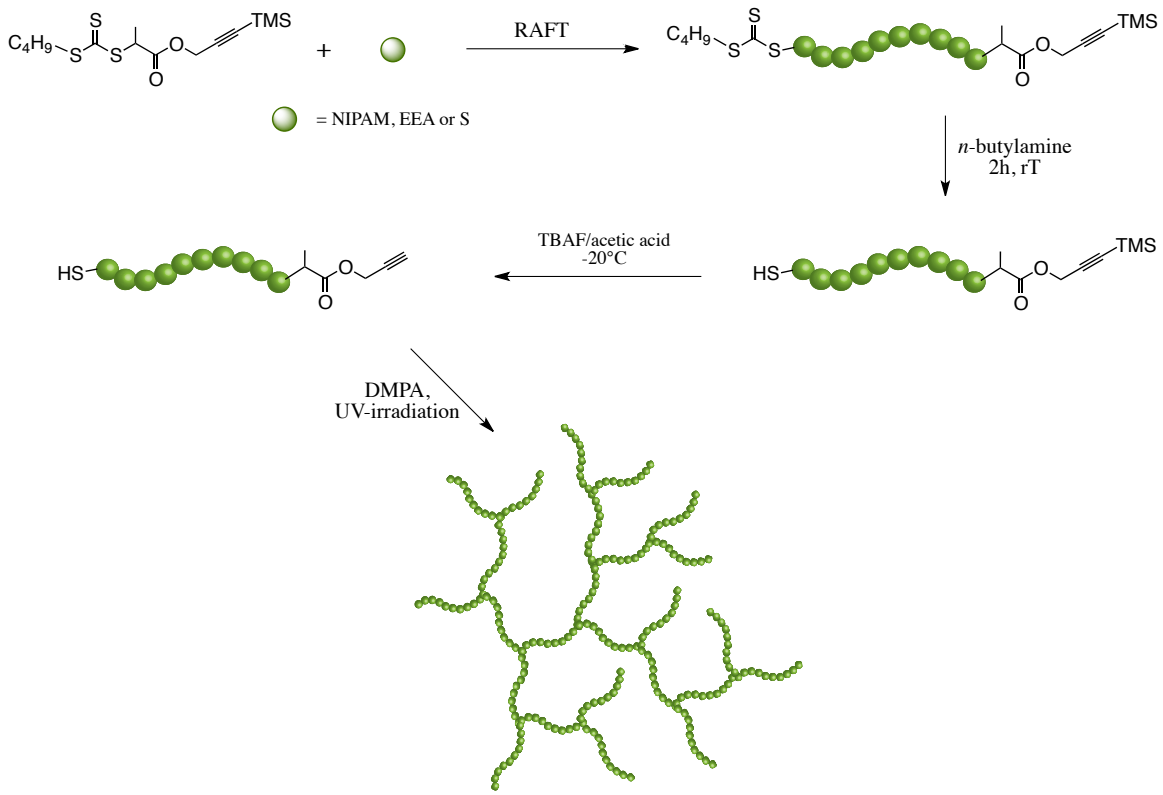

Scheme IV-1: General scheme of the synthesis of hyperbranched polymers via thiol-yne chemistry starting from an A'B_2 CTA which is subsequently used for the RAFT polymerization of NIPAM, EEA or S. After aminolysis and deprotection, UV-curing yields the hyperbranched structures.

IV.2.1 Synthesis of the A'B_2 chain transfer agent

For the preparation of the AB_2 oligomers *via* RAFT, a specific A'B_2 RAFT agent was synthesized. This functional CTA contains an (protected) alkyne functionality at the α-chain end (= B_2 functionality), while the thiocarbonylthio group serves as a protecting group for a thiol (= A' functionality). After polymerization, the aminolysis of the thiocarbonylthio group and the desilylation of the alkyne functionality result into the desired AB_2 oligomers.

In the first stage of this project, the commercially available 2-(dodecylthiocarbonothioylthio)-2-methylpropionic acid (DDMAT) was esterified with 3-(trimethyl silyl)propargyl alcohol to yield an appropriate CTA (Figure IV-1). However, because of the large amount of CTA needed (aiming for low molecular weight polymers) and the high price of DDMAT, it was initially chosen to synthesize this RAFT agent ourselves. Despite many attempts, low yields were obtained (≤ 20%).

Hawkett *et al.* reported the synthesis of 2-(((Butylsulfanyl)carbonothioyl) sulfanyl)propanoic acid (BuPAT), another CTA with a carboxylic acid at the ω-chain end, which is already industrially applied by BASF.[17] Therefore, as an alternative for DDMAT, this CTA was synthesized with high yields (79%) and subsequently esterified with protected propargyl alcohol, yielding BUPAT-TMS, a CTA with a protected alkyne moiety at the α-chain end (Figure IV-2). The completion of this reaction was confirmed *via* ^{1}H NMR (Figure IV-3). The trimethylsilyl (TMS) group was used for protecting the alkyne group from radical attacks during the radical polymerization.

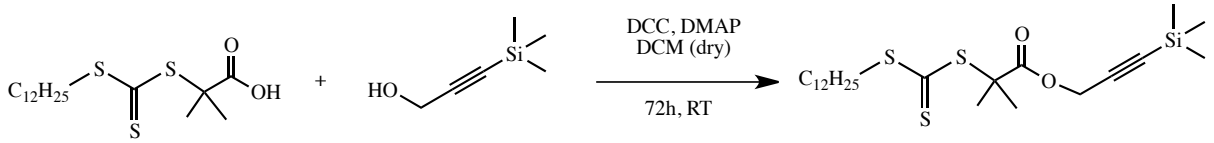

Figure IV-1: Esterification of DDMAT with protected propargyl alcohol resulting a CTA containing a protected alkyne functionality at the α-chain end.

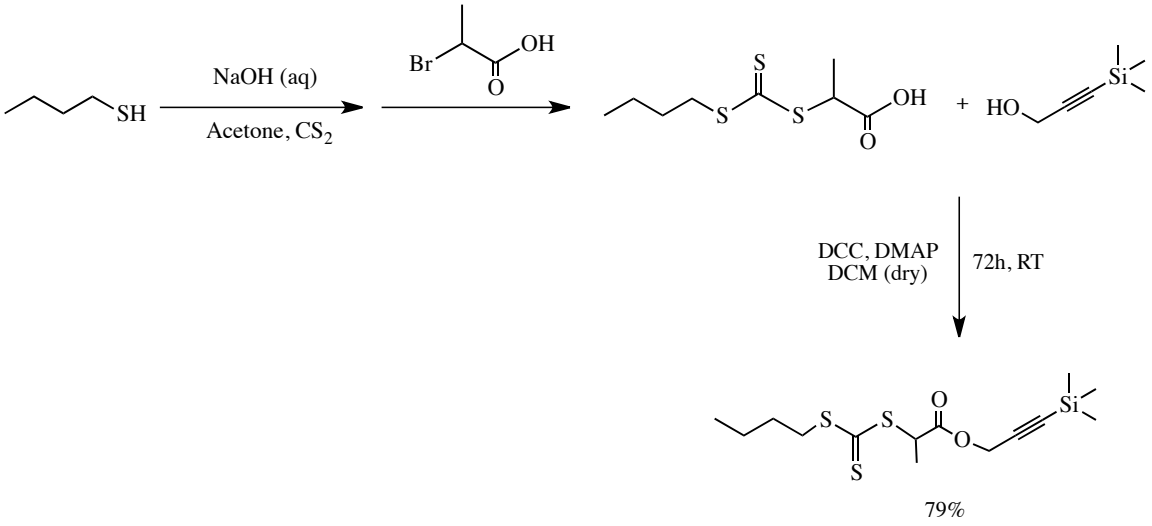

Figure IV-2: Synthesis of BuPAT starting from commercially available, cheap compounds and subsequent esterification with 3-(trimethylsilyl)propargyl alcohol, yielding a CTA (BuPAT-TMS) with a protected alkyne at the α-chain end.

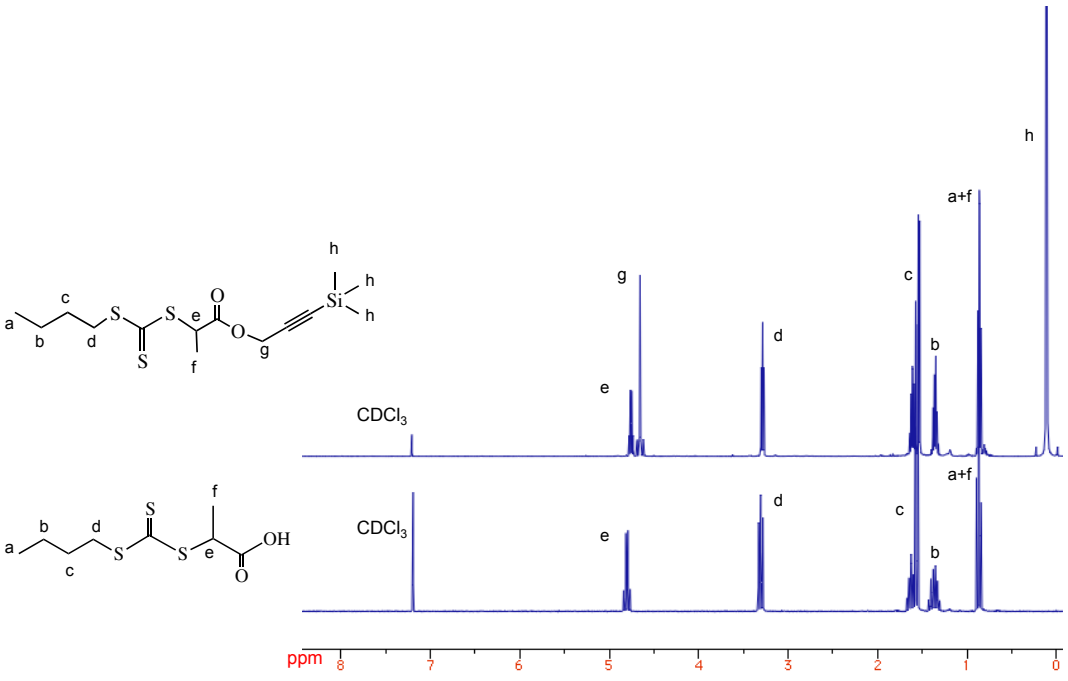

Figure IV-3: ^{1}H NMR ($CDCl_3$; 500 MHz) of BuPAT (bottom) and BuPAT-TMS (top) proven the conversion of the carboxylic acid to the trimethylsilyl protecting group upon esterification with TMS-propargyl alcohol.

IV.2.2 Synthesis of A'B_2 oligomers by RAFT polymerization

In a next stage, the protected alkyne containing CTA, BuPAT-TMS, has been used for the RAFT polymerization of three different types of monomers: styrene (S), *N*-isopropyl acrylamide (NIPAM) and ethoxyethyl acrylate (EEA). These three monomers are chosen to prove the versatility of the CTA, as they represent three major types of monomers that are used frequently in polymer science: acrylates; acrylamides and styrenics. Moreover, EEA is a monomer that has been used for other research projects in our research group.[18-21] The polymerizations of NIPAM and EEA were performed in dry 1,4-dioxane at 65°C in the presence of AIBN as initiator, while styrene is polymerized in bulk at 85°C, also in the presence of AIBN. To obtain low molecular weight oligomers, to ensure a better reaction between the A-functionalities and B_2 functionalities, small ratios between the monomer concentration and the CTA concentration were applied (50/1 and 30/1 ratio) (Table IV-1).

Table IV-1: Summary of the optimized reaction conditions and results of the RAFT polymerization of NIPAM, EEA and S mediated by BuPAT-TMS.

Entry	Monomer	$[M]_0/[CTA]_0/[I]_0$	t [h]	$M_{n,\,SEC}$ [g/mol]	$M_{n,\,th}$ [g/mol]	Đ	Conv.[e] [%]
1	NIPAM[a]	30/1/0.11	5	5300[c]	3100	1.22[c]	79
2	NIPAM[a]	30/1/0.11	3	3800[c]	2500	1.15[c]	63
3	EEA[a]	30/1/0.11	5	5200[c]	3850	1.15[c]	80
4	S[b]	50/1/0.11	5	5100[d]	3500	1.23[d]	60
5	S[b]	50/1/0.11	3	4000[d]	2500	1.17[d]	40

[a]Reaction performed at 65°C in 1,4-dioxane; [b]Reaction performed at 85°C in bulk; [c]SEC, calibrated with PMMA standards, DMA as eluent; [d]SEC, calibrated with PS standards, THF as eluent; [e]Calculated from ^{1}H NMR. $M_{n,\,th} = M_w(CTA) + conv\ x$ [M]/[CTA] x M_w(M).

For all polymerizations a kinetic investigation was performed. As depicted in Figure IV-4, a first-order kinetic plot $\ln([M]_0/[M])$ as a function of the time was observed for the RAFT polymerization of NIPAM. Moreover, the molecular weight increases linearly with the monomer conversion while the dispersities remain lower than 1.25, indicating effective controlled polymerization resulting into homopolymers with molecular weights which are in good agreement with the theoretically expected and low dispersities. Furthermore, both MALDI-TOF MS and NMR analysis confirmed a high end-group fidelity (≥ 90%) after polymerization (by comparison of the S-C**H**

signal from the α-chain end and the C**H** signal of the NIPAM repeating unit in the ^{1}H NMR spectrum). Those properties were obtained even at conversions of 70%, which is an important feature in the synthesis strategy of hyperbranched polymers.

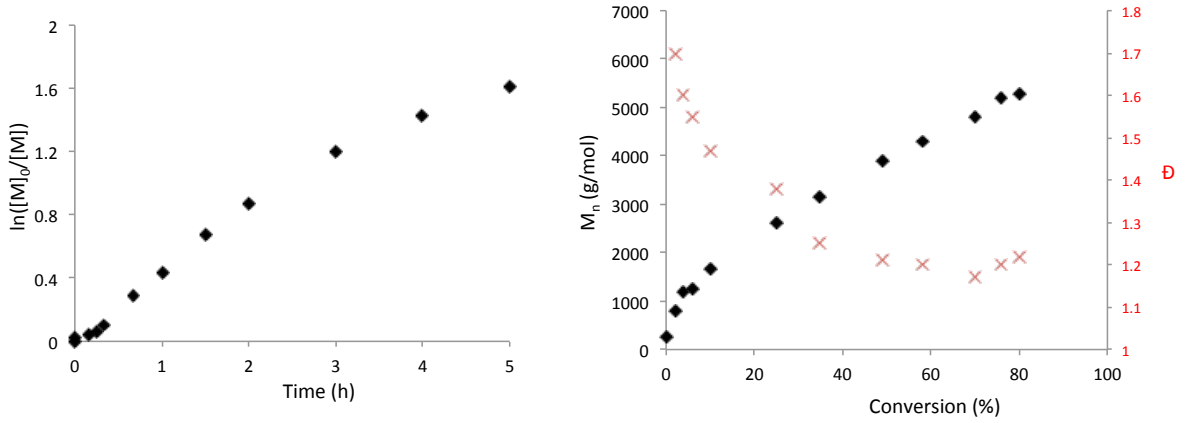

Figure IV-4: RAFT polymerization of NIPAM using BUPAT-TMS as CTA at 65°C in 1,4-dioxane as solvent with AIBN as thermal initiator (I); $[M]_0/[CTA]_0/[I]_0$ = 40/1/0.11. First-order kinetic plot (left) and molecular weight and dispersity evolution as a function of monomer conversion (right).

A similar kinetic plot was observed for the polymerization of EEA, meaning that the RAFT polymerization of EEA proceeds at similar rate as NIPAM using BuPAT-TMS as CTA. However, for the RAFT polymerization of styrene a small induction period of approximate 20 minutes is observed which is evidenced from the conversion vs. time plot (Figure IV-5). This observation has been reported earlier for RAFT polymerizations and is the result of the RAFT equilibrium establishment. Nevertheless, a linear relationship between the monomer conversion and molecular weight and dispersity indicates the controlled character of the polymerization. Again, both MALDI-TOF MS and combination of ^{1}H NMR analysis with UV-Vis analysis proves the high end-group fidelity (≥ 90%) even at conversion of 60%.

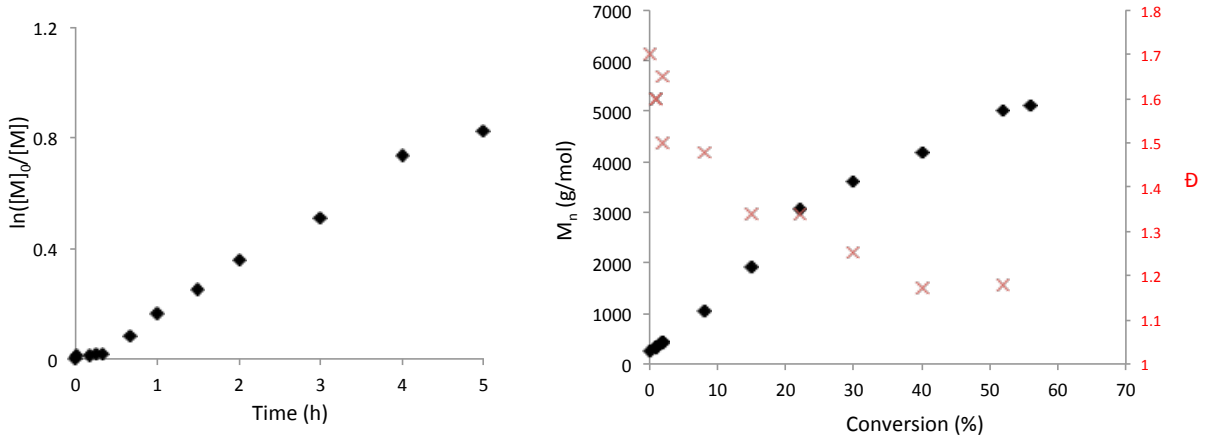

Figure IV-5: RAFT polymerization of styrene using BuPAT-TMS as CTA at 85°C in bulk with AIBN as thermal initiator (I); $[M]_0/[CTA]_0/[I]_0$ = 80/1/0.11. First-order kinetic plot (left) and molecular weight and dispersity evolution in function of monomer conversion (right).

Summarizing, it can be concluded that BuPAT-TMS is a good chain transfer agent for all three types of monomers as it provides polymers with molecular weights that are good agreement with the theoretically expected, low dispersities and high end-group fidelity.

IV.2.3 Aminolysis and desilylation yielding the AB_2 monomers

The polymers obtained *via* RAFT polymerization using BuPAT-TMS as CTA (Entries 2 and 5, Table IV-1), are in a next step transformed in AB_2 oligomers where A stands for a thiol functionality while B_2 is an alkyne moiety. First, the trithiocarbonate end-group at the ω-chain end is converted into a thiol upon aminolysis at ambient temperature in the presence of *n*-butylamine as nucleophile. For this reaction, an equimolar amount of amine in principle is needed for the aminolysis of the thiocabonylthio group.[22-24] Yet, to ensure completeness of the conversion, a 20 molar excess of amine with respect to the trithiocarbonate group is applied. Under these conditions, the aminolysis proceeds fast at room temperature, reaching near completion within 2 hours. Moreover, the excess of *n*-butylamine could be easily removed by two-fold precipitation of the aminolyzed polymer in the non-solvent (cold diethylether for PNIPAM and cold methanol for PS). Moreover, drying the polymer overnight at 40°C under reduced pressure ensures the removal of all remaining solvent and *n*-butylamine.

As stated above (section III.2), the completion of the aminolysis could visually be followed by the change in colour of the solution from yellow to colourless due to the removal of the trithihocarbonate group. Moreover, UV-Vis spectroscopy shows the disappearance of the signal at 310 nm, which corresponds to the maximum absorption of the trithiocarbonate group, after aminolysis, proving the complete conversion to the thiol functionality (Figure IV-6, left). To avoid disulfide formation during the reaction, a few drops of *n*-tributylphosphine, a frequently used mild reducing agent, is added to the solution. SEC analysis indeed confirms the absence of disulfides as the SEC traces are monomodal and symmetrical while the dispersity remains low (≤ 1.20) after aminolysis (Figure IV-6, right).

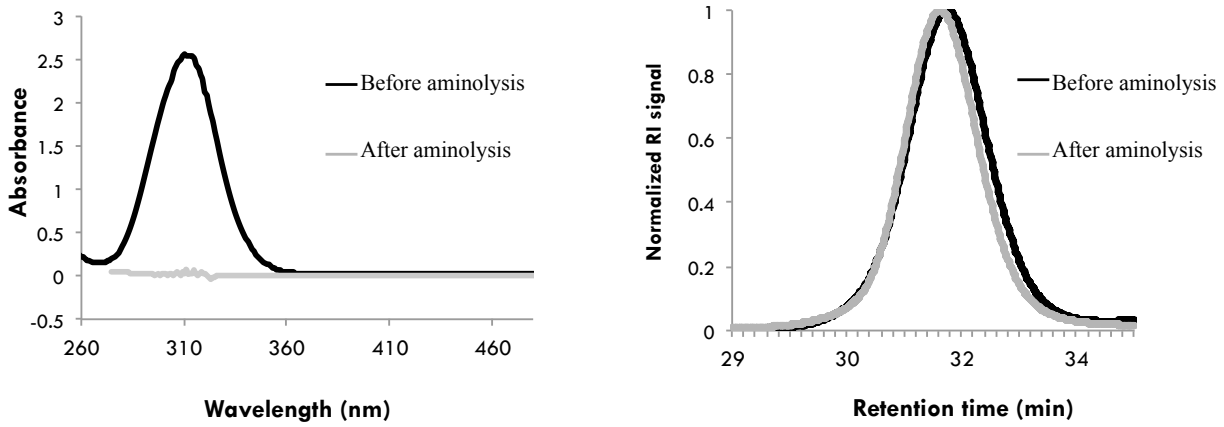

Figure IV-6: Typical UV-Vis spectra of PNIPAM (entry 2; Table IV-1) before (black line) and after (grey line) aminolysis, confirming the complete conversion of the trithiocarbonate into a thiol functionality (left) upon reaction with n-butylamine; SEC traces of PNIPAM before (black line) and after (grey line) aminolysis proving the absence of disulfides as the traces remain monomodal and symmetrical in combination with low dispersities (right).

In the next step, deprotection of the trimethylsilyl group of the alkyne moiety was performed by treatment of the aminolyzed polymer with tetrabutylammonium fluoride (TBAF) in the presence of acetic acid as buffer agent in THF at -20°C.[25-27] Under these conditions, a virtually yield of 100% of the expected terminal alkyne polymers can be provided. The complete removal of the trimethylsilyl protecting group was proven by ^{1}H NMR where the typical C-**CH** alkyne signal at 2.55 ppm appeared while the signals from the methyl functionalities from the protecting group (Si**$(CH_3)_3$**) at 0.25 ppm disappeared. Moreover, SEC analysis revealed that, as expected, the hydrodynamic volume after deprotection has decreased while the dispersity remained almost unchanged. Both the aminolyis and the deprotection of the alkyne functionality provides the AB_2 thiol-alkyne, which in the presence of a photo-initiator can further react to hyperbranched polymers upon thiol-yne chemistry.

IV.2.4 Thiol-yne chemistry yielding hyperbranched polymers

In the next phase, the AB_2 polymers (Entry 2, Table IV-1) are tested on the ability to undergo thiol-yne reaction upon UV-irradiation using 2,2-dimethoxy-2-phenylacetophenone (DMPA) as photoinitiator yielding hyperbranched polymers. As the RAFT polymerization can be used to synthesize well-defined polymers from a variety of functional monomers, a wide range of different hyperbranched polymers can be synthesized using this approach. To illustrate the robustness of the thiol-yne reaction, AB_2 thiol-alkyne PNIPAM was further reacted *via* thiol-yne chemistry in the presence of 5 wt% DMPA under UV-irradiation (365 nm) at 40°C (= temperature inside the UV-curing box). According to literature, the amount of photoinitiator should be limited as model studies revealed that some compounds can react with the formed radical fragments.[28]

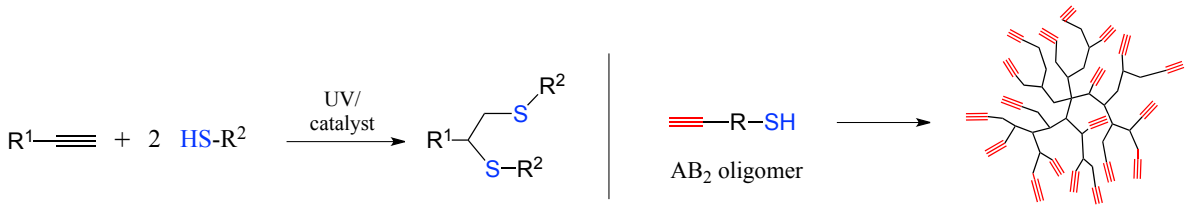

Figure IV-7: Principle of radical thiol-yne chemistry (left) and synthesis of hyperbranched structures out of AB_2 thiol-alkyne oligomers using this method (right).

SEC analysis of the obtained polymers revealed an increase in molecular weight and dispersity, indicating the proceeding of the thiol-yne reaction. Moreover, ^{1}H NMR analysis revealed that the signal at 2.5 ppm from unreacted alkyne functionalities broadened while little or no additional signals in the region of 5-6.5 ppm were observed meaning that no or small amount of double bonds (linear units) are present in the structure (Figure IV-8). This evidences the high degree of branching (DB) (≥ 85%), which was expected when thiol-yne chemistry is applied for the synthesis of hyperbranched polymers, due to the fact that the thiol addition to the vinylthioether occurs three times faster than the thiol addition to the alkyne functionality.[29] This means that the hyperbranched structures possess DB almost as high as those obtained for dendrimers, while having different architecture. This DB is much higher than those for the conventional hyperbranched polymers obtained through AB_2 polymerizations (DB = 0.5). While it is expected that hyperbranched polymers possess a high dispersity due to the statistical nature of the AB_2 thiol-yne reaction, the disperisities of these hyperbranched structures are rather low. Most possible this can attributed to the relatively large spacing between the branching point as result of working with AB_2 oligomers.

Table IV-2: SEC data for the hyperbranched polymers achieved by UV-irradiation of Entry 2.

Entry	t [min]	$M_{n, SEC}$ [g/mol]	Đ
1_HB	360	13200	2.4
2_ HB	420	15100	2.5
3_HB	420	19800	2.9

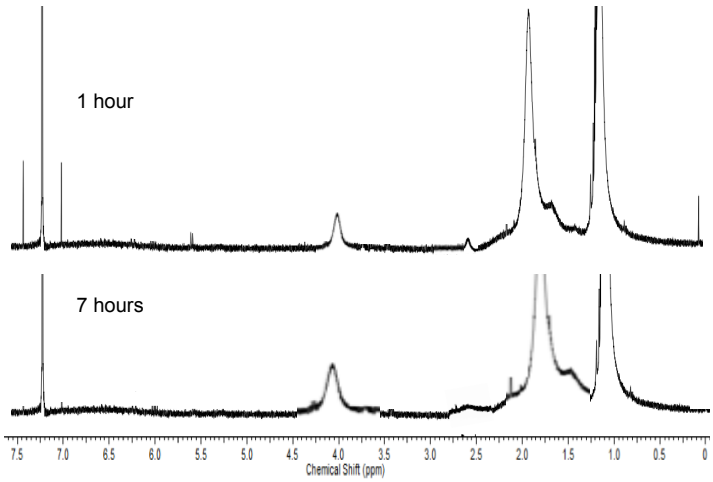

Figure IV-8: ^{1}H NMR of the hyperbranched PNIPAM structure after 1 hour reaction time and after 7 hours reaction time.

The peculiarity of this strategy is that after the thiol-yne reaction, hyperbranched polymers are obtained with a large amount of terminal alkyne groups that in a second step, a post-modification reaction, can further react upon thiol-yne or Cu(I)-catalyzed azide-alkyne cycloaddition reaction. This makes this strategy versatile to prepare a wide range of (thermo-responsive) hyperbranched polymers containing a wide range of functionalities, starting from the same structures.

Using this strategy, it is possible to prepare a range of hyperbranched polymers, for example thermo-responsive HB, through choice of the precursor AB_2 oligomers. Moreover, this technique allows the incorporation of different functional groups upon post-modification reactions with the preserved alkyne functionalities in the hyperbranched polymer, broadening its possibilities in application fields (see section VI.2.6).

IV.3 Approach 2: Synthesis of hyperbranched polymers upon ring-opening of the thiolactone moiety with amino-terminated oligomers and subsequent thiol-yne chemistry

The above strategy for the synthesis of hyperbranched polymers is straightforward and allows the formation of different kinds of structures, as the RAFT polymerization is tolerant for a wide variety of functional monomers. However, incorporation of other functional groups is only possible *via* post-polymerization reaction of the alkyne moieties.[30] As described in Chapter III, the advantage of the use of thiolactone moiety, which can be opened upon aminolysis generating a thiol, is the simultaneous introduction of a new functionality *via* the reaction with the amine. This has stimulated us to develop a new strategy where a combination of RAFT and thiolactone chemistry is applied. For this, an alkyne-thiolactone compound, which can be seen as an $A'B_2$ monomer, is synthesized whereby the ring is opened upon reaction with a RAFT-derived polymer containing a primary amine at the ω-chain end (for the synthesis of these compounds: see Chapter III), yielding AB_2 polymers. Formation of the highly functional hyperbranched structures is achieved by using UV-light (365 nm), in the presence of DMPA as photoinitiator.

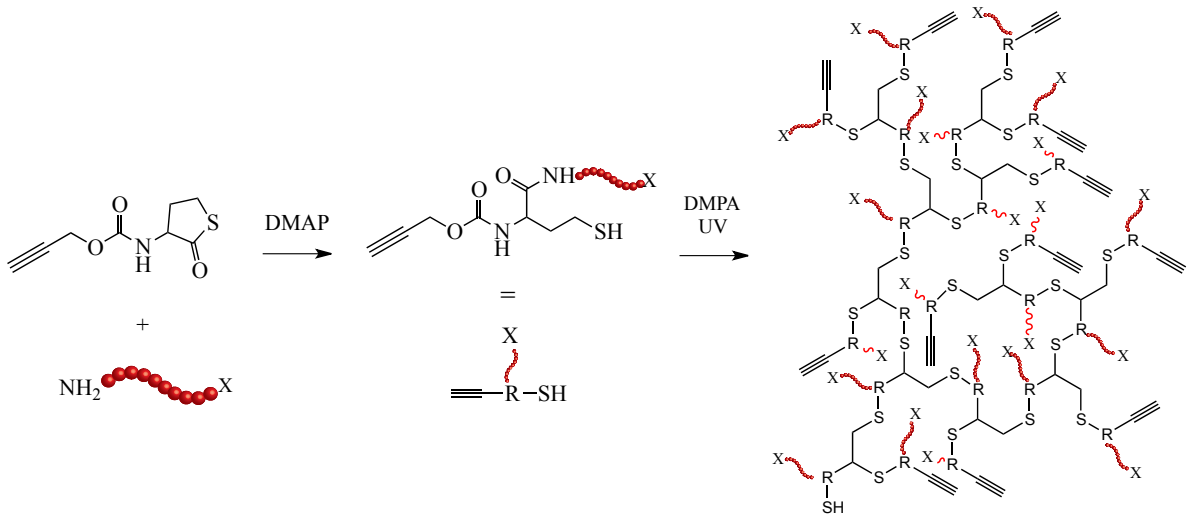

Scheme IV-2: General scheme of the synthesis of hyperbranched polymers via thiol-yne chemistry starting from an $A'B_2$ alkyne-thiolactone monomer and an oligomer containing a primary amine at the ω-chain end. Opening of the thiolactone ring yields the hyperbranched structure upon UV-irradiation.

IV.3.1 Synthesis of the alkyne-thiolactone monomer

The synthesis of the monomer containing both a triple bond and a thiolactone unit was straightforward as in our research group alloc-thiolactone monomers were already synthesized for the preparation of polyurethane structures.[31] In this case, combination of the thiolactone moiety, which can be considered as a latent thiol, with an alkyne functionality, yields a $A'B_2$ monomer (Figure IV-9). Reaction of DL-homocysteine thiolactone hydrochloride, available in large scale, with propargyl chloroformate in the presence of $NaHCO_3$ enables the introduction of the triple bond in the compound, yielding the $A'B_2$ monomer. Purification of the product was done *via* flash chromatography, resulting in a colourless oil with an overall yield of 88% (Figure IV-10).

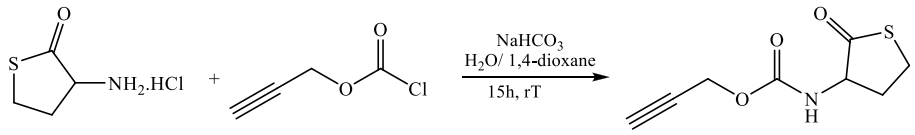

Figure IV-9: Synthesis of the alkyne-thiolactone $A'B_2$ monomer from DL-homocysteine thiolactone hydrochloride and propargyl chloroformate in the presence of $NaHCO_3$.

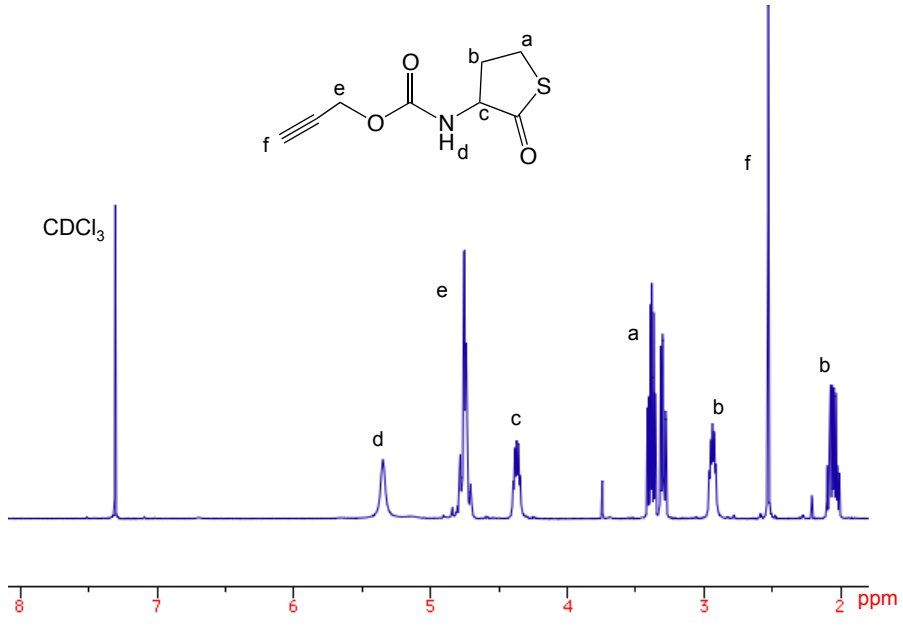

Figure IV-10: ^1H NMR ($CDCl_3$; 500 MHz) of the alkyne-thiolacton monomer synthesized by reaction of DL-homocysteine thiolactone hydrochloride with propargyl chloroformate.

IV.3.2 Synthesis of hyperbranched structures upon aminolysis

The reactivity of the alkyne-thiolactone monomer was investigated in our research group by a model reaction with *n*-propylamine and is fully described in the PhD thesis of dr. Fabienne Goethals.[31, 32] In this project, the formation of hyperbranched polymers is achieved by ring-opening of the alkyne-thiolactone monomer upon aminolysis with NH_2-PNIPAM oligomers and subsequent UV-curing (365 nm) in the presence of DMPA as photoinitiator. NH_2-PNIPAM was chosen as reactant as it will result into thermo-responsive hyperbranched polymers. The synthesis of such NH_2-PNIPAM homopolymers is fully described in Chapter III. As reversible addition-fragmentation chain transfer (RAFT) is the chosen polymerization technique for the synthesis of those oligomers, a wide range of functionalities can be introduced at the ω-chain end *via* thiol-X chemistry. As such, the advantage of this concept is that the functionality at the ω-chain end of the oligomer (depicted as functionality X in Scheme VI-2), is introduced in the hyperbranched structure and this on each branching unit. In this way, a whole range of new properties can be given to the structure, according to the introduced functionality, making this approach broadly applicable. Moreover, this strategy can be applied by the use of a one-pot two-step system (using UV-irradiation) where all components are present from the start. In this way, the released thiol is able to immediately react further with the alkyne upon thiol-yne chemistry. Alternatively, when applying the two steps consecutively, the complete conversion of the thiolactone in the corresponding thiol can be ensured prior to the thiol-yne reaction.

Earlier reports on the reactivity of the thiolactone ring with polymers containing primary amine end-groups (NH_2-polymer) reveal that the reaction proceeds rather slow.[33] These studies show that, because of the relatively high reactivity of the triple bonds towards thiyl radicals, the first step of the two-step reaction is rate-determining. A kinetic study of the rate of aminolysis of γ-thiobutyrolactone upon reaction with the primary amine-terminated oligomer NH_2-PNIPAM (M_n = 3500 g/mol, Đ = 1.15) was performed as model reaction (Figure IV-11). The reaction kinetics were determined *via* GC, by following the disappearance of the γ-thiobutyrolactone signal as a function of time (Figure IV-12). When using a two-fold excess of NH_2-oligomer and 10 mol% of 4-dimethylaminopyridine (DMAP), the reaction is complete after 16 hours. However, LC-MS analysis revealed that not only the expected thiol product was obtained, but also the disulfide product.

Figure IV-11: Model reaction performed to determine the kinetics of the thiolactone ring opening with the primary amine-terminated oligomers (X = primary alcohol functionality).

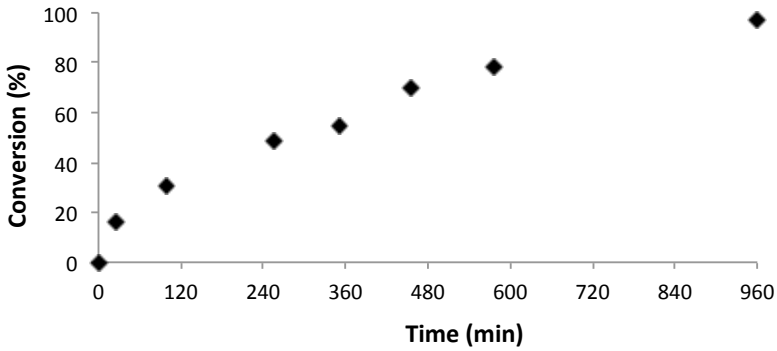

Figure IV-12: Aminolysis of γ-thiobutyrolactone with NH_2-PNIPAM: conversion as a function of time.

In a next stage, the alkyne-thiolactone $A'B_2$ molecule is reacted with 2 equivalents of primary amine-terminated oligomer and 10 mol% of DMAP in THF under UV-irradiation in the presence of DMPA as photoinitiator (Figure IV-13). Under these conditions, hyperbranched polymers are prepared using a one-pot reaction mixture, whereby the ring-opening is immediately followed by the thiol-yne reaction.

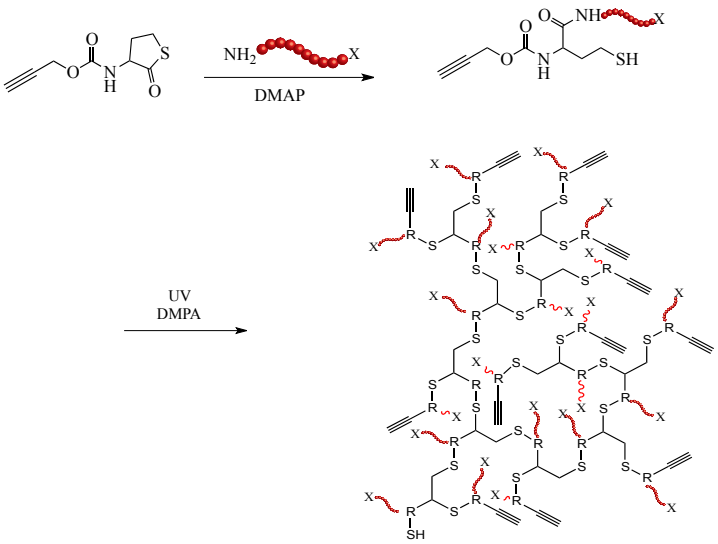

Figure IV-13: Nucleophilic ring-opening of the alkyne-thiolactone, followed by a thiol-yne reaction under UV-irradiation leading to hyperbranched polymers.

However, the amount of photoinitiator is kept low as its radical fragments can react with the amine end-groups of the polymer, creating a whole range of undesired side-products.[34] The reaction is followed by SEC analysis, which shows a maximum conversion after 25 hours (the molecular weight didn't increase anymore with longer reaction times). Moreover, increasing the amount of DMPA (from 3 w% to 7 w%) or amine-terminated oligomer (up to 5 equivalents) did not increase the reaction rate or the maximum conversion. Again, the dispersities are low for hyperbranched polymers due to the large space between each branching point.

Table IV-3: Overview of the molecular weight characteristics of HB1, HB2 and HB3, for different reaction times.

Entry	t [h]	$M_{n, SEC}$ [g/mol]	Đ	DB
HB1	25	16500	2.8	n.d
HB1	27	16600	2.7	≥ 80
HB2	24	17500	2.4	n.d
HB2	28	17700	2.5	≥≥90
HB3	25	19000	3.1	n.d.

n.d =not determined

The DB of the hyperbranched polymers was determined *via* ^{1}H NMR analysis by following the decrease of the signal at 4.6 ppm, due to the reaction of the alkyne with the thiol functionality with the formation of a thioether and a double bond. Moreover, the intensity of the signals of the double bond protons retained low, indicating a low presence of linear units. This means a high amount of dendritic units is present in the structure, leading to a high degree of branching. This is a reflection of the fact that the second addition of the thiol to the vinylthioether is much faster than the first addition to the alkyne, implicating the B functionalities have a different reactivity, which confirms the findings of Fairbanks.[35] Furthermore, a maximum molecular weight of 20 kDa was obtained after 25 hours, due to steric hindrance of the compounds.

IV.4 Conclusion

Two different approaches were applied for the synthesis of functional hyperbranched polymers starting from AB_2 precursors, where A is a thiol moiety and B_2 an alkyne functionality. In a first approach, a suitable chain transfer agent containing a protected alkyne at the α-chain end, is synthesized and used for the RAFT polymerization of different functional polymers. Kinetic investigation of different monomers using this specific CTA was performed. In the next step, the AB_2 prepolymers were obtained upon desilylation of the alkyne functionality and aminolysis of the trithiocarbonate RAFT group. Applying UV-irradiation in the presence of a photoinitiator, the thiol was able to react with both π-bonds of the alkyne functionality leading to hyperbranched structures with a high degree of branching. In this way, a high amount of alkyne functionalities are left in the structure, which are available for further modification.

In the second strategy, an alkyne-thiolactone monomer is synthesized, which can be considered as as $A'B_2$ precursor. The thiolactone functionality (A') is modified into a thiol (A) upon aminolysis with a NH_2-PNIPAM prepolymer. This prepolymer is synthesized *via* the RAFT polymerization technique as such that it contains a primary amine functionality at the α-chain end. Like in the first approach, applying UV-irradiation in the presence of a photoinitiator, hyperbranched polymers are obtained. The advantage of this strategy is that next to a high amount of terminal alkyne functionalities, also an additional functionality originating from the prepolymer is present on every branching unit in the hyperbranched structure. As such, functionalities can be incorporated from the start without additional modification reactions.

IV.5 Experimental part

IV.5.1 Materials

1-Butanethiol (Aldrich, 99%), carbon disulfide (Aldrich, ≥ 99%), *N*-(bromomethyl)phthalimide (Aldrich, 97%), chloroform (Aldrich, HPLC grade), triethylamine (Aldrich, HPLC grade), dry DMF (Aldrich, 99.8%), *n*-hexane (Aldrich, HPLC grade), toluene (Aldrich, HPLC grade), H_2SO_4 (Aldrich, 99.9%), potassium hydroxide (KOH) (Aldrich, 90%), *tert*-butanol (Aldrich, ≥ 99%), *N,N'*-dicyclohexylcarbodiimide (DCC) (Aldrich, 99%), 4-dimethylaminopyridine (DMAP) (Aldrich, ≥ 99%), 2,2-dimethoxy-2-phenyl acetophenone (DMPA, Acros, 99%), propargyl chloroformate (Aldrich, 96%), ethyl acetate (Fluka, HPLC), methanol (Sigma Aldrich, HPLC grade) were used as received.

N-Isopropyl acrylamide (NIPAM) (Aldrich) was recrystallized twice from a 50/50 toluene/*n*-hexane mixture. 2-([(butylsulfanyl)carbonothioyl]sulfanyl)propanoic acid (BuPAT), 1-ethoxyethyl acrylate (EEA) were prepared following a literature procedure.[17, 36] Styrene (Acros Organics, 99%, extra pure) was passed through a column of basic alumina to remove the inhibitor. THF (Aldrich, >99%) was destilled over Na/benzophenone prior to use. 2,2'-Azobis(isobutyronitrile) (AIBN) (Aldrich) was recrystallized twice from methanol. 1,4-Dioxane (Aldrich, HPLC grade) was dried by distillation from sodium/benzophenone.

IV.5.2 Characterization and equipment

^{1}H and ^{13}C NMR (Attached Proton Test, APT) spectra were recorded in $CDCl_3$ (Eurisotop), DMSO-*d6* (Eurisotop) on a Bruker AM500 spectrometer at 500 MHz or on a Bruker Avance 300 at 300 MHz.

An Agilent technologies 1100 series LC/MSD system equipped with a diode array detector and single quad MS detector (VL) with an electrospray source (**ESI-MS**) was used for classic reversed phase L*C-MS (liquid chromatography mass spectroscopy) and MS analysis.* Analytic reversed phase HPLC was performed with a Phenomenex C18 (2) column (5 µ, 250 x 4.6 mm) using a solvent gradient (0 → 100% acetonitrile in H_2O in 15 min) and the eluting compounds were detected v*ia U*V-detection (λ = 214 nm).

Size Exclusion Chromatography (SEC) was performed on a Waters instrument, with a refractive-index (RI) detector (2414 Waters), equipped with 3 Polymer Standards Services SEC serial columns (1 X GRAM Analytical 30 Å, 10 µm and 2 x GRAM Analytical 1000 Å, 10 µm) at 35 °C. Poly(methyl methacrylate) (PMMA) standards were used for calibration and N,*N*-*d*imethylacetamide (DMA), containing LiBr (0.42 g/mL) was used as an solvent at a flow rate of 1 mL/min. Molecular weight and dispersity were determined using the Empower software.

UV curing was performed by irradiation with 365 nm UV lamps (9 x 9 W) positioned in a metal cylindrical container.

UV-Vis measurements were performed on an AnalytikJena Specord 200 in quartz cuvettes with a thickness of 10 mm at a wavelength range of 200 to 700 nm. The concentration of each sample was 1 mg/mL.

Matrix assisted laser desorption/ionization time of flight mass spectroscopy (MALDI-TOF MS) was performed on an Applied Biosystems Voyager De STR MALDI-TOF mass spectrometer equipped with 2 m linear and 3 m reflector flight tubes, and a 355 nm Blue Lion Biotech Marathon solid state laser (3.5 ns pulse). All mass spectra were obtained with an accelerating potential of 20 kV in positive ion mode and in reflectron mode. *Trans*-2-[3-(4-*tert*-butylphenyl)-2-methyl-2-propenylidene]malononitrile, (DCTB) (30 mg/mL in DCM) was used as a matrix, NaTFA (19 mg/mL in acetone) was used as a cationizing agent, and polymer samples were dissolved in THF (4 mg/mL). Analyte solutions were prepared by mixing 10 µL of the matrix, 10 µL of the polymer and 1 µL of the salt solution. Subsequently, 0.5 µL of this mixture was spotted on the sample plate, and the spots were dried in air at room temperature. A poly(ethylene oxide) standard (Mn = 2000 g/mol) was used for calibration. All data were processed using the Data Explorer 4.0.0.0 (Applied Biosystems) software package.

IV.5.3 Synthesis of 2-([(butylsulfanyl)carbonothioyl]sulfanyl)propanoic acid

This compound was synthesized according to a procedure described in literature.[17]. A 50% NaOH solution (32.00 g, containing 16.00 g, 400 mmol of NaOH) was added to a stirred mixture of butanethiol (36.00 g, 400 mmol) and water (60 mL). Acetone (20 mL) was then added, and the resulting clear, colourless solution was stirred for 30 minutes and then cooled to near-room temperature and treated with carbon disulfide (27 mL, 34.2 g, 450 mmol) to give a clear orange solution. This was stirred for 30 minutes and then cooled in an ice bath to an internal temperature below 10°C. 2-Bromopropanoic acid (62.73 g, 410 mmol) was then added at such a rate that the temperature did not exceed 30°C followed by 50% NaOH (32.80 g, 410 mmol), also added at such a rate that the temperature did not exceed 30°C. When the exotherm had stopped, the ice bath was removed and water (60 mL) was added. The reaction was stirred at ambient temperature for 24 h then diluted with water (100 mL) and stirred and cooled in an ice bath while 10 M HCl (60 mL) was added at a rate which kept the temperature below 10°C. A yellow oil separated, and stirring of the mixture was continued at ice temperature until the oil solidified. The solid was collected by suction filtration, pressed and washed with cold water, and dried under reduced pressure to a state of semi-dryness. The lumps were crushed with a spatula; the now-granular solid was resuspended in fresh cold water and stirred for 15 min then refiltered. The residue was washed with cold water and air-dried to afford a powdery yellow solid, 84.98 g, which was recrystallized from hexane (180 mL) with gentle stirring to give bright yellow microcrystals (yield = 88 %). ^{1}H NMR ($CDCl_3$; 500 MHz); δ (ppm): 4.85 (q, 1H, SC**H**), 3.37 (t, 2H, C$\mathbf{H_2}$S), 1.69 (q, 2H, C$\mathbf{H_2}$$CH_2$S), 1.63 (d, 3H, SCHC$\mathbf{H_3}$), 1.44 (m, 2H, CH_3C$\mathbf{H_2}$$CH_2$), 0.94 (t, 3H, C$\mathbf{H_3}$$CH_2$). ^{13}C NMR ($CDCl_3$, 75 MHz); δ (ppm): 221.8 -**C**S), 177.1 -CO), 47.5 (S**C**H), 37.2 (**C**H_2S), 30.8 (**C**$H_2$$CH_2$S), 22.3 ($CH_3$**C**$H_2$), 16.7 (SCH**C**$H_3$), 13.7 ($CH_2$**C**$H_3$).

BuPAT-TMS. To a solution of BuPAT (5 g; 21 mmol) and 3-(trimethyl silyl)propargyl alcohol (2.24 g, 18 mmol) in dry dichloromethane (100 mL), DCC (4,51 g, 22mmol) is added with a catalytic amount of DMAP. This solution was stirred for 72 hours at room temperature under N_2 atmosphere. The salts formed are removed *via* filtration and the solution was concentrated under reduced pressure. The product was purified *via* flash chromatography (*n*-hexane/ethyl acetate 98/2) resulting a yellow viscous oil with a yield of 79%. ^{1}H NMR ($CDCl_3$; 500 MHz); δ (ppm): 4.85 (q, 1H, SC**H**), 4.60 (s, 2H, O-C$\mathbf{H_2}$-C-),3.37 (t, 2H, C$\mathbf{H_2}$S), 1.69 (q, 2H, C$\mathbf{H_2}$$CH_2$S), 1.63 (d, 3H, SCHC$\mathbf{H_3}$), 1.44 (m, 2H, CH_3C$\mathbf{H_2}$$CH_2$), 0.94 (t, 3H, C$\mathbf{H_3}$$CH_2$), 0.25 (s, 9H SI-C$\mathbf{H_3}$). ^{13}C NMR ($CDCl_3$, 75 MHz); δ (ppm): 221.8 (CS), 177.3 (CO), 47.5 (S**C**H), 37.2 (**C**H_2S), 30.0 (**C**$H_2$$CH_2$S), 22.1 ($CH_3$**C**$H_2$), 27.3 ($CH_2$) 16.7 (SCH**C**$H_3$), 13.6 ($CH_2$**C**$H_3$).

IV.5.4 Polymerizations and post-modification procedures

Typical RAFT polymerization procedure for NIPAM. In a typical experiment, NIPAM (4.86 g, 43 mmol), CTA (0.5 g, 0.00143 mol), AIBN (0,0259 g, 0.158 mmol) as the thermal initiator ($[CTA]_0$:$[AIBN]_0$ = 1:0.11) and dry 1,4-dioxane were placed in a 20 mL Schlenk flask, which was degassed by three freeze-pump-thaw cycles, backfilled with nitrogen, sealed and heated under stirring to 65°C. After 3 hours, the reaction was quenched by placing the flask in an ice/water bath under air. The polymer was isolated by a two-fold precipitation in cold diethyl ether and dried under vacuum, yielding a slightly yellow fine powder. Similar procedures were applied for the RAFT polymerization of EEA.

Typical RAFT polymerization procedure for styrene (S). In a typical experiment, S (7.45 g, 72 mmol), CTA (0.5 g, 0.00143 mol) and AIBN (0,0259 g, 0.158 mmol) as the thermal initiator ($[CTA]_0$:$[AIBN]_0$ = 1:0.11) were placed in a 20 mL Schlenk flask, which was degassed by three freeze-pump-thaw cycles, backfilled with nitrogen, sealed and heated under stirring to 85°C. After 3 hours, the reaction was quenched by placing the flask in an ice/water bath under air. The polymer was isolated by a two-fold precipitation in cold methanol and dried under vacuum, yielding a slightly yellow fine powder.

Aminolysis of the trithiocarbonate group. The polymer was reacted with an excess (20 equivalents) *n*-butylamine in THF (0.2 M) for two hours. The colour of the solution changed from light yellow to colourless. A few drops of *n*-tributylphosphine were added to the mixture to minimize disulfide formation. The polymer was subsequently isolated by two-fold precipitation in cold diethyl ether (for PNIPAM) or cold methanol (for PS) and obtained as a white solid after drying.

Deprotection of the alkyne moiety.[37] The protected polymer was dissolved in THF with a concentration of 0.10 M and 1.5 equivalents of acetic acid, according to the protected alkyne functions, were added. After bubbling for 10 minutes with argon, the solution was cooled to -20°C and a 0.2 M solution of TBAF in H_2O (1.5 equivalents relative to the trimethylsilyl protection groups) was added dropwise with a syringe. After stirring for 30 minutes, the solution was allowed to reach room temperature and continued to stirr for additional 2 hours. Subsequently, the mixture was passed through a short silica column to remove TBAF x $3H_2O$ and, after washing the column with

additional THF, the solution was concentrated under reduced pressure before precipitating the polymer into the anti-solvent (cold diethyl ether for PNIPAM and cold methanol for PS).

Hyperbranching: thiol-alkyne: The alkyne-thiol AB_2 oligomer (0.2 g; 0.057 mmol) was dissolved in THF and 3 to 5 w% DMPA as photoinitiator was added. Three freeze-pump-thaw cycles were performed to guarantee oxygen-free atmosphere. Next, the reaction mixture is placed under UV-irradiation (365 nm, 9 x 9W) while stirring. Test experiment reveals that without photoinitiator nothing happens.

Alkyne-thiolactone monomer. To a suspension of $NaHCO_3$ (42 g; 0.5 mol) in H_20/1,4-dioxane (1/1; 200 mL), DL-homocysteine thiolactone hydrochloride (15.4 g; 0.1 mol) was slowly added and the mixture was stirred for 30 minutes. Propargyl chloroformate (23.7 g; 0.2 mol) was added dropwise during a period of 10 minutes and the mixture was stirred overnight. The reaction was terminated by dilution with brine (400 mL) and extracted with water (4 x 250 mL). The organic phase was collected, dried over magnesium sulphate and concentrated under reduced pressure. The product was purified by flash chromatography with DCM/ethyl acetate (98/2) as eluens, furnishing the product as a colourless viscous oil with a yield of 88%. $C_8H_9NO_3S$ (199.2 g/mol); *m/z* (ESI-MS) 199, 171, 127, 111. ^{1}H NMR ($CDCl_3$, 500 MHz); δ (ppm): 2.04 (m, 1H); 2.5 (s, 1H); 2.85 (m 1H); 3.29 (m, 2H); 4.35 (m, 1H); 4.72 (dt, 2H); 5.35 (s, 1H). ^{13}C NMR ($CDCl_3$, 75 MHz) δ (ppm): 205.1 (C), 156.2 (C), 132.6 (CH), 118.2 (CH_2), 66.2 (CH_2), 60.9 (CH), 32.0 (CH_2), 27.3 (CH_2).

Hyperbranching: thiolactone-alkyne: The alkyne-thiolactone monomer (51.8 mg; 0.25 mmol) and 2 equivalents of the NH_2-PNIPAM (1.75 g; 0.5 mmol) were dissolved in THF in the presence of DMPA (2 to 5 w%). Three freeze-pump-thaw cycles were performed to guarantee oxygen-free atmosphere. In a subsequent step, the reaction mixture is placed under UV-irradiation (365 nm, 9 x 9W).

IV.6 References

[1] D. Yan, C. Gao, H. Frey, "*Hyperbranched Polymers: Synthesis, properties and applications"*, John Wiley & Sonc, Inc, **2009**.
[2] A. P. Vogt, B. S. Sumerlin, *Macromolecules* **2008**, *41*, 7368.
[3] J. M. J. Frechet, M. Henmi, I. Gitsov, S. Aoshima, M. R. Leduc, R. B. Grubbs, *Science* **1995**, *269*, 1080.
[4] C. J. Hawker, J. M. J. Frechet, R. B. Grubbs, J. Dao, *J. Am. Chem. Soc.* **1995**, *117*, 10763.
[5] S. G. Gaynor, S. Edelman, K. Matyjaszewski, *Macromolecules* **1996**, *29*, 1079.
[6] J. A. Yoon, T. Young, K. Matyjaszewski, T. Kowalewski, *Acs Appl. Mater.* **2010**, *2*, 2475.
[7] K. Matyjaszewski, S. G. Gaynor, A. Kulfan, M. Podwika, *Macromolecules* **1997**, *30*, 5192.
[8] B. L. Liu, A. Kazlauciunas, J. T. Guthrie, S. Perrier, *Polymer* **2005**, *46*, 6293.
[9] B. L. Liu, A. Kazlauciunas, J. T. Guthrie, S. Perrier, *Macromolecules* **2005**, *38*, 2131.
[10] W.-J. Wang, D. Wang, B.-G. Li, S. Zhu, *Macromolecules* **2010**, *43*, 4062.
[11] S. Carter, S. Rimmer, A. Sturdy, M. Webb, *Macromol. Biosci.* **2005**, *5*, 373.
[12] D. Konkolewicz, A. Gray-Weale, S. Perrier, *J. Am. Chem. Soc.* **2009**, *131*, 18075.
[13] D. Konkolewicz, M. J. Monteiro, S. Perrier, *Macromolecules* **2011**, *44*, 7067.
[14] M. Semsarilar, V. Ladmiral, S. Perrier, *Macromolecules* **2010**, *43*, 1438.
[15] H. C. Kolb, M. G. Finn, K. B. Sharpless, *Angew. Chem.-Int. Edit.* **2001**, *40*, 2004.
[16] A. B. Lowe, C. E. Hoyle, C. N. Bowman, *J. Mater. Chem.* **2010**, *20*, 4745.
[17] C. J. Ferguson, R. J. Hughes, D. Nguyen, B. T. T. Pham, R. G. Gilbert, A. K. Serelis, C. H. Such, B. S. Hawkett, *Macromolecules* **2005**, *38*, 2191.
[18] W. Van Camp, F. E. Du Prez, S. A. F. Bon, *Macromolecules* **2004**, *37*, 6673.
[19] D. Wouters, W. Van Camp, B. Dervaux, F. E. Du Prez, U. S. Schubert, *Soft Matter* **2007**, *3*, 1537.
[20] P. Escale, W. Van Camp, F. Du Prez, L. Rubatat, L. Billon, M. Save, *Polym. Chem.* **2013**, *4*, 4710.
[21] S. De Smet, S. Lingier, F. E. Du Prez, *Polym. Chem.* **2014**, *5*, 3163.
[22] C. Boyer, A. Granville, T. P. Davis, V. Bulmus, *J. Polym. Sci. Pol. Chem.* **2009**, *47*, 3773.
[23] M. Le Neindre, B. Magny, R. Nicolay, *Polym. Chem.* **2013**, *4*, 5577.
[24] J. Xu, J. He, D. Fan, X. Wang, Y. Yang, *Macromolecules* **2006**, *39*, 8616.
[25] V. Ladmiral, G. Mantovani, G. J. Clarkson, S. Cauet, J. L. Irwin, D. M. Haddleton, *J. Am. Chem. Soc.* **2006**, *128*, 4823.
[26] M. T. Stone, J. S. Moore, *Org. Lett.* **2004**, *6*, 469.
[27] S. H. Chanteau, J. M. Tour, *J. Org. Chem.* **2003**, *68*, 8750.
[28] P. Derboven, D. R. D'hooge, M. M. Stamenovic, P. Espeel, G. B. Marin, F. E. Du Prez, M.-F. Reyniers, *Macromolecules* **2013**, *46*, 1732.
[29] B. D. Fairbanks, E. A. Sims, K. S. Anseth, C. N. Bowman, *Macromolecules* **2010**, *43*, 4113.
[30] R. Barbey, S. Perrier, *Acs Macro Letters* **2013**, *2*, 366.
[31] P. Espeel, F. Goethals, F. E. Du Prez, *J. Am. Chem. Soc.* **2011**, *133*, 1678.
[32] F. Goethals, "Multistep reactions based on thiolactones for the synthesis of functionalized polymers", Ghent University, Ghent, 2014.
[33] P. Espeel, F. Goethals, F. Driessen, L.-T. T. Nguyen, F. E. Du Prez, *Polym. Chem.* **2013**, *4*, 2449.
[34] N. B. Cramer, S. K. Reddy, M. Cole, C. Hoyle, C. N. Bowman, *J. Polym. Sci. Pol. Chem.* **2004**, *42*, 5817.
[35] B. D. Fairbanks, T. F. Scott, C. J. Kloxin, K. S. Anseth, C. N. Bowman, *Macromolecules* **2009**, *42*, 211.
[36] R. Hoogenboom, U. S. Schubert, W. Van Camp, F. E. Du Prez, *Macromolecules* **2005**, *38*, 7653.
[37] A. Krieg, C. R. Becer, R. Hoogenboom, U. S. Schubert, *Macromol. Symp.* **2009**, *275–276*, 73.

Abstract

In this chapter the optimization of the Cu(0)-mediated polymerization of *n*-butyl acrylate and 2-methoxyethyl acrylate is reported using an automated parallel synthesizer. Using this robot, up to 16 kinetic reactions could be performed in parallel, resulting in a fast screening of different reaction conditions. Several parameters were optimized to determine the optimal reaction conditions with regard to control over the polymerization and reaction rate. These optimal reaction conditions were then used for the one-pot two-step synthesis of diblock copolymers by sequential monomer addition.

This chapter was published as:

L. Voorhaar, S. Wallyn, F. E. Du Prez, R. Hoogenboom, Polymer Chemistry 2014, 5, 4268.

Chapter V

Cu(0)-mediated polymerization *via* high-throughput experimentation

As alternative CRP technique to RAFT, which is used in the previous chapters, Cu(0)-mediated polymerization was considered as a technique to synthesize the AB_2 oligomers. This recently developed technique is identified to be fast, proceeds at ambient temperatures and yields polymers with high end-group fidelity even at high conversions. As describes in Chapter II, this end-group fidelity is an important feature for the synthesis of hyperbranched polymers. Therefore, in collaboration with the research group of prof. dr. Hoogenboom, the optimal polymerization conditions and parameters have been determined using a high throughput methodology.

V.1 Introduction

Over the past decades, several types of controlled radical polymerization methods have been developed. The most popular methods are atom transfer radical polymerization (ATRP)[1-3], reversible addition–fragmentation chain transfer (RAFT) polymerization[4] and nitroxide mediated polymerization (NMP).[5] One of the more recently developed techniques, which appears to be very promising, is the Cu(0)-mediated polymerization.[6, 7] With this method, polymers with low dispersity can readily be synthesized at room temperature and even below with high end-group fidelity even at high conversions.[8, 9] In contrast to ATRP, which also uses the change in the oxidation state of a transition metal catalyst, Cu(0)-mediated polymerization can only be performed in polar solvents, sometimes in combination with apolar solvents. In these solvents and in combination with an appropriate nitrogen containing ligand, it is theorized that Cu(I)X species will disproportionate into Cu(0) and Cu(II)X_2 species.[10] Atomic Cu(0) species will activate the process and Cu(II)X_2 will mediate

the deactivation, resulting in a mechanism that facilitates a fast controlled radical polymerization. However, the exact mechanism through which Cu(0)-mediated polymerization occurs is still under debate.[11-14]

Recent publications have shown significant progress in the area of Cu(0)-mediated polymerization. Among the monomers that have been polymerized in a controlled manner *via* Cu(0)-mediated polymerization are acrylates[6, 15-17], methacrylates[6, 18], vinyl chloride[6] and (meth)acrylamides[19-21]. Also the synthesis of more complex polymeric architectures, such as multiblock copolymers,[22-24] star[25, 26] and graft polymers[27] has been shown. However, for each monomer the polymerization conditions should be optimized, which is in general a time-consuming task.

Applying Cu(0)-mediated polymerization using an automated parallel synthesizer seems to be ideally suited for fast optimization of reaction conditions. In the past, such a parallel synthesis robot has already been used for controlled radical polymerization *via* RAFT,[28-31] ATRP,[32, 33] MADIX[34] and NMP.[35, 36] Because many reactions can simultaneously be performed, it is much more time efficient than manually performing a large number of individual reactions. Moreover, the reproducibility of the automated parallel polymerization reactions is also improved because of the similar conditions within the parallel reactors, as opposed to performing many reactions separately.

In this part of this PhD project, the optimization of the Cu(0)-mediated polymerization of *n*-butyl acrylate (BA) and 2-methoxyethyl acrylate (MEA) using an automated parallel synthesizer is described. These two monomers serve as examples for regularly applied acrylates. At first, the ability of Cu(0)-mediated polymerization reactions to be performed in a controlled and reproducible fashion in the robot system is investigated. Subsequently, different parameters and their effect on the polymerization kinetics are evaluated to find the optimal reaction conditions. The parameters that are varied include the type of ligand and initiator, the amount of Cu(0), Cu(II) and ligand, and the monomer to initiator (M/I) ratio. The optimum reaction conditions were then used for the one-pot two-step synthesis of diblock copolymers by sequential monomer addition.

V.2 Optimization of different polymerization parameters

V.2.1 Reproducibility of automated Cu(0)-mediated polymerization

In the first stage of this project, the settings of the automated synthesizer were optimized to get reproducible results. Problems like the inaccuracy of the liquid transfers by the syringe and liquid pumps of the automated synthesizer at higher transfer speeds could lead to inaccurate concentrations. To avoid such problems, the optimized liquid transfer speed of each of the components was determined.

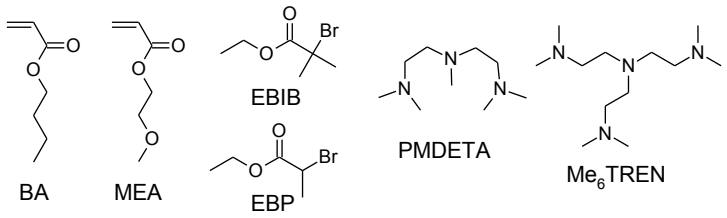

Figure V-1: Structure of n-butyl acrylate (BA), 2-methoxyethyl acrylate (MEA), ethyl α-bromoisobutyrate (EBiB), ethyl 2-bromopropionate (EBP), N,N,N',N'',N''-pentamethyldiethylenetriamine (PMDETA), Tris[2-(dimethylamino)ethyl]amine (Me_6TREN), which are used in this research.

In many polymerization reactions, the reaction solvent has been used as an internal standard to calculate the monomer conversion. However, for Cu(0)-mediated polymerization reactions in the automated synthesizer this was not possible. When all components of the reaction are added together, the polymerization immediately starts, leaving no time to take an accurate sample at zero conversion. Therefore, a small amount of 1,2-dichlorobenzene (0.1 mL in a total reaction volume of 4 mL) was added together with the monomer into the reactors to serve as an internal standard. Then, most of the other stock solutions were added and a sample for zero conversion was taken. Subsequently the final component, in most cases the initiator, was added to start the reaction. Using both visual observation and the log of the automated synthesizer, the exact times that the stock solutions are added and at which time each sample is taken can be exactly determined, enabling accurate kinetic studies. Due to the robustness and relatively high reaction rate of Cu(0)-mediated polymerization, it was found that in some cases the reaction still continued within the sample vials after sampling, leading to irreproducible kinetic plots. To prevent this, the radical inhibitor phenothiazine was added to the solvent in the sample vials, which ensures that no further polymerization takes place after sampling.

As the Cu(0)-mediated polymerization of acrylates is an exothermic reaction, the heat that is produced during the reaction may lead to an increase in the polymerization temperature and, thus, could influence the polymerization kinetics. Therefore, a polymerization was conducted with an internal temperature probe revealing that there was only a minor 0.5°C increase in temperature in the first few minutes, immediately after the start of the polymerization. As this minor temperature increase is not expected to have a significant effect on the polymerization kinetics, it was not further taken into account. To prove that these settings lead to reproducible polymerization, eight reactions were performed under similar conditions (Figure V-2). BA was polymerized using a ratio of [BA]:[EBiB]:[PMDETA]:[Cu(II)] equal to 100:1:0.24:0.05 at a monomer concentration of 2.2 M in DMF at 25°C.

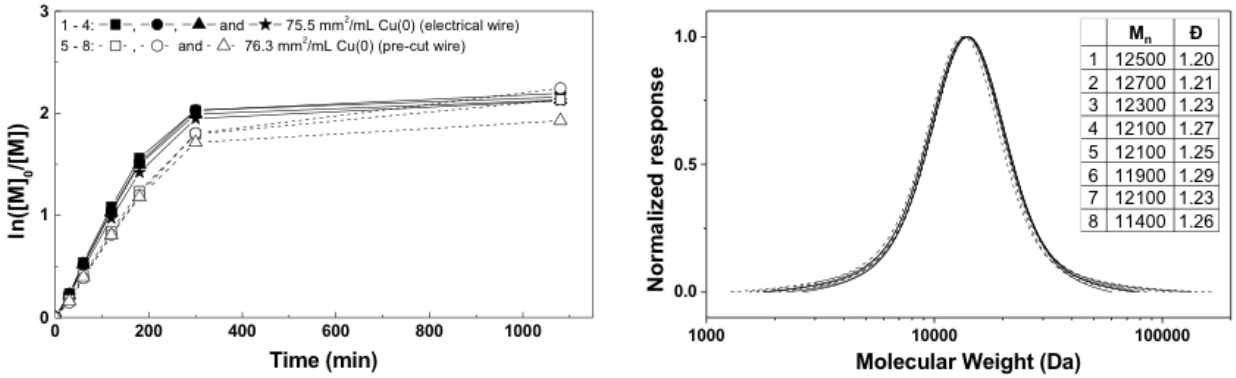

Figure V-2: Left: a first order kinetic plot for Cu(0)-mediated polymerization of BA using [BA]:[EBiB]:[PMDETA]:[Cu(II)] = 100:1:0.24:0.05, 2.2 M monomer concentration in DMF at 25 °C. Right: SEC traces of the eight individual pBA polymers at the end of the reaction.

Two types of Cu(0) were used, namely a 5 cm piece of electrical wire (with a surface area of 75.5 $mm^2\,mL^{-1}$), bent in such a shape that it fits in the reactor, and small pieces of pre-cut copper wire (with a surface area of 76.3 $mm^2\ mL^{-1}$). As shown in Figure V-2, both the conversion plots and SEC traces almost exactly overlap and the molecular weight distribution is relatively narrow, with dispersities (Đ) ranging from 1.2 to 1.3, demonstrating that reproducible Cu(0)-mediated polymerization reactions can be performed in the synthesis robot. Control over the polymerization is evident from the low Đ as well as the close to linear first order kinetic plot up to a $\ln([M]_0/[M])$ value of 2, corresponding to a conversion of 87%. For future reactions, it was decided to use the pre-cut copper wire, because it is much easier to handle and to vary the amounts compared to the electrical wire. These optimized experimental procedures were further used in this work to study the effects of various parameters on the Cu(0)-mediated polymerization.

V.2.2 Investigation of the amount of Cu(0) and initiator type

As it was considered at the moment of this research that Cu(0) is the driving force behind the Cu(0)-mediated polymerization mechanism, it was expected that changing the amount of Cu(0), *i.e.* the available surface area, would have a significant influence on the reaction kinetics. Several series of reactions were performed with different amounts of Cu(0) to study this effect. In the first series of reactions (Figure V-3) a constant ratio of [BA]:[EBiB]:[PMDETA]:[$CuBr_2$] equal to 100:1:0.18:0.05 was used with a monomer concentration of 2.2 M in DMF.[23]

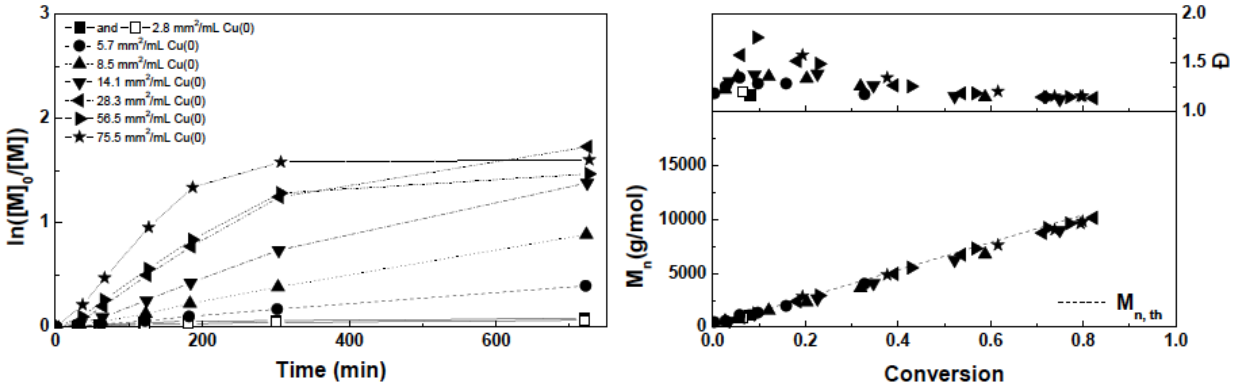

Figure V-3: Left: a first order kinetic plot for Cu(0)-mediated polymerization of BA using [BA]:[EBiB]:[PMDETA]:[Cu(II)] = 100:1:0.18:0.05, 2.2 M monomer concentration in DMF at 25°C, using different amounts of Cu(0) expressed as surface area. Right: the corresponding molecular weight and dispersity vs. conversion plot.

It is clear that an increase in the amount of Cu(0) increases the speed of the polymerization during the early stages of the reaction. However, after several hours the fastest reactions show more termination, as is evident from a decrease in the slope of the first order kinetic plot, resulting in a lower monomer conversion towards the end of the reaction. Nonetheless, the measured M_n*'s* for all polymerization reactions increase linearly with conversion and are in close agreement with the theoretical M_n. Dispersities are around 1.2 - 1.5 in the early stages of the reactions and decrease to around 1.15 with increasing monomer conversion.

For the second series of reactions with different amounts of Cu(0), Me_6TREN was applied as the ligand (Figure V-4, top). This ligand is more generally used in Cu(0)-mediated polymerization reactions because of its higher k_{act}/k_{deact} ratio, which leads to faster polymerization rates and increased control. The [BA]:[EBiB]:[Me_6TREN]:[$CuBr_2$] ratio was 100:1:0.18:0.05 for all reactions and in addition to Cu(0) wire also Cu(0) powder was used. All reactions were performed in duplicate

showing good reproducibility. While the surface area of the powder is close to that of the highest amount of Cu(0) wire, the polymerization is significantly faster during the first hour, likely caused by a difference in accessibility of the Cu(0) for the ligand. After a fast start, the reaction with powder terminates at a monomer conversion of 87%.

Other reactions with Cu(0) wire show near linear first order kinetics up to full monomer conversion. The reactions with 12.5 and 25 mm^2 mL^{-1} Cu(0) wire show similar reaction rates, indicating that this is the maximum reachable k_p, most probably limited by the solubility of Cu(0) in DMF. The M_n's are mostly in agreement with the theoretical M_n, except for the reactions using 25 mm^2 mL^{-1} Cu(0), which show higher M_n, possibly due to termination reactions. Dispersities are around 1.5 at low conversion, and decrease to 1.05 above 40% conversion. In the case of 25 mm^2 mL^{-1} Cu(0) the dispersity at full conversion is slightly higher (1.08), also demonstrating slightly lower control over the polymerization.

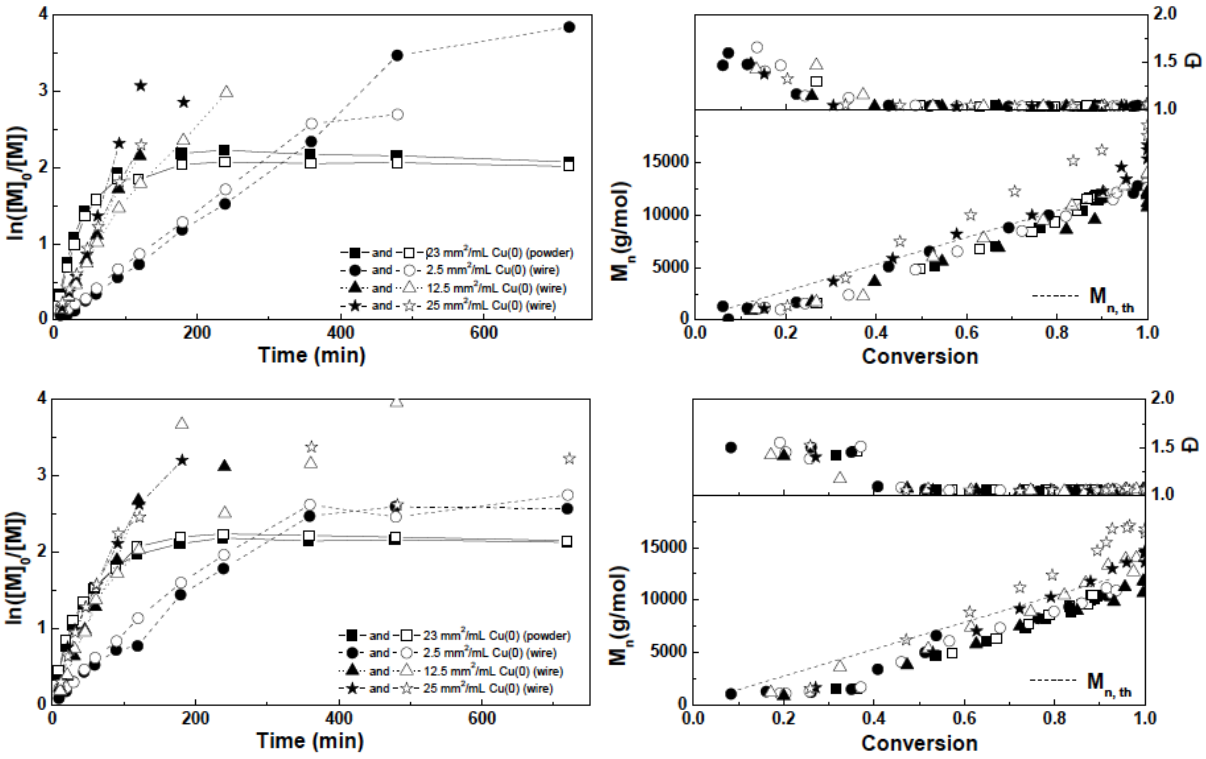

Figure V-4: Top left: a first order kinetic plot for Cu(0)-mediated polymerization of BA using [BA]:[EBiB]:[Me$_6$TREN]:[Cu(II)] = 100:1:0.18:0.05, 3 M monomer concentration in DMF at 25°C, using different amounts of Cu(0). Bottom left: same as top using EBP as the initiator instead of EBiB. Right: corresponding molecular weight and dispersity vs. conversion plots.

The third series of reactions (Figure V-4, bottom) was performed with EBP as the initiator and [BA]:[EBP]:[Me_6TREN]:[$CuBr_2$] equal to 100:1:0.18:0.05, revealing very similar results as obtained with EBiB. However, the initiation of the polymerization reactions was slightly faster, indicating that EBP is the more suitable initiator of the two tested ones, in agreement with the theory that the initiator structure should mimic the structure of dormant propagating macroradicals. However, a recent study oppositely suggested that EBiB is a better initiator for acrylates.[37] EBP was chosen as the initiator for further reactions based on our results. As using PMDETA as a ligand results in slower reactions and higher dispersities, it is clear that Me_6TREN is a better ligand for the polymerization of BA *via* Cu(0)-mediated polymerization. In both series with Me_6TREN the reactions using the highest amount of Cu(0) show a deviation from the theoretical molecular weights and slightly higher dispersities. Based on all obtained results, it was decided to use a 12.5 mm^2 mL^{-1} surface area Cu(0) wire in further reactions in combination with EBP as the initiator and Me_6TREN as the ligand.

V.2.3 Investigation of ligand concentration

The amount of Me_6TREN was subsequently varied from 0 to 0.5 equivalents with all other amounts being kept constant at [BA]:[EBP]:[$CuBr_2$] equal to 100:1:0.05 (Figure V-5). As expected, a larger amount of Me_6TREN results in a faster reaction because more Cu(0) can be dissolved. However, the reactions using 0.5 eq. of Me_6TREN show a lower conversion in the last samples, than those containing 0.3 or 0.2 eq. It is likely that more termination reactions occur with a higher amount of Me_6TREN as more Cu(0) will lead to a higher radical concentration. In contrast, the reactions involving 0.025 and 0 eq. Me_6TREN show almost no conversion. Even though all reactions revealed a linear increase of M_n with conversion close to $M_{n,th}$, dispersities are somewhat higher for the reactions with higher amounts of Me_6TREN. This can also be seen in the SEC traces of these polymers (Figure V-8), which show a shoulder at higher molecular weight, indicating coupling between chains. At 0.15 eq. Me_6TREN (and lower) this shoulder was not observed, indicating that a lower amount of the ligand provides a better controlled reaction.

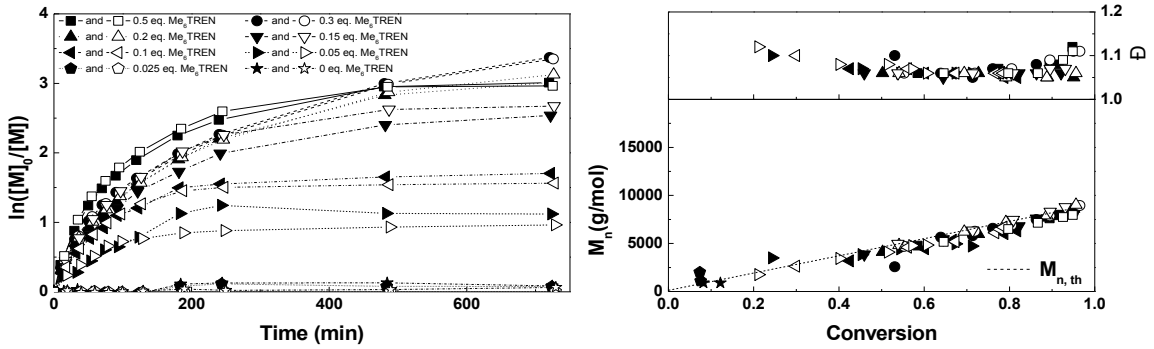

Figure V-5: Left: a first order kinetic plot for Cu(0)-mediated polymerization of BA using [BA]:[EBP]:[Cu(II)] = 100:1:0.05, 3 M monomer concentration in DMF at 25°C, using 12.5 mm^2 mL^{-1} Cu(0) wire and different amounts of Me_6TREN. Right: corresponding molecular weight and dispersity vs. conversion plot.

V.2.4 Investigation of Cu(II) concentration

The Cu(II) in the form of $CuBr_2$ is important in the Cu(0)-Cu(II) equilibrium that determines the control over the polymerization. Therefore it is expected that changing the amount of Cu(II) will not only have a large effect on the speed of the polymerization, but also on the molecular weight distribution. The [BA]:[EBP]:[Me_6TREN] ratio was kept constant at 100:1:0.18. As seen in Figure V-6, a larger amount of Cu(II) slows down monomer conversion, with no conversion using 0.5 eq. of Cu(II), relative to the initiator. The polymerization without Cu(II) or up to 0.05 eq. of Cu(II) proceeds at similar rates. SEC results show that a higher amount of Cu(II) leads to more controlled molecular weights and lower dispersities. As can be seen in the SEC traces (Figure V-7, top), a Cu(II) ratio of 0.05 eq. or lower leads to a small tailing at higher molecular weights, which could be indicative of the presence of low amounts of chain termination termination by coupling as a result of a too high radical concentration, which is not observed at Cu(II) ratios of 0.1 and higher. From these results it was concluded that a Cu(II) ratio of 0.1 results in the most controlled polymerization while maintaining a high polymerization speed. MALDI-TOF MS analysis of one of the samples confirmed high end-group fidelity (Figure V-7, bottom). The zoom in Figure V-7 (bottom) shows a peak spacing of 128 corresponding to the molecular weight of BA while the exact mass corresponds to the polymer with both the initiation fragment and bromide end-groups as well as a sodium ion, present to charge the polymer.

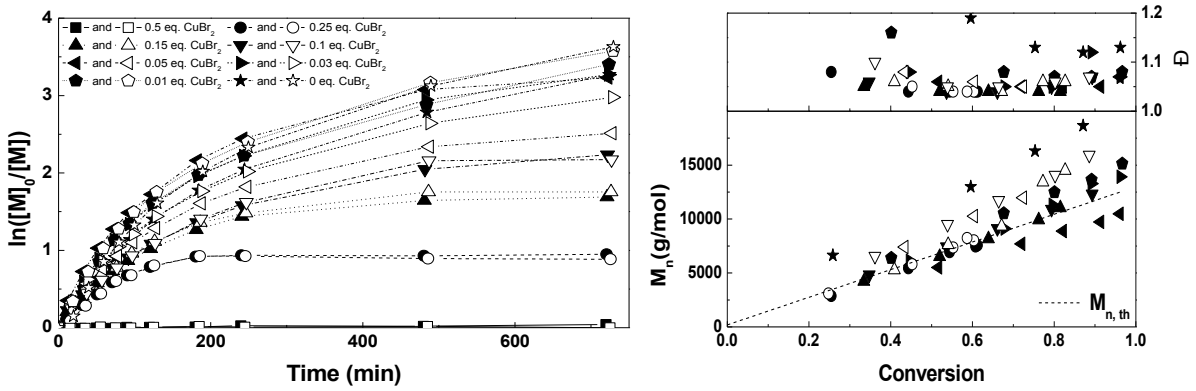

Figure V-6: Left: a first order kinetic plot for Cu(0)-mediated polymerization of BA using [BA]:[EBP]:[Me₆TREN] = 100:1:0.18, 3 M monomer concentration in DMF at 25°C, using 12.5 mm² mL⁻¹ Cu(0) wire and different amounts of Cu(II). Right: the corresponding molecular weight and dispersity vs. conversion plot.

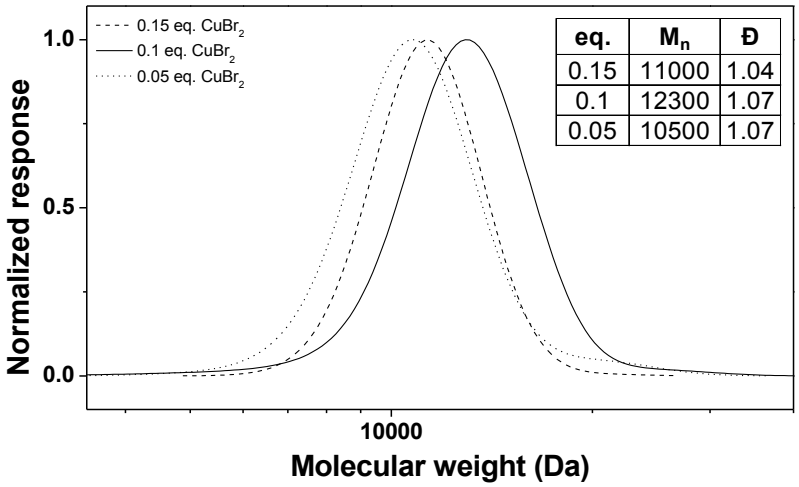

eq.	M_n	Đ
0.15	11000	1.04
0.1	12300	1.07
0.05	10500	1.07

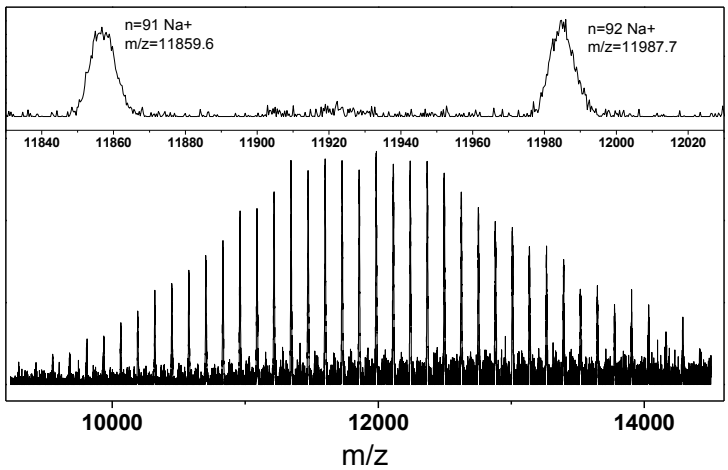

Figure V-7: Top: SEC traces of pBA polymers synthesized using [BA]:[EBP]:[Me₆TREN] = 100:1:0.18, 3M monomer concentration in DMF at 25°C, using 12.5 mm² mL⁻¹ Cu(0) wire and different amounts of Cu(II). Bottom: a MALDI-TOF MS spectrum of pBA synthesized using a [BA]:[EBP]:[Me₆TREN]:[CuBr₂] ratio of 100:1:0.18:0.1.

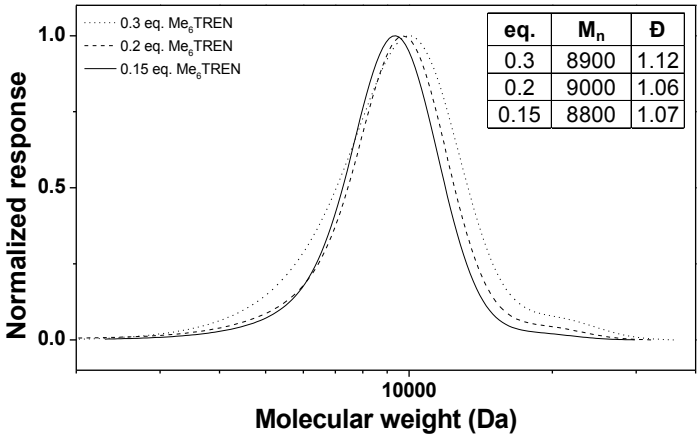

eq.	M_n	Đ
0.3	8900	1.12
0.2	9000	1.06
0.15	8800	1.07

Figure V-8: SEC traces of pBA polymers synthesized using [BA]:[EBP]:[Cu(II)] = 100:1:0.05, 3 M monomer concentration in DMF at 25°C, using 12.5 mm^2 mL^{-1} Cu(0) wire and different amounts of Me$_6$TREN.

V.2.5 Investigation of the variation of M/I ratio

Several experiments were performed to determine optimal conditions for polymerization reactions with different M/I ratios to find the limit in M_n reachable by Cu(0)-mediated polymerization. The reactions were performed with both BA and MEA as monomers to test whether the optimized conditions are applicable for other acrylates than BA. The investigated M/I ratios are 50, 100, 200 and 400. In the first experiment (Figure V-9), the ratio of [M]:[EBP]:[Me$_6$TREN]:[Cu(II)] was kept constant at [M]:1:0.15:0.1, resulting in lower concentrations of Me$_6$TREN and Cu(II) with increasing M/I ratio. The amount of Cu(0) was 12.5 mm^2 mL^{-1} in all reactions. As seen in Figure V-9, this resulted in a slower reaction for higher M/I ratios and a lower monomer conversion after 48 hours, due to more termination earlier in the reaction.

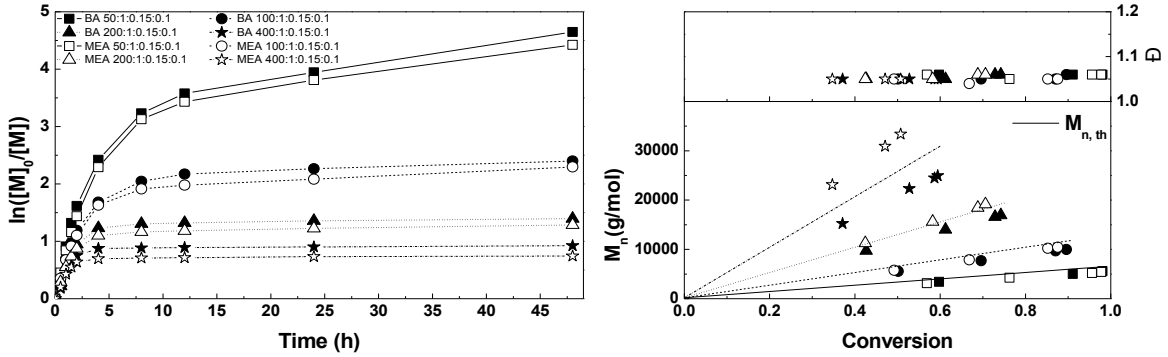

Figure V-9: Left: a first order kinetic plot for Cu(0)-mediated polymerization of BA and MEA using different [M]:[EBP]:[Me$_6$TREN]:[Cu(II)] ratios, 3 M monomer concentration in DMF at 25°C, and 12.5 mm^2 mL^{-1} Cu(0) wire. Right: the corresponding molecular weight and dispersity vs. conversion plot.

However, dispersities were in all cases around 1.05, indicating a well-controlled polymerization. The conversions of BA and MEA are very similar, indicating that these optimal reaction conditions are also applicable to other acrylates with similar hydrophobicity. The measured M_n's of MEA are higher than those of BA, which is especially clear at the highest M_n's. This is ascribed to a better solubility of pMEA in the eluent (THF), leading to a larger hydrodynamic volume and thus a higher M_n calculated relative to polystyrene standards. Overall the M_n's are in good agreement with the theoretical M_n*'s* up to masses of about 30 000 g mol^{-1}. For the second experiment, the amount of Cu(0) was adjusted to the amount of the ligand. This resulted in polymerization rates similar to those of the previous experiment with a slightly longer inhibition period. Dispersities were somewhat higher, namely 1.09 for the higher M/I polymerization. This indicates that a constant amount of 12.5 mm^2 mL^{-1} Cu(0) wire, independent of the M/I ratio, gives the best results, even though all ligand is likely saturated with copper in either case. For a third experiment the concentrations of monomer, Me_6TREN and Cu(II) and the amount of Cu(0) were kept constant, while only varying the EBP concentration to adjust the M/I ratio, leading to different [EBP]:[Me_6TREN]:[$Cu_{(II)}$] ratios. This resulted in somewhat higher monomer conversion, but also a large increase in dispersity at higher conversions, indicating a loss of control over the polymerization.

According to these results, the best way to synthesize BA and MEA polymers of different lengths is to use a [M]:[EBP]:[Me_6TREN]:[Cu(II)] ratio of [M]:1:0.15:0.1, regardless of which M/I ratio is used. A constant Cu(0) wire amount of 12.5 mm^2 mL^{-1} leads to slightly better results than adjusting the amount of Cu(0) to the amount of the ligand.

V.2.6 Sequential addition of a second monomer

To study the livingness of the polymerization and the feasibility of one-pot two-step block copolymerization by sequential monomer addition, a BA polymerization was performed for several hours, after which MEA was added as the second monomer to the polymerization mixture (Figure V-10). The initial [BA]:[EBP]:[Me_6TREN]:[$CuBr_2$] ratio was set to 50:1:0.15:0.1. After a certain time (3, 6, 12 or 24 hours) a 3 M solution of MEA in DMF was added to the reactors, leading to a total M/I ratio of 100. A similar experiment was performed using [BA]:[EBP]:[Me_6TREN]:[$CuBr_2$] = 100:1:0.15:0.1 and a total M/I ratio of 200 after the addition of MEA, showing similar results.

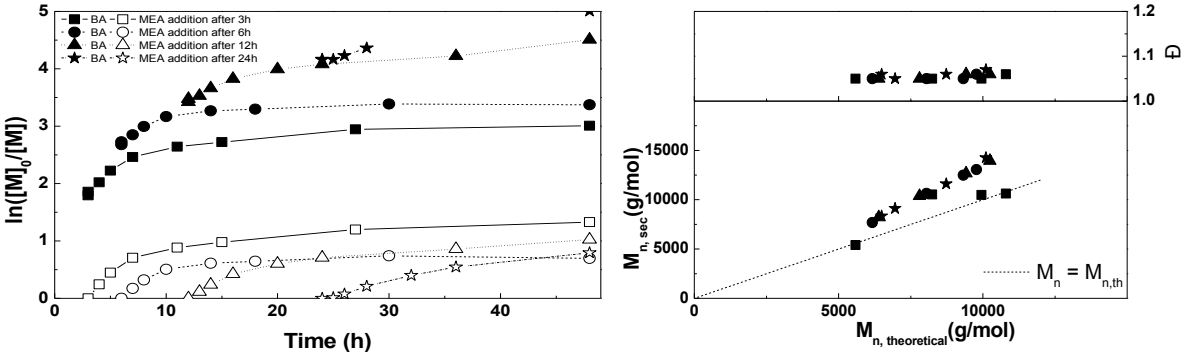

Figure V-10: Left: a first order kinetic plot for Cu(0)-mediated polymerization of BA with sequential addition of MEA using [BA]:[EBP]:[Me$_6$TREN]:[Cu(II)] = 50:1:0.15:0.1 and [MEA]:[EBP] = 50:1, 3 M monomer concentration in DMF at 25°C and 12.5 mm^2 mL^{-1} Cu(0) wire. Right: the corresponding molecular weight and dispersity vs. theoretical molecular weight plot.

The results show that, in general, a higher MEA conversion is obtained when the second monomer is added at an earlier time, demonstrating that more pBA chains are still "living." However, too short BA polymerization times do not result in perfect block copolymers, because some of the BA is also incorporated into the polymer chain after addition of the MEA. From those results, the best moment for adding the second monomer is 12 hours after the start of the polymerization. The conversion of BA at that moment is around 97%, and almost no BA is converted after addition of the MEA. In this case the MEA reaches a monomer conversion of 64% 48 hours after the start of the polymerization. Dispersities were below 1.1 in all cases. SEC traces of the block copolymers at different times during the reaction (Figure V-11) show that almost all the pBA homopolymer is converted into a block copolymer as only a very small shoulder is observed at low molecular weight in the final SEC trace. Even though the second block does not reach full conversion, quasi-perfect block copolymers can be obtained in this one-pot two-step approach.

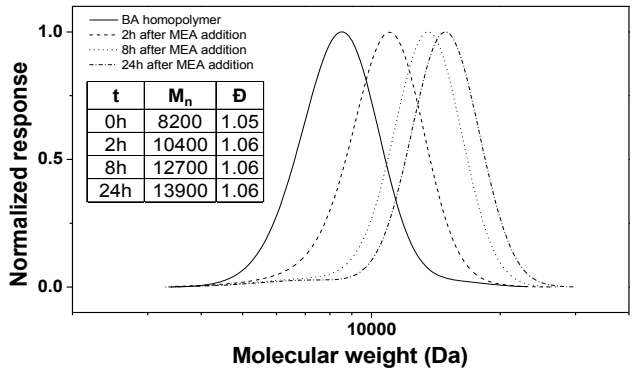

t	M_n	Đ
0h	8200	1.05
2h	10400	1.06
8h	12700	1.06
24h	13900	1.06

Figure V-11: SEC traces of pBA-b-pMEA block copolymers at different times during the polymerization after sequential addition of MEA at 12 hours BA polymerization time, using [MEA]:[EBP] = 50:1.

V.3 Conclusion

Reproducible Cu(0)-mediated polymerization could be performed in an automated parallel synthesizer. Good near-linear first order kinetics up to almost full conversion were found in many cases, showing that Cu(0)-mediated polymerization leads to controlled polymerization under a variety of reaction conditions. The best results with good control over molecular weight (distribution) while maintaining a high reaction speed were obtained with a [M]:[EBP]:[Me_6TREN]:[$CuBr_2$] ratio of [M]:1:0.15:0.1 with 12.5 mm^2 mL^{-1} Cu(0) wire. Applying those conditions, it was possible to make polymers with narrow molecular weight distributions over a large range of molecular weights.

One-pot block copolymerization reactions could also be performed, although these did not cause full conversion of the second monomer. Altogether, this work shows the power of high-throughput optimization of Cu(0)-mediated polymerization reaction conditions. As such, it may serve to accelerate optimization of Cu(0)-mediated polymerization conditions and aid in gaining fundamental understanding of the effects of various parameters on the Cu(0)-mediated polymerization. Examples of effects that could be studied further using high-throughput Cu(0)-mediated polymerization are the cooperative and synergistic effects of mixtures of solvents on the disproportionation of copper and subsequent rate of polymerization[39, 40] and the role of particle size and surface area of the copper.[41, 42] Furthermore, this high throughput methodology allows fast preparation of libraries of defined (block co)polymers by Cu(0)-mediated polymerization.

This research has given us a better insight in this recent CRP technique and the optimal conditions were applied in the next chapter to prepare well-defined AB_2 oligomers.

V.4 Experimental part

V.4.1 Materials

N,N-Dimethylformamide (DMF) was purchased from Biosolve. Copper(II)bromide ($CuBr_2$, 99%) was purchased from Fluka and used as received. Copper powder (spheroidal, 10 mm, 99%), ethyl α-bromoisobutyrate (EBiB, 98%), ethyl 2-bromopropionate (EBP, 99%), and N,N,N',N'',N''-pentamethyldiethylenetriamine (PMDETA, 99%) were purchased from Sigma-Aldrich and used as received. N-Butyl acrylate (BA, 99%) and 2-methoxyethyl acrylate (MEA, 98%) were purchased from Sigma-Aldrich and purified by passing over a basic aluminium oxide column to remove the inhibitor. Tris[2-(dimethylamino)ethyl]amine (Me_6TREN) was synthesized according to a previously published procedure.[43] Pre-cut copper wire (Sigma-Aldrich, 99.9%) and copper wire (from the core of an electrical wire, hardware store) were stirred in sulphuric acid, milliQ water and acetone before use.

V.4.2 Automated Cu(0)-mediated polymerization

Reactions were performed using a Chemspeed ASW2000 automated synthesizer equipped with 16 parallel reactors with a volume of 13 mL, a Huber Petite Fleur thermostat for heating/cooling, a Huber Ministat 125 for reflux and a Vacuumbrand PC 3000 vacuum pump. Stock solutions of all components were prepared and bubbled with argon for at least 30 minutes before being introduced into the robot system and then kept under an argon atmosphere. The hood of the automated synthesizer was continuously flushed with nitrogen and the reactors were flushed with argon to ensure an inert atmosphere. Before starting the polymerization, the reactors were degassed through ten vacuum–argon cycles. Stock solutions were transferred to the reactors using the syringe of the automated synthesizer leading to a polymerization mixture with the desired ratio of reagents and a total volume of 4 mL. During the reactions, 50 mL samples were taken at preset time intervals and directly injected into 1.5 mL sample vials, each containing a 0.1 mg mL^{-1} solution of phenothiazine in either THF or acetone to quench the reaction. For a more detailed description of the automated parallel synthesis protocol the reader is referred to the literature.[29]

V.4.3 Gas chromatography

The samples were measured with GC to determine the monomer conversion from the ratio of the integrals from the monomer and the internal standard. GC was performed on an Agilent 7890A system equipped with a VWR Carrier-160 hydrogen generator and an Agilent HP-5 column of 30 m length and 0.320 mm diameter. A FID detector was used and the inlet was set to 240°C with a split injection ratio of 25:1. Hydrogen was used as the carrier gas at a flow rate of 2 mL min^{-1}. The oven temperature was increased at 20°C min^{-1} from 50°C to 120°C, followed by a ramp of 50°C min^{-1} to 150°C.

V.4.4 Size exclusion chromatography

The samples were run over a short aluminium oxide column tobremove residual copper before the SEC measurements. The measurements were performed on a Varian PL-GPC 50 Plus system using THF at 1 mL min^{-1} as an eluent, and equipped with two PLgel 5 mm MIXED-D columns, a PL-AS RT autosampler and five detectors: RI, light scattering at 15° and 90°, a viscometer and a UV Knauer Wellchrom Spectro-Photometer K-2501. Molecular weights were determined with the RI detector using polystyrene standards as many of the polymers were too small for accurate detection by light scattering of viscometry.

V.4.5 MALDI-TOF MS

Matrix assisted laser desorption/ionization time of flight mass spectroscopy (MALDI-TOF MS) was performed on an Applied Biosystems Voyager De STR MALDI-TOF mass spectrometer equipped with 2m linear and 3m reflector flight tubes. All mass spectra were obtained with an accelerating potential of 20 kV in positive ion mode and in reflectron mode. Dithranol (25 mg mL^{-1} in THF) was used as a matrix, NaI (20 mg mL^{-1} in THF) was used as a cationizing agent, and polymer samples were dissolved in THF (5 mg mL^{-1}). Analyte solutions were prepared by mixing 20 mL of the matrix, 10 mL of the polymer and 10 mL of the salt solution. Subsequently, 0.5 mL of this mixture was spotted on the sample plate, and the spots were dried in air at room temperature. A poly(ethylene oxide) standard (M_n = 2000 g mol^{-1}) was used for calibration. All data were processed using the Data Explorer 4.0.0.0 (Applied Biosystems) software package.

V.5 References

[1] W. A. Braunecker, K. Matyjaszewski, *Prog. Polym. Sci.* **2007**, *32*, 93.
[2] M. Ouchi, T. Terashima, M. Sawamoto, *Chem. Rev.* **2009**, *109*, 4963.
[3] S. E. Averick, C. G. Bazewicz, B. F. Woodman, A. Simakova, R. A. Mehl, K. Matyjaszewski, *Eur. Polym. J.* **2013**, *49*, 2919.
[4] G. Moad, E. Rizzardo, S. H. Thang, *Aust. J. Chem.* **2009**, *62*, 1402.
[5] C. J. Hawker, A. W. Bosman, E. Harth, *Chem. Rev.* **2001**, *101*, 3661.
[6] V. Percec, T. Guliashvili, J. S. Ladislaw, A. Wistrand, A. Stjerndahl, M. J. Sienkowska, M. J. Monteiro, S. Sahoo, *J. Am. Chem. Soc.* **2006**, *128*, 14156.
[7] B. M. Rosen, V. Percec, *Chem. Rev.* **2009**, *109*, 5069.
[8] F. Nystroem, A. H. Soeriyadi, C. Boyer, P. B. Zetterlund, M. R. Whittaker, *J. Polym. Sci. Pol. Chem.* **2011**, *49*, 5313.
[9] N. H. Nguyen, M. E. Levere, V. Percec, *J. Polym. Sci. Pol. Chem.* **2012**, *50*, 860.
[10] N. H. Nguyen, M. E. Levere, J. Kulis, M. J. Monteiro, V. Percec, *Macromolecules* **2012**, *45*, 4606.
[11] D. Konkolewicz, Y. Wang, P. Krys, M. Zhong, A. A. Isse, A. Gennaro, K. Matyjaszewski, *Polym. Chem.* **2014**, *5*, 4396.
[12] F. Alsubaie, A. Anastaski, V. Nikolaou, A. Simula, G. Nurumbetov, P. Wilson, K. Kempe, D. M. Haddleton, *Macromolecules* **2015**, *48*, 5517.
[13] S. R. Samanta, V. Nikolaou, S. Keller, M. J. Monteiro, D. A. Wilson, D. M. Haddleton, V. Percec, *Polym. Chem.* **2015**, *6*, 2084.
[14] D. Konkolewicz, Y. Wang, M. Zhong, P. Krys, A. A. Isse, A. Gennaro, K. Matyjaszewski, *Macromolecules* **2013**, *46*, 8749.
[15] G. Lligadas, V. Percec, *J. Polym. Sci. Part A* **2008**, *46*, 2745.
[16] X. Leng, N. H. Nguyen, B. van Beusekom, D. A. Wilson, V. Percec, *Polym. Chem.* **2013**, *4*, 2995.
[17] S. R. Samanta, V. Percec, *Polym. Chem.* **2014**, *5*, 169.
[18] S. Fleischmann, V. Percec, *J. Polym. Sci. Part A* **2010**, *48*, 2243.
[19] N. H. Nguyen, B. M. Rosen, V. Percec, *J. Polym. Sci. Part A* **2010**, *48*, 1752.
[20] C. Waldron, Q. Zhang, Z. Li, V. Nikolaou, G. Nurumbetov, J. Godfrey, R. McHale, G. Yilmaz, R. K. Randev, M. Girault, K. McEwan, D. M. Haddleton, M. Droesbeke, A. J. Haddleton, P. Wilson, A. Simula, J. Collins, D. J. Lloyd, J. A. Burns, C. Summers, C. Houben, A. Anastasaki, M. Li, C. R. Becer, J. K. Kiviaho, N. Risangud, *Polym. Chem.* **2014**, *5*, 57.
[21] N. H. Nguyen, C. Rodriguez-Emmenegger, E. Brynda, Z. Sedlakova, V. Percec, *Polym. Chem.* **2013**, *4*, 2424.
[22] C. Boyer, A. H. Soeriyadi, P. B. Zetterlund, M. R. Whittaker, *Macromolecules* **2011**, *44*, 8028.
[23] A. H. Soeriyadi, C. Boyer, F. Nystrom, P. B. Zetterlund, M. R. Whittaker, *J. Am. Chem. Soc.* **2011**, *133*, 11128.
[24] A. Anastasaki, C. Waldron, P. Wilson, C. Boyer, P. B. Zetterlund, M. R. Whittaker, D. Haddleton, *ACS Macro Letters* **2013**, 896.
[25] W. Ding, C. Lv, Y. Sun, H. Luan, T. Yu, G. Qu, *Polymer Bulletin* **2011**, *67*, 1499.
[26] C. Boyer, A. Derveaux, P. B. Zetterlund, M. R. Whittaker, *Polym. Chem.* **2012**, *3*, 117.
[27] A. Ding, G. Lu, H. Guo, X. Zheng, X. Huang, *J. Polym. Sci. Part A* **2013**, *51*, 1091.
[28] M. W. M. Fijten, M. A. R. Meier, R. Hoogenboom, U. S. Schubert, *J. Polym. Sci. Part A* **2004**, *42*, 5775.
[29] C. R. Becer, A. M. Groth, R. Hoogenboom, R. M. Paulus, U. S. Schubert, *QSAR Comb. Sci.* **2008**, *27*, 977.
[30] C. Guerrero-Sanchez, L. O'Brien, C. Brackley, D. J. Keddie, S. Saubern, J. Chiefari, *Polym. Chem.* **2013**, *4*, 1857.
[31] J. J. Haven, C. Guerrero-Sanchez, D. J. Keddie, G. Moad, *Macromol. Rapid Commun.* **2013**, n/a.
[32] H. Zhang, M. W. M. Fijten, R. Hoogenboom, R. Reinierkens, U. S. Schubert, *Macromol. Rapid Commun.* **2003**, *24*, 81.
[33] H. Zhang, H. Abeln Caroline, W. M. Fijten Martin, S. Schubert Ulrich, "High-throughput experimentation applied to atom transfer radical polymerization: Automated optimization of the copper catalysts removal from polymers", in *e-Polymers*, 2006, p. 6/90.
[34] P. Chapon, C. Mignaud, G. Lizarraga, M. Destarac, *Macromol. Rapid Commun.* **2003**, *24*, 87.
[35] A. W. Bosman, A. Heumann, G. Klaerner, D. Benoit, J. M. J. Frechet, C. J. Hawker, *J. Am. Chem. Soc.* **2001**, *123*, 6461.

[36] T. M. Eggenhuisen, C. R. Becer, M. W. M. Fijten, R. Eckardt, R. Hoogenboom, U. S. Schubert, *Macromolecules* **2008**, *41*, 5132.
[37] N. H. Nguyen, B. M. Rosen, V. Percec, *J. Polym. Sci. Pol. Chem.* **2011**, *49*, 1235.
[38] A. Anastasaki, C. Waldron, P. Wilson, R. McHale, D. M. Haddleton, *Polym. Chem.* **2013**, *4*, 2672.
[39] X. Jiang, S. Fleischmann, N. H. Nguyen, B. M. Rosen, V. Percec, *J. Polym. Sci. Part A* **2009**, *47*, 5591.
[40] N. H. Nguyen, B. M. Rosen, X. Jiang, S. Fleischmann, V. Percec, *J. Polym. Sci. Part A* **2009**, *47*, 5577.
[41] G. Lligadas, B. M. Rosen, C. A. Bell, M. J. Monteiro, V. Percec, *Macromolecules* **2008**, *41*, 8365.
[42] N. H. Nguyen, B. M. Rosen, G. Lligadas, V. Percec, *Macromolecules* **2009**, *42*, 2379.
[43] M. Ciampolini, N. Nardi, *Inorg. Chem.* **1966**, *5*, 41.

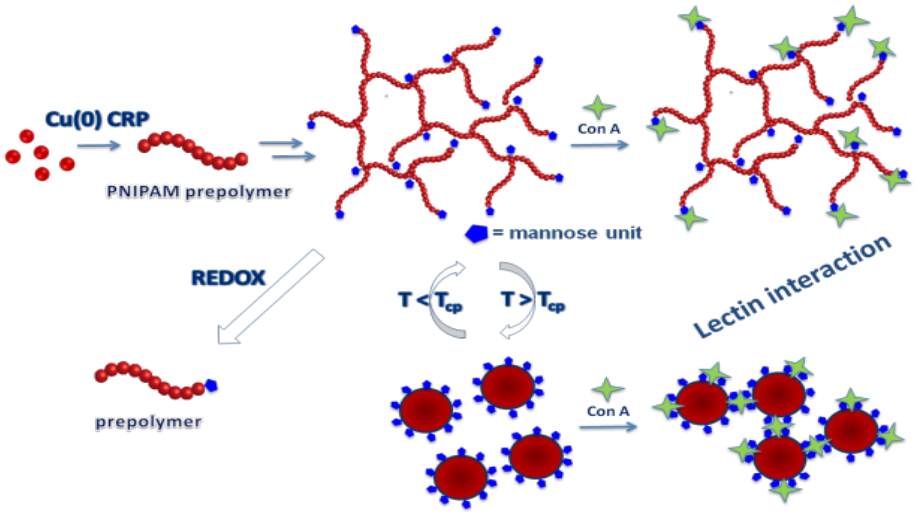

Abstract

Preparation of stimuli-responsive hyperbranched glycopolymers that are able to simultaneously enhance and control the lectin-polymer interaction has been challenging. Hyperbranched glycopolymers have been prepared in which thermo-responsive poly(*N*-isopropylacrylamide) (PNIPAM), connected by redox-responsive disulfide bonds, forms the skeleton and for which mannose units are present at each branching point. Degradation of the hyperbranched structure via chemical reduction of the disulfide bond was demonstrated. Moreover, the thermo-responsive behaviour of the glycopolymer was studied. Finally, the lectin-polymer interaction was investigated to understand the influence of both the polymer concentration and different chain conformations below and above cloud point, respectively.

Furthermore, it has also been attempted to prepare thermo-responsive hyperbranched glycopolymers with adjustable amount of sugar units per branching unit.

Part of this chapter was published as:

S. Vandewalle, S. Wallyn, S. Chattopadhyay, C. R. Becer, F. Du Prez, Eur. Polym. J. 2015, 69, 490.

Chapter VI

Synthesis of hyperbranched glycopolymers

VI.1 Introduction

Synthetic glycopolymers have attracted great interest as an alternative or mimics of naturally occurring biopolymers due to their multivalency and recognition properties.[1, 2] The latter depends largely on the accessibility of sugar units in the polymer backbone. The properties and application can be tuned by preparing suitable sugar containing polymers. Two major approaches to synthesize glycopolymers can be distinguished (see section II.4.2): (*i*) The first approach starts from the polymerization of suitable glycomonomers. For example, Stenzel *et al.* reported the synthesis of glycomonomers, followed by the preparation of polymers via RAFT polymerization.[3] Haddleton *et al.* reported the synthesis of sugar methacrylate monomers by CuAAC click reactions.[4] A series of glycopolymers were prepared via atom transfer radical polymerization (ATRP) using these monomers. (*ii*) The second approach relies on a post-polymerization modification. In this approach, suitable functional polymers were prepared using different polymerization techniques. In the subsequent steps clickable, sugar units were reacted with the polymer backbone, via various click reactions. In one of the first examples, Haddleton *et al.* reported the preparation of polymers containing reactive propargyl units by ATRP. The propargyl groups act as a clickable scaffold to introduce a variety of sugar units resulting in the generation of a library of polymers.[4] Another interesting example was demonstrated by Zi-Chen *et al.* on the preparation of biodegradable block copolymers of poly(caprolactone) and poly (bromo caprolactone) by ring opening polymerization.[5] In the subsequent step, bromine groups were replaced by azide groups, which acted as a scaffold to introduce sugar units, and thus to obtain the final biodegradable glycopolymers. In a recent article published by our group we reported the synthesis of glycopolymer nanoparticles.[6] Sugar units were introduced by a post polymer modification approach using thiolactone rings as a scaffold to generate thiol groups that acted as a suitable nucleophile to introduce the sugar units.

Besides knowledge about the synthesis, understanding the lectin-polymer interactions is crucial from the application point of view. Glycopolymers exhibit specific interactions with lectins and proteins, which were observed to be stronger than that from single carbohydrate molecules due to the 'glycocluster effect'.[7] In different biological applications these polymers play important role as either inhibitors or effectors depending on their mechanism of interactions; i.e., steric stabilization, chelating effect, and statistical rebinding etc.[8, 9] The binding rate of the polymers depends on several parameters: the density of sugar units, the type of the sugar units and the shape of the glycopolymers.[10, 11] Extensive reports have already been published on this topic in the last decade, highlighting the synthesis of different glycopolymers with variety of shapes, composition etc. and the influence of the different parameters on the binding capacities with lectins and proteins.[12, 13] At this stage, it is indispensable to continue the preparation of novel series of responsive glycopolymers with the aim to (*i*) maximise their interaction with lectins by controlling the shape of the polymer and (*ii*) understand the possibility of controlling the polymer-lectin interactions by making use of external stimuli. This kind of studies will definitely help to improve the performance of polymer based delivery systems.

In this chapter, two synthetic strategies to prepare thermo-responsive hyperbranched glycopolymers are reported. Next to the frequently used RAFT technique, the Cu(0)-mediated radical polymerization has been applied as CRP technique to prepare the AB_2 oligomers which can further react into hyperbranched structures. The latter technique, which has been extensively described and investigated in Chapter V, has been depicted as an excellent polymerization technique for the preparation of well-defined polymer structures and is therefore applied for the preparation of hyperbranched glycopolymers.

In the first strategy, hyperbranched glycopolymers with mannose units present in each branching point and a skeleton based on PNIPAM, made by Cu(0)-mediated radical polymerization, have been synthesized (Strategy 1; Scheme VI-1). The thermo-responsive behaviour is related to the PNIPAM skeleton, while mannose was chosen as sugar unit because of its specific binding ability with lectin ConA.[14] One can expect that such hyperbranched polymers will have enhanced interactions with lectins, despite the presence of a low number of sugar units in the polymer backbone, because the mannose moieties, situated at each branching point, should be more available for cluster formation, compared to linear analogues. Furthermore, as a result of the thermo-responsive

behaviour of these types of polymers, different conformations of the polymers below and above the cloud point temperature should influence the lectin-polymer interaction.

In a second strategy, hyperbranched glycopolymers have been synthesized by RAFT copolymerization of NIPAM and propargyl acrylate, followed by the CuAAC reaction with azide mannose and subsequent thiol-Michael reaction (Strategy 2, Scheme VI-1). In this strategy, an adaptable amount of sugar moieties per branching point can be introduced, varying the interaction strength with their specific lectins.

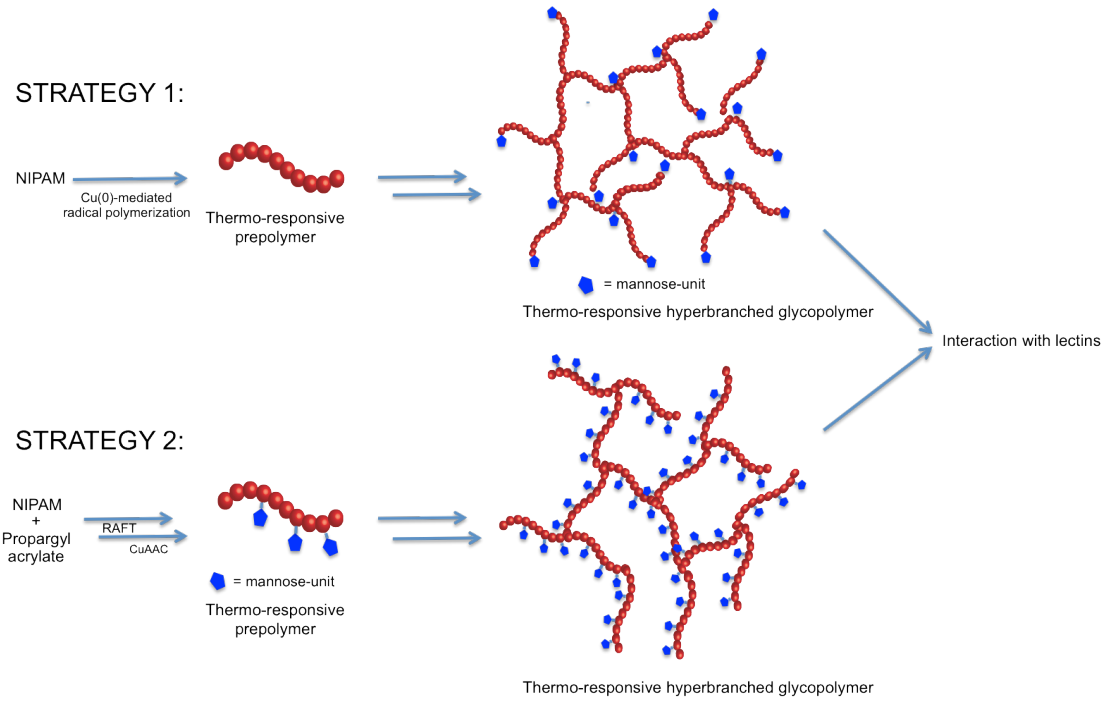

Scheme VI-1: General overview of the two applied strategies for the synthesis of thermo-responsive hyperbranched glycopolymers. Strategy 1: Cu(0)-mediated polymerization approach whereby a thiolactone containing intiator is used for the polymerization of NIPAM, which is opened with mannose-amine yielding hyperbranched structures upon thiol-yne chemistry. Strategy 2: RAFT approach whereby CuAAC is combined with thiol-X chemistry for the formation of hyperbranched glycopolymers with sugar-units along the backbone.

VI.2 Strategy 1: Synthesis of thermo-responsive hyperbranched glycopolymer using Cu(0)-mediated polymerization

Hyperbranched glycopolymers with mannose units at the branching points were synthesized via a three step procedure (Figure VI-1). In the first step, a functional branched AB_2 type initiator was synthesized, where A and B represents the thiolactone and bromo-propionyl functionality respectively (Figure VI-2). Using this AB_2 type initiator, linear PNIPAM polymers were synthesized *via* Cu(0)-mediated controlled radical polymerization (**2**, Figure VI-1). In a next step, the bromine end-groups are modified into methanethiosulfonate groups which can be considered as protected thiol functionalities. Upon opening of the thiolactone ring with amine sugar, a thiol is released which reacts with the methanethiosulfonate groups, yielding hyperbranched glycopolymers upon disulfide formation. Following this strategy, glycopolymers containing one sugar moiety per branching unit are synthesized.

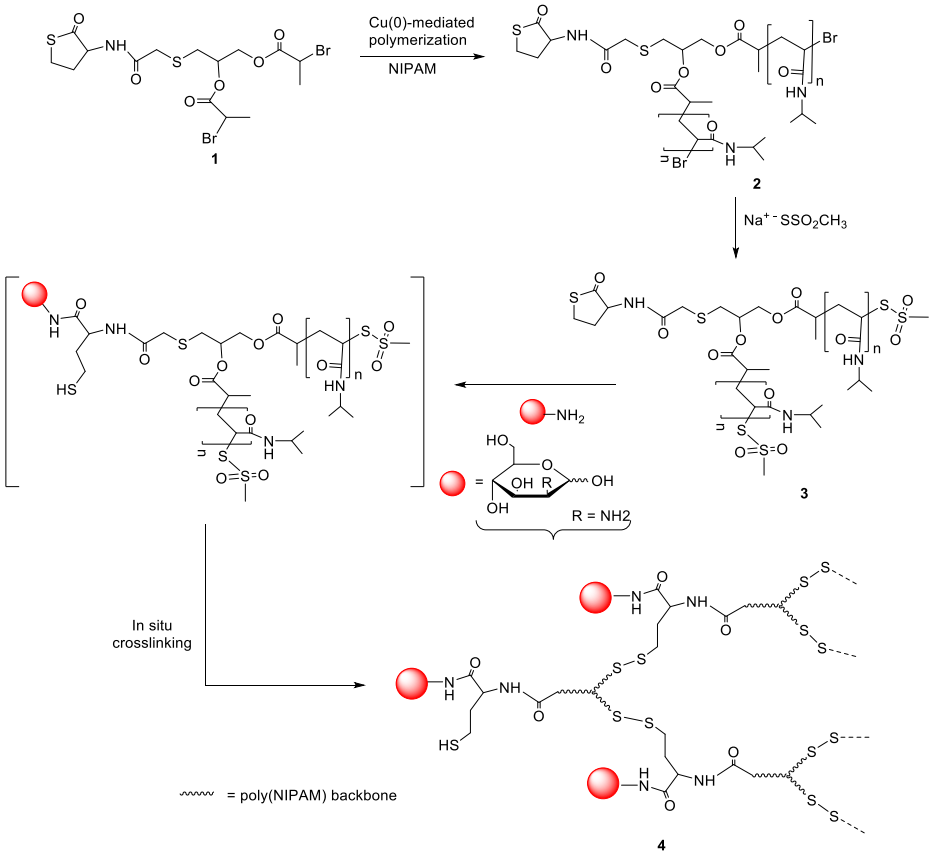

Figure VI-1: Synthesis scheme of the Cu(0)-mediated polymerization strategy for the synthesis of thermo-responsive hyperbranched glycopolymers.

VI.2.1 Synthesis of the AB_2 initiator for Cu(0)-mediated polymerizations

The first step in this synthesis strategy for the hyperbranched glycopolymers is the synthesis of a suitable initiator, which contains both a thiolactone moiety and two secondary bromide initiator groups (Figure VI-2). This was achieved *via* a straightforward three-step reaction starting from the commercially available DL-homocysteine thiolactone hydrochloride. Reaction with 2-bromoacetyl bromide in the presence of K_2CO_3, followed by the thiol-bromo reaction with 1-thioglycerol yielded a branched compound containing one thiolactone moiety and two hydroxyl groups. Modification of these hydroxyl groups into secondary bromide initiator groups upon reaction with 2-bromopropionyl bromide yields the desired AB_2 initiator as a yellowish oil. The product was purified *via* flash chromatography (eluents: *n*-hexane/ethyl acetate: 80/20) and the overall yield amounts 65%.

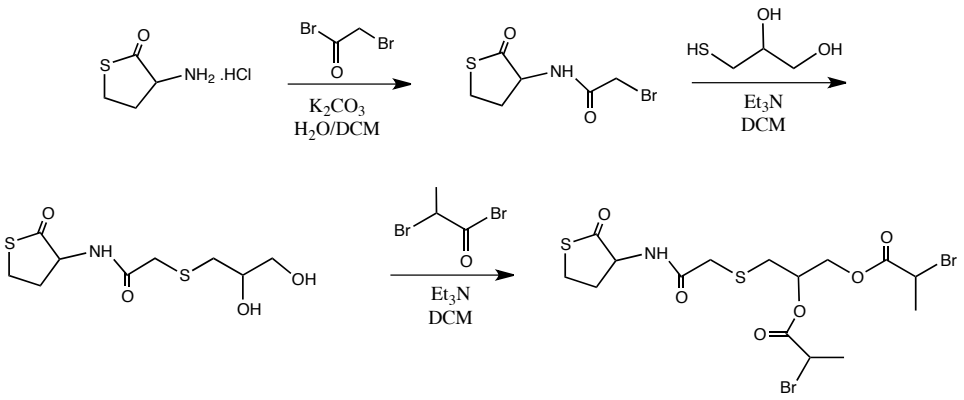

Figure VI-2: The different steps in the synthesis route of the thiolactone containing initiator for Cu(0)-mediated polymerization starting from the commercially available DL-homocysteine thiolactone hydrochloride.

VI.2.2 Synthesis of the thermo-responsive prepolymers

In a next step, the synthesized AB_2 initiator is used for the Cu(0)-mediated living radical polymerization of NIPAM to obtain thermo-responsive AB_2 prepolymers (Figure VI-3). This polymerization technique is known to be fast and yields polymers with high end-group fidelity, when applying the optimal conditions, which has been determined in Chapter V. This high end-group fidelity is an important feature for the synthesis of hyperbranched polymers in general.

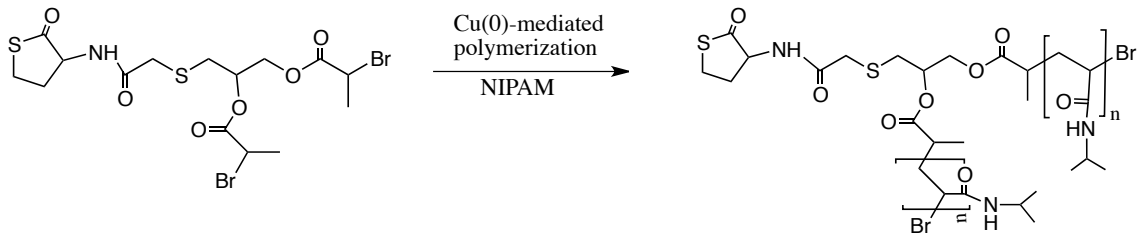

Figure VI-3: Cu(0)-mediated polymerization of NIPAM using the thiolactone containing AB_2 initiator yielding thermo-responsive prepolymers.

In this project, two different approaches of the polymerization technique are applied for reasons of comparison, namely the direct use of Cu(0) pellets as active species and the disproportionation of Cu(I) to Cu(0). In the first approach, Cu(0) is used in the form of pellets which promotes the reproducibility of the reaction, while in the second approach Cu(I) was stirred under inert atmosphere during one hour in the presence of the ligand Me_6Tren allowing the reduction to Cu(0). This reduction is confirmed by the formation of copper(0) particles that are clearly visible in the solution. For more information, the reader is referred to the experimental section.

In both approaches, the polymerization reactions were performed at room temperature and water was applied as solvent. A small amount of DMF was added to enhance the solubility of the initiator. After polymerization, the PNIPAM prepolymer was purified by two-fold precipitation in cold diethyl ether, yielding a white powder.

Table VI-1: Reaction conditions and results of the Cu(0)-mediated polymerization of NIPAM by the direct use of Cu(0) pellets.

Entry	$[M]_0/[I]_0/[L]_0/[CuBr_2]_0$	t [h]	$M_{n,\,SEC}$ [a] [g/mol]	$M_{n,\,NMR}$ [g/mol]	Đ	Conv. [b] [%]
1	50/1/0.12/0.05	4	3500	2600	1.14	75
2	100/1/0.12/0.05	6	6300	4300	1.09	89
3	100/1/0.12/0.05	4	5000	3200	1.10	95
4	50/1/0.12/0.05	4	4500	2900	1.09	95

Polymerizations performed in H_2O (+ minimum amount of DMF) at room temperature. [a]SEC, calibrated with PMMA standards; [b]Determined via ^{1}H NMR.

Table VI-2: Reaction conditions and results of the Cu(0)-mediated polymerization of NIPAM by the disproportionation of Cu(I) to Cu(0).

Entry	$[M]_0/[I]_0/[L]_0/[CuBr]_0$	t [h]	$M_{n,\,SEC}$ [a] [g/mol]	$M_{n,\,NMR}$ [g/mol]	Đ	Conv. [b] [%]
5	50/0.8/0.4/0.4	4	7800	4600	1.13	85
6	50/1/0.4/0.4	6	4500	3200	1.08	90
7	50/1/0.5/0.5	4	5000	4100	1.10	95
8	100/1/0.5/0.5	4	8900	6100	1.09	95

Polymerizations performed in H_2O (+ minimum amount of DMF) at room temperature. [a]SEC, calibrated with PMMA standards; [b]Determined via ^1H NMR.

The excellent end-group fidelity was proven *via* MALDI-TOF MS analysis (Figure VI-4) as the experimental masses are in good agreement with the theoretical calculated masses. Both approaches resulted in similar homopolymers with an average relative molecular weight (M_n) between 3500 and 8900 g/mol and low dispersities (below 1.15)

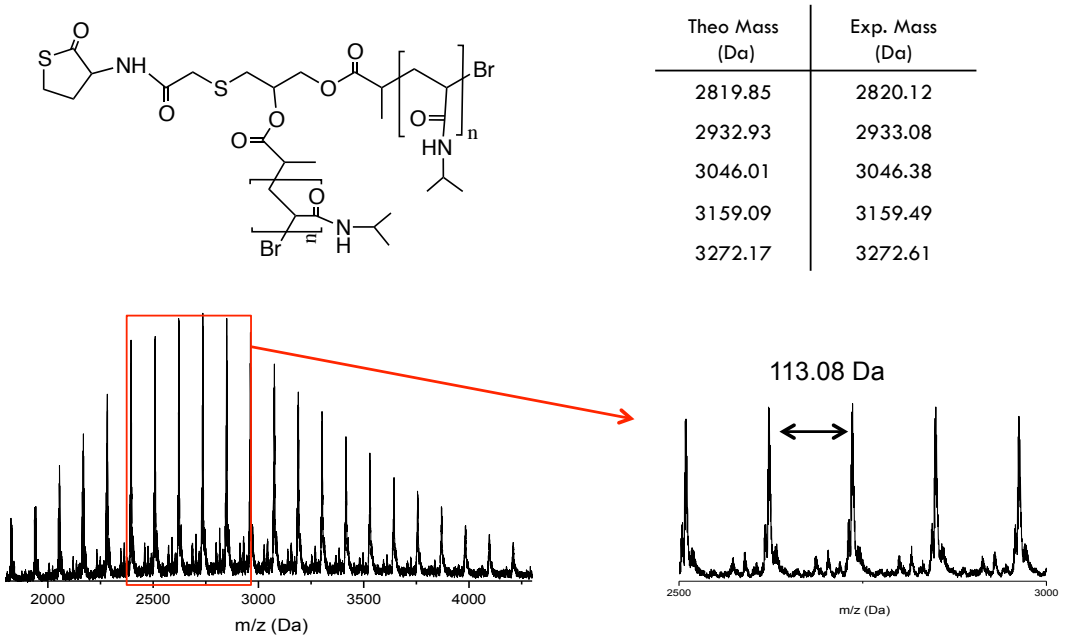

Figure VI-4: MALDI-TOF analysis of PNIPAM prepolymer (Entry 6, Table VI-2). The experimental masses are in good agreement with the theoretical masses, confirming the presence of the bromine end-groups after Cu(0)-mediated polymerization.

VI.2.3 Post-modification with sodium methanethiosulfonate

Next, the bromine end-groups of these PNIPAM prepolymers were modified into methanethiosulfonate groups via a S_N2 reaction in the presence of triethylamine. This procedure is a straightforward method for the transformation of halide end-groups into activated disulfides using methanethiosulfonate, which can further react with thiols yielding disulfide containing compounds.[15] The nucleophilic substitution reaction was performed in DMF as solvent at 40°C for 16 hours in the presence of sodium methanethiosulfonate with a [bromide]/[sodium methanethiosulfonate] ratio equal to 1/3 (Figure VI-5). After the reaction, the excess of methanethiosulfonate was removed by several consecutive precipitations in THF. Finally, the polymers were purified by two-fold precipitation in cold diethyl ether, yielding a white powder.

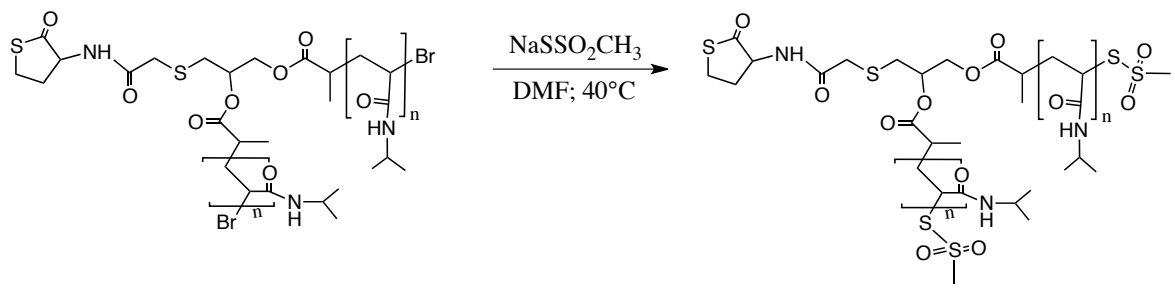

Figure VI-5: Post-modification of the bromide end-groups of the prepolymers into methanethiosulfonate group via nucleophilic substitution with sodium methanethiosulfonate at 40°C in DMF for 16 hours.

MALDI-TOF MS analysis again confirmed the successful replacement of the bromine end-groups with the methanethiosulfonate groups (Figure VI-6). Moreover, the presence of the methanethiosulfonate groups was also proven by ^{1}H NMR analyses via the appearance of a new signal at δ = 3.2 ppm, which could be attributed to methyl functionality of the methanethiosulfonate (Figure VI-7). It is noteworthy that sodium methanethiosulfonate is insoluble in chloroform, the applied NMR solvent, which indicates that the presence of the new signal could not arise from contamination. Moreover, SEC analysis showed no characteristic change in dispersity before and after end-groups modification.

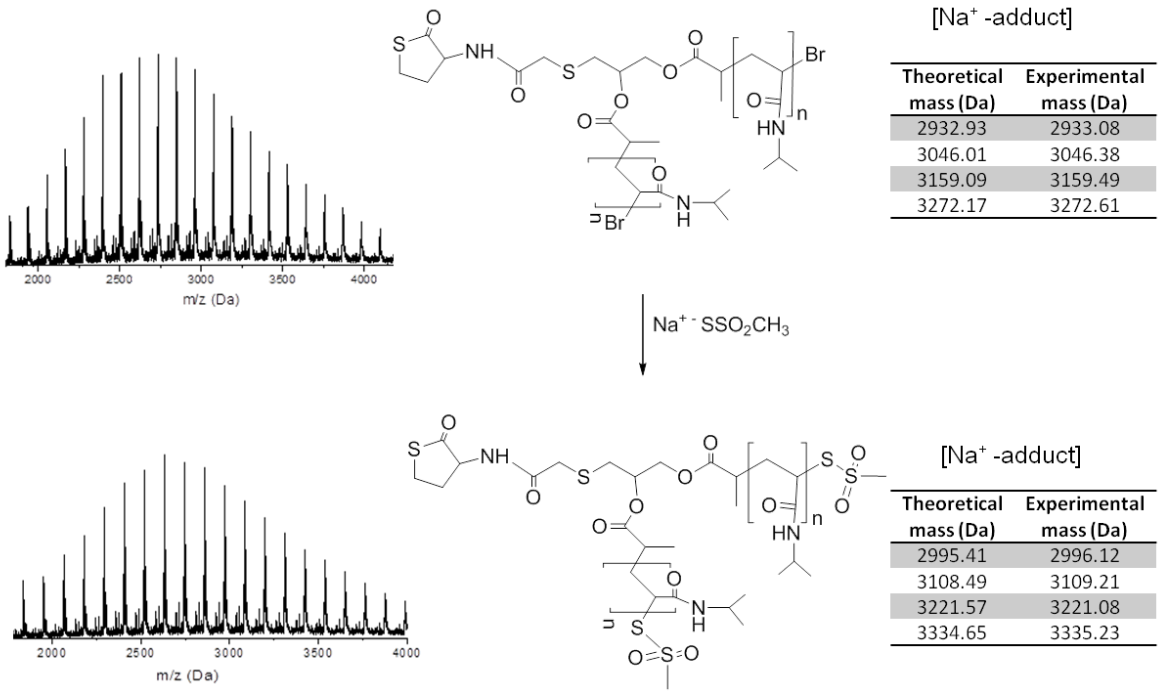

Theoretical mass (Da)	Experimental mass (Da)
2932.93	2933.08
3046.01	3046.38
3159.09	3159.49
3272.17	3272.61

Theoretical mass (Da)	Experimental mass (Da)
2995.41	2996.12
3108.49	3109.21
3221.57	3221.08
3334.65	3335.23

Figure VI-6: MALDI-TOF analysis of PNIPAM (Entry 6, Table VI-2) after modification of the bromide end-groups into methanethiosulfonate groups. The experimental masses are in good agreement with the theoretical masses, confirming the completeness of the modification reaction.

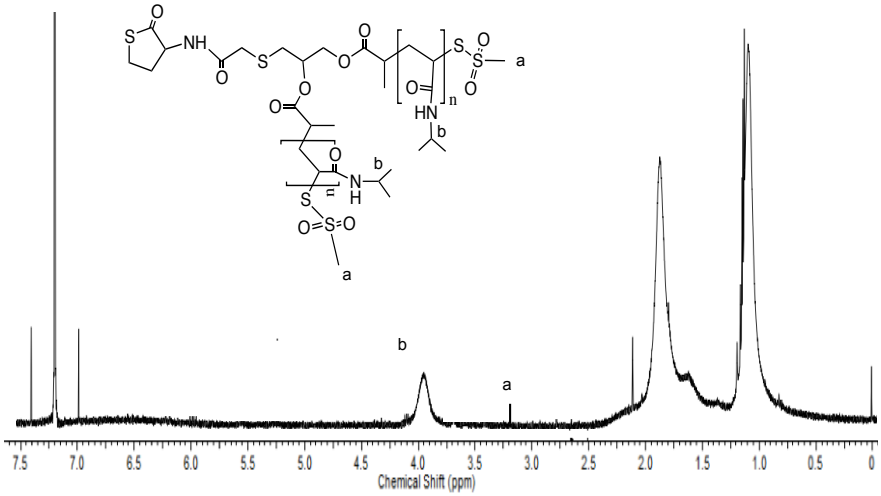

Figure VI-7: ^{1}H NMR (CDCl3; 500 MHz) of the PNIPAM oligomer after post-modification with sodium methanethiosulfonate.

VI.2.4 Opening of the thiolactone ring and subsequent formation of hyperbranched polymers

In the final step of this approach, aiming for the preparation of hyperbranched polymers (Figure VI-1, **4**), two known reactions were combined: (i) ring-opening of the thiolactone with an amine to generate thiol groups[16, 17] and (ii) the reaction of methanethiosulfonate with thiols upon formation of disulfide bonds.[18] The thiolactone moiety on the PNIPAM chain end was opened by reaction with the commercially available D-(+)-mannosamine hydrochloride, leading to the introduction of mannose units in the polymer chain and the simultaneous generation of functionalities. At the same time, the thiol groups can *in situ* react with the methanethiosulfonate groups upon disulfide formation, resulting in the formation of thermo-responsive hyperbranched polymers containing one sugar moiety per branching unit (Figure VI-8).

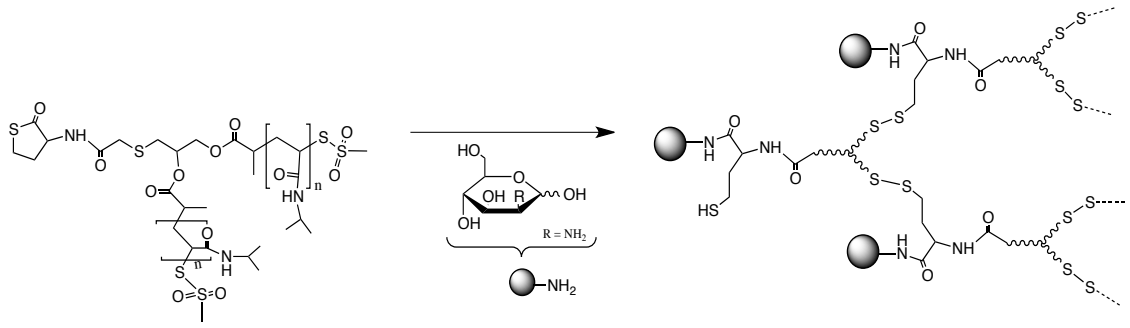

Figure VI-8: Ring-opening of the thiolactone moiety upon aminolysis with the commercially available mannosaminehydrochloride, releasing a thiol. This thiol can subsequently react with the methanethiosulfonate groups upon disulfide formation, yielding thermo-responsive hyperbranched polymers.

Hereby it is chosen to work with highly concentrated solutions (6 M) to promote the formation of hyperbranched structures and to reduce the intern ring formation. Moreover, DMSO is used as solvent for two reasons. First of all, it is one of the few solvents the mannosamine compound is fully soluble in and secondly disulfide formation is promoted in this solvent,[19] which is an important feature for the formation of the hyperbranched polymers. The solution was stirred for 6 hours while samples were taken for SEC and NMR analysis. After 6 hours, the solution became as viscous that stirring was not possible anymore. The reaction completion, yielding the hyperbranched polymers was confirmed via SEC analysis. SEC traces reveal that both the molecular weight and dispersity increased a lot, which is typical for hyperbranched polymers (Đ = 7.3) (Figure VI-9, 2).

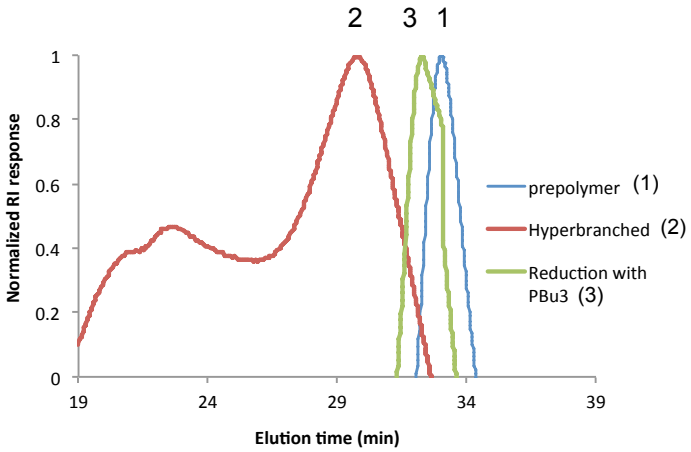

Figure VI-9: SEC traces of the PNIPAM prepolymer (1), the hyperbranched structure (2) and the reduced structure (3).

VI.2.5 Degradation and thermo-responsive behaviour studies of the hyperbranched polymer

As the PNIPAM prepolymers are connected to each other via disulfide bonds, the structure can be reduced into its prepolymers each containing one sugar unit. This degradation behaviour could be applied in the area of drug or gene delivery applications.[20] To demonstrate this reducability, the hyperbranched polymer was treated with *n*-tributylphosphine, a frequently used reducing agent. SEC analysis showed that a linear polymer with low molecular weight (M_n = 4900 g/mol) and dispersity (≤ 1.25) was obtained, which are similar to those from the earlier prepared prepolymers (Figure VI-9, 3). This degradation behaviour could be applied in the area of drug or gene delivery applications.

Besides the fact that the hyperbranched polymers can be degraded to their prepolymers, it is expected that they also possess a thermo-responsive character as they are built up out of PNIPAM prepolymers. PNIPAM is a well-known thermo-responsive polymer, generally having a cloud point temperature (T_{cp}) in the range of 28°C - 32°C. To understand the thermo-responsive behaviour of the newly prepared hyperbranched polymers, the cloud point temperature was determined *via* turbidimetry. This temperature is directly related to the interaction of the polymer with water and thus its conformation in solution. Below the cloud point, the polymer is present in coil form while above the cloud point, the coil conformations collapse to form globular structures. In this work, the cloud point for the prepared linear PNIPAM prepolymers was 32°C (Figure VI-10, 1). The introduction of hydrophilic mannose units in the polymer chain has an impact on the cloud point temperature and,

thus, for the hyperbranched polymers, the T_{cp} increases from 32°C to 39°C. This increase can be attributed to the fact that introduction of hydrophilic mannose units in the polymer chain leads to a favourable enthalpic interaction of the polymer with water.

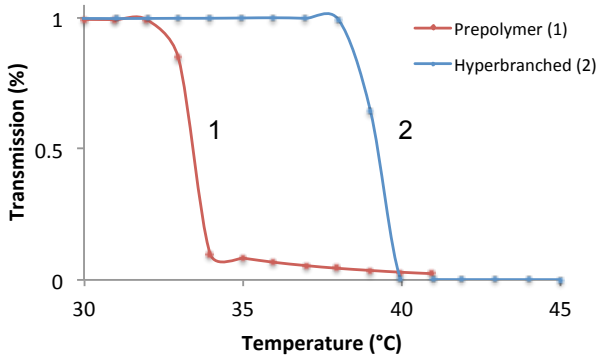

Figure VI-10: Turbidimetry measurements of the PNIPAM prepolymer (1) and the hyperbranched glycopolymer (2) indicating the cloud point temperature increased from 32°C to 39°C as a result of the introduction of the hydrophilic sugar units.

VI.2.6 Interaction of the hyperbranched glycopolymer with Con A

The investigation of the lectin-glycopolymer interaction is of huge importance for the applications of the relevant glycopolymers.[10, 21, 22] The potencies of glycopolymers acting as inhibitor or effectors in biological applications depend on the specific operating mechanism, such as the chelate effect, steric stabilization, substrate binding, receptor clustering, etc. It is already proven that the specific features of the glycopolymer (architecture, dispersity and epitope density) determine the binding efficiency.[23, 24] This part of the project has been performed in collaboration with Dr. Becer, an expert on the characterization of glycopolymers.

As mentioned in the introduction, the interaction of the glycopolymers with lectins is well known and a lot of work was already performed to understand the influence of different parameters such as the type of sugar unit and polymer architecture. However, the interaction of thermo-responsive hyperbranched glycopolymers with lectins has not been described yet to our knowledge. The two aims of this part of the study is to understand (i) their interaction with lectins as a function of polymer concentration and (ii) the influence of different conformations of the polymers in solution present below and above cloud point (T_{cp}).

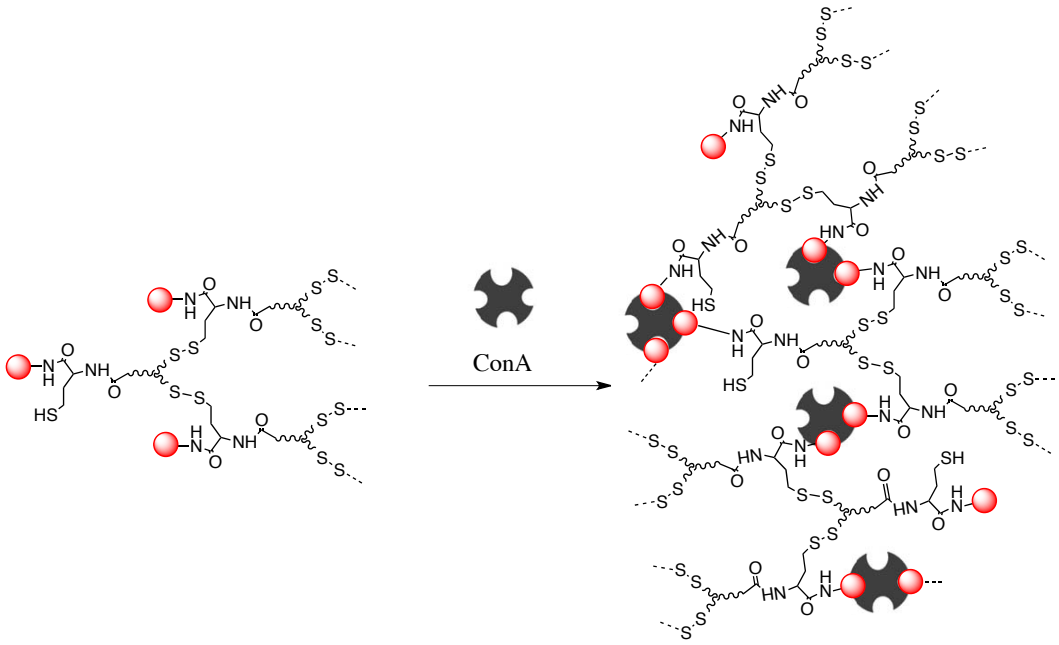

Figure VI-11: Schematic representation of the interaction of lectins with the hyperbranched glycopolymer.

For the current study, Con A was chosen as a model lectin due to its signaling properties and excellent complex forming abilities with sugar units.[25] Solutions of hyperbranched glycopolymers were added to a known concentration of Con A (2 mg/mL) and the rate of interaction was determined by UV-Vis measurements. The lectin-glycopolymer interaction leads to precipitation of the polymer-lectin clusters, which can be monitored by analyzing the transmission of light (wavelength 420 nm) through the solution using a UV-Vis spectrometer. Three different concentrations of the polymer solution were first studied to understand the interaction of the polymer with Con A. As expected, the lectin-polymer interaction is faster with increasing polymer concentration, mainly due to the higher presence of mannose units that are responsible for lectin binding (Figure VI-12, left).

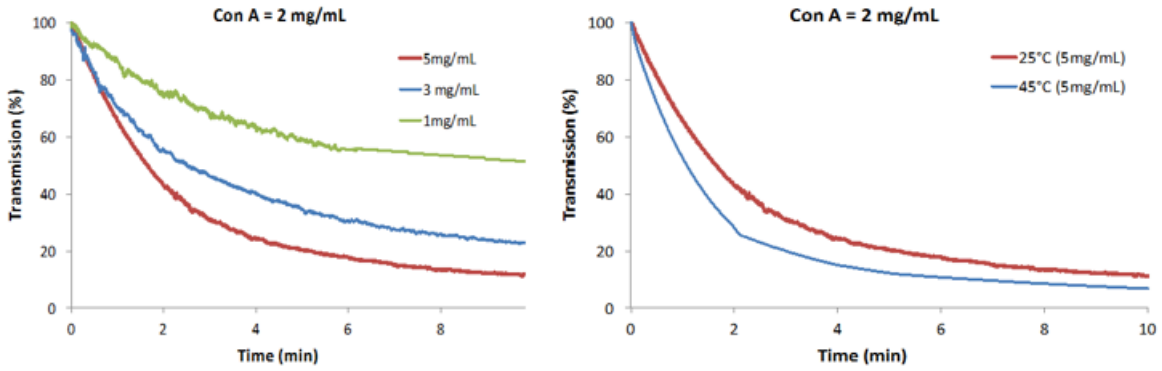

Figure VI-12: UV-Vis turbidimetry measurements for determining the rate of interaction of the hyperbranched glycopolymers with the Con A lectin (left). Determination of the interaction rate for different concentrations of the hyperbranched glycopolymer with a fixed concentration of Con A (right). Determination of the interaction rate of the hyperbranched glycopolymer with Con A above and below the cloud point temperature.

The hyperbranched glycopolymers exhibit a thermo-responsive behaviour (T_{cp} = 39°C), which indicates the presence of coiled forms below T_{cp} and a collapsed globule structure above T_{cp}. This conformational change is expected to have an impact on the interaction properties with lectins because the availability of the mannose units should be different in the coil and globule structure. This hypothesis was examined by studying the lectin-polymer interaction above or below the cloud point temperature. It was observed that the interaction occurs faster above the cloud point temperature (Figure VI-12, right). This phenomenon could be explained by the presence of the globular structure above T_{cp}, which leads to a higher concentration of hydrophilic mannose moieties at the outer part of the globules. In this way, it is assumed that the availability of mannose units is higher, thus resulting in faster ConA-glycopolymer interaction.

VI.3 Strategy 2: Synthesis of thermo-responsive hyperbranched glycopolymers using RAFT

The aim of this second strategy is to prepare thermo-responsive hyperbranched glycopolymers, which contain a variable amount of sugar moieties. This can be achieved by the copolymerization of NIPAM with propargyl acrylate in different ratios *via* RAFT and subsequent post-modification reactions to introduce the sugar units. It is believed that this higher amount of sugar units will have an improved effect on the binding properties with their specific lectins.

The synthesis scheme of this second strategy is depicted in Scheme VI-2. In the first step, a suitable chain transfer agent (CTA), containing two primary hydroxyl groups at the ω-chain end and a trithiocarbonate functionality, is synthesized. This CTA is subsequently used for the RAFT copolymerization of *N*-isopropyl acrylamide (NIPAM) and propargyl acrylate (Pro A) in certain ratios, yielding thermo-responsive prepolymers. In a next step, the two hydroxyl groups at the α-chain end are reacted with acryloyl chloride, resulting in two acrylate groups, while the pendant alkyne groups are clicked with azide-mannose compounds upon CuAAC reaction. Aminolysis of the ω-trithiocarbonate group yields a thiol functionality, which subsequently reacts upon Michael-addition with the acrylate groups resulting in thermo-responsive hyperbranched glycopolymers.

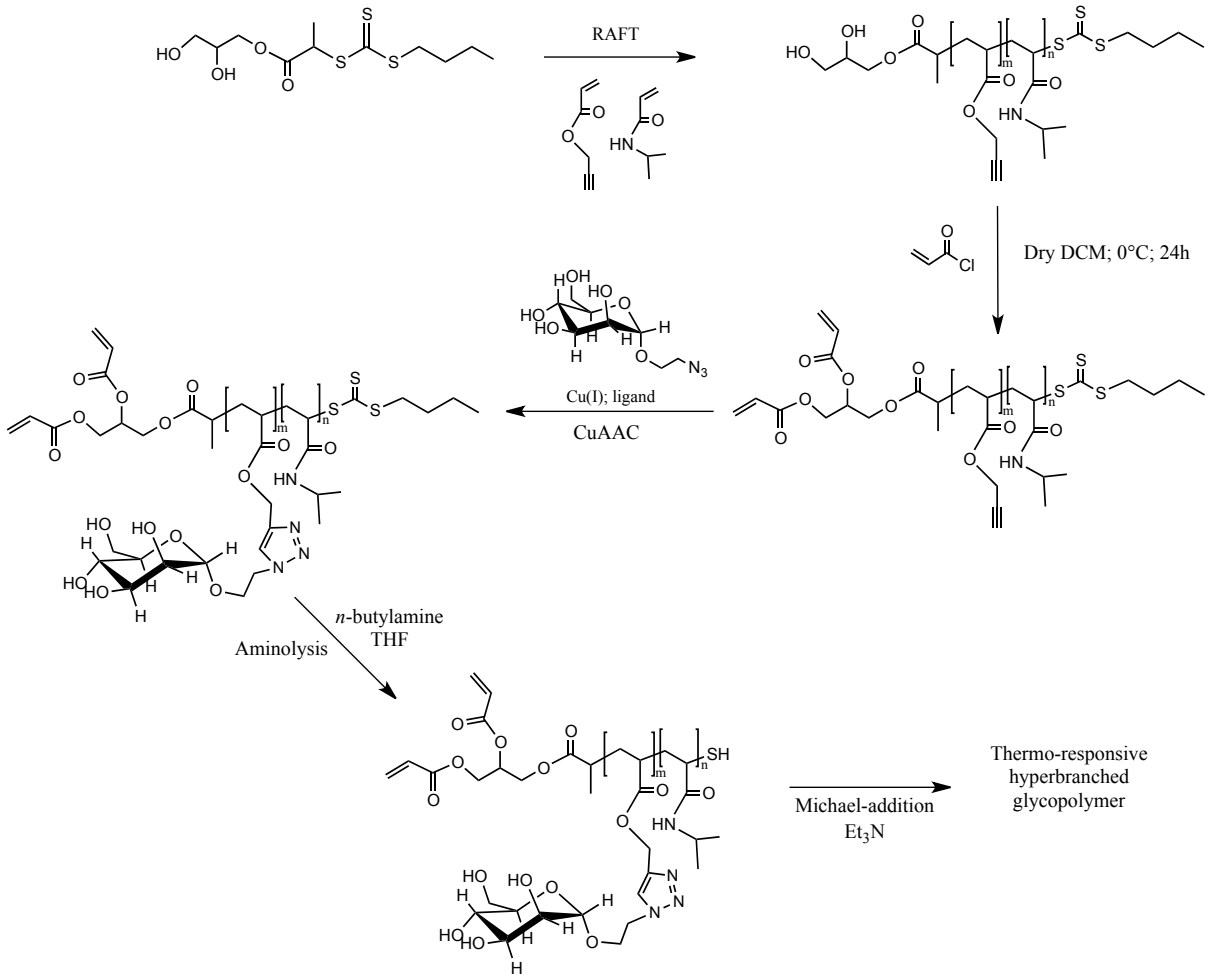

Scheme VI-2: General overview of the different steps used in the RAFT strategy for the synthesis of thermo-responsive hyperbranched glycopolymers.

VI.3.1 Synthesis of the DPBCP RAFT agent

The CTA (2,3-dihydroxypropyl-2-(((butylthio)carbonothioyl)thio) propanoate (DPBCP) (Figure VI-13, 3) was synthesized via a three step reaction. First of all BuPAT (Figure VI-13, 1) was synthesized according to a procedure described in section IV.2.1 (Figure IV-2).[26] The carboxylic acid at the α-chain end was subsequently modified into an acetonide group by esterification with solketal in the presence of DCC and a catalytic amount of DMAP in dry DCM. After three days of stirring at room temperature, the salts obtained (DCU) are filtered off and the product was concentrated under reduced pressure with an overall yield of 65%. Both NMR (^{1}H NMR, ^{13}C APT and 2D-HSQC) as well as LC-MS confirmed the complete conversion of both steps. By esterification of BuPAT with solketal, different additional signals appear in ^{1}H NMR. The two specific signals, arising from the two methyl groups from the esterified BuPAT (Figure VI-13, 2) at 1.29 ppm and 1.38 ppm disappear after deprotection under acidic

conditions proving the complete deprotection of the acetal group into the two corresponding hydroxyl groups (Figure VI-13, 3). 2D-HSQC is used to correctly assign the different signals. Moreover, the broad signal at 2.3 ppm could be assigned to the two hydroxyl groups at the α-chain end of the synthesized CTA. Furthermore, the integration and couplings of the different signals in 2D-HSQC are in good agreement with the desired product.

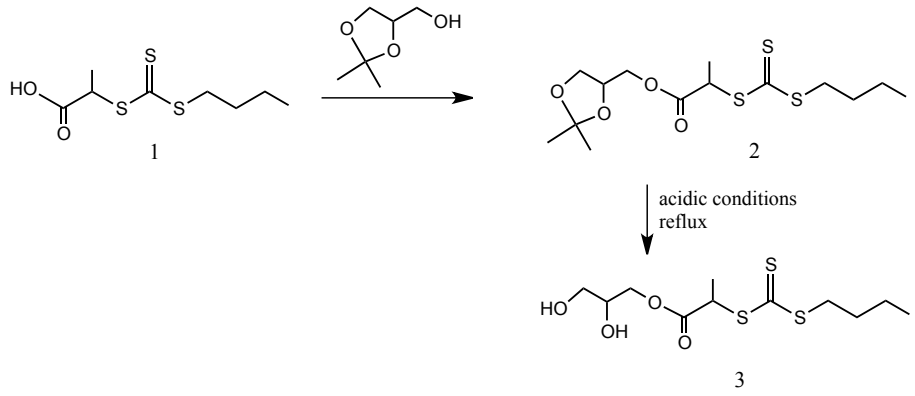

Figure VI-13: Applied synthesis strategy for the preparation of the DPBCP (3) starting from BuPAT (1) by esterification with solketal followed by deprotection under acidic conditions.

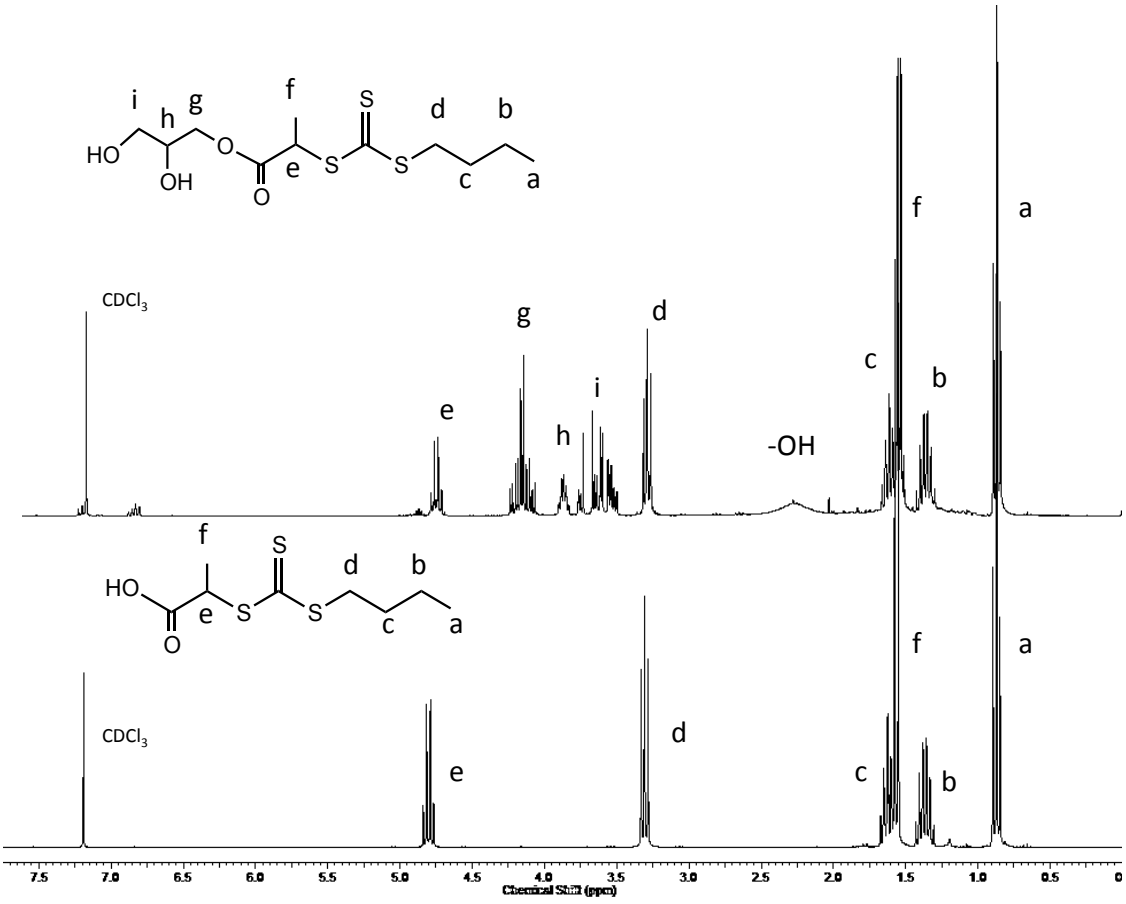

Figure VI-14: ^{1}H NMR spectra ($CDCl_3$; 300 MHz) of the CTA with a carboxylic acid at the α-chain end (bottom) and of the CTA with a diol at the α-chain end (top).

VI.3.2 RAFT copolymerization of *N*-isopropylacrylamide and propargyl acrylate

In response to the expectations of advanced polymer synthesis, RAFT polymerization has clearly demonstrated the ability to control the polymerization of a broad range of functional monomers. Considering this, the present work extends the use of the combination of NIPAM and propargyl acrylate (ProA) monomers in RAFT polymerization, allowing for the preparation of well-defined copolymers with adjustable alkyne content and T_{cp}, predictable molecular weights (M_w) and low dispersities (Đ). These copolymerizations were done using the optimized conditions of the homopolymerization of NIPAM as at these conditions a good control over the copolymerization was observed. As such, the RAFT polymerization was performed in THF at 65°C using DPBCP as CTA in the presence of the thermal radical initiator AIBN. Different monomer ratios were studied, taking into account the preferable alkyne content, and thus in a later stage sugar moieties and T_{cp} of the copolymers.

In a first stage of this strategy, a kinetic study of the copolymerization was performed to provide a better insight in the rate characteristics of the copolymerization. It is chosen to perform a copolymerization with a monomer ratio NIPAM/ProA of 10/1 as at this ratio the copolymers exhibit a cloud point temperature as well as enough alkyne groups that, in a later stage, can be converted into sugar units to yield thermo-responsive glycopolymers. At specific time, samples for NMR, SEC and GC are taken. This latter technique was used to determine the conversion of both monomer as a function of the time while SEC was applied for the determination of the molecular weight and dispersities. NMR was used to confirm the end-group fidelity of this copolymerization.

This kinetic study revealed a controlled polymerization process with a steady increase of both monomer conversions versus time, while the molecular weight of the copolymer linearly evolved with the average monomer conversion, yielding monomodal molecular weight distribution and narrow dispersities Đ (Figure VI-15). Moreover it was observed that both monomers are incorporated with similar rates, indicating that the experimental ratios of the monomers are in good agreement with the theoretical ones. Furthermore, high end-group fidelity was confirmed using ^{1}H NMR and ^{13}C NMR (90%). UV-Vis analysis confirmed the presence of the trithiocarbonate group in the copolymer after purification (two-fold precipitation in cold diethyl ether) as an absorbance at 310 nm was observed which is attributed to the trithiocarbonate group.

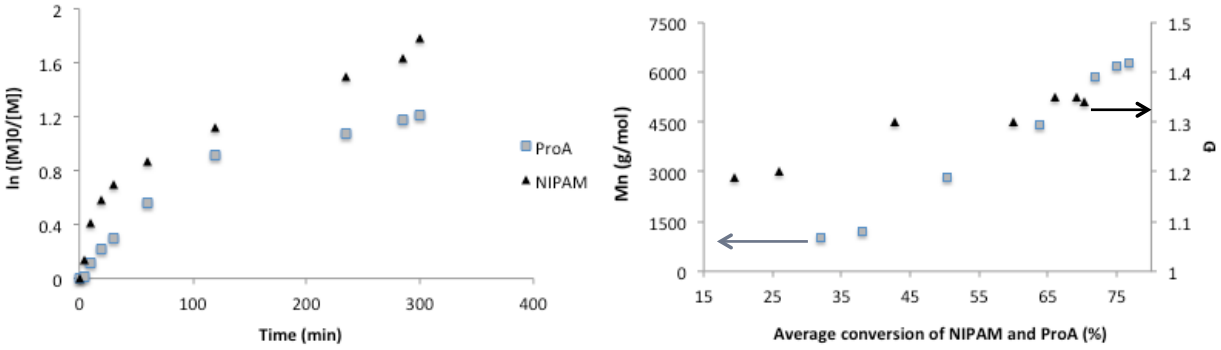

Figure VI-15: Copolymerization of NIPAM and ProA using DPBCP as CTA, at 65°C in 50 vol% THF and with 0.1 eq. AIBN as the radical source (NIPAM+ ProA)/DDMAT 30/1 (Entry 1, Table 1): (left) straight kinetic plots; (right) copolymer molecular weight and evolution of dispersity with the average monomer conversion.

Table VI-3: Summary of the reaction conditions and results of the RAFT copolymerization of NIPAM and ProA mediated by DPBCP.

Entry	$[M]_0/[CTA]_0/[I]_0$	NIPAM/ProA	t [h]	$M_{n,\,SEC}$ [g/mol]	Đ	Conv. NIPAM[a] [%]	Conv. ProA[a] [%]
1	30/1/0.11	5/1	4	4000	1.21	67	60
2	50/1/0.11	5/1	4	5600	1.19	65	55
3	50/1/0.11	9/1	3	6400	1.30	60	48
4	30/1/0.11	10/1	3	4000	1.24	66	65

All polymerizations were performed at 65°C in 50 vol% THF; initiator: AIBN; CTA: DPBCP; [a)] determined via ^{1}H NMR and SEC analysis.

In Table VI-3 the different applied reaction conditions and analysis results are depicted. As expected from the kinetic study, the experimental monomer ratio is in good agreement with the theoretical, as both monomers are incorporated in the polymer with similar rate. This ratio is determined via ^{1}H NMR by the ratio of the integration of specific NIPAM signal at 4.05 ppm (*CH*-signal) with the integration of the specific ProA signal at 4.5 ppm (*CH_2-signal)*. In Figure VI-16 the example is given for Entry 1 where the specific signals are identified in the structure.

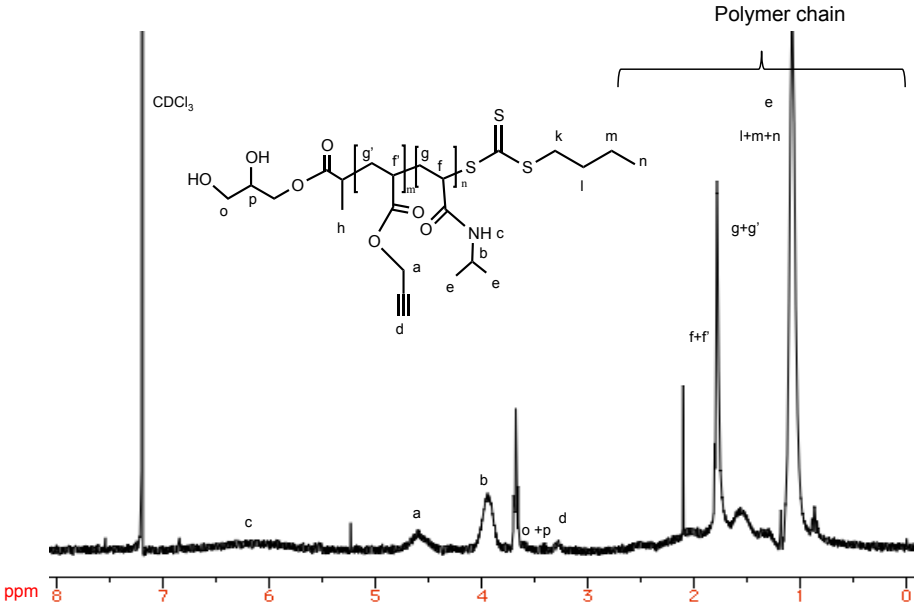

Figure VI-16: ^{1}H NMR ($CDCl_3$; 300 MHz) of Entry 1 : determination of the ratio NIPAM/ProA in the copolymer by taking the ratio of signals a/2b.

Moreover, the T_{cp} of some synthesized copolymers is determined and compared with each other. Turbimetry analysis gives the transmission plot as a function of the temperature from which the T_{cp} can be determined as the point where the transmission starts to drop. As is clear for the transmission curve in Figure VI-17, the T_{cp} of Entry 1 is a few degrees lower as that from Entry 3. This can easily be explained by the fact that the NIPAM/ProA ratio in Entry 1 is lower, resulting in a more hydrophobic structure. Since the cloud point temperature of PNIPAM is independent of the molecular weight,[27] the T_{cp} only depends on the incorporated amount of alkyne groups in the copolymer: the higher the ProA/NIPAM ratio, the lower the T_{cp} as a result of the higher amount of hydrophobic alkyne moieties in the copolymer chain.

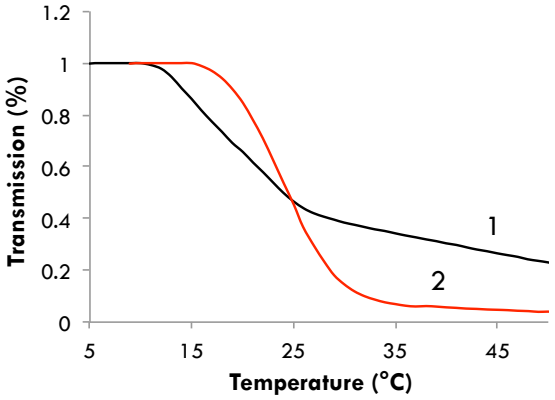

Figure VI-17: Cloud point temperature determination of Entry 1 (NIPAM/ProA = 5/1) (1) and Entry 3 (NIPAM/ProA = 9/1) (2) via UV-Vis measurements.

VI.3.3 Post-modification of P(NIPAM-co-ProA)

VI.3.3.1 *Modification of the hydroxyl groups with acryloyl chloride*

P(NIPAM-co-ProA), synthesized via RAFT, has been subjected in the next step to a post-modification reaction of the hydroxyl groups with acryloyl chloride. Upon esterification reaction, the hydroxyl groups at the α-chain end can be modified in acrylate groups which are know to easily react with thiols upon Michael addition in the presence of a base (see section II.2.2.1.3) (Figure VI-18). P(NIPAM-co-ProA) was functionalized, using 8 times excess of acryloyl chloride, in the presence of Et_3N in dry DCM. The reaction was carried out at 0°C for 72 hours and the product was purified by two-fold precipitation in cold diethyl ether and dried overnight under vacuum. The purified copolymer was analyzed by SEC, UV-Vis and NMR spectroscopy.

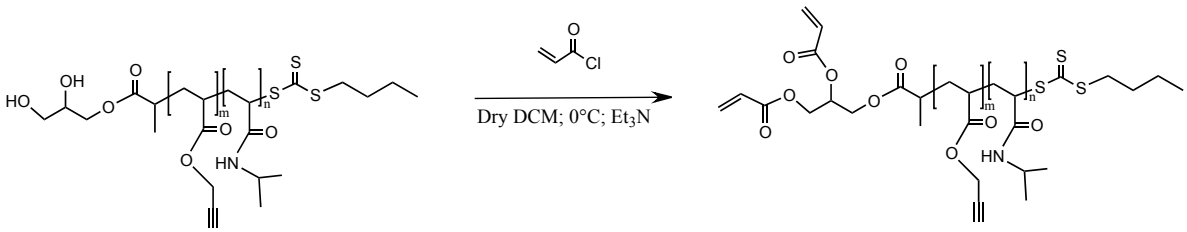

Figure VI-18: Post-modification of the terminal hydroxyl groups in P(NIPAM-co-ProA) with acryloyl chloride upon thiol-Michael addition, resulting in two terminal acrylate groups.

In Table VI-4 the molecular weight and the dispersities of the different modified copolymers are shown. After modification, a noticeable increase in molecular weight is observed, while the dispersities almost did not change. The acrylate end groups are able to give the copolymer another folding, resulting in a different hydrodynamic volume, which can lead to a higher increase in molecular weight than expected by SEC. This result was a first indication that the post-modification reaction was successful.

Table VI-4: SEC analsysis results of P(NIPAM-co-ProA) before (Entries 1 and 2) and after (Entries 1a and 2a) modification with acryloyl chloride.

Entry	NIPAM/ProA	$M_{n,\,SEC}$ [a] [g/mol]	Đ
1	5/1	4000	1.2
1a	5/1	5500	1.3
2	9/1	6400	1.3
2a	9/1	7150	1.3

Via turbidimetry analysis the T_{cp} of the copolymer after post-modification was determined and compared with the T_{cp} before the post-modification reaction. This was done for entries 1 and 1a. The corresponding transmission curves are depicted in Figure VI-19. For both copolymers, a decrease in T_{cp} was observed due to the modification of the more hydrophilic hydroxyl groups into acrylate groups. This observation was the second indication of the success of the modification into the acrylate groups at the α-chain end of the copolymer chain.

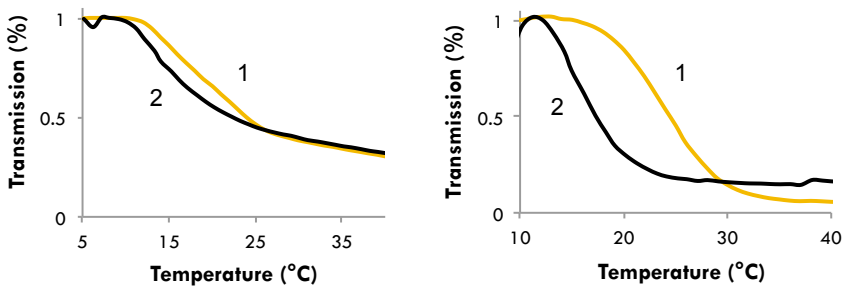

Figure VI-19: Cloud point determination of Entry 1 before (1) and after (2) modification with acryloyl chloride (left) and of Entry 2 before (1) and after (2) the post-modification reaction (right) via UV-Vis measurements. It is observed that the cloud point has dropped with a few degrees after post-modification reaction in both cases.

The analysis of the modified copolymer via ^{1}H NMR was not straightforward,as the typical acrylate signals (5.5 - 6.5 ppm) appear in the same region as the broad N-H signal of the NIPAM groups. Nevertheless, at this stage of the research, it was assumed that the post-modification reaction was successful due to the presence of some small signals on top of the broad N-H signal (Figure VI-20). However, in section VI.3.3.3, it will become clear that the modification into acrylates at the α-chain end was not complete.

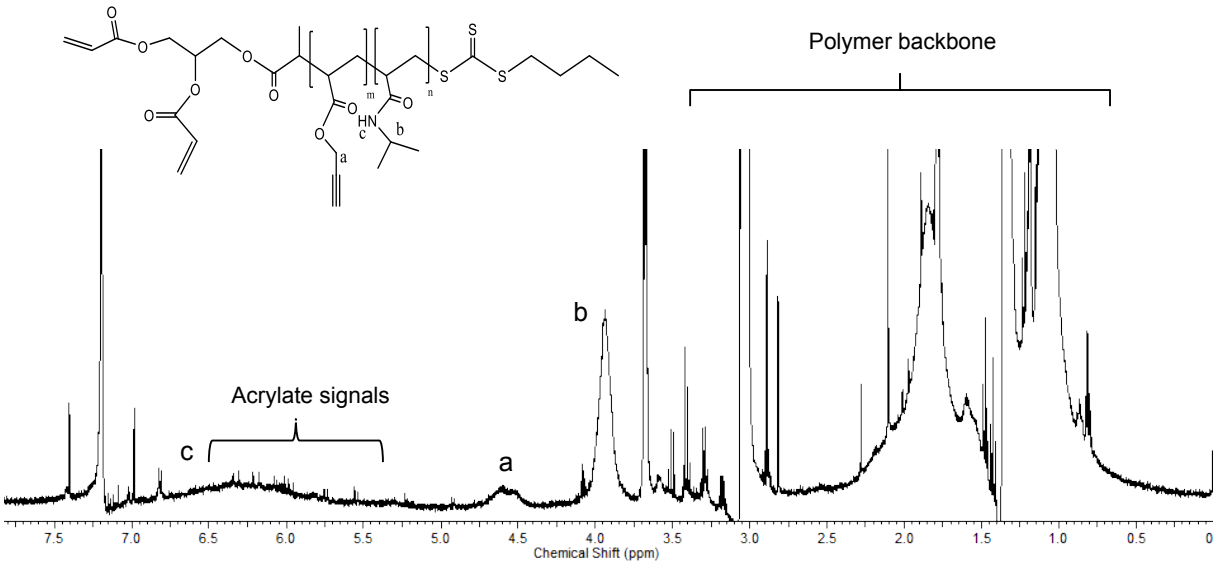

Figure VI-20: ^{1}H NMR ($CDCl_3$; 500 MHz) of the copolymer after modification with acryloyl chloride.

VI.3.3.2 *CuAAC reaction of the alkyne groups with azide-mannose*

The alkyne groups present in the copolymer have subsequently been reacted with azide-mannose. This post-modification reaction, which is depicted in Figure VI-21, catalyzed by Cu(I) in the presence of the ligand PMDETA. Due to the slight solubility of the sugar compound, the reaction was performed in DMF at 40°C for 4 hours. This reaction is followed with an online-infrared technique by following the decrease of the typical azide signal at 2100 cm^{-1}. The modified copolymer was purified by two-fold precipitation in cold diethyl ether, dried under vacuum and analyzed by SEC, UV-Vis and NMR spectroscopy.

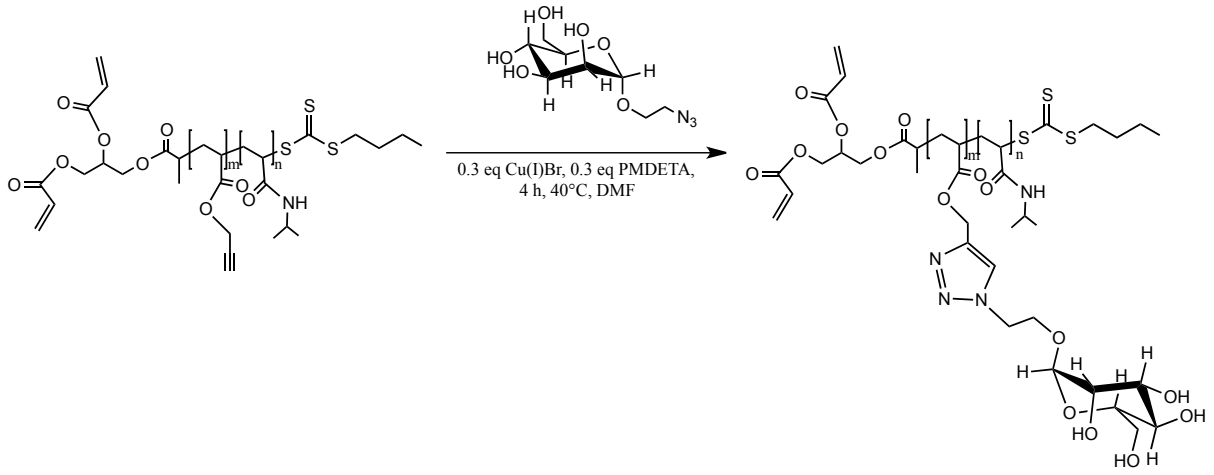

Figure VI-21: CuAAC reaction of the modified P(NIPAM-co-ProA) with azide mannose in the presence of PMDETA in DMF yielding thermo-responsive glycopolymers.

VI.3.3.2.1 Synthesis of the azide mannose

The synthesis route of the azide mannose is shown in Figure VI-22.[28] It was chosen to use a mannose compound characterized with an azide group at the 1-position connected with an ethylene linker. By applying this ethylene spacer, it is expected that the reactivity towards lectins will be higher than that from sugar compound where no linker is present.

In the first step of the synthesis route, D-(+)-mannose is acetylated with acetic acid anhydride in dry pyridine yielding product (1), whereby the hydroxyl groups are protected as acetyl functionalities. This protection allows the selective substitution of the acetyl group at the anomer 1-position with 2-bromoethanol. This reaction was performed in DCM and catalysed by boron trifluoride etherate. In the third step, the halide group is modified into an azide functionality upon a straightforward S_N2 reaction with sodium azide, yielding product 4. In the final step, the product was deprotected by treatment in methanol in the presence of a catalytic amount of potassium carbonate. The overall yield of this synthesis route is 45%.

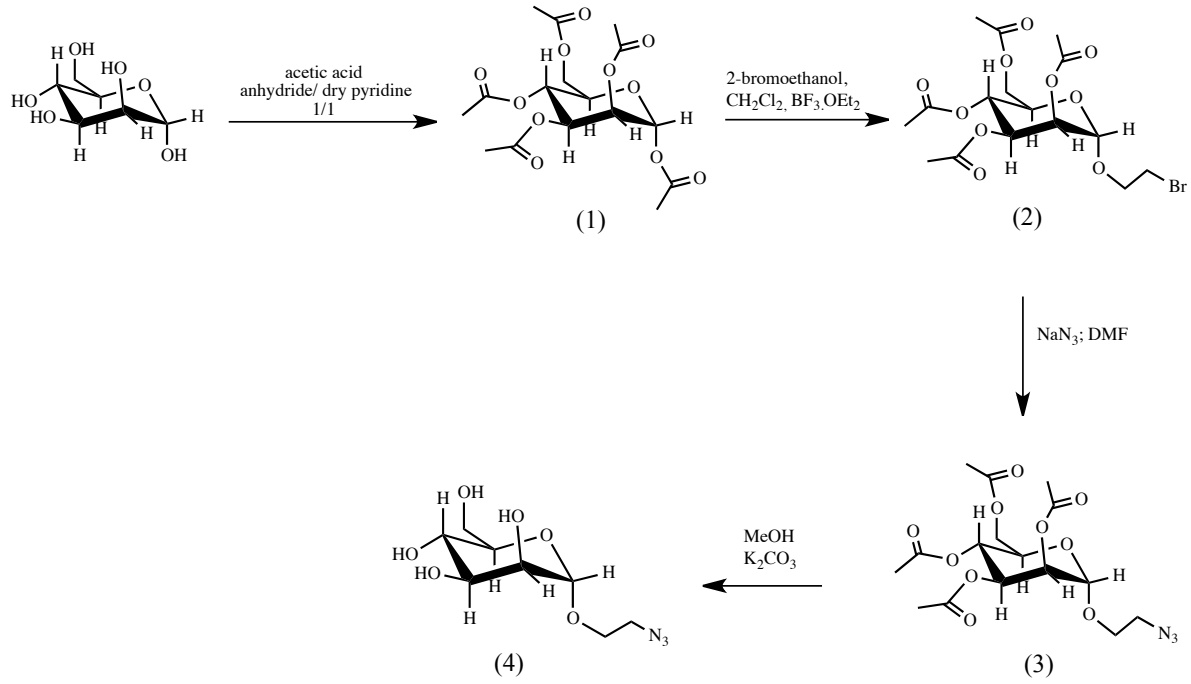

Figure VI-22: Synthesis strategy for the preparation of the azide-mannose sugar compound via a four step route.

Each synthesis step was followed by characterization via NMR, LC-MS and IR analysis. Via IR it is possible to follow the reaction in an easy way, because each step, except for step 2, is accompanied with measureable change in IR spectrum. The IR spectra of D-(+)-mannose, product (1), product (3) and product (4) are depicted in Figure VI-23.

D-(+)-mannose is characterized by an intense stretching vibration between 3200 and 3600 cm^{-1}, originating from the hydroxyl groups present in the C-glycoside. On the other hand, product (1), acetylated mannose, is characterized by an intense stretching vibration at 1730 cm^{-1}, arising from the carbonyl groups of the acetyl functionalities. Moreover, no vibration in the region between 3200 and 3600 cm^{-1} was observed, indicating the completion of the protection of all hydroxyl groups. The characterization of product (2) was exclusively done by ^1H NMR, confirming the success of the S_N2 reaction. An intense stretching vibration at 1730 cm^{-1} is observed when analysing product (3) arising from the carbonyl functionalities. Besides this vibration, also a vibration at 2100 cm^{-1} is present, which is a typical vibration for azide functionalities. The final compound, product (4), shows just like product (3) a stretching vibration at 2100 cm^{-1}, the azide, and an intense vibration in the region between 3200 and 3600 cm^{-1}, the hydroxyl groups, while the signal at 1730 cm^{-1} has disappeared. This analysis

confirms the deprotection of the hydroxyl groups and the incorporation of the azide functionality. Moreover, LC-MS and ^{1}H NMR of the end-product prove the synthesis of product (4). For the characterization via ^{1}H NMR, the reader is referred to the experimental part (VI.5.8).

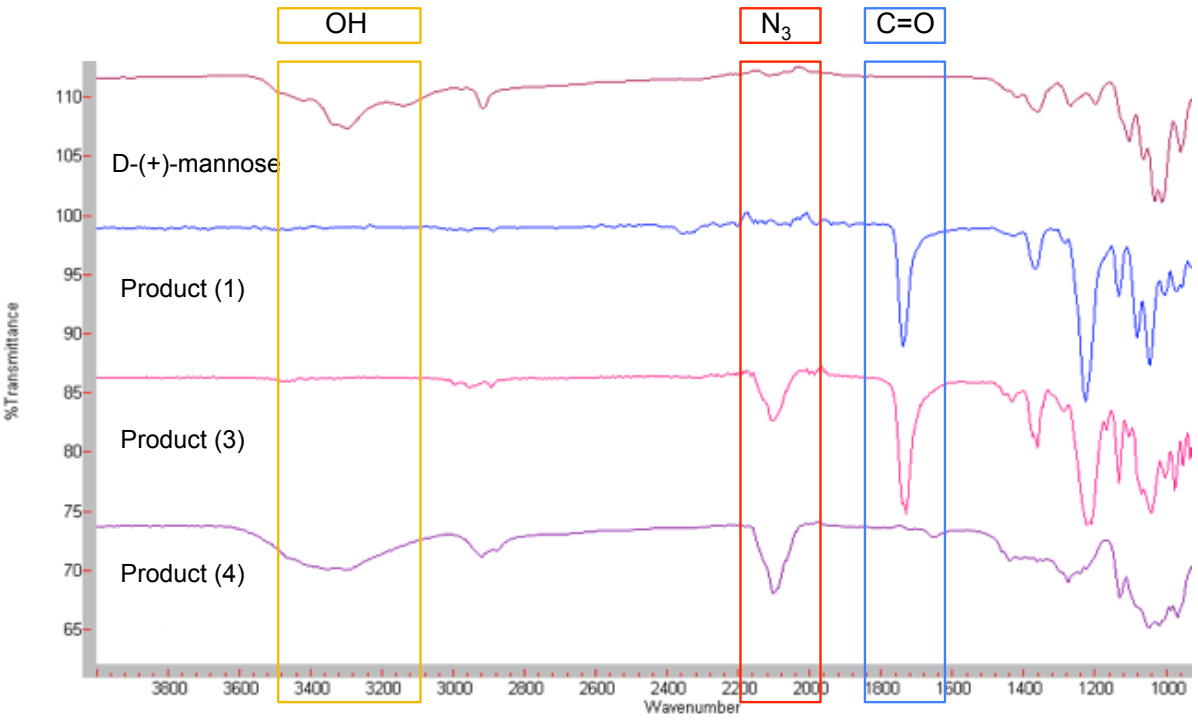

Figure VI-23: IR spectra of D-(+)-mannose and the different products, whereby the most important, specific vibrations are designated.

VI.3.3.2.2 Post-modification via CuAAC

The synthesized P(NIPAM-co-ProA) contains a certain amount of alkyne groups along the polymer chain which are reacted with the azide functionality of the mannose-compound. Via this click reaction, glycopolymers with mannose-unit in the polymer chain are obtained. The incorporation of the mannose units along the polymer chain increases the molecular weight of the copolymer. For Entry 1a, which contains 7 alkyne groups per polymer chain, an increase of about 1750 Da is observed. In Figure VI-24 the SEC curves of Entry 1 after each modification step are depicted. There is a clear increase in molecular weight observed after coupling of the sugar units at the polymer chain while the dispersities remained almost constant. The click reaction with the mannose sugar at the P(NIPAM-co-ProA) results in the fact that the copolymer is much more hydrophilic, which accompanied with an increase in T_{cp} of about 20°C.

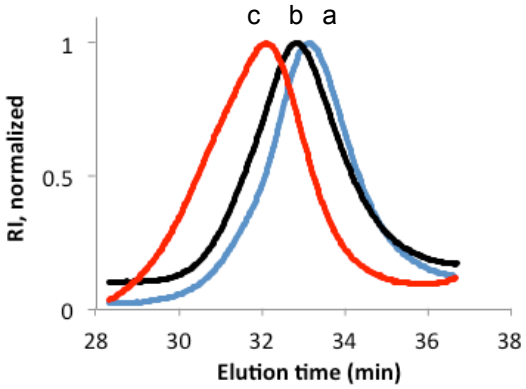

Entry	$M_{n,SEC}$ (g/mol)	Đ
8a	4900	1.35
8b	5600	1.35
8c	9800	1.35

Figure VI-24: SEC curves and results of Entry 8 before post-modification (a), after modification of the hydroxyl groups into acrylates (b) and after CuAAC with the mannose units (c).

In Figure VI-25 the transmission curves of Entry 8 before and after CuAAC reaction are depicted, which shows the increase of the T_{cp} from 11°C and 33°C.

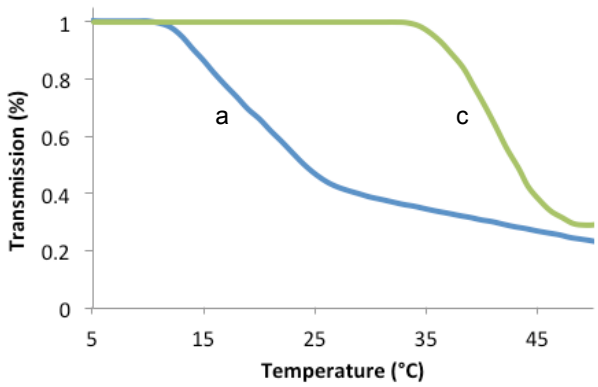

Figure VI-25: Determination of the T_{cp} via turbimetry analysis of Entry 8 before post-modification (a) (11.5°C) and after CuAAC reaction with azide-mannose (c) (33°C).

The glycopolymer was analyzed via ^{1}H NMR in which new signals appear arising from the click reaction with the mannose units (Figure VI-26). A new signal at 7.94 ppm is observed which represents the proton d of the triazole ring indicating the success of the click reaction. Moreover, some additional signals in the range of 4.3-5.3 ppm, which represent the CH-signals of the coupled mannose units, are seen.

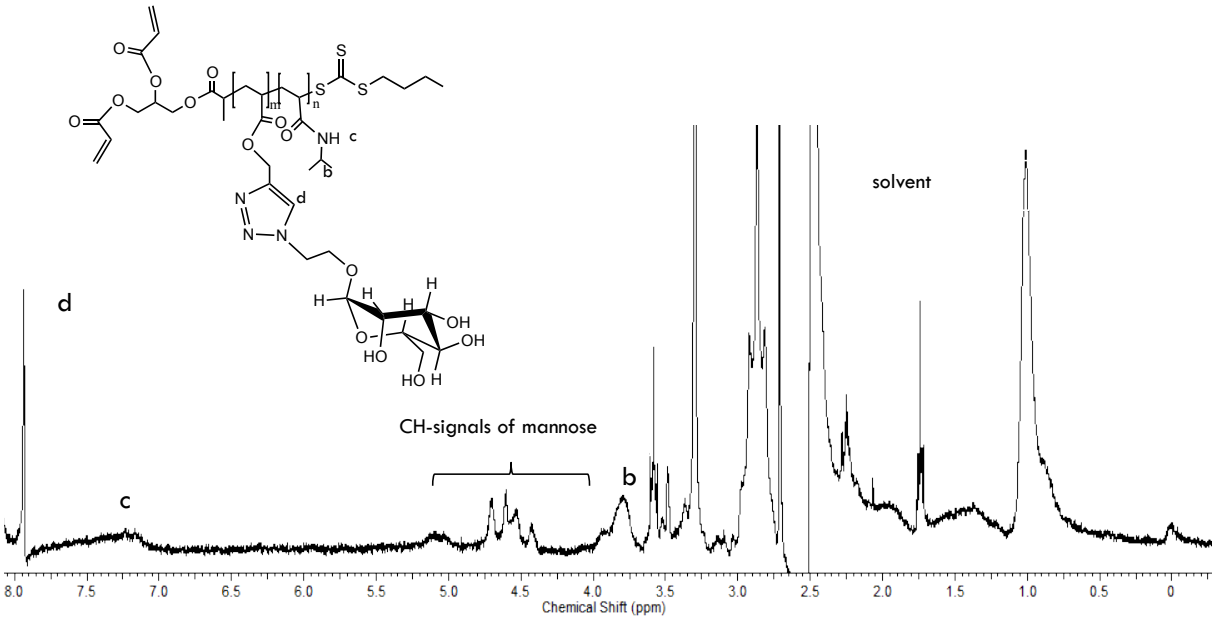

Figure VI-26: ^{1}H NMR (DMSO-d_6, 300 MHz) of the copolymer P(NIPAM-co-ProA) after click reaction with the azide mannose.

VI.3.3.3 *Synthesis of hyperbranched glycopolymers*

The glycopolymer P(NIPAM-co-ProA) was subsequently reacted with n-propylamine which transforms the trithiocarbonate group into a thiol upon aminolysis. From literature it is known that this primary amine shows a higher reactivity towards the trithiocarbonate group compared to acrylates.[29] This means that the two acrylate groups at the α-chain end should remain unreacted while the trithiocarbonate group is modified into a thiol functionality which is proven by UV-Vis spectroscopy. The typical absorption signal of the trithiocarbonate groups at 310 nm disappears after aminolysis, confirming the transformation into the thiol functionality. The aminolysis was done in THF by using an excess of the primary amine for 3 hours at room temperature. After reaction, the polymer was purified by precipitation in cold diethyl ether and dried under vacuum.

As consequence of the aminolysis of the trithiocarbonate group, a thiol functionality is released, which subsequently could react with the α-acrylates upon Michael-thiol addition. From this point of view, the polymer structures can be considered as AB_2 precursors for the synthesis of the hyperbranched glycopolymers. The thiol functionality (A-unit) can only react with the acrylates (B-units) via Michael-thiol addition, yielding hyperbranched glycopolymers.

However, after addition of Et_3N and reacting overnight, no addition reaction was observed. SEC analysis revealed that the molecular weight and dispersity nearly did not change, while a huge increase was expected due to the formation of hyperbranched polymers. Since this reaction was performed at high concentrations and thiols are known to react fast with acrylate groups, it was investigated if all previous steps of this strategy were successful.

Therefore, each step of the synthesis strategy was analyzed once more into more detail to detect the problem. From this extensive study, it can be concluded that the problem probably lies in either the inefficient coupling of the acrylate groups on the polymer chain or to the reaction of the acrylate with the excess of *n*-propylamine. As already stated above, the analysis by ^{1}H NMR of the coupling of the acrylates on the hydroxyl groups could not be done because the specific acrylate signals are overlapping with the strongly broadened NH-signal of the NIPAM units. On the other hand, due to the fact that the modified polymer is difficult to isolate from the excess of ProA monomer, the observed NMR-signals at 5.5-6.5 ppm could also be ascribed to the monomer instead of the acrylates.

On account of the failure of the acrylate coupling on the polymer chain, three alternative methods have been applied for the substitution of the terminal hydroxyl groups. First of all, the esterification with acryloyl chloride was performed under very dry conditions in dry pyridine at -20°C. These conditions are chosen to avoid the possible elimination reactions of the hydroxyl groups, which can appear as side reaction. A second applied method makes use of the esterification of the hydroxyl groups with acrylic acid in the presence of DCC and DMAP. As final attempt, the hydroxyl groups were modified into bromide functionalities by the use of 2-bromopropionyl bromide. These bromide groups can in a next step be reacted with thiols upon thiol-bromo reaction. Unfortunately, none of these three alternatives for the post-modification of the hydroxyl groups were successful, according to the NMR analyses.

At this point, further research could not be done anymore (end of PhD). In the future, other synthesis strategies could be applied to make this RAFT strategy successful for the preparation of thermo-responsive hyperbranched glycopolymers with sugar units along the polymer backbone. The first idea is the synthesis of a CTA with two primary hydroxyl groups at the α-chain end to avoid the possible elimination reaction (Figure VI-27).

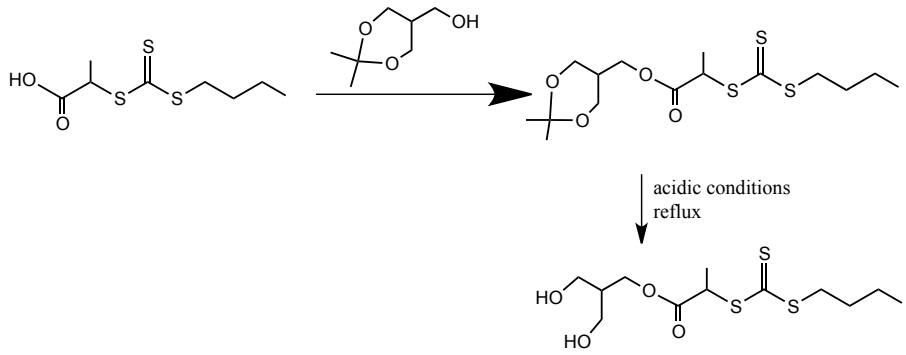

Figure VI-27: Synthesis scheme of the CTA with two primary hydroxyl groups at the α-chain end.

Moreover, another idea is to copolymerize NIPAM with a mannose acrylate via Cu(0)-mediated polymerization technique using the AB_2 initiator (Figure VI-2). Therefore, a mannose monomer would first be synthesized via the click reaction of the azide monomer (Figure VI-28). with propargyl acrylate. In a next step, this monomer would be copolymerized with NIPAM using different monomer ratios (90/10; 50/50; 10/90) applying the same conditions as for the homopolymerization of NIPAM. In this way, the mannose units are directly incorporated in the copolymer chain. By post-modification with sodium methanethiosulfonate followed by ring-opening of the thiolactone with a functional primary amine, hyperbranched glycopolymers should be obtained (Figure VI-28). An additional advantage of this strategy is the introduction of another functionality originating from the primary amine, which is used to open the thiolactone ring.

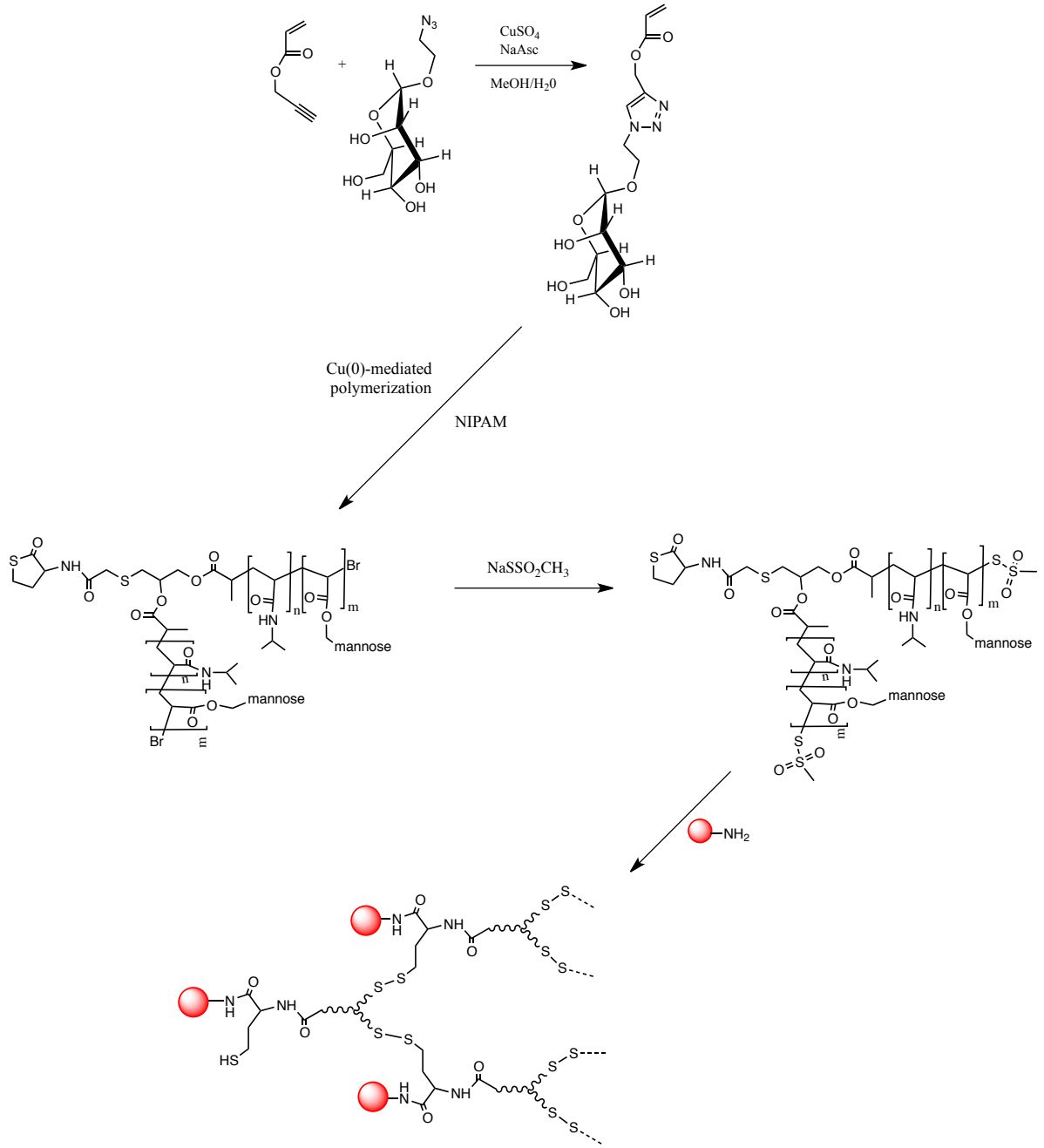

Figure VI-28: Synthesis of the mannose monomer by CuAAC reaction of the azide-mannose with propargyl acrylate (top). This monomer is subsequently copolymerized with NIPAM via the Cu(0)-mediated polymerization technique using a suitable AB_2 initiator. By post-modification with sodium methanethiosulfonate followed by the ring-opening of the thiolactone with a primary amine, hyperbranched polymers could be obtained.

VI.4 Conclusion

Due to the increasing popularity of glycopolymers in polymer science, the aim of this project was to synthesize hyperbranched glycopolymers by the use of controlled radical polymerization (CRP) techniques in combination with efficient post-modification reactions. In a first strategy, Cu(0)-mediated polymerization was used, while a second technique makes use of RAFT. In both strategies, NIPAM is applied as monomer which provide thermo-responsiveness to the polymer structures.

In the first strategy (Scheme VI-3), the synthesis of a thermo-responsive hyperbranched glycopolymer containing sugar moieties in each branching point and redox-degradable links is described. Degradation of the hyperbranched PNIPAM-containing structure was demonstrated by chemically reducing the disulfide bond at the branching point. The hyperbranched polymer shows thermoresponsive behaviour with a cloud point of 39°C. In the lectin-polymer interaction study, it was found that the interaction increases with the concentration of the polymer. Also, it was demonstrated that the polymer-lectin interaction is higher above the cloud point, as a result of the easier access of the mannose units in the globular conformation.

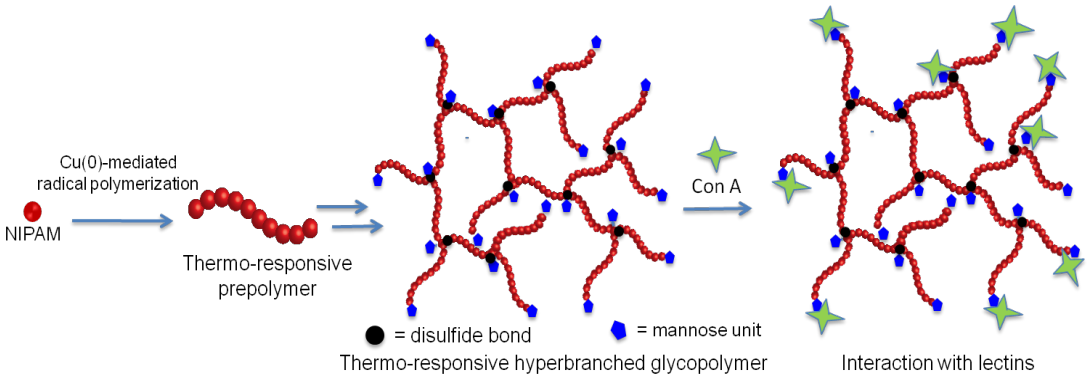

Scheme VI-3: Graphical scheme of the synthesis and lectin interactions of the thermo-responsive hyperbranched glycopolymers applying the first strategy.

In a second strategy, a functional CTA was synthesized and subsequently used for the copolymerization of NIPAM with ProA in different ratios yielding well-defined structures. After performing a kinetic study to obtain the optimal reaction conditions, the hydroxyl groups at the α-chain end were converted into acrylate groups. Next, sugar units are introduced by the CuAAC reaction of the alkyne groups of the ProA units with azide mannose. In a final step, the typical trithiocarbonate group at the ω-chain end is reacted with a primary amine upon aminolysis, releasing a thiol that subsequently can react with the acrylate groups at the α-chain end, yielding the hyperbranched thermo-responsive glycopolymers. Since no hyperbranched structures are formed, the different synthesis steps have been analyzed in more detail. It was observed that the esterification reaction of the hydroxyl groups with acryloyl chloride probably failed. Different other post-modification reactions are performed but none of them has been successful. Other potential strategies have been proposed at the end of this PhD chapter.

VI.5 Experimental part

VI.5.1 Materials

Ethanol (95%; Chem-Labs), diethyl ether (≥ 99.8%; Aldrich), *n*-toluene (99.9%; Aldrich), *n*-hexane (98%; Aldrich); methanol (≥ 99%; Chem-labs), *N,N*-dimethylformamide (DMF) (≥ 99%; Acros), tetrahydrofuran (THF) (≥ 99.9%; Aldrich), dimethylsulfoxide (DMSO) (≥ 99.9%; Aldrich), ethyl acetate (≥ 99.8%; Aldrich), dichloromethane (DCM) (≥ 99.8%; Aldrich), pyridine (≥ 99.9%; Aldrich), N,N-dimethylacetamide (DMA) (99%; Aldrich), ProA (98%; Aldrich), acrylic acid (99%; Aldrich), acetic acid (≥ 99.8%; Acros), acetic acid anhydride (≥ 98%; Aldrich), citric acid (≥ 99.5%; Aldrich), trifluoroacetic acid (TFA) (≥ 99%; TCI), sodium trifluoroacetic acid (NaTFA) (98%; Aldrich), K_2CO_3 (≥ 99%; Roth), $MgSO_4$ (pure; Boom), boortrifluoride diethyletherate (≥ 46.5%; Aldrich), triethyl amine (Et_3N) (99%; Acros), phenothiazine (99%; Acros), aluminiumoxide (Al_2O_3) (Aldrich), trans-2-(3-(4-tert-butylphenyl)-2-methyl-2-propenylidene) malononitrile (DCTB) (≥ 98%; TCI), isopropylidene glycerol (solketal) (98%; Aldrich), 4-dimethylaminopyridine (DMAP) (99%; Aldrich), *N,N*-dicyclohexylcarbodiimide (DCC) (99%; Acros), copper(II) dibromide (99%, Aldrich), D-(+)-mannose (≥ 99%; Aldrich), 2-bromoethanol (97%; Acros), sodium azide (99%; Acros), D-(+)-mannosamine hydrochloride (≥ 99; Aldrich), acryloyl chloride (96%; Aldrich), DL-homocysteine thiolactone hydrochloride (99%; Acros), 2-bromoacetylbromide (≥98%; Aldrich), 1-thioglycerol (≥ 97%; Aldrich), 2-bromopropionyl bromide (97%; Aldrich), tributylphosphine (95%; Acros), and Concanavalin A from *Canavalia ensiformis* (type IV; Aldrich) were used as received. *N*-Isopropyl acrylamide (NIPAM) (≥ 98%; TCI) was recrystallized twice from a 50/50 toluene/*n*-hexane mixture. 2,2'-Azobis(isobutyronitrile) (AIBN) (98%; Aldrich) was recrystallized twice from methanol. 1,4-Dioxane (HPLC grade; Aldrich) was dried by distillation from sodium/benzophenone. Copper(I) bromide (98; Aldrich) is treated with acetic acid for 24 hours, filtered off, washed with ethanol and diethyl ether and dried overnight at 70°C under vacuum. Me_6TREN is synthesized according to a procedure described in literature.[30]

VI.5.2 Characterization and equipment

VI.5.2.1 *^{1}H- and ^{13}C-NMR, SEC, UV-Vis and MALDI-TOF MS analysis see Chapter III*

VI.5.2.2 *LC-MS analysis*

An Agilent technologies 1100 series LC/MSD system equipped with a diode array detector and single quad MS detector (VL) with an electrospray source (ESI-MS) was used for classic reversed phase liquid chromatography-mass spectroscopy (LC-MS) and MS analysis. Analytic reversed phase HPLC was performed with a Phenomenex C18 (2) column (5 µ, 250 x 4.6 mm) using a solvent gradient (0 → 100% acetonitrile in H_2O in 15 min) and the eluting compounds were detected via UV-detection (λ = 254 nm).

VI.5.2.3 *Time-resolved online ATR FT-IR*

Time-resolved *online ATR FT-IR* spectra were recorded on a React-IR 4000 Instrument (Mettler Toledo AutoChem ReactIR) equipped with a silicon ATR probe (SiComp, optical range 4400–650 cm^{-1}). For *online* monitoring, the silicon probe was introduced into a two-necked glass flask containing the reaction mixture and spectra were recorded every minute. The solvent spectrum was recorded at the reaction temperature and subtracted to enhance the signal of the reaction species.

VI.5.3 Synthesis of the AB_2 initiator (Figure VI-2)

VI.5.3.1 *Synthesis of 2-bromo-N-thiolactone acetamide (step 1; Figure VI-2)*

DL-homocysteine thiolactone hydrochloride (9.2 g; 60 mmol) and potassium carbonate (25 g; 180 mmol) are dissolved in 200 mL H_2O followed by the addition of 200 mL CH_2Cl_2. This two-phase system is cooled to 0°C and a solution of 2-bromoacetyl bromide (10.5 mL; 120 mmol) in CH_2Cl_2 (40 mL) is added dropwise over a periode of 30 minutes.Next, the solution is stirred for another hour at room temperature. The two phases are separated and the organic phase is washed two times with a 5% aqueous solution of citric acid (40 mL) and two times with H_20 (40 mL) before drying over $MgSO_4$. The solvent was removed under reduced pressure to obtain a white solid with a yield of 86%.

VI.5.3.2 *Synthesis of 2-((2,3-dihydroxypropyl)thio)-N-thiolactone acetamide (step 2; Figure VI-2)*

To a solution of 2-bromo-*N*-thiolactone acetamide (5 g; 21 mmol) and 1-thioglycerol (4.54 g; 42 mmol) in dichloromethane (40 mL), a solution of Et_3N (12.8 g; 126 mmol) in dichloromethane (10 mL) was added dropwise at room temperature. The conversion of the reaction is followed via TLC (eluens: DCM/ EtOAc: 7/1) (R_f*:* 0.6 to R_f: 0.15).

VI.5.3.3 *Synthesis of the branched thiolactone initiator (step 3; Figure VI-2)*

After complete conversion, determined via TLC, the reaction solution 2-((2,3-dihydroxypropyl)thio)-N-thiolactone acetamide is cooled to 0°C and a solution of 2-bromopropionyl bromide (27.2; 126 mmol) in CH_2Cl_2 (40 mL) is added dropwise over a period of 45 minutes. The reaction mixture is subsequently stirred for two hours at room temperature whereby the conversion is followed by TLC (eluens: DCM/EtOAc: 7/1). Next, the mixture is diluted with diethyl ether (100 mL) and washed with H_2O (2 x 50 mL) and with a saturated solution of $NaHCO_3$. The organic phase is dried over $MgSO_4$ and concentrated under reduced pressure. The residue is purified via flash chromatography (eluens: hexane/EtOAc: 4/1), yielding a brownish oil with a overall yield of 65%. **^{1}H NMR** (300 MHz, $CDCl_3$); δ(ppm): 1.77 (d, 6H, 2x C**H**$_3$); 1.99 (m, 1H, C**H**$_2$); 2.77 (m, 1H, C**H**$_2$); 2.85 (m, 2H, C**H**$_2$S); 3.26 (m, 4H, C**H**$_2$S and C**H**$_2$O); 4.11-4.73 (m, 2H, 2x C**H**Br), 4.11-4.73 (m, 2H, SC**H**$_2$CO); 4.11-4.73 (m, 1H, N(H)C**H**CO); 5.21 (m, 1H, C**H**O); 6.94 (m, 1H, N**H**). **^{13}C-APT** (300MHz, $CDCl_3$); δ(ppm): 21.78 (2 x **C**H$_3$); 27.55 (**C**H$_2$S); 31.51 (**C**H$_2$CH$_2$); 32.79 (**C**H$_2$S); 36.28 (**C**H$_2$O); 39.89 (2x **C**HBr); 59.76 (N(H)**C**HCO); 64.50 (S**C**H$_2$CO); 71.75 (**C**HO); 169.13 (**C**(O)O); 170 (**C**(O)S); 205 (**C**(O)NH). M.W.= 535.27 g/mol; ESI-MS (m/z): 536.5 g/mol [M+H$^+$].

VI.5.4 Homopolymerization of NIPAM using the AB_2 initiator

VI.5.4.1 *Direct use of Cu(0) as catalyst*

In the first sealed flask, foreseen of 5 Cu(0) pellets, the monomer NIPAM is dissolved together with the AB_2 initiator (VI.5.3) in water with a minimum amount of DMF to enhance the solubility of the initiator. In a second flask, $CuBr_2$ and Me_6TREN are dissolved in water. The conditions of the reaction are chosen as followed: $[M]_0/[I]_0/[L]_0/[CuBr_2]_0$ = 100 or 50/1/0.12/0.05 whereby the monomer

concentration is 2.5 mol/L. Both solutions are bubbled with N_2 gas for 45 minutes to remove all oxygen from the reaction mixtures. Subsequently, the solution of the second flask is added to the first flask, which starts the actual polymerization. The polymerization is performed at room temperature for 3 or 4 hours depending on the desired molecular weight. After polymerization, toluene is added to the reaction mixture and the mixture is concentrated under reduced pressure. Filtration over Al_2O_3 is done to remove all the copper from the reaction mixture and the filter is washed several times with THF. The colorless solution is concentrated under reduced pressure to a smaller volume (+/- 10 mL) and subsequently precipitated in cold diethyl ether (2 times), filtered and washed with diethyl ether to obtain a white solid.

VI.5.4.2 *Disproportionation of Cu(I)Br/Me_6TREN in Cu(0) and $CuBr_2$ in H_2O*

In the first sealed flask, the ligand Me_6TREN is dissolved in water where subsequently Cu(I)Br is added. The solution became blue after addition of the copper(I) and after 45 minutes of stirring some purple/red powders could be observed in the suspension. The stirring was further allowed at ambient temperature for another 30 minutes under nitrogen protection. The monomer NIPAM, the AB_2 initiator and water with a minimum amount of DMF were charged in a second flask fitted with a rubber septum and the mixture was deoxygenated by bubbling N_2 gas through the solution. The conditions were chosen as such: $[M]_0/[I]_0/[L]_0/[CuBr]_0$= 50/1/0.4/0.4 with a monomer concentration of 2.5 mol/L. The degassed monomer/initiator was then transferred with a degassed syringe to the first flask, starting the polymerization. The mixed solution is allowed to stir at room temperature for 3 to 5 hours depending on the desired molecular weight. Samples are taken during the reaction to determine the conversion. Catalyst residues are removed by filtering through a column of aluminium oxide.

VI.5.5 Post-modification of the PNIPAM with sodium methanethiosulfonate

VI.5.5.1 *Synthesis of sodium methanethiosulfonate*

Sodium methanethiosulfonate was synthesized according a procedure described in literature.[31] Sodium sulphide nonahydrate (72.1 g; 0.3 mol) was dissolved in water (80 mL) with gentle heating to about 60°C. The solution was cooled to 0- 5°C in an ice bath with stirring. Methanesulfonyl chloride (23.3 mL, 34.5 g, 0.3 mol) was added dropwise over 1 hour. The mixture turned yellow, then orange-brown, and finally colorless. Some sulfur was precipitated. The mixture was heated under reflux for 18 hours and then cooled. At this stage, the reaction mixture was brown. The solution was evaporated on a high-vacuum rotary evaporator giving a white solid. The solid was

dried for 24 h in a vacuum desiccator over calcium chloride, ground with a pestle and mortar, and replaced in the vacuum desiccator for an additional 24 h. The white solid was extracted with dry ethanol (ca. 15 x 100 mL), and the slurry was filtered after each extraction. The filtrate was evaporated down to a thick slurry of precipitated sodium methanethiosulfonate which was collected by filtration. The filtrate thus obtained was evaporated further and refiltered. Sodium methanethiosulfonate (32.5 g, 87%) was obtained as white crystals. **^{1}H NMR** (300 MHz, D_2O); δ(ppm): 3.24 (s, SC**H**$_3$);44; ^{13}C NMR (300 MHz, D_2O); δ(ppm): 54.9 (**C**H$_3$).

VI.5.5.2 *Post-polymerization reaction*

The poly(*N*-isopropyl acrylamide) (2 g; 0.44 mmol) is dissolved in DMF (100 mL) and sodium methanethiosulfonate (177.08 mg; 1.32 mmol) is added. The reaction mixture is subsequently stirred at 40°C for 16 hours. The excess of sodium methanethiosulfonate is subsequently removed by precipitation in THF. After filtration, the solution was concentrated under reduced pressure and the polymer was isolated by two-fold precipitation in cold diethyl ether.

VI.5.5.3 *Formation of hyperbranched glycopolymers by opening the thiolactone ring*

The thiolactone ring of the PNIPAM prepolymers was opened by adding the deprotected D-(+)-mannosamine (179 mg; 1 mmol) to a solution of the polymer (500 mg; 0.1 mmol) in DMSO as solvent to promote the formation of disulfide bonds. Hereby it was chosen to work with highly concentrated solutions (6 M) to favour the formation of hyperbranched structures and to reduce ring formation. The solution was stirred for 6 hours while samples were taken for SEC and NMR analysis. After 6 hours, the solution became so viscous that stirring was not possible anymore and the polymer was investigated by SEC.

VI.5.5.4 *Degradation of the hyperbranched glycopolymer via chemical reduction of the disulfide bond*

The hyperbranched glycopolymer (40 mg, 0.0016 mmol) was dissolved in THF. To this solution *n*-tributylphosphine (6.47 mg , 0.032 mmol) was added. The reaction mixture was allowed to stir for 2 hours and the reduced polymer was isolated by two-fold precipitation in cold diethyl ether and investigated by SEC. The obtained 'prepolymers' could again be converted into hyperbranched

glycopolymers by dissolving the polymer in DMSO, a known solvent that promotes disulfide bond formation. Hereby hyperbranched polymers were again formed, although a fraction of the prepolymers stayed unreacted in the mixture.

VI.5.6 Interaction measurements of the glycopolymers with Con A via turbimetry measurements

These measurement are performed following a procedure described by Kiessling *et al.*[25] Con A (2mg/mL) was completely dissolved in a HBS buffer (0.1M Tris-HCl pH 7.5, 90 µM NaCl, 1 mM $CaCl_2$, 1 mM $MnCl_2$). Subsequently, the concentration was diluted to a concentration of 1 mM. After addition of a certain concentration of glycopolymer in HBS buffer into a polycarbonate cuvette, the cuvette was placed in the UV-Vis spectrometer. Following addition of the diluted Con A solution into the cuvette via a pipette, the absorbance of the mixture was quickly recorded at 420 nm for 10 min every 0.12 s. The relative rate of interaction was determined by a linear fit of the steepest portion of the initial aggregation. Each experiment was repeated three times. This procedure was done at room temperature to investigate the binding rate and at higher temperatures to investigate the effect of the thermo-responsiveness of the glycopolymer on the interaction rate.

VI.5.7 Synthesis of the CTA DPBCP (Figure VI-13)

VI.5.7.1 *Synthesis of 2-([[(Butylsulfanyl)carbonothioyl]sulfanyl)propanoic acid) (BUPAT) (1)*

The CTA BuPAT is prepared via a one-pot synthesis with a yield of 85%, according to a synthesis procedure described in literature and section IV.5.3.[26]

VI.5.7.2 *Synthesis of (2,2-dimethyl-1,3-dioxolan-4-yl)methyl 2-(((butylthio)carbonothioyl)thio)propanoate (2)*

The esterification of BuPAT (10 g; 42 mmol) with solketal (4.35 mL; 35 mmol) is performed in dry DCM (100 mL) in the presence of DMAP (1.71 g; 14 mmol) and DCC (9 g ; 43.75 mmol) in a dry one-neck flask sealed with a rubber septum. The reaction mixture is then stirred for 3 days at room temperature. The formed salts (DCU) are filtered and washed with DCM. The eluens is concentrated under reduced pressure yielding a yellow oil which is purified via flash chromatography (eluens*: n*-hexane/EtOAc: 9/1). **^{1}H NMR** (300 MHz, $CDCl_3$); δ(ppm): 0.86 (t, 3H, C**H**$_3$); 1.29 (s, 3H, C**H**$_3$); 1.36 (m,

2H, C**H**$_2$); 1.38 (s, 3H, C**H**$_3$); 1.54 (d, 3H, C**H**$_3$); 1.61 (m, 2H, C**H**$_2$); 3.3 (t, 2H, C**H**$_2$); 3.69 (m, 1H, C**H**$_2$); 4.00 (m, 1H, C**H**$_2$); 4.12 (m, 2H, C**H**$_2$); 4.24 (m, 1H, C**H**); 4.76 (m, 1H, C**H**).

VI.5.7.3 *Synthesis of 2,3-dihydroxypropyl 2-(((butylthio)carbonothioyl)thio) propanoate (3)*

Product 2 is dissolved in 75 mL DCM and stirred at room temperature. Next, 25 mL TFA is added dropwise to the solution during a period of 30 min and the mixture is allowed to stir for another 5 hours at room temperature. The product is subsequently concentrated under reduced pressure to yield a brownish-yellow product (overall yield of 65%). **^{1}H NMR** (300 MHz, $CDCl_3$); δ(ppm): 0.86 (t, 3H, C**H**$_3$); 1.36 (m, 2H, C**H**$_2$); 1.54 (d, 3H, C**H**$_3$); 1.61 (m, 2H, C**H**$_2$); 2.23 (s, 1H, O**H**); 3.3 (t, 2H, C**H**$_2$); 3.55 (m, 1H, C**H**$_2$); 3.67 (m, 1H, C**H**$_2$); 3.89 (m, 1H, C**H**); 4.20 (m, 2H, C**H$_2$**); 4.76 (m, 1H, C**H**). **^{1}3 C-APT NMR** (300 MHz, $CDCl_3$); δ(ppm): 13.58 (**C**H$_3$); 16.40 (**C**H$_3$); 22.05 (**C**H$_2$); 30.09 (**C**H$_2$); 37.20 (**C**H$_2$); 47.85 (**C**H); 63.19 (**C**H$_2$); 66.40 (**C**H$_2$); 69.67 (**C**H); 171.50 (**C**$_q$).

VI.5.8 Synthesis of 2'-azidoethyl-O-α-D-mannopyranoside (Figure VI-22)

VI.5.8.1 *Synthesis of 1,2,3,4,6-penta-O-acetyl-α-D-mannospyranoside (1)*

To a solution of the commercially available D-(+)-mannose (5 g; 27.75 mmol) in dry pyridine (11.8 mL; 138 .75 mmol), acetic acid anhydride (13.1 mL; 138.75 mmol) is added and the reaction mixture is allowed to stir overnight at room temperature. Next, the excess of acetic acid anhydride is removed by filtration over silica and the filter was washed several times with toluene. The product is subsequently concentrated under reduced pressure and dissolved again in toluene to remove all the remaining pyridine. This procedure is repeated 3 times to obtain product (1) as a white solid with a yield of 87%. **^{1}H NMR** (300 MHz, $CDCl_3$); δ(ppm): 1.94 (s, 3H, C**H$_3$**CO); 1.98 (s, 3H, C**H$_3$**CO); 2.04 (s, 3H, C**H$_3$**CO); 2.10 (s, 3H, C**H$_3$**CO); 2.12 (s, 3H, C**H$_3$**CO); 3.92-4.12 (d, 2H, C**H$_2$**OC=O); 4.17-4.27 (m, 1H, C**H**CH$_2$); 5.03-5.44 (3H, m, C**H**, C**H**, C**H**); 6.00 (s, 1H, C**H**OCO).

VI.5.8.2 *Synthesis of 2'-bromoethyl 2,3,4,6-tetra-O-acetyl-α-D-mannopyranoside (2)*

To a solution of product (1) (7.6 g; 19.47 mmol) and 2-bromoethanol (1.87 mL; 20.68 mmol) in dry DCM, borotrifluoride etherate (9.26 mL; 75.29 mmol) is added dropwise over a period of 15 minutes. The reaction mixture is stirred overnight at room temperature under N_2 atmosphere in the

absence of light. Next, DCM (50 mL) is added and the mixture is neutralized with $NaHCO_3$. The organic phase is washed three times with H_2O and concentrated under reduced pressure. The product crystallizes to a pale white powder which is further purified by recrystallization in EtOAc/*n*-hexane (1/1) yielding a white powder (yield: 68%). **^{1}H NMR** (300 MHz, $CDCl_3$); δ(ppm): 1.94 (s, 3H, C**H$_3$**CO); 1.98 (s, 3H, C**H$_3$**CO); 2.04 (s, 3H, C**H$_3$**CO); 2.10 (s, 3H, C**H$_3$**CO); 3.46 (t, 2H, C**H$_2$**Br); 3.87 (m, 2H, C**H$_2$**O); 4.06 (d, 2H, C**H$_2$**OC=O); 4.20 (m, 1H, C**H**CH$_2$); 4.81 (s, 1H, C**H**O); 5.18-5.33 (3H, m, C**H**, C**H**, C**H**). **^{13}C-APT NMR** (300 MHz, $CDCl_3$); δ(ppm): 20.65-20.92 (4 x OC=O**C**H$_3$); 26.60 (**C**H$_2$Br); 62.44 (**C**H$_2$); 66.00 (**C**H); 68.50 (**C**H); 68.94 (**C**H); 69.05 (**C**H); 69.43 (**C**H); 97.75 (O**C**HO); 169.76-170.60 (4 x O**C**=OCH$_3$).

VI.5.8.3 *Synthesis of 2'-azidoethyl-2,3,4,6-tetra-O-acetyl-α-D-mannopyranoside (3)*

To a solution of product (2) (3 g; 6;59 mmol) in DMF, sodium azide (2.57 g; 39.54 mmol) is slowly added. The reaction mixture is allowed to react for three hours at 60°C. The reaction is followed via TLC analysis with EtOAc/*n*-hexane (2/1) (starting product R_f = 0.7; end product R_f = 0.55). The solution is concentrated under reduced pressure and redissolved again in DCM. This mixture is subsequently 4 times washed with H_2O (50 mL) and the organic phase is dried over $MgSO_4$ and concentrated under reduced pressure. A yellowish powder is obtained which is purified by recrystallization in EtOAc/*n*-hexane (2/1). Yield: 89%. **^{1}H NMR** (300 MHz, $CDCl_3$); δ(ppm): 1.94 (s, 3H, C**H$_3$**CO); 1.98 (s, 3H, C**H$_3$**CO); 2.04 (s, 3H, C**H$_3$**CO); 2.10 (s, 3H, C**H$_3$**CO); 3.32-3.48 (m, 2H, C**H$_2$**N$_3$); 3.56-3.66 (m, 1H, C**H$_2$**O); 3.76-3.85 (m, 1H, C**H$_2$**O); 3.94-4.09 (m, 2H, C**H$_2$**OC=O); 4.17-4.27 (m, 1H, C**H**CH$_2$); 4.80 (s, 1H, C**H**O); 5.18-5.33 (3H, m, C**H**, C**H**, C**H**). **^{13}C-APT NMR** (300 MHz, $CDCl_3$); δ(ppm): 20.66-20.87 (4 x OC=O**C**H$_3$); 50.36 (**C**H$_2$N$_3$); 62.46 (**C**H$_2$); 66.00 (**C**H); 68.50 (**C**H); 68.94 (**C**H); 69.05 (**C**H); 69.43 (**C**H); 97.75 (O**C**HO); 169.76-170.60 (4 x O**C**=OCH$_3$).

VI.5.8.4 *Synthesis of 2'-azidoethyl-O-α-D-mannopyranoside (4)*

To a solution of product (3) in anhydrous methanol, a catalytic amount of K_2CO_3 is added. The reaction mixture is stirred under N_2 atmosphere at room temperature for three hours. The mixture is concentrated under reduced pressure to obtain a pale white product with a yield of 85%. **^{1}H NMR** (300 MHz, DMSO); δ(ppm); 3.29-3.71 (m, 9H, 2x C**H**OH, C**H**OCH$_2$ C**H$_2$**OH, C**H$_2$**N$_3$, C**H$_2$**O); 3.72-3.83 (m, 1H, C**H**CH**$_2$**); 3.90-4.60 (s, 4H, 4x O**H**); 4.68 (d, 1H, OC**H**O). M.W.= 249.10 g/mol; ESI-MS (m/z): 267.20 g/mol [M+NH_4^+].

VI.5.9 Copolymerization of NIPAM and ProA (P(NIPAM-co-ProA))

NIPAM and ProA are added in a certain ratio (5/1 or 10/1) to a solution of the RAFT agent DPBCP and AIBN in THF as such that $[M]_0/[CTA]_0/[I]_0$= 30/1/0.11. The reaction mixture was charged to a schlenk tube and the solution was deoxygenated via freeze-pump-thaw cycles for 3 times. The degassed solution was then heated to 65°C and the polymerization was started. After 5 hours, the reaction was quenched by placing the flask in an ice/water bath under air. The copolymer was isolated by a three-fold precipitation in cold diethyl ether. The copolymer was then redissolved in THF and concentrated under reduced pressure at 50°C to ensure the elimination of the excess of ProA-monomer. Next, the copolymer is precipitated again in cold diethyl ether and dried under vacuum.

VI.5.10 Post-modification of P(NIPAM-co-ProA)

VI.5.10.1 *Reaction with acryloyl chloride (P(NIPAM-co-ProA)2)*

The copolymer P(NIPAM-co-ProA) (2.8 g; 1.12 mmol) is dissolved together with Et_3N (1.25 mL; 8.96 mmol) in dry CH_2Cl_2 (25 mL). To this solution, acryloyl chloride was added dropwise during 30 minutes at 0°C and subsequently allowed to stir for 24h at room temperature. Next, a minimal amount of phenothiazine was added and the solvent and excess of acryloyl chloride were removed under reduced pressure. The yellow product is subsequently dissolved in CH_2Cl_2 and isolated by two-fold precipitation in cold diethyl ether and dried under vacuum to obtain a yellowish powder.

VI.5.10.2 *CuAAC reaction with 2'-azidoethyl-O-α-D-mannospyranoside*

The modified P(NIPAM-co-ProA)2 copolymer (2 g; 0.4 mmol), Cu(I)Br (17.21 mg; 0.12 mmol) and PMDETA (25.06 µL; 0.12 mmol) are dissolved in DMF in a one-neck flask. Next, the azide-mannose (2'-azidoethyl-O-α-D-mannopyranoside) (109.66 mg; 0.44 mmol) dissolved in DMF is added and the mixture is allowed to stir at room temperature for 4 hours under N_2 atmosphere. The copper is removed from the mixture by multiple filtration through Al_2O_3 and washing with THF. After concentration under reduced pressure to a volume of 5 mL, the polymer is isolated by precipitation in cold diethyl ether, yielding a light green solid.

VI.5.10.3 *Aminolysis of the trithiocarbonate group*

The with sugar modified copolymer (0.424 g; 0.0597 mmol) is dissolved in THF (10 mL). Next, *n*-propylamine (0.1 mL; 1.194 mmol) is added and the reaction is allowed to stir at room temperature under N_2 atmosphere. The reaction process is followed via UV-Vis analysis. Completion of the reaction is confirmed by the disappearance of the absorbance signal at a wavelength of 310 nm. Next, triethylamine is added to the mixture as catalyst for the Michael-addition reaction between the thiol and the acrylate groups. This mixture is stirred overnight at room temperature.

VI.5.10.4 *Reaction of the hydroxyl groups with acryloyl chloride*

P(NIPAM-co-ProA) (2.8 g; 1.12 mmol) is dissolved in dry pyridine and is subsequently concentrated under reduced pressure (2 times) under N_2 atmosphere. The polymer was dissolved again in dry pyridine and distillated acryloyl chloride is added dropwise at a temperature of -20°C for 15 min. The reaction mixture is allowed to stir at room temperature for 10 min and methanol is added subsequently. The formed salts are precipitated in THF and the polymer is isolated by precipitation in cold diethyl ether and dried under vacuum.

VI.5.10.5 *Reaction of the hydroxyl groups with acrylic acid*

P(NIPAM-co-ProA) (2 g; 0.8 mmol) is dissolved in a mixture of DMAP (0.04 g; 0.32 mmol), DCC (0.206 g; 1 mmol) and acrylic acid (0.066 mL; 0.96 mmol) in dry CH_2Cl_2. This reaction is stirred for 24 hours at room temperature. Next, a catalytic amount of phenothiazine (radical inhibitor) is added and the reaction mixture is concentrated under reduced pressure to remove the solvent. The excess of acrylic acid is removed by adding pyridine and subsequent evaporation under reduced pressure. The polymer is isolated by two-fold precipitation in cold diethyl ether.

VI.5.10.6 *Reaction of the hydroxyl groups with 2-bromopropionyl bromide*

To a mixture of P(NIPAM-co-ProA) (2.8 g; 1.12 mmol) in dry CH_2Cl_2, EtN_3 (1.25 mL; 8;96 mmol) is added. Next, 2-bromopropionyl bromide (0.93 mL; 8.96 mmol) is added dropwise to the reaction mixture at 0°C. The mixture is stirred for 24 hours at room temperature. The solvent and the excess van 2-bromopropionyl bromide are removed under reduced pressure. The polymer was subsequently isolated by two-fold precipitation in cold diethyl ether.

VI.6 References

[1] L. Valtola, A. Rahikkala, J. Raula, E. I. Kauppinen, H. Tenhu, S. Hietala, *Eur. Polym. J.* **2014**, *59*, 282.
[2] L. L. Kiessling, J. C. Grim, *Chem. Soc. Rev.* **2013**, *42*, 4476.
[3] M. Hetzer, G. Chen, C. Barner-Kowollik, M. H. Stenzel, *Macromol. Biosci.* **2010**, *10*, 119.
[4] L. Nurmi, J. Lindqvist, R. Randev, J. Syrett, D. M. Haddleton, *Chem. Commun.* **2009**, 2727.
[5] N. Xu, R. Wang, F.-S. Du, Z.-C. Li, *J. Polym. Sci. Part A* **2009**, *47*, 3583.
[6] S. Reinicke, P. Espeel, M. M. Stamenovic, F. E. Du Prez, *Acs Macro Letters* **2013**, *2*, 539.
[7] J. J. Lundquist, E. J. Toone, *Chem. Rev.* **2002**, *102*, 555.
[8] J. E. Gestwicki, C. W. Cairo, L. E. Strong, K. A. Oetjen, L. L. Kiessling, *J. Am. Chem. Soc.* **2002**, *124*, 14922.
[9] V. Ladmiral, G. Mantovani, G. J. Clarkson, S. Cauet, J. L. Irwin, D. M. Haddleton, *J. Am. Chem. Soc.* **2006**, *128*, 4823.
[10] C. R. Becer, *Macromol. Rapid Commun.* **2012**, *33*, 742.
[11] K. Lin, A. M. Kasko, *Biomacromolecules* **2013**, *14*, 350.
[12] S. Slavin, J. Burns, D. M. Haddleton, C. R. Becer, *Eur. Polym. J.* **2011**, *47*, 435.
[13] C. R. Becer, M. I. Gibson, J. Geng, R. Ilyas, R. Wallis, D. A. Mitchell, D. M. Haddleton, *J. Am. Chem. Soc.* **2010**, *132*, 15130.
[14] Y. Gou, J. Geng, S.-J. Richards, J. Burns, C. Remzi Becer, D. M. Haddleton, *J. Polym. Sci. Part A* **2013**, *51*, 2588.
[15] C. Boyer, A. H. Soeriyadi, P. J. Roth, M. R. Whittaker, T. P. Davis, *Chem. Commun.* **2010**, *47*, 1318.
[16] P. Espeel, F. Goethals, F. E. Du Prez, *J. Am. Chem. Soc.* **2011**, *133*, 1678.
[17] P. Espeel, F. Goethals, M. M. Stamenovic, L. Petton, F. E. Du Prez, *Polym. Chem.* **2012**, *3*, 1007.
[18] C. Boyer, A. Granville, T. P. Davis, V. Bulmus, *J. Polym. Sci. Pol. Chem.* **2009**, *47*, 3773.
[19] J. P. Tam, C. R. Wu, W. Liu, J. W. Zhang, *J. Am. Chem. Soc.* **1991**, *113*, 6657.
[20] V. Sharma, S. Anandhakumar, M. Sasidharan, *Mater. Sci. Eng. C-Mater. Biol. Appl.* **2015**, *56*, 393.
[21] S. R. S. Ting, G. Chen, M. H. Stenzel, *Polym. Chem.* **2010**, *1*, 1392.
[22] G. Yilmaz, C. R. Becer, *Eur. Polym. J.* **2013**, *49*, 3046.
[23] M. Ahmed, R. Narain, *Biomaterials* **2012**, *33*, 3990.
[24] Y. Chen, G. Chen, M. H. Stenzel, *Macromolecules* **2010**, *43*, 8109.
[25] C. W. Cairo, J. E. Gestwicki, M. Kanai, L. L. Kiessling, *J. Am. Chem. Soc.* **2002**, *124*, 1615.
[26] C. J. Ferguson, R. J. Hughes, D. Nguyen, B. T. T. Pham, R. G. Gilbert, A. K. Serelis, C. H. Such, B. S. Hawkett, *Macromolecules* **2005**, *38*, 2191.
[27] Y. Zhang, S. Furyk, L. B. Sagle, Y. Cho, D. E. Bergbreiter, P. S. Cremer, *J. Phys. Chem. C* **2007**, *111*, 8916.
[28] W. Hayes, H. M. I. Osborn, S. D. Osborne, R. A. Rastall, B. Romagnoli, *Tetrahedron* **2003**, *59*, 7983.
[29] P. Espeel, F. Goethals, F. Driessen, L.-T. T. Nguyen, F. E. Du Prez, *Polym. Chem.* **2013**, *4*, 2449.
[30] M. Ciampoli, N. Nardi, *Inorg. Chem.* **1966**, *5*, 41.
[31] E. J. Grayson, S. J. Ward, A. L. Hall, P. M. Rendle, D. P. Gamblin, A. S. Batsanov, B. G. Davis, *J. Org. Chem.* **2005**, *70*, 9740.

Chapter VII

Summary and conclusions

The aim of this work was to develop a straightforward and versatile procedure for the synthesis of functional hyperbranched polymers. Combinations of controlled radical polymerization (CRP) techniques and recent developments in thiol-X chemistry are applied in different strategies for the preparation of such hyperbranched structures. The interest in those highly branched structures has grown a lot the last decade as they possess unique properties compared to their linear analogues of equivalent molecular masses, making them attractive for different applications.[1-6] Hyperbranched polymers differ from the structurally perfectly uniform dendrimers as they are irregularly structured with randomly distributed branching points. Moreover, while the preparation of dendrimers requires extensive purifications steps and is expensive, hyperbranched polymers can be prepared via much more straightforward procedures, most often via a one-pot synthesis using simple and efficient reactions. The self-condensing vinyl polymerization of AB* monomers (where A is a vinyl group and B stands for initiator) and the step-growth polymerization of AB_x monomers (where A and B are functionalities that selectively react with each others, and $x \geq 2$) are the most known of such reactions.

In this work well-defined AB_2 macromonomers are synthesized *via* CRP techniques and then further reacted upon thiol-X chemistry resulting in functional hyperbranched polymers. Next to frequently used reversible addition-fragmentation chain transfer (RAFT), the Cu(0)-mediated radical polymerization has been applied as CRP technique. The latter technique has been recently developed and is known to be fast, can proceed at ambient conditions and yields polymers with high end-group fidelity even at high conversions. These features make this technique attractive for the synthesis of well-defined functional macromolecules. Not only the kinetics using different monomers and functional initiators are investigated, also other parameters, such as the amount of ligand, have been optimized *via* high throughput experiments. Using the robot, up to 16 reactions could be performed

in parallel, resulting in a fast screening of different reaction conditions enabling the determination of the optimized reaction conditions for this CRP technique.

The synthesized AB_2 macromonomers (where A and B selectively react with each other under certain conditions) are able to further react upon thiol-X chemistry yielding hyperbranched polymers. Thiol-X chemistry has gained a lot of interest in polymer science, due to its high reactivity and ability to react as thiyl radical as well as thiolate anion. However, this reactivity towards a whole range of substrates directly implies a restriction, as a lot of side reactions are possible. To circumvent this problem, the use of protecting groups for thiols, such as disulfides or thiocarbonylthio groups, is required. However, a lot of these methods require a protecting and a deprotecting step, which is unfavourable in terms of atom-efficiency and overall yield. In this work, a thiolactone moiety is used as precursor for the thiol functionality, which can be obtained upon aminolysis without any further deprotection or purification step, while at the same time an additional functionality is introduced in the structure. As such, opening of the thiolactone ring with glucosamine resulted into hyperbranched glycopolymers that are able to interact with certain lectins, making them applicable in different medical fields.

In **Chapter II**, not only the recent advances in the different CRP techniques, but also the developments in click chemistry in general are described. It was seen that in polymer science, where a huge need for efficient reaction is needed, thiol-X chemistry has gained a lot of attention. The different new insights in this chemistry and some examples are given to stress its applicability in polymer science. In the second part of this chapter, the unique features and different possible synthesis strategies of hyperbranched polymers are reported, next to some recent examples where the thiol-X chemistry and hyperbranched structures have been combined. Finally, the synthesis and the advantages of the use of glycopolymers is shortly described, together with their interaction possibilities with certain lectins making them applicable in certain fields.

In the next chapter, **Chapter III**, the use of RAFT as CRP technique for the straightforward synthesis of heterotelechelic, hydrophilic polymers with a primary amine and thiol group at the α– and ω-chain end is described. End-group conversion during each step of the synthesis was monitored by ^{1}H NMR spectroscopy, MALDI-TOF MS analysis and UV-Vis spectroscopy, confirming quantitative modifications. Grafting the amino groups with citraconic anhydride resulted in the creation of dual

temperature- and pH-responsive polymer/gold nanohybrids. Furthermore, incorporation of two different dye components in the PNIPAM structure yielded thermo-responsive polymeric dyes whose sensing capacities were demonstrated by using a biphasic aqueous/organic system below and above the cloud point temperature of the polymeric structure.

Chapter IV reports the findings on the use of thiol-yne chemistry of AB_2 oligomers for the preparation of functional hyperbranched polymers. In this context, two different approaches were followed. In the first approach, a suitable CTA, containing an alkyne functionality at the ω-chain end, was synthesized and evaluated on its polymerization capacities of different monomer types. Aminolysis yielded the AB_2 thiol-alkyne oligomers, which were further reacted to hyperbranched polymers applying photo (UV)-initiated thiol-yne chemistry. In the other approach, aminolysis of the thiolactone moiety of an $A'B_2$ thiolactone-alkyne monomer was used with a RAFT-derived oligomer containing a primary amine at the α-chain end. Using this strategy, a new functionality is introduced into the structure originating from the amine molecule. Also here, photo(UV)-initiated thiol-yne chemistry was applied for the preparation of hyperbranched structures.

In **Chapter V,** the reproducible Cu(0)-mediated polymerization performed in an automated parallel synthesizer, has been described. Good near-linear first order kinetics up to almost full conversion were obtained in most cases, indicating the controlled characteristics of the Cu(0)-mediated polymerization. It was found that the best results with good control over molecular weight (distribution) while maintaining a high reaction speed were obtained with a [M]:[EBP]:[Me_6TREN]:[$CuBr_2$] ratio of [M]:1:0.15:0.1 with 12.5 mm^2 mL^{-1} Cu(0) wire. Applying those conditions, it was possible to make polymers with narrow molecular weight distributions over a large range of molecular weights. Moreover, one-pot block copolymerization reactions have also been performed, although these did not cause full conversion of the second monomer.

Finally, in **Chapter VI**, the synthesis of hyperbranched glycopolymers in which thermo-responsive poly(*N*-isopropylacrylamide) (PNIPAM), connected by redox-responsive disulfide bonds, forms the skeleton and for which mannose units are present at each branching point are described. Degradation of the hyperbranched structure via chemical reduction of the disulfide bond was demonstrated. Moreover, the thermo-responsive behaviour of the glycopolymer was studied. Finally, the lectin-polymer interaction was investigated to understand the influence of both the polymer

concentration and different chain conformations below and above cloud point, respectively. Furthermore, it has been attempted to prepare thermo-responsive hyperbranched glycopolymers with adjustable amount of sugar units per branching unit.

VII.1 Perspectives

The recent advances of controlled radical polymerization allow for the synthesis of complex polymer structures, which begin to find their way in industrial applications. In this project, the synthesis of functional hyperbranched polymers via a straightforward and versatile procedure is described, making them available for large scale production and applicable in different fields. However, further investigation of post-modification reactions of the functional hyperbranched polymers upon click chemistry would promote their versatility. Not only the azide-alkyne based click reactions are suitable for the post-modification, but also a whole rang of thiol-based efficient reactions meet the requirements for industrial processes. In this way, a large amount of functional groups can be introduced in the hyperbranched structure making them applicable in different fields. For instance, introduction of target molecules, sugar units of drug compounds makes the functional hyperbranched structures applicable in the pharmaceutical field. It is believed that these structures give other performances compared to their linear analogous. Testing and evaluation these performances should be done intensively.

Another perspective deals with the synthesis of hyperbranched glycopolymers with an adjustable amount of sugar moieties per branching unit. It is believed that such hyperbranched glycopolymers would show a higher interaction with their specific lectins compared to the hyperbranched glycopolymers with only one sugar unit at each branching point. A part of this approach is already described in Chapter VI, but further investigation on both the synthesis and the interaction approach are needed.

VII.2 References

[1] D. A. Tomalia, J. M. Frechet, *Prog. Polym. Sci.* **2005**, *30*, 217.
[2] D. A. Tomalia, J. M. J. Frechet, *J. Polym. Sci. Pol. Chem.* **2002**, *40*, 2719.
[3] C. Gao, D. Yan, *Prog. Polym. Sci.* **2004**, *29*, 183.
[4] D. Astruc, E. Boisselier, C. Ornelas, *Chem. Rev.* **2010**, *110*, 1857.
[5] D. Konkolewicz, M. J. Monteiro, S. Perrier, *Macromolecules* **2011**, *44*, 7067.
[6] M. Calderon, M. A. Quadir, S. K. Sharma, R. Haag, *Adv. Mater.* **2010**, *22*, 190.

Chapter VIII

Nederlandstalige samenvatting

(Dutch summary)

Het doel van deze thesis was de ontwikkeling van een eenvoudige en veelzijdige procedure voor de synthese van functionele hypervertakte polymeren. Een combinatie van gecontroleerde radicalaire polymerisatie (CRP) technieken en de recente ontwikkelingen in de thiol-X chemie werden aangewend in verschillende strategieën voor de synthese van dergelijke hypervertakte polymeren. De interesse in deze hoogvertakte structuren is de laatste jaren sterk toegenomen dankzij hun unieke eigenschappen in vergelijking met hun lineaire analogen van eenzelfde moleculaire massa, wat hen aantrekkelijk maakt in verschillende toepassingsgebieden.[1-6] Het feit dat hypervertakte polymeren onregelmatig gestructureerd zijn met willekeurig verdeelde vertakkingspunten onderscheidt hen van de structureel perfecte, uniforme dendrimeren. In tegenstelling tot de synthese van dendrimeren, die vaak tijdrovend en kostelijk is, kunnen hypervertakte polymeren bereid worden via een éénpotssynthese gebruikmakend van eenvoudige en efficiënte reacties. Vinyl condensatiepolymerisatie van AB* monomeren (waarbij A een vinylgroep en B een initiator voorstellen) en de stapsgewijze polymerisatie van AB_x monomeren (waarbij A en B functionele groepen zijn die selectief met elkaar reageren, en $x \geq 2$) zijn de meest gekende van dergelijke reacties.

In dit werk werden goed gedefinieerde AB_2 macromonomeren gesynthetiseerd met behulp van CRP technieken en die vervolgens gebruikmakend van thiol-X chemie verder gereageerd werden tot functionele hypervertakte polymeren. Naast de frequent gebruikte reversibele additie-fragmentatie ketentransfer (RAFT) techniek, werd ook de Cu(0)-gemedieerde radicalaire polymerisatie aangewend als CRP techniek voor de synthese van de AB_2 macromonomeren. Deze laatstgenoemde techniek werd recent ontwikkeld en is gekend om snel te zijn, door te kunnen gaan

bij kamertemperatuur en polymeren op te leveren met een hoog eindgroepbehoud, zelfs bij hoge conversies. Deze eigenschappen maken de techniek aantrekkelijk voor de synthese van goed gedefinieerde functionele macromoleculen. Niet alleen de kinetiek van verschillende monomeren en functionele initiatoren zijn onderzocht, ook parameters zoals de ligandconcentratie zijn geoptimaliseerd geweest *via* 'high throughput' experimenten. Gebruikmakend van een syntheserobot konden tot 16 reacties tergelijkertijd uitgevoerd worden, leidend tot een snelle screening van verschillende reactiecondities. Dit maakte de bepaling van de geoptimaliseerde reactiecondities van deze CRP techniek op een snelle manier mogelijk.

Deze gesynthesieerde AB_2 macromonomeren (waar A en B selectief met elkaar kunnen reageren onder bepaald condities) zijn in staat om verder te reageren via thiol-X chemie, met de vorming van hypervertakte polymeren tot gevolg. Thiol-X chemie heeft de laatste tijd sterk aan interesse gewonnen binnen de polymeerwetenschap, dankzij de hoge reactiviteit en de mogelijkheid om te reageren als thiyl radicalen alsook als thiolaatanionen. Deze reactiviteit ten opzichte van een hele reeks van substraten, legt echter ook een beperking op daar vele zijreacties mogelijk zijn. Om dit probleem te omzeilen is het gebruik van beschermgroepen voor thiolen zoals disulfides of thiocarbonylthiogroepen een vereiste. Desondanks vereisen vele van deze methodes een beschermings- en ontschermingsstap, welke in termen van atoom-efficiëntie en totale opbrengst ongunstig zijn. In dit werk werd een thiolacton-eenheid gebruikt als precursor voor een thiolfunctionaliteit, welke kan verkregen via aminolyse zonder enig verdere ontschermings- of opzuiveringsstap, terwijl tergelijkertijd een extra functionaliteit in de structuur is ingevoerd. Zo leidde de opening van de thiolactonring met glucosamine tot hypervertakte glycopolymeren die in staat zijn om interactie aan te gaan met bepaalde lectines, welke hen toepasbaar maakt in verschillende medische sectoren.

In **Hoofdstuk II**, werden niet alleen de recente vooruitgangen in de verschillende CRP technieken beschreven, ook de ontwikkelingen in click chemie in het algemeen werden besproken. Er werd gezien dat in de polymeerwereld, waar er een hoge nood is aan efficiënte reacties, thiol-X chemie enorm aan interesse gewonnen heeft. De verschillende nieuwe inzichten in deze chemie en enkele voorbeelden zijn gegeven om hun toepasbaarheid binnen de polymeerwereld te onderstrepen. In een tweede deel van dit hoofdstuk, werden de unieke eigenschappen en de verschillende mogelijke synthesestrategieën voor hypervertakte polymeren gerapporteerd, naast enkele voorbeelden waar thiol-X chemie en hypervertakte structuren werden gecombineerd. Als

laatste werden de synthese en de voordelen van het gebruik van glycopolymeren kort beschreven, samen met hun interactiemogelijkheden met bepaalde lectines, welke hen toepasbaar maakt in verschillende specifieke sectoren.

In het volgend hoofdstuk, **Hoofdstuk III**, werd het gebruik van RAFT als CRP techniek voor de eenvoudige synthese van heterotelechelische, hydrofiele polymeren met een primair amine en thiol groep aan respectievelijk de α- en de ω-keteneinde beschreven. Eindgroepconversie gedurende de verschillende stappen van de synthese werden via ^{1}H NMR spectroscopie, MALDI-TOF MS analyse en UV-Vis spectroscopie bepaald, welke kwantitatieve modificaties bevestigen. Het graften van de amino-groepen met een citraconzuuranhydride leidde tot de vorming van temperatuurs- en pH-responsieve polymeer/goud-nanohybride structuren (Figuur VIII-1). Verder leidde de incorporatie van twee verschillende kleurcomponenten in de PNIPAM structuren tot thermoresponsieve polymerische kleurstoffen. De mogelijkheid van deze structuren om als sensoren aangewend te worden, werd aangetoond door het gebruik van een tweefasensysteem boven en onder de witwordingstemperatuur van de polymeerstructuur.

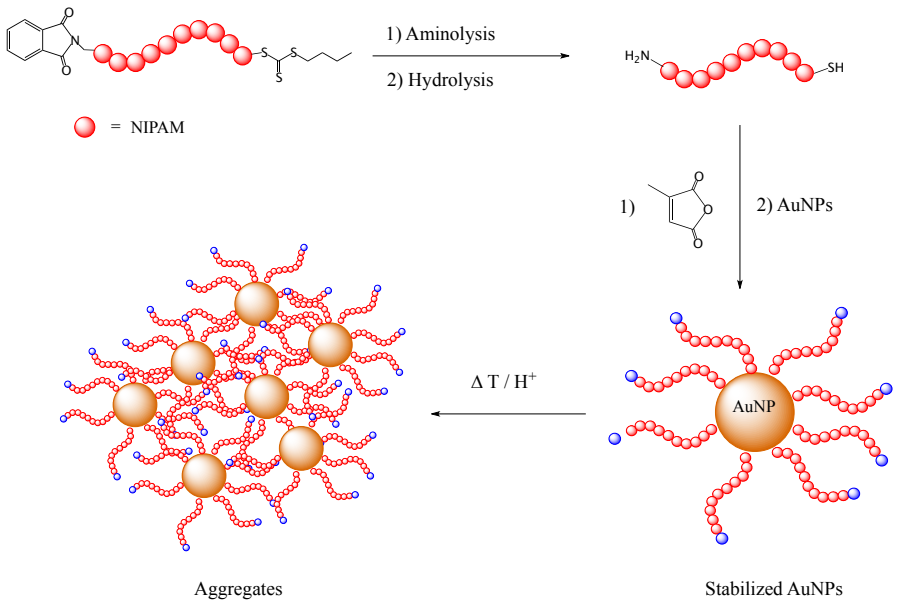

Figuur VIII-1: Schema van de verschillende stappen voor de synthese van responsieve goud nanohybride structuren.

Hoofdstuk IV beschrijft de bevindingen over het gebruik van thiol-yn chemie op de AB_2 macromonomeren voor de synthese van functionele hypervertakte polymeren. In deze context, werden twee verschillende benaderingen gebruikt. In de eerste strategie werd een geschikt ketentransferreagens (CTA), met een alkynfunctionaliteit aan de ω-ketenuiteinde, gesynthetiseerd en vervolgens geëvalueerd op zijn polymerisatiecapaciteiten van verschillende monomeertypes. Aminolyse leidde tot de AB_2 thiol-alkyn-oligomeren, die verder gereageerd werden tot hypervertakte polymeren gebruikmakend van foto(UV)-geïnitieerde thiol-yn chemie. In de tweede strategie werd de aminolyse van de thiolactoneenheid van een $A'B_2$ thiolactone-alkyn-monomeer uitgevoerd met een RAFT-afgeleid oligomeer dat een primair amine bezit aan het α-ketenuiteinde. Het toepassen van deze strategie laat toe om een nieuwe functionaliteit afkomstig van de aminemolecule in te voeren. Ook hier werd foto(UV)-geïnitieerde thiol-yn chemie aangewend voor de synthese van de hypervertakte structuren.

In **Hoofdstuk V**, werd de reproduceerbaarheid van de Cu(0)-gemedieerde polymerisatie techniek uitgevoerd in een geautomatiseerde parallelle robot, beschreven. Zo goed als een lineaire eerste orde kinetiek en volledige conversies warden verkregen in de meeste gevallen, wat de gecontroleerde karakteristieken van deze technieken aangeven. Er werd gezien dat de beste resultaten met een goede controle over het moleculaire gewicht met behoud van een hoge reactiesnelheid werden behaald met een [M]:[EBP]:[Me_6TREN]:[$CuBr_2$] verhouding van [M]:1:0.15:0.1 met 12.5 mm^2 mL^{-1} Cu(0) draad. Het toepassen van deze condities maakte het mogelijk om polymeren met een nauwe moleculaire gewichtsdistributie voor een hele reeks moleculaire gewichten te synthetiseren. Bovendien werden ook enkele blokcopolymerisaties in één pot uitgevoerd, hoewel deze niet leidden tot de volledige conversie van het tweede monomeer.

Tot slot, in **Hoofdstuk VI**, werd de synthese van hypervertakte glycopolymeren waarbij thermoresponsieve PNIPAM ketens, verbonden door redox-responsieve disulfidebindingen, het skelet vormen beschreven (Figuur VIII-2). Bovendien werd de synthesestrategie zo gekozen dat er een mannose-eenheid in elk vertakkingspunt aanwezig is. Verder werden de degradatie van de hypervertakte structuur via chemische reductie van de disulfidebinding aangetoond en het thermoresponsief karakter van het glycopolymeer onderzocht. Vervolgens werd ook de lectine-polymeerinteractie onderzocht om een beter inzicht te verwerven over de invloed van zowel de polymeerconcentratie als de verschillende polymeerconformaties respectievelijk onder en boven de witwordingstemperatuur. Als laatste werd er gepoogd om thermoresponsieve hypervertakte

glycopolymeren met een aanpasbare hoeveelheid suikereenheden per vertakkingseenheid te synthetiseren.

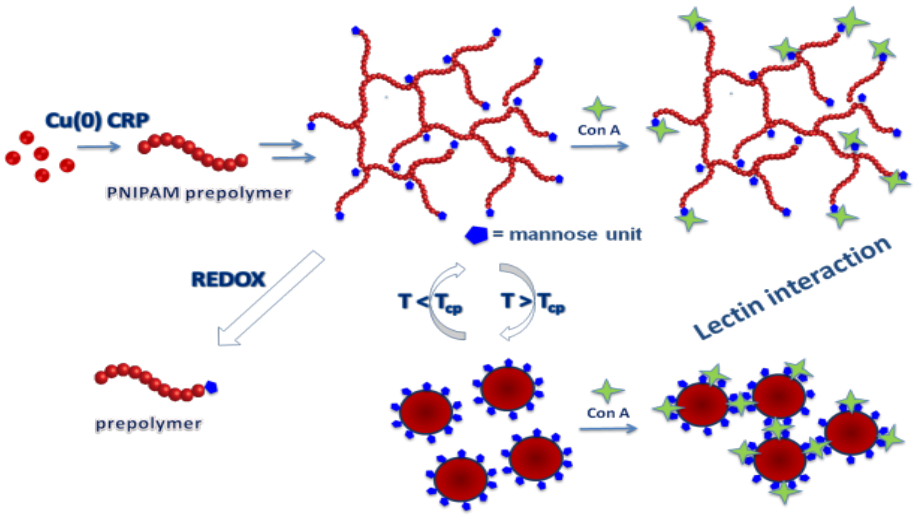

Figuur VIII-2: Grafische voorstelling van de verschillende stappen in de aangewende synthesestrategie voor een hypervertakt glycopolymeer.

VIII.1 Vooruitzichten

De recente vooruitgangen binnen de gecontroleerde radicalaire polymerisatietechnieken laat de synthese van complexe polymeerstructuren welke hun weg beginnen te vinden in industriële toepassingen, toe. In dit project, werd de synthese van functionele hypervertakte polymeren gebruikmakend van een eenvoudige en veelzijdige procedure beschreven, wat hen beschikbaar maakt voor productie op grote schaal in verschillende sectoren. Verder onderzoek van postmodificatiereacties op de functionele hypervertakte polymeren via klikchemie zou hun veelzijdigheid verder verhogen. Niet enkel de azide-alkyn gebaseerde klikreacties komen in aanmerking voor post-modificatie, maar ook een hele reeks thiolgebaseerde efficiënte reacties voldoen aan de vereisten voor industriële processen. Op deze manier kan een grote waaier aan functionele groepen in de hypervertakte structuur geïntroduceerd worden, wat hen inzetbaar maakt in verschillende toepassingsgebieden. Zo maakt de introductie van targetmoleculen, suikereenheden of drugcomponenten de functionele hypervertakte structuren toepasbaar in de farmaceutische sector. Het wordt aangenomen dat deze structuren andere prestaties leveren in vergelijking met hun lineaire analogen. Het testen en de evaluatie van deze prestaties zouden dan ook uitgebreid bestudeerd moeten worden.

Een ander vooruitzicht behandelt de synthese van hypervertakte glycopolymeren met een aanpasbaar aantal suikereenheden per vertakkingseenheid. Er wordt van uitgegaan dat dergelijke hypervertakte glycopolymeren een hogere interactie vertonen met hun specifieke lectines in vergelijking met de hypervertakte glycopolymeren met slechts één suikereenheid per vertakkingspunt. Een deel van deze benadering werd reeds beschreven in **Hoofdstuk VI**, maar verder onderzoek naar zowel de synthese- als naar de interactiestrategieën zijn noodzakelijk.

VIII.2 Referenties

[1] D. A. Tomalia, J. M. Frechet, *Prog. Polym. Sci.* **2005**, *30*, 217.
[2] D. A. Tomalia, J. M. J. Frechet, *J. Polym. Sci. Pol. Chem.* **2002**, *40*, 2719.
[3] C. Gao, D. Yan, *Prog. Polym. Sci.* **2004**, *29*, 183.
[4] D. Astruc, E. Boisselier, C. Ornelas, *Chem. Rev.* **2010**, *110*, 1857.
[5] D. Konkolewicz, M. J. Monteiro, S. Perrier, *Macromolecules* **2011**, *44*, 7067.
[6] M. Calderon, M. A. Quadir, S. K. Sharma, R. Haag, *Adv. Mater.* **2010**, *22*, 190.

List of Publications

Publications included in this PhD manuscript:

1. Wallyn, S.; Zhang, Z.; Driessen, F.; Pietrasik, J.; De Geest, B. G.; Hoogenboom, R.; Du Prez, F. E., Straightforward RAFT Procedure for the Synthesis of Heterotelechelic Poly(acrylamide)s. *Macromol. Rapid Commun.* **2014,** *35*, 405-411.

2. Voorhaar, L.; Wallyn, S.; Du Prez, F. E.; Hoogenboom, R., Cu(0)-mediated polymerization of hydrophobic acrylates using high-throughput experimentation. *Polymer Chemistry* **2014,** *5*, 4268-4276.

3. Vandewalle, S.; Wallyn, S.; Chattopadhyay, S.; Becer, C. R.; Du Prez, F., Thermoresponsive hyperbranched glycopolymers: Synthesis, characterization and lectin interaction studies. *European Polymer Journal* **2015,** *69*, 490-498.

Publications not included in this PhD manuscript:

1. Lammens, M.; Skey, J.; Wallyn, S.; O'Reilly, R. K.; Du Prez, F., Polymeric ligands as homogeneous, reusable catalyst systems for copper assisted click chemistry. *Chemical Communications* **2010,** *46*, 8719-8721.

2. Wallyn, S.; Lammens, M.; O'Reilly, R. K.; Du Prez, F., Highly Active, Thermo-Responsive Polymeric Catalytic System for Reuse in Aqueous and Organic CuAAC Reactions. *J. Polym. Sci. Pol. Chem.* **2011,** *49*, 2878-2885.